

Electronic Thesis and Dissertation Repository

4-15-2011 12:00 AM

Evaluation of Wind-Induced Resuspension on the Performance of a Mine Tailings Storage Facility

Laxmi Kant Kachhwal
The University of Western Ontario

Supervisor
Dr. Ernest K. Yanful
The University of Western Ontario

Graduate Program in Civil and Environmental Engineering
A thesis submitted in partial fulfillment of the requirements for the degree in Doctor of Philosophy
© Laxmi Kant Kachhwal 2011

Follow this and additional works at: <https://ir.lib.uwo.ca/etd>



Part of the [Environmental Engineering Commons](#), and the [Geotechnical Engineering Commons](#)

Recommended Citation

Kachhwal, Laxmi Kant, "Evaluation of Wind-Induced Resuspension on the Performance of a Mine Tailings Storage Facility" (2011). *Electronic Thesis and Dissertation Repository*. 123.
<https://ir.lib.uwo.ca/etd/123>

This Dissertation/Thesis is brought to you for free and open access by Scholarship@Western. It has been accepted for inclusion in Electronic Thesis and Dissertation Repository by an authorized administrator of Scholarship@Western. For more information, please contact wlsadmin@uwo.ca.

**EVALUATION OF WIND-INDUCED RESUSPENSION ON THE
PERFORMANCE OF A MINE TAILINGS STORAGE FACILITY**

(Spine title: Study of Water Cover Technology for Reactive Mine Tailings)

(Thesis format: Integrated-Article)

by

Laxmi Kant Kachhwal

Graduate Program in Civil & Environmental Engineering

A thesis submitted in partial fulfillment
of the requirements for the degree of
Doctor of Philosophy

The School of Graduate and Postdoctoral Studies
The University of Western Ontario
London, Ontario, Canada

© Laxmi Kant Kachhwal 2011

THE UNIVERSITY OF WESTERN ONTARIO
SCHOOL OF GRADUATE AND POSTDOCTORAL STUDIES

CERTIFICATE OF EXAMINATION

Supervisor

Dr. Ernest K. Yanful

Supervisory Committee

Dr.

Examiners

Dr. Mustafa Samad

Dr. Robert A. Schincariol

Dr. Raouf E. Baddour

Dr. Jon Southen

The thesis by

Laxmi Kant Kachhwal

entitled:

**Evaluation of Wind-Induced Resuspension on the Performance of a
Mine Tailings Storage Facility**

is accepted in partial fulfillment of the
requirements for the degree of
Doctor of Philosophy

Date _____
Chair of the Thesis Examination Board

ABSTRACT

Proper management of sulphide rich reactive mine tailings is a growing concern for mining industries. Oxidation of tailings can release acids and toxic metals into the surroundings, which can potentially pollute the ecosystem. Confining tailings under shallow water covers is one of the most successfully applied technologies for long-term storage. The water has lower solubility and diffusivity of oxygen than air and can significantly reduce the influx of oxygen to the bed tailings. However, wind-induced waves and currents in the water can resuspend bed tailings and ultimately result in oxidation.

Extensive field investigations were carried out to evaluate the performance of the existing Shebandowan tailings storage facility, Thunder Bay, Ontario, Canada. Sediment traps and optical backscatter sensor data showed some amount of resuspension occurring at this site under existing conditions. The role of wind induced circulation currents in the resuspension was not clear from previous studies. A semi empirical approach was used to determine the total bed shear stress in the tailings pond, where the current fraction of the bed shear stress was obtained by fitting the Log-Law to mean velocity profiles measured using acoustic Doppler current profiler (ADCP). This was the first study, where the actual currents were measured in a tailings pond. The results showed that wave-current interactions increased the total bed shear stress. A graphical approach was developed to obtain the critical shear stress and erosion rate characteristics of the bed tailings using field recorded resuspension. Previous studies obtained these parameters from laboratory column and flume experiments that did not necessarily represent field conditions.

Based on the field investigations, some major improvements were made to an existing model of water cover design and the results show that wave-current interactions significantly increase the required depth of water from 3.9 m in the absence of wave-current interaction to 6.3 m to completely eliminate tailings resuspension in the west cell of the tailings pond. However, the optimized water depths of less than 2.2 m, 1.1 m, and 2.0 m for the west, middle and east cells were sufficient to reduce tailings concentration to values within the regulatory limit of 15 mg/L, respectively.

Keywords: Mine tailings; shallow water cover; resuspension; wind waves and currents; wave-current interaction; sediment traps; OBS sensors; ADCP; water cover design model; critical shear stress; erosion characteristics; Log-Law; optimization.

CO-AUTHORSHIP

The following work was carried out by Laxmi Kant Kachhwal under the supervision of Prof. Ernest K. Yanful. The field and laboratory work was conducted by Laxmi Kant Kachhwal. Prof. Yanful was involved in field visits, experimental data collection, editing, and interpretation of the results. Prof. Yanful was a co-author on the publication arising from Chapter 3 and will also be co-author on the publications from Chapters 4, 5, and 6. Ms. Lisa Lanteigne of Decommissioning Department, ValeInco Limited, Canada was involved in the editing of the publication arising from Chapter 3 and was also a co-author on the publication. Dr. Collin D. Rennie, Department of Civil Engineering, University of Ottawa, Canada co-supervised the ADCP data collection and analysis conducted in Chapter 4 and will be a co-author on the publication arising from that chapter.

Chapter 3

Water Cover Technology for Reactive Tailings Management: A Case Study of Field Measurement and Model Predictions

Laxmi Kant Kachhwal, Ernest K. Yanful, and Lisa Lanteigne

Water Air Soil Pollution (2011) 214: 357-382

Copyright License in Appendix-VI

Chapter 4

A Semi-Empirical Approach for Estimation of Bed Shear Stress in a Tailings Pond

Laxmi Kant Kachhwal, Ernest K. Yanful, and Collin D. Rennie

Submitted to Environmental Earth Sciences

Chapter 5

Estimating the Erosion Characteristics of Tailings Using Field Resuspension Data

Laxmi Kant Kachhwal, and Ernest K. Yanful

Submitted to Marine Geology

Chapter 6

An Improved Model for the Design of Water Cover for Reactive Mine Tailings

Laxmi Kant Kachhwal, and Ernest K. Yanful

To be submitted.

ACKNOWLEDGEMENTS

First of all, I want to thank almighty god for giving me strength and ability to successfully complete this work.

I am heartily thankful to my supervisor, Professor Ernest K. Yanful for providing me the opportunity to work with him and whose encouragement, guidance, and support from the initial to the final level enabled me to develop an understanding of the subject. It has truly been a blessing working with Dr. Yanful over the past five years. He taught me critical thinking and has given me all the necessary tools to be a successful researcher. I feel privileged to be his student.

I am grateful to Dr. Collin D. Rennie, associate professor, Department of Civil Engineering, University of Ottawa, Canada who gave necessary training for the use of acoustic Doppler current profiler and helped in the data analysis. This research would not have been possible without the help of onsite staff which includes Jakkoo, Christian and other personnel of Denison Environmental Services, Shebandowan Mine, Thunder Bay, Ontario, Canada.

I greatly acknowledge the enormous help and support from my friends and colleagues, faculty and staff at the Civil and Environmental Engineering Department. The administrative and technical staffs Joanne Lemon, Connie Walter, Cynthia Quintus, Kathy Moser, Stephanie Laurence, Charlene Kruzynski, Wilbert Logan, Tim Stephens, and Melody Richards have all assisted me in various ways and I am sincerely grateful for their help.

Finally with all the respect, I would like to express my most sincere gratitude to my father Bhim Raj Kachhwal, my mother Pushpa Kachhwal, my wonderful wife Rashmi, and my adorable son Manan for their love, support, patience, and understanding throughout my time in graduate study.

The research was supported by the Natural Sciences and Engineering Research Council of Canada and ValeInco Limited through a Collaborative Research and Development Grant awarded to Prof. Ernest K. Yanful.

TABLE OF CONTENTS

TITLE PAGE.....i

CERTIFICATION OF EXAMINATION.....ii

ABSTRACT.....iii

CO-AUTHORSHIP.....v

ACKNOWLEDGEMENTS.....vii

TABLE OF CONTENTS.....ix

LIST OF TABLES.....xiv

LIST OF FIGURES.....xvi

NOTATIONS.....xxii

CHAPTER 1: INTRODUCTION..... 1

1.1 GENERAL.....1

1.2 OBJECTIVES5

1.3 ORIGINALITY AND CONTRIBUTION OF THE THESIS6

1.4 THESIS ORGANIZATION.....8

1.5 REFERENCES..... 12

CHAPTER 2: LITERATURE REVIEW 14

2.1 ENVIRONMENTAL GEOCHEMISTRY OF MINE TAILINGS..... 14

2.2 TAILINGS MANAGEMENT/STORAGE FACILITY 18

2.3 WATER COVER TECHNOLOGY 22

2.4 DESIGN APPROACH OF SHALLOW WATER COVER 27

2.4.1	<i>Estimation of Bed Shear Stress</i>	28
2.4.2	<i>Erosion Characteristics</i>	38
2.5	MOTIVATION FOR THE PRESENT RESEARCH	46
2.6	REFERENCES	49

CHAPTER 3: WATER COVER TECHNOLOGY FOR REACTIVE TAILINGS MANAGEMENT: A CASE STUDY OF FIELD MEASUREMENT AND MODEL PREDICTIONS..... 60

3.1	INTRODUCTION	60
3.2	THE STUDY SITE	64
3.3	METHODS AND MATERIALS	65
3.3.1	<i>Weather Station</i>	65
3.3.2	<i>Measurement of Resuspension</i>	67
3.3.3	<i>Characteristics of Bed Tailings</i>	72
3.3.4	<i>A New Approach to Predicting Resuspension</i>	72
3.3.5	<i>Critical Shear Stress</i>	80
3.4	RESULTS AND DISCUSSION	82
3.4.1	<i>Wind Data Analysis</i>	82
3.4.2	<i>Evaporation and Precipitation</i>	83
3.4.3	<i>Water Cover Depth to Eliminate Resuspension</i>	86
3.4.4	<i>Resuspension Measured with Sediment Traps</i>	90
3.4.5	<i>Mineralogical and Elemental Analysis of Suspended and Bed Material</i>	93
3.4.6	<i>Resuspension Data from OBS Sensors</i>	98
3.4.7	<i>Predicted and Measured Resuspension</i>	107
3.5	CONCLUSIONS	113
3.6	REFERENCES	116

CHAPTER 4: A SEMI-EMPIRICAL APPROACH FOR ESTIMATION OF BED SHEAR STRESS IN A TAILINGS POND	121
4.1 INTRODUCTION.....	121
4.1 STUDY SITE	125
4.2 METHODS AND MATERIALS.....	125
4.2.1 <i>The Acoustic Doppler Current Profiler (ADCP) Data Collection</i>	125
4.2.2 <i>Estimation of Bed Shear Stress</i>	128
4.3 RESULTS AND DISCUSSION.....	131
4.3.1 <i>ADCP Measured Flow</i>	131
4.3.2 <i>The Bed Shear Stress</i>	137
4.3.3 <i>Sources of Error</i>	146
4.4 CONCLUSIONS	148
4.5 REFERENCES.....	149
CHAPTER 5: ESTIMATING THE EROSION CHARACTERISTICS OF TAILINGS USING FIELD RESUSPENSION DATA.....	152
5.1 INTRODUCTION.....	152
5.2 STUDY SITE	156
5.3 METHODS AND MATERIALS.....	158
5.4 DATA COLLECTION.....	162
5.5 DATA ANALYSIS.....	167
5.6 RESULTS AND DISCUSSION.....	168
5.7 CONCLUSIONS	173
5.8 REFERENCES.....	175

CHAPTER 6: AN IMPROVED MODEL FOR THE DESIGN OF WATER COVER FOR REACTIVE MINE TAILINGS	178
6.1 INTRODUCTION.....	178
6.2 METHODS AND MATERIALS.....	182
6.2.1 <i>The Total Bed Shear Stress</i>	182
6.2.2 <i>Prediction of Currents</i>	183
6.2.3 <i>Erosion Characteristics of Bed Material</i>	186
6.3 RESULTS AND DISCUSSION.....	186
6.3.1 <i>Results from Existing Samad and Yanful (2005) Model</i>	186
6.3.2 <i>Comparison of Model Predicted and Field Measured Currents</i>	189
6.3.3 <i>Wave-Current Interactions</i>	191
6.3.4 <i>Optimized Water Cover Depths</i>	205
6.4 CONCLUSIONS	207
6.5 REFERENCES.....	208
CHAPTER 7: CONCLUSIONS AND SCOPE FOR FUTURE WORK.....	211
7.1 CONCLUSIONS	211
7.2 APPLICATIONS.....	217
7.3 RECOMMENDATIONS FOR FUTURE WORK.....	217
7.4 REFERENCES.....	219
APPENDIX-I: CALIBRATION OF OBS SENSORS.....	220
APPENDIX-II: MINEROLOGY OF BED TAILINGS	229
APPENDIX-III: FIELD MEASURED CURRENT VELOCITY PROFILES.....	238

APPENDIX-IV: DERIVATION OF SIMPLIFIED EQUATION FOR TOTAL BED SHEAR STRESS.....	250
APPENDIX-V: MISCELLANEOUS PHOTOS OF SITE SHOWING DEPLOYMENT OF VARIOUS INSTRUMENTS.....	257
APPENDIX-VI: COPYRIGHT LICENSE FOR PUBLICATION OF CHAPTER 3.....	268
CURRUCULAR VITAE	274

LIST OF TABLES

TABLE	DESCRIPTION	PAGE
CHAPTER 2		
LITERATURE REVIEW		
2.1	Summary of various types of engineered cover options for reactive tailings management	20
CHAPTER 3		
WATER COVER TECHNOLOGY FOR REACTIVE TAILINGS MANAGEMENT: A CASE STUDY OF FIELD MEASUREMENT AND MODEL PREDICTIONS		
3.1	Some basic characteristic properties of bed tailings	74
3.2	On site recorded precipitation and calculated evaporation during different trips	85
3.3	Total suspended solids (TSS) collected in sediment traps and corresponding water cover depth	91
3.4	Total suspended solids (TSS) collected in sediment traps and corresponding water cover depth	96
3.5	Tailings Composition: Trace elements in $\mu\text{g/g}$ by ICP-AES (BT = Bed Tailings & ST = Suspended Tailings)	97
3.6	Concentration of selected elements in tailings compared to typical crustal composition (Fe is in weight % as oxide and other elements in $\mu\text{g/g}$)	98
CHAPTER 4		
A SEMI-EMPIRICAL APPROACH FOR ESTIMATION OF BED SHEAR STRESS IN A TAILINGS POND		
4.1	Comparison of log linear profile fitted with different number of measurement points at location 10	147

LIST OF TABLES

TABLE	DESCRIPTION	PAGE
CHAPTER 6	AN IMPROVED MODEL FOR THE DESIGN OF WATER COVER FOR REACTIVE MINE TAILINGS	
6.1	Input data and results of water cover depth predictions using the existing Samad and Yanful (2005) model	187
6.2	Comparison of field measured and model predicted bed shear velocities under similar wind conditions	190
6.3	Erosion characteristics derived from field measured resuspension data and model predicted water cover depth with and without wave-current interactions	193
6.4	Model predicted resuspended tailings concentrations after applying depth restrictions under conditions of with and without wave-current interactions	201
6.5	Optimized water cover depths for allowed maximum resuspended tailings concentrations of 15 mg/L	206

LIST OF FIGURES

FIGURE	DESCRIPTION	PAGE
CHAPTER 2		
LITERATURE REVIEW		
2.1	Effect of pH on release of metals (Aube and Zinck 2003)	16
2.2	Schematic diagram of tailings pond hydrodynamics in presence of winds (Yanful and Catalan 2002)	29
2.3	Comparison of wave heights predicted by SMB and CEM methods with measured data (Samad and Yanful 2005)	33
2.4	Shield's diagram: the relationship between dimensionless critical shear stress and shear velocity Reynolds number (Yang 1977)	41
CHAPTER 3		
WATER COVER TECHNOLOGY FOR REACTIVE TAILINGS MANAGEMENT: A CASE STUDY OF FIELD MEASUREMENT AND MODEL PREDICTIONS		
3.1	Map of Shebandowan Mine tailings storage facility showing the location of sediment traps (ST) and OBS sensors	66
3.2	Schematic diagram of sediment trap (Adu-Wusu et al. 2001)	68
3.3	Field calibration curves of OBS sensors for West and Middle cell tailings	71
3.4	Particle size distribution curve of bed tailings samples collected from location of each sediment trap	73
3.5	Wind direction frequency distribution plotted for summer (May to November) months of year 2006, 2007 and for long-term wind data	83

LIST OF FIGURES

FIGURE	DESCRIPTION	PAGE
CHAPTER 3	WATER COVER TECHNOLOGY FOR REACTIVE TAILINGS MANAGEMENT: A CASE STUDY OF FIELD MEASUREMENT AND MODEL PREDICTIONS	
3.6	Total precipitation and total average evaporation during each Trip	86
3.7	Shebandowan mine tailings pond boundary and location of square grids of 50 m interval for whole pond and west, middle and east cells	87
3.8	Contour plots of fetch length (in m) for whole pond (without wave breaks) and each cell (with wave breaks)	88
3.9	Contours of minimum required water cover depth to completely eliminate resuspension for whole pond and each cell	89
3.10	Total suspended solids collected in sediment traps versus depth of water cover	92
3.11	X-ray diffractograms of resuspended material collected at ST2 during Trip-1 and bed tailings at ST-2 and ST-5	94
3.12	Case I: Time series results of total suspended solids concentration (TSS) measured by OBS-1 and OBS-2 on July19 to 21, 2007 in the middle cell with corresponding wind data	100
3.13	Case II: Time series results of total suspended solids concentration (TSS) measured by OBS-1 and OBS-2 on July21 to 23, 2007 in the west cell with corresponding wind data	102

LIST OF FIGURES

FIGURE	DESCRIPTION	PAGE
CHAPTER 3		
WATER COVER TECHNOLOGY FOR REACTIVE TAILINGS MANAGEMENT: A CASE STUDY OF FIELD MEASUREMENT AND MODEL PREDICTIONS		
3.14	Case III: Time series results of total suspended solids concentration (TSS) measured by OBS-1 and OBS-2 on October 04, 2007 in the west cell with corresponding wind data	104
3.15	Case IV: Time series results of total suspended solids concentration (TSS) measured by OBS-1 and OBS-2 on October 09, 2007 in the west cell with corresponding wind data	106
3.16	Contours of total bed shear stress (Pa) and predicted resuspension concentration (mg/L) in the west cell after applying depth restriction of 0.9 m	108
3.17	Change in total bed shear stress (Pa) with increasing water cover depth (m)	110
3.18	Change in resuspended solids concentration (mg/L) with water cover depth	110
CHAPTER 4		
A SEMI-EMPIRICAL APPROACH FOR ESTIMATION OF BED SHEAR STRESS IN A TAILINGS POND		
4.1	The map of Shebandowan tailings storage facility, the Middle cell, and ADCP data collection locations in the Middle cell	126
4.2	Boat mounted Workhorse Rio Grande 1200 kHz ADCP with mounting assembly	127
4.3	Plot of wind data during ADCP data collection	132
4.4	Contour map of water cover depth or bathymetry of the middle cell	133

LIST OF FIGURES

FIGURE	DESCRIPTION	PAGE
CHAPTER 4		
A SEMI-EMPIRICAL APPROACH FOR ESTIMATION OF BED SHEAR STRESS IN A TAILINGS POND		
4.5	Three-dimensional visualization of current flow pattern with bathymetry in the Middle cell viewed from different angles (Note: Vector color represents velocity magnitude and pond color represents depths as shown in color scale legends for both)	134
4.6	Two-dimensional near bed currents flow circulation pattern	136
4.7	Contour map of estimated bed shear stress due to wind induced wave orbital velocities	138
4.8	Log linear current velocity profile for locations 10 and 14	140
4.9	Contour map of estimated bed shear stress due to wind induced circulatory current velocities	141
4.10	Contour map of estimated bed shear stress due to combined wave current interaction	143
4.11	Comparison of wind wave and current induced bed shear stresses	145
4.12	Log current velocity profile at location 10 with linear regression line fitted for three points and for full profile	147
CHAPTER 5		
ESTIMATING THE EROSION CHARACTERISTICS OF TAILINGS USING FIELD RESUSPENSION DATA		
5.1	Map of Shebandowan tailings storage facility showing the OBS data collection locations in the west and middle cells and location of weather station	157
5.2	OBS recorded suspended solids concentration (SSC) and corresponding wind data in the west cell of the tailings pond on July October 09-10, 2007	164

LIST OF FIGURES

FIGURE	DESCRIPTION	PAGE
CHAPTER 5 ESTIMATING THE EROSION CHARACTERISTICS OF TAILINGS USING FIELD RESUSPENSION DATA		
5.3	OBS recorded suspended solids concentration (SSC) and corresponding wind data in the middle cell of the tailings pond on July 25-27, 2008	166
5.4	Time series of total bed shear stress (in Pa) calculated from wind data corresponding to OBS data collected in (a) the west cell or Case-1 and (b) the middle cell or Case-2	169
5.5	Plot of calculated erosion rates versus total bed shear stress data to obtain critical shear stress values for the (a) west cell and (b) middle cell	170
5.6	Plot of logarithm of erosion rate versus logarithm of bed shear stress over the critical shear stress to obtain erosion rate parameters of the bed tailings in the (a) west cell and (b) middle cell	172
CHAPTER 6 AN IMPROVED MODEL FOR THE DESIGN OF WATER COVER FOR REACTIVE MINE TAILINGS		
6.1	Contour map of minimum required water cover depth without wave-current interaction in the each cell of tailings pond	194
6.2	Contour map of minimum required water cover depth with wave-current interaction in the each cell of tailings pond	195
6.3	Contour map of minimum required water cover depth without wave-current interaction in the whole pond in absence of wave breaks	196
6.4	Contour map of minimum required water cover depth with wave-current interaction in the whole pond in absence of wave breaks	197

LIST OF FIGURES

FIGURE	DESCRIPTION	PAGE
CHAPTER 6	AN IMPROVED MODEL FOR THE DESIGN OF WATER COVER FOR REACTIVE MINE TAILINGS	
6.5	Contour map of predicted resuspension without wave-current interaction for restricted depth of 1.0 m over the entire tailings pond area	199
6.6	Contour map of predicted resuspension with wave-current interaction for restricted depth of 1.0 m over the entire tailings pond area	200
6.7	Contour map of predicted resuspension without wave-current interaction for restricted depth of 2.0 m over the entire tailings pond area	203
6.8	Contour map of predicted resuspension with wave-current interaction for restricted depth of 2.0 m over the entire tailings pond area	204
6.9	Contour map of optimized water cover depths in the each cell with allowed resuspension of under 15 mg/L	206

NOTATIONS

Notation	Description	Unit
U	Wind speed measured at 10 m above the water surface	m/s
U_a	Wind stress factor ($= 0.71 * U^{1.23}$)	
u^*_a	Wind shear velocity	m/s
u^*_s	Surface shear velocity of water	m/s
u	Near bed velocity measured at elevation above the bed z	m/s
F	Fetch length or the distance of water surface over which wind blows	m
h	Water cover depth	m
H_s	Significant wave height	m
T_s	Significant wave period	s
L	Wave length	m
τ_b	Total bed shear stress	N/m^2 or Pa
τ_w	Bed shear stress due to wind induced waves	N/m^2 or Pa
τ_c	Bed shear stress due to circulation currents	N/m^2 or Pa
τ_s	Bed shear stress due to seiche motion	N/m^2 or Pa
τ_m	Mean shear stress	N/m^2 or Pa
τ_{cr}	Critical bed shear stress	N/m^2 or Pa
E	Erosion rate	$mg/m^2.s$
α	Coefficient of erosion rate equation	
M	Exponent of erosion rate equation	

Notation	Description	Unit
D	Sediment Particle diameter	m
D ₅₀	Particle size (50% finer than)	mm
ν	Kinematic viscosity of water	m ² /s
ρ_s	Density of sediments	kg/m ³
ρ_w	Density of water	kg/m ³
γ_w	Specific weight of water	N/m ³
γ_s	Unit weight of sediment	N/m ³
γ_{bo}	Unit weight of consolidated sediment	N/m ³
γ_b	Unit weight of sediment on the bed	N/m ³
g	Gravitational acceleration	m/s ²
k	Constant = 2.9x10 ⁻⁴	N/m
ϕ	Angle of repose or friction angle	Degrees
G _s	Specific gravity of sediments	
c	Cohesion	N/m ² or Pa
u _{bm}	Maximum horizontal bottom velocity in shallow water	m/s
a _m	Maximum displacement of fluid particles corresponding to maximum bottom velocity	m
f _w	Wave friction factor	
R _w	Wave Reynold's number	
z _{sh}	Surface characteristic length	m
z _{bh}	Bottom characteristic length	m
λ	Constant depends on intensity of turbulence in water and varies 0.2 to 0.5	
C _{ssc}	Suspended solids concentration	mg/L

Notation	Description	Unit
E_0	Total evaporation	m
E_n	Net evaporation due to radiation	m
E_a	Mass transfer/aerodynamic evaporation	m
Δ	Rate of change in saturation vapor pressure with temperature	m
γ	Psychometric constant ($\cong 0.66 \text{ mb}^0\text{C}^{-1}$)	mb^0C^{-1}
e_s	Saturation vapor pressure of air	mb
e_a	Vapor pressure of air	mb
f_{rh}	Relative humidity	%
Q_n	Net radiation	cal/cm ² .day or W/m ²
L_v	Latent heat of vaporization	cal/g
u_{*cw}	Combined wave-current bed shear velocity	m/s
u_{*c}	Current bed shear velocity	m/s
u_{*w}	Wave bed shear velocity	m/s
θ_c	Angle between wave and current at any location	Degrees
κ	Von Karman's constant (~ 0.40)	
z_0	Bed roughness length	m
z	Elevation above the bed	m
OBS	Optical backscatter sensor	
ST	Suspended tailings sample	
BT	Bed tailings sample	
ADCP	Acoustic Doppler current profiler	
SSC	Suspended solids concentration	mg/L

CHAPTER 1: INTRODUCTION

1.1 GENERAL

Metal mines typically can be classified into three main categories as (1) ferrous, (2) precious, and (3) base metals, depending on the importance of the end products after exploration of metals.

1. Ferrous-metal mines produce primarily iron and metals such as niobium and tantalum that are alloyed with steel.
2. Precious-metal mines produce primarily gold, silver, palladium, and uranium.
3. Base-metal mines include all the remaining metallic commodities, the most important being nickel, copper, zinc, lead, molybdenum, magnesium and cobalt.

In Canada metal mining is associated with the largest and the oldest geological formation known as the Canadian Shield, which represents about half of the land area in Canada. The Canadian Shield is composed of igneous, sedimentary and metamorphosed rocks. According to Natural Resources Canada (2009), the Canadian Shield extends from the eastern Northwest Territories and southern Nunavut, through north-eastern Alberta, northern Saskatchewan and Manitoba, western and central Ontario, most of Quebec north of the St. Lawrence River, to Labrador and Baffin Island in the form of a great circle around Hudson's Bay. The majority of metal mines in Canada are in the Canadian Shield stretching southeast from the gold mines of Yellowknife, through Flin Flon, Red Lake,

Timmins, Sudbury, Rouyn-Noranda, Val d'Or and Chibougamau, to the iron mines of Labrador City. The remaining areas of metal mining are found within the mountains along the western and south-eastern coasts (Natural Resources Canada 2009).

Canada has reserves of major metals copper, nickel, lead, zinc, molybdenum, silver, and gold. Four provinces in Canada, Ontario, British Columbia, New Brunswick, and Quebec, were dominant in terms of probable mineable reserves of major metals during 2005 (Reed 2005). Ontario has the largest metal mining sector of all the provinces in Canada, and accounts for one-third of Canada's mineral production. Ontario's mining industry generates \$5-7 billion each year, primarily through exports. Nickel, gold and copper generate the greatest economic value among all the minerals mined in Ontario. Ontario had 55% of the nickel, 52% of the gold, and 40% of the copper, plus 24% of the silver, 21% of the zinc, and 5% of the lead in Canada. In almost the last 100 years Ontario has mined (Reed 2005):

- 166 million ounces of gold
- 1 billion ounces of silver
- 10.8 million tons of nickel
- 13.8 million tons of copper
- 10.2 million tons of zinc

In Ontario alone, over 6,000 inactive or abandoned exploration or mining sites exist. Metal mines produce two common types of solid waste (1) waste rock and (2) tailings. A single mine, in general, produces tens of millions of tonnes of solid waste during its life span. Modern mines process huge quantities of ore, on the order of tens of

thousands to hundreds of thousands of tonnes a day. A rough estimate is that Canadian mines produce about two tonnes of solid waste every day containing toxic metals, which is the largest amount of waste production among all industrial wastes (Mining Watch Canada 2009; Environmental Mining Council of BC 2010). Once blasted and hauled from the mine shaft or pit, ore is crushed and processed using massive volumes of water and a variety of chemical and physical processes. The mineral content of an ore can be in the 5 % range for base metals or as low as 0.00005% for precious metals like gold. This means that 95% to 99.9995% of the mined and processed ore becomes a waste product known as tailings (Mining Watch Canada 2009). For example, in Canada, the average grades of mined copper are under 1 %, meaning that for every tonne of copper extracted, 99 tonnes of waste material (waste rock and tailings) is generated (Environmental Mining Council of BC 2010).

In nature, most metals are found in the form of their sulphide minerals such as pyrite (FeS_2), galena (PbS), sphalerite (ZnS), covellite (CuS) and many others. Mine tailings is the waste left behind after processing and extraction of valuable metals from the ore. In general, tailings are composed of residual metal minerals, sulphur, and other processing chemicals. These sulphide rich mine tailings are highly reactive with the environment. On exposure to environmental oxygen and moisture, sulphide minerals oxidize and generate sulphuric acid and release toxic metals to the environment. This problem is commonly known as acid rock drainage (ARD) or acid mine drainage (AMD) when the oxidation and resulting drainage are associated with either an open pit mine or underground mine. Toxic pollutants that are commonly found in mine tailings include: cyanide (Cn), mercury (Hg), copper (Cu), lead (Pb), arsenic (As), cadmium (Cd),

selenium (Se), zinc (Zn) and nickel (Ni) (Ljungberg and Ohlander 2001; Armienta et al. 2003; Da Silva et al. 2005). If left unconfined and exposed to the environment, these heavy metals can leach out into surface and ground water systems causing serious pollution problems for generations. In Canada, there are an estimated 351 million tonnes of waste rock and 510 million tonnes of sulphide tailings which have the potential to produce acidic drainage. Cleanup of existing acid-generating mines in Canada will cost between \$ 2 to 5 billion (Environmental Mining Council of BC 2010).

Water cover technology is one of the most promising methods available for storing mine tailings in the long-term with minimal environmental impact. In this method, oxidation of tailings is eliminated or minimized by submerging them under a confined water cover of lower solubility and diffusivity of oxygen in comparison to those of air. However, wind induced resuspension of the bed tailings poses a major threat to the effectiveness of the method. A number of previous studies have demonstrated the occurrence of wind induced resuspension and subsequent oxidation of mine tailings under shallow water covers, which underscores the inadequacy of traditionally designed water cover depths to eliminate resuspension (Adu-Wusu et al. 2001; Yanful and Catalan 2002; Mian and Yanful 2003; Mian and Yanful 2004). These studies have also shown that water cover depth plays an important role in controlling wind-induced resuspension of already submerged tailings, which could otherwise still potentially oxidize due to near saturation levels of dissolved oxygen in the water during turbulence (Li et al. 1997; Samad and Yanful 2005).

A resuspension model, such as the one developed by Samad and Yanful (2005), can prove to be an important tool in either designing a new tailings storage facility or managing an existing one. The lack of field representative data on return currents, critical shear stress and erosion rate parameters can limit the use of such models. Apart from this, the role of return currents in resuspension is not clear from the available studies in literature and needs to be further investigated. In most published studies, the wind induced circulation currents were determined using theoretical and empirical relations such as those developed by Wu and Tsanis (1995). These theoretical models were developed under laboratory conditions and have not been verified for field conditions, especially for small closed water bodies such as tailings ponds.

The work presented in this thesis is the result of extensive field work carried out to study the wind-induced resuspension of tailings stored under shallow water cover in an existing tailings storage facility. The field data were used to address some of the unresolved issues of water cover technology pointed out in the prior work by many researchers and, also, to develop a new methodology to estimate the erosion characteristics of bed tailings. As a major outcome of this research, the thesis was able to improve an existing water cover design model developed by Samad and Yanful (2005).

1.2 OBJECTIVES

The research presented in this thesis was undertaken to address issues associated with the functioning of water covers over reactive mine tailings. The main objectives of the study were to:

1. Evaluate the performance of the Shebandowan tailings storage facility, which is divided into three cells by means of two internal wave breaks (dykes), under its existing conditions. This included the effect of the two wave breaks and their locations on the overall resuspension management of the facility.
2. Compare field measured resuspension results with predictions from the Samad and Yanful (2005) model.
3. Measure field circulation currents and study their effect on total bed shear stress.
4. Compare field measured currents with those predicted from counter-current model such as Wu and Tsanis (1995) under similar wind conditions.
5. Develop a simple design method to calculate total bed shear stress in shallow water conditions.
6. Develop a new methodology to calculate critical shear stress and erosion parameters of bed material using field measured resuspension results.
7. Develop an improved resuspension model to design and optimize the water cover depth over mine tailings.

1.3 ORIGINALITY AND CONTRIBUTION OF THE THESIS

The research work presented in this thesis involved extensive field data collection, laboratory experiments, and theoretical data analysis. The field data collection include measurements of accumulated suspended sediments with sediment traps deployed over certain time periods, optical backscatter (OBS) measurements of real time resuspended solids concentrations in water, and real-time measurements of wind-induced circulation

currents in the water columns with the help of an acoustic Doppler current profiler (ADCP). Continuous weather data, which included wind speed and direction, were also collected. The results provided both quantitative and qualitative understanding of the process of tailings resuspension and the parameters on which it depends. The outcomes of the study were used in improving the methodologies of resuspension prediction in tailings ponds and in designing optimized water cover depths over tailings.

1. The combination of sediment traps, optical backscatter (OBS) and computer modelling results helped to understand resuspension under conditions existing in the tailings pond. The geochemical analysis of suspended and bed tailings showed that the material collected in the sediment traps were resuspended bed tailings.
2. The effect of two wave-breaks and their locations in the tailings pond was studied with the help of the resuspension model. None of the published work to date has dealt with an assessment of resuspension in a tailings pond subdivided into cells by wave breaks. The wave breaks or internal dykes are generally installed in tailings ponds to decrease the fetch (distance over which wind blows) and eliminate or reduce resuspension to insignificant levels.
3. The thesis provides measurements of wind-induced circulation currents in a tailings pond with the help of an acoustic Doppler current profiler (ADCP). This was the first study, where actual circulation currents were measured in a tailings pond. In most previous resuspension studies, currents were determined using empirical relations.
4. The field measurement and quantitative analysis of circulation currents showed that wave-current interaction may enhance the total bed shear stress and should be

considered in the analysis. Previous studies conducted on tailings ponds ignored this important part.

5. A simplified equation was derived to estimate the wind-induced total bed shear stress in tailings ponds under shallow water cover conditions using wind speed, fetch length and water depth data. This equation reduces the lengthy process of bed shear stress estimation from a single equation, which also incorporates the wave-current interaction term.
6. A new graphical method has been developed for the estimation of erosion characteristics of the bed tailings. The optical backscatter data collection of suspended solids concentrations along with wind data were used to estimate the critical shear stress and erosion rate parameters using actual field measured resuspension. These estimated values are probably more reliable than those obtained from laboratory experiments conducted on disturbed bed tailings and under simulated conditions.
7. The outcomes of the research resulted in an improved model to design water covers over reactive mine tailings, reliable prediction of resuspension under given conditions, and optimization of water cover depth for known regulatory limit of suspended solids concentration in water.

1.4 THESIS ORGANIZATION

The thesis is written in an integrated-article format, with each of the articles in individual chapters containing separate introduction, tables, figures, results and discussion, and

references. There are seven major chapters in the thesis including chapters on Introduction, Literature Review, and Conclusions and Recommendations. Some additional relevant information is presented in appendices at the end of thesis. The organization of thesis is as follows:

Chapter 1: This chapter provides background information on the metal mine tailings origin and management issues, water cover technology and problem of wind induced resuspension. This chapter also defines the objectives undertaken for this research.

Chapter 2: This chapter provides detailed literature review of metal mine tailings managements using water cover technology. The review of published work on geochemistry of mine tailings, management techniques, water cover technology, wind-induced resuspension, and water cover design modelling have been provided to improve understanding of unresolved issues associated with water cover technology and hence delineate the motivation for the research.

Chapter 3: The chapter presents field measured results of wind induced resuspension at the Shebandowan tailings pond, ON, Canada. Resuspension was measured by means of eight sediment traps and two optical backscatter sensors (OBS). Sediment traps collected the suspended material over a certain period during four sampling campaigns, while OBS sensors recorded real time suspended solids concentration in the water. The Samad and Yanful (2005) model was applied to study the effect of internal wave breaks on the minimum required water cover depths. Field measured and model predicted results were compared and found to be in good agreement.

Chapter 4: This chapter shows the measurement of current circulation patterns recorded using an Acoustic Doppler Current Profiler, or ADCP. In this chapter a semi-empirical approach was developed to calculate the total bed shear stress. This approach involved the use of empirical wind wave hindcasting formulas, the well-known Log Law and wave-current interaction. ADCP provided measured currents and their directions at different locations in the tailings pond which make it possible to incorporate the wave-current interaction term in the model. The result showed that wave-current interaction may enhance the total bed shear stress.

Chapter 5: In this chapter a new method of estimation of critical shear stress and erosion rate parameters of bed material is discussed. In the method, in-situ recorded wind data and real time resuspension recorded by OBS were used to graphically obtain characteristic parameters of bed sediments. The results obtained using this method were more representative than those obtained by empirical equations or laboratory experiments. Also, a new equation was derived to simplify the estimation of total bed shear stress under shallow water conditions by using wind speed, fetch length, and water cover depth data.

Chapter 6: This chapter provides the results of an improved model to design water covers over reactive mine tailings. The work and approach discussed in chapters 4 and 5, was incorporated into the existing model (Samad and Yanful 2005). Results obtained from the existing model and improved model were also provided. The results obtained from the improved model were found to be more reliable to apply in the field.

Chapter 7: Finally, this chapter summarizes the major outcomes and conclusions of the thesis and also highlights recommendations for future work.

Appendices: The thesis includes five appendices. Appendix-I provides detailed laboratory calibration procedure of two OBS sensors for field bed tailings. In Appendix-II, X-ray diffractograms of suspended tailings samples collected in eight sediment traps and corresponding bed tailings samples have been provided as discussed in Chapter 3. Appendix-III provides current velocity profiles measured in the middle cell using an ADCP used in Chapter 4. Appendix-IV provides the derivation of the simplified equation for bed shear stress estimation under shallow water conditions. Appendix-V contains photos of instrumentation deployed in the field. The copyright license obtained for the publication of Chapter 3 has been provided in Appendix-VI.

1.5 REFERENCES

1. Adu-Wusu, C., Yanful, E.K., Mian, M.H., et al. (2001). Field evidence of resuspension in a mine tailings pond. *Canadian Geotechnical Journal*, 38(4): 796-808.
2. Armienta, M.A., Talavera, O., Morton, O., & Barrera, M. (2003). Geochemistry of metals from mine tailings in Taxco, Mexico. *Bulletin of Environmental Contamination and Toxicology*, 71: 387-393.
3. Da Silva, E.F., Fonseca, E.C., Matos, J.X., Patinha, C., Reis, P., & Oliveira, J.M.S. (2005). The effect of unconfined mine tailings on the geochemistry of soils, sediments and surface waters of the Lousal area (Iberian Pyrite Belt, Southern Portugal). *Land Degradation and Development* 16: 213-228.
4. Environmental Mining Council of BC (2010). Acid mine drainage, mining and water pollution issues in BC. Victoria, BC, Canada.
5. Li, M.G., Aube, B., & St-Arnaud, L. (1997). Considerations in the use of shallow water covers for decommissioning reactive tailings. *Proceedings 4th International Conference on Acid Rock Drainage, Vancouver, B.C.*, 1: 115-130.
6. Ljungberg, J., & Ohlander, B. (2001). The Geochemical dynamics of oxidising mine tailings at Laver, northern Sweden. *Journal of Geochemical Exploration* 74: 57-72.
7. Mian, M.H., & Yanful, E.K. (2003). Tailings erosion and resuspension in two mine tailings ponds due to wind waves. *Advances in Environmental Research*, 7: 745-765.

8. Mian, M.H., & Yanful, E.K. (2004). Optical backscatter measurements of tailings resuspension in a mine tailings pond. Proceedings 57th Canadian Geotechnical Conference, Session 7D: 38-45.
9. Mining Watch Canada (2009). Two million tonnes a day, a mine waste primer. Mining Watch Canada, Ottawa, ON, Canada, December 2009.
www.miningwatch.ca
10. Natural Resources Canada (2009). The atlas of Canada-metal mining. Natural Resources Canada, Accessed December 25, 2010.
http://atlas.nrcan.gc.ca/auth/english/maps/economic/mining/metal_mines/1
11. Reed, A. (2005). Canadian reserves of selected major metals and recent production decisions. Canadian Minerals Yearbook, 2005, Natural Resources Canada.
12. Samad, M. A., & Yanful, E.K. (2005). A design approach for selecting the optimum water cover depth for subaqueous disposal of sulfide mine tailings. Canadian Geotechnical Journal, 42, 207-228.
13. Yanful, E.K., & Catalan, L.J.J. (2002). Predicted and field measured resuspension of flooded mine tailings. Journal of Environmental Engineering, ASCE, 128(4): 341-251.
14. Wu, J., & Tsanis, I.K. (1995). Numerical study of wind induced water currents. Journal of Hydraulic Engineering, ASCE, 121(5): 388-395.

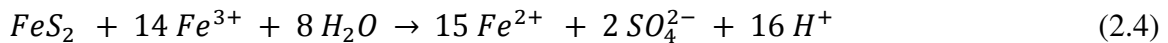
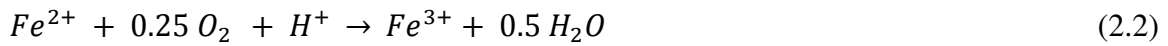
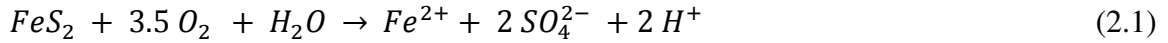
CHAPTER 2: LITERATURE REVIEW

2.1 ENVIRONMENTAL GEOCHEMISTRY OF MINE TAILINGS

In nature, most base metals are found in the form of their sulphide minerals. The mineralogy of ores is different for different mining locations but is commonly composed of sulphide minerals such as pyrite (FeS_2), chalcopyrite (CuFeS_2), galena (PbS), sphalerite (ZnS), pyrrhotite (FeS), marcasite (FeS_2), bournonite (CuPbSbS_2), tetrahedrite ($\text{Cu}_{12}\text{Sb}_4\text{S}_{13}$), arsenopyrite (FeAsS), cobaltite (CoAsS), and argentite (Ag_2S) (Ljungberg and Ohlander 2001; Armienta et al. 2003; Da Silva et al. 2005).

It is well known that acid mine drainage (AMD) originates from the oxidation of the above mentioned sulphide minerals which tend to be abundant in mining residues known as mine tailings (Ritcey 1989; Salomons 1995; Environment Canada 2009; Mining Watch Canada 2009). In general, mine tailings contain residual metal minerals and sulphur which are left behind after extraction of valuable metals up to the extent of economic feasibility. Sulphide rich mine tailings, especially iron bearing sulphides, are highly reactive and if exposed to environmental oxygen and moisture, will oxidize generating sulphuric acid and releasing toxic metals to the environment. This problem is commonly known as acid rock drainage (ARD) or acid mine drainage (AMD) when the oxidation and resulting drainage are associated with either an open pit mine or underground mine (Ritcey 1989; Salomons 1995; Environment Canada 2009; Mining Watch Canada 2009).

The process of sulphide mineral oxidation is quite complex, but may be represented by a series of simplified reactions involving pyrite (FeS_2) oxidation in the presence of two common bacteria *Acidithiobacillus ferrooxidans*, and *Acidithiobacillus thiooxidans* as below (Evangelou 1995; Bennett 2002).



In these pyrite oxidation reactions ferrous ion oxidizes to ferric ion. *Acidithiobacillus ferrooxidans* and *Acidithiobacillus thiooxidans* bacteria, which are available naturally, do not directly take part in the chemical reactions but act as a catalyst. From these chemical reactions, it is evident that pyrite oxidation occurs in the presence of oxygen and moisture and releases the free iron metal (Fe^{2+}) and acid (H^+) in the environment. Both of these end products are potentially responsible for environmental degradation. Acidity lowers the pH of the water and accelerates the mobility of other toxic metal ions such as: arsenic (As), cadmium (Cd), chromium (Cr), cobalt (Co), copper (Cu), cyanide (Cn), lead (Pb), manganese (Mn), mercury (Hg), nickel (Ni), selenium (Se), and zinc (Zn). Aube and Zinck (2003) showed the effect of pH on the mobility of metals by metal hydrolysis (Figure 2.1). It can be noted that the concentration

of metals in solution increases with increasing acidity or decreasing pH and at higher pH values most metals precipitate in their hydroxide forms.

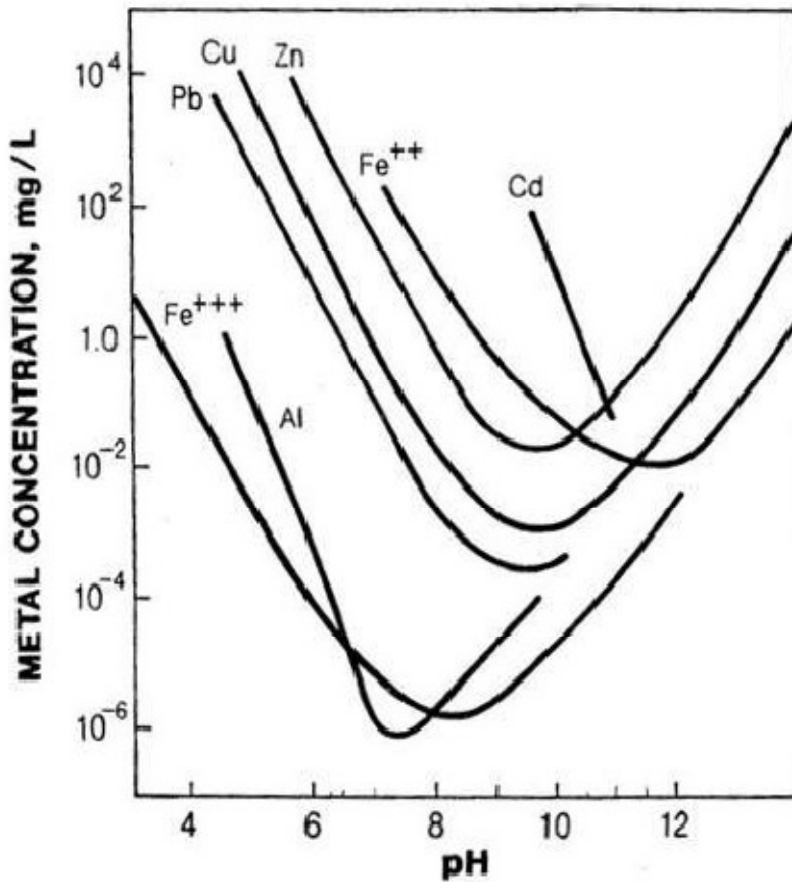


Figure 2.1 Effect of pH on release of metals (Aube and Zinck 2003)

Oxidation of reactive mine tailings can adversely affect the environment. In environmental risk assessment studies involving mine tailings, the effect on the following key environmental factors must be included (Environment Canada 2009):

1. Ground water

2. Surface water
3. Air quality
4. Vegetation
5. Livestock (wildlife and aquatic life)

In an acidic environment, toxic pollutants that are commonly found in tailings include: arsenic (As), cadmium (Cd), chromium (Cr), cobalt (Co), copper (Cu), cyanide (Cn), lead (Pb), manganese (Mn), mercury (Hg), nickel (Ni), selenium (Se), and zinc (Zn). Ljungberg and Ohlander (2001) studied the geochemistry of oxidising mine tailings from Laver, northern Sweden. Based on the analysis of 60 tailings samples, these authors predicted that the tailings deposits can be divided into three zones (i) a top most zone which was highly oxidized, (ii) the oxidation front where oxidation was occurring, and (iii) the bottom non-oxidized zone. The oxidation front was estimated to be moving downward at 2.8 cm/year and was predicted to reach the groundwater within 15-30 years. In another study, Da Silva et al. (2005) studied the effect of unconfined metal mine tailings on the soils and surface water systems of Lousal village on the southwest limb of the Lousal anticline, Portugal, located at the former Lousal Mine, which closed in 1988. Da Silva et al. (2005) found significantly high amounts of toxic metals As, Cu, Hg, Pb, and Zn from soil samples collected from the surrounding mine area. Waters affected by acid mine drainage had pH ranging from 1.9 to 2.9. Sulphate (SO_4^{2-}) concentration, ranged from 9249 to 20700 mg/L. The stream water mixed with acid mine drainage effluents was found carrying higher SO_4^{2-} , Fe, Al, As, Cu, Pb, Zn, and Cd than the Fresh Water Aquatic Life Acute Criteria.

Changul et al. (2009) characterised the geochemistry of tailings generated at the Akara Gold Mine, Thailand. The most toxic metals found were Co, Cu, Cd, Cr, Pb, Mn, Ni and Zn analysed on the basis of the United States Environmental Protection Agency (EPA 3052) guidelines. Acid-base counting and net acid generation tests showed that the tailings samples contain abundant sulphur and were therefore, potentially acid generating. The results of leaching experiments showed that leachates of low pH had heavy metals concentrations that were higher than the regional standards.

The above studies showed the risk of potential environmental hazards if reactive mine tailings are left exposed to the environment without an effective management plan. A proper disposal plan may include a physical barrier of any material that can stop or minimize oxygen influx to tailings also remain environmentally stable in the long term. There are several types of barriers such as water cover, earthen cover, vegetation cover, and geo-synthetic cover. In the next section a brief review of each of these barrier technologies is provided.

2.2 TAILINGS MANAGEMENT/STORAGE FACILITY

To stop or minimize the oxidation of sulphide minerals present in tailings, a properly planned disposal and management strategy is required. An effective tailings management plan must minimize the impact on each of five already mentioned environmental factors (section 2.1). A good management technique must include (O`Kane and Wels 2003):

1. Dust control

2. Erosion control
3. Chemical stabilisation of acid-forming mine waste (through control of oxygen ingress)
4. Contaminant release control (through control of infiltration)
5. Provision of a growth medium for the establishment of sustainable vegetation

There are several techniques available that have been studied and implemented successfully in the field as well. The most common techniques involve application of different kinds of engineered cover materials to eliminate or minimize oxygen influx into tailings. Some of the most effective covers include earthen or soil cover, vegetation cover, synthetic cover and water cover. In a long term disposal plan each of these covers have inherent advantages and disadvantages as briefly summarized in the Table 2.1.

Field implementation of the above mentioned cover technologies depends on many factors such as site conditions, climate conditions, tailings composition, resources availability, regional laws and regulations, and economic feasibility. A site specific assessment is needed before selecting one or combinations of these cover techniques. The Department of Fisheries and Oceans Canada, Environment Canada, and Natural Resources Canada work together to conduct a thorough analysis of tailings management options provided by the developer (Environment Canada 2009).

In this thesis, the focus is on water cover technology. Relative to other methods, water cover technology is one of the most economical approaches in tailings management in Canada where natural water resources are readily available. Water covers have been extensively studied and applied in many parts of Canada, Scandinavian countries, United

Table 2.1 Summary of various types of engineered cover options for reactive tailings management

Type of Cover	Approach	Advantages	Disadvantages or Issues	Major Example Site
Earthen or Soil Cover	Single or multi layered compacted soil cover of low hydraulic conductivity	<ol style="list-style-type: none"> 1. Long term stability 2. Variety of materials selection 	<ol style="list-style-type: none"> 1. High cost 2. Erosion 3. Requires large area on land 	Kam Kotia Mine Site, north-eastern Ontario, Canada (Herlin 2007)
Vegetation Cover	Vegetation type depends on composition of tailings	<ol style="list-style-type: none"> 1. Acid neutralization 2. Segregation of tailings 3. Erosion prevention 4. Aesthetically good 	<ol style="list-style-type: none"> 1. Extensive pre-assessment of climate conditions, physical, chemical and microbial properties needed 	Ekati Diamond Mine, Yellowknife, NWT, Canada (Reid and Naeth 2005)

Synthetic Cover	Cover of engineered geosynthetic material eg. Geosynthetic Clay Liner (GCL), Geomembrane (GM)	<ol style="list-style-type: none"> 1. Light weight 2. Easy to install 3. Very low hydraulic conductivity 	<ol style="list-style-type: none"> 1. Long term durability 2. Fragile 3. Should cover large area 4. Construction and maintenance cost 	Premier Gold Project, Stewart, BC, Canada (Renken et al. 2005)
Water Cover	Tailings deposited under a shallow water cover contained by perimeter dams, which has low diffusivity and solubility of oxygen	<ol style="list-style-type: none"> 1. Aesthetically good 2. No dust and erosion 3. Easy to manage by maintaining a designed water cover depth 	<ol style="list-style-type: none"> 1. Strong wind induced resuspension 2. Dam stability 3. Seepage 	Shebandowan Mine, Thunder Bay, ON, Canada (Kachhwal et al. 2010)

States and many other parts of the world. In Canada, at present, there are several existing mining sites where water cover technology has been used for long term storage of both oil sands and metal mine tailings. Some of existing tailings ponds designed to store metal mine tailings in Canada are listed below:

1. Heath Steel Upper and Lower Cells, New Brunswick, Canada
2. Louvicourt Tailings Area, Val d'Or, Quebec, Canada
3. Whistle Mine, Sudbury, Ontario, Canada
4. Quirke Waste Management Area, Elliot Lake, Ontario, Canada
5. Falconbridge Mine Tailings Pond, Sudbury, Ontario, Canada
6. Shebandowan Tailings Storage Facility, Thunder Bay, Ontario, Canada

2.3 WATER COVER TECHNOLOGY

The placement of tailings under a cover of water has been shown to be an effective method of minimizing acid generation and metal release from reactive tailings. The effectiveness of water cover technology is based on the fact that oxygen has lower solubility and diffusivity in water (8.6 g/m^3 and $2 \times 10^{-9} \text{ m}^2/\text{s}$ at 25°C , respectively), than in air (285 g/m^3 and $1.78 \times 10^{-5} \text{ m}^2/\text{s}$ at 25°C). These parameters mean that the influx of oxygen to the tailings is low; hence oxidation is significantly reduced (Dave et al. 1997; Simms et al. 2001; Adu-Wusu et al. 2001). A water cover also eliminates wind erosion and dust from potentially toxic tailings and, in the long term, provides an anoxic or

reducing environment for sulphate reduction and generation of alkalinity for the precipitation of metals (Yanful and Catalan 2002).

Vigneault et al. (2001) applied a water cover of 0.3 m in experimental field cells (size 21 x 21 x 3 m deep) over fresh sulphide rich tailings and monitored the interstitial water chemistry over a period of two years. The results of the study showed that a water cover of 0.3 m was effective in reducing the rate of tailings oxidation, but evidence of progressive oxidation of tailings was found. The penetrations of the oxidation front was found to be less than 7 mm. The results also showed mobilization of toxic metals, such as cadmium (Cd), Copper (Cu), and Zinc (Zn). In that study, wind-induced turbulence was not considered. The main conclusion from the study was that a water cover of 0.3 m was sufficient to slow down the rate of tailings oxidation, but did not completely stop the oxidation reaction.

A major challenge with implementing a water cover over tailings is the presence of strong winds which can induce waves and currents in the water. The waves and currents can disturb the tailings and resuspend them. Lick (1982) found that large variations in suspended solids concentrations in the western basin of Lake Erie were directly related to high bottom shear stresses caused by wind induced wave action. Halfman and Scholz (1993) studied suspended sediment concentrations in water-column profiles in Lake Malawi using a light transmissometer and found that wind induced waves and currents were one of the potential causes of sediment resuspension in Lake Malawi. The total suspended solids concentrations were reported between 0.1 and 0.5

mg/L. Similarly, Jin and Wang (1998) predicted that wind induced waves were the main reason for sediment resuspension in Lake Okeechobee.

In a tailings pond, wind waves deliver energy to the water cover to generate currents which, along with the waves, can initiate sediment motion. Wind induced turbulence in the water also keeps the dissolved oxygen concentration at saturation level (Li et al. 1997; Samad and Yanful 2005). Strong winds sustained over a long period can cause resuspension of tailings in water that contains dissolved oxygen, and result in a greater potential for tailings to oxidize and impact the water quality in the pond and at the outlet. Wind induced resuspension alters both the surface water quality and geochemistry of bed tailings.

Yanful and Verma (1999) studied the oxidation of resuspended pyrrhotite mine tailings flooded under a shallow water cover (0.8 m) in laboratory column experiments. Resuspension of tailings was generated by a paddle rotated at prescribed speeds in the water. The water quality was monitored continuously for 126 days. The results showed that pH and DO (dissolved oxygen) of stirred water were relatively lower than those of static water covers. The sulphate production was increased by about 26-64 times, while the release of metals such as zinc, copper, and nickel was 1020, 318 and 138 times greater, respectively. Tailings oxidation and metal release increased with increasing stirrer speed and decreasing water depth. Similar results for tailings oxidation were obtained by Gautam et al. (2000) in a laboratory wave tank (4.5 x 1.5 x 1 m size) study, where imposed waves were specially designed to allow simulation of field measured wave height: water depth ratios. However, the oxidation rate of mine tailings exposed to

the environment depends on the geochemistry and mineralogy of the tailings, a detailed discussion of which is outside the scope of the present thesis.

Environment Canada specifies the environmental code of practice for metal mine tailings stored under water cover, which addresses the following key aspects of tailings management (Environment Canada 2009):

1. Dam stability
2. Changes in tailings geochemistry
3. Effects of seepage past the dam and from the base of the facility
4. Surface water management and discharge
5. Dust generation
6. Access and security
7. Wildlife entrapment
8. Special considerations for some types of mines such as uranium mines

A deep water cover is generally favourable to prevent wind induced turbulence from reaching otherwise stable bed material. A deep water cover can be implemented by placing the tailings in existing natural lakes and water bodies or artificial impoundments by constructing perimeter dams. Engineered deep water covers require large land areas and high perimeter dams, which increase construction costs and raise dam stability concerns. Natural lakes can provide a long-term, stable environment for storing mining waste. They have a lower risk of failure than engineered or artificial impoundment areas.

Department of Fisheries and Oceans Canada and Environment Canada requires that mine tailings are managed in natural water bodies in accordance with the Metal Mining Effluent Regulations (MMER 2002), under section 36 of the Fisheries Act with no net loss of natural habitats. The act requires that any mining company planning to use a natural water body for tailings storage should compensate for the lost habitat under the monitoring of Department of Fisheries and Oceans Canada (Environment Canada 2003). However, under new regulations it is almost impossible to obtain approval to use natural water bodies, such as lakes and ponds, to store the tailings.

An alternate to deep water covers by constructing artificial impoundments is to store tailings under engineered shallow water covers. An engineered shallow water cover has relatively low implementation cost and improved dam stability. It is generally implemented by maintaining a certain water cover depth sufficient to stop oxygen influx to the bed. Most of the existing mine tailings ponds mentioned in section 2.2 involved shallow water covers. Typically, a water cover depth of 1 m is adopted over reactive mine tailings as an industrial practice (Mian 2004). As mentioned, wind-induced erosion and subsequent resuspension of bed tailings is a major challenge in the implementation and management of engineered or shallow water covers. A number of previous studies have demonstrated the occurrence of wind induced resuspension and oxidation of mine tailings under shallow water covers, which underscore the inadequacy of traditionally designed water cover depths to eliminate resuspension (Adu-Wusu et al. 2001; Yanful and Catalan 2002; Mian and Yanful 2003; Mian and Yanful 2004).

All of these authors have noted that resuspension of tailings depends on variables such as wind speed, wind direction, pond geometry or fetch length, water cover depth and also on tailings properties such as particle size distribution and critical shear stress of the bed material. Strong winds of high frequency blowing in the direction of maximum pond fetch for a significantly long period may cause tailings resuspension under shallow water cover depths. Under such conditions, shear stress generated at the tailings bed generally exceeds the critical shear stress or erosion resistance of the tailings (Adu-Wusu et al. 2001; Yanful and Catalan 2002; Samad and Yanful 2005).

2.4 DESIGN APPROACH OF SHALLOW WATER COVER

Water cover depth is a key parameter that must be known either in the design of a new tailings pond or in the management of an existing facility. A minimum water cover depth must be determined to prevent the erosion of bed material from wind-induced wave activity and subsequent resuspension. MEND manual (2001) provides a method to estimate a minimum water cover depth based on the approach by Lawrence et al. (1991). The method is based on the assumption that, to avoid resuspension, wind-wave induced near bed velocity must not exceed the critical velocity for erosion. This method prescribes a single water cover depth for the entire pond, which may be unrealistic because the mobilized bed shear stress is not the same everywhere in the pond. Also, the contribution of return currents in the bed shear stress is ignored which is not always valid (Lawrence et al. 1991; Samad and Yanful 2005).

Samad and Yanful (2005) resolved these problems and developed a method for calculating the minimum water cover depth involving the discretization of the pond area into a mesh of square grid cells and calculation of water cover depth at the center of each grid cell taking into account the fetch length for that grid cell. The method is based on the same premise that erosion and subsequent resuspension of bed sediment occur when the total bed shear stress induced by waves and return currents exceeds the critical shear stress of the bed material. The water cover depth required to eliminate resuspension can be selected by comparing predominant wind induced total bed shear stress with the critical shear stress of the bed material. The critical shear stress is a characteristic property of the bed sediments which must be determined experimentally. It is the minimum shear stress required to entrain the bed sediments and is a complex function of particle size, degree of consolidation, cementation, and geochemistry of the material. In order to obtain the design water depth, knowledge of wind-induced total shear stress on the sediment bed and critical shear stress of the bed sediments is necessary. Following is a review of approaches used to determine these parameters.

2.4.1 Estimation of Bed Shear Stress

Wind induced bed shear stress in a closed water body such as a mine tailings pond, where wind is the only driving force, is made up of two parts (i) bed shear stress due to orbital waves and (ii) bed shear stress due to circulatory currents. Figure 2.2 presents a schematic diagram of tailings pond hydrodynamics in the presence of wind (adopted from

Yanful and Catalan 2002). The effect of wind in the tailings pond induces wave orbital velocities and return currents.

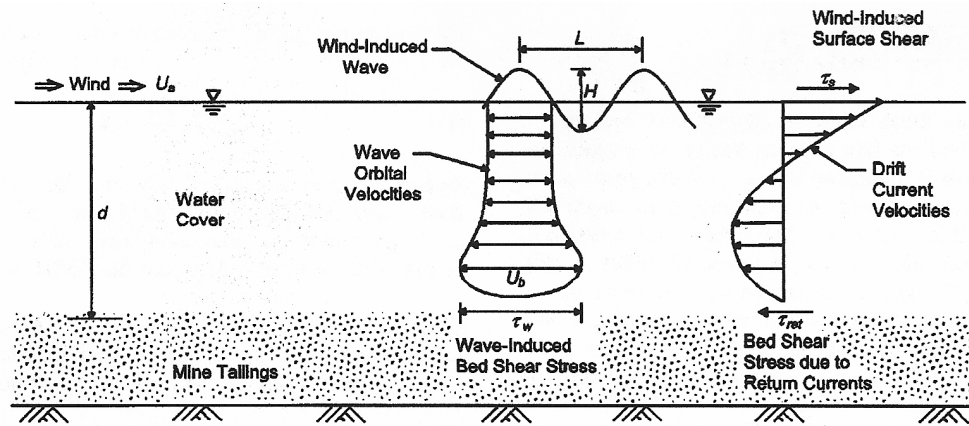


Figure 2.2 Schematic diagram of tailings pond hydrodynamics in presence of winds (Yanful and Catalan 2002)

2.4.1.1 Wind Wave Action

According to Philips (1957), wind blowing over the water surface transfers its energy and generates waves in the water. The reason for energy transfer is the fluctuation of air pressure associated with turbulent eddies. Small waves then grow with time due to resonance between wind-induced atmospheric pressure fluctuations and the developing waves. The characteristics of the waves or wave parameters such as wave period (T), wave height (H), and wave length (L) depend on the wind and water body conditions such as wind speed (U), duration of persistent wind, wind direction, water cover depth (h), and fetch length or the distance of water surface over which wind blows (F).

There are several semi-empirical methods available to predict wave parameters. The two most common approaches for wind wave predictions, which are also employed in the Samad and Yanful (2005) model, are: (i) the significant wave approach or SMB method, and (ii) the wave spectrum approach or CEM method. These methods are briefly described as follows:

1. The SMB Method

The Sverdrup-Munk-Bretschneider (SMB) approach based on measured wave statistics and frequency distributions was developed by Sverdrup and Munk (1947) and later modified by Bretschneider (1957). Details of this approach are available in CERC (1984). The approach provides two sets of equations to determine wave parameters one for deep water conditions ($h/L > 0.5$) and the other for intermediate and shallow water conditions ($h/L < 0.5$). The significant wave height (H_s) and wave period (T_s) are given by following equations:

Deep water conditions ($h/L > 0.5$)

$$H_s = 0.0016 \sqrt{\frac{FU_a^2}{g}} \quad (2.5)$$

$$T_s = 0.2714 \sqrt[3]{\frac{FU_a}{g^2}} \quad (2.6)$$

Intermediate and shallow water conditions ($h/L < 0.5$)

$$H_s = 0.283 \frac{U_a^2}{g} \tanh \left[0.530 \left(\frac{gh}{U_a^2} \right)^{3/4} \right] \tanh \left\{ \frac{0.00565 \left(\frac{gF}{U_a^2} \right)^{1/2}}{\tanh \left[0.530 \left(\frac{gh}{U_a^2} \right)^{3/4} \right]} \right\} \quad (2.7)$$

$$T_s = 7.54 \frac{U_a}{g} \tanh \left[0.833 \left(\frac{gh}{U_a^2} \right)^{3/8} \right] \tanh \left\{ \frac{0.0379 \left(\frac{gF}{U_a^2} \right)^{1/3}}{\tanh \left[0.833 \left(\frac{gh}{U_a^2} \right)^{3/8} \right]} \right\} \quad (2.8)$$

where, F is fetch length, U_a is wind stress factor ($= 0.71 U^{1.23}$), U is wind speed measured at 10 m above the water surface, g is gravitational acceleration.

The SMB method has been used widely in several wind-wave sediment erosion and transport studies. Adu-Wusu et al. (2001) used the SMB method in the analysis and found that strong wind induced waves were the cause of tailings resuspension at the Quirke Waste Management Area. Bentzen et al. (2009) studied the wind induced resuspension of highway detention pond deposits using the SMB method of wave prediction along with the linear wave theory. In the present thesis, the SMB method has been used for the calculations of wave characteristics and subsequent determination of the bed shear stress exerted by wind waves.

2. The CEM Method

The Coastal Engineering Manual or CEM method is based on the wave spectrum approach which was introduced by Pierson, Neumann and James in 1955 assuming that wave growth is best described as a spectral phenomenon (CERC 2002). This approach resulted in the following equations for calculating the two wave parameters, significant wave height (H_s) and peak wave period (T_p).

$$H_s = 0.0413 \frac{u_{*a}^2}{g} \sqrt{\left(\frac{gF}{u_{*a}^2}\right)} \quad (2.9)$$

$$T_p = 0.751 \frac{u_{*a}}{g} \sqrt[3]{\left(\frac{gF}{u_{*a}^2}\right)} \quad (2.10)$$

where, u_{*a} is the wind shear velocity, which can be calculated using Equation 2.11 (CERC 2002)

$$C_D = \frac{u_{*a}^2}{U^2} \text{ and } C_D = 0.001(1.1 + 0.035 * U) \quad (2.11)$$

where, C_D is the drag coefficient.

Samad and Yanful (2005) compared the results of wave height obtained from the SMB and CEM methods and from field measurements. As shown in Figure 2.3, both the SMB and CEM methods predicted results within reasonable accuracy, however the SMB method yielded higher magnitudes compared to the CEM method. Once the wave characteristics or parameters have been obtained by

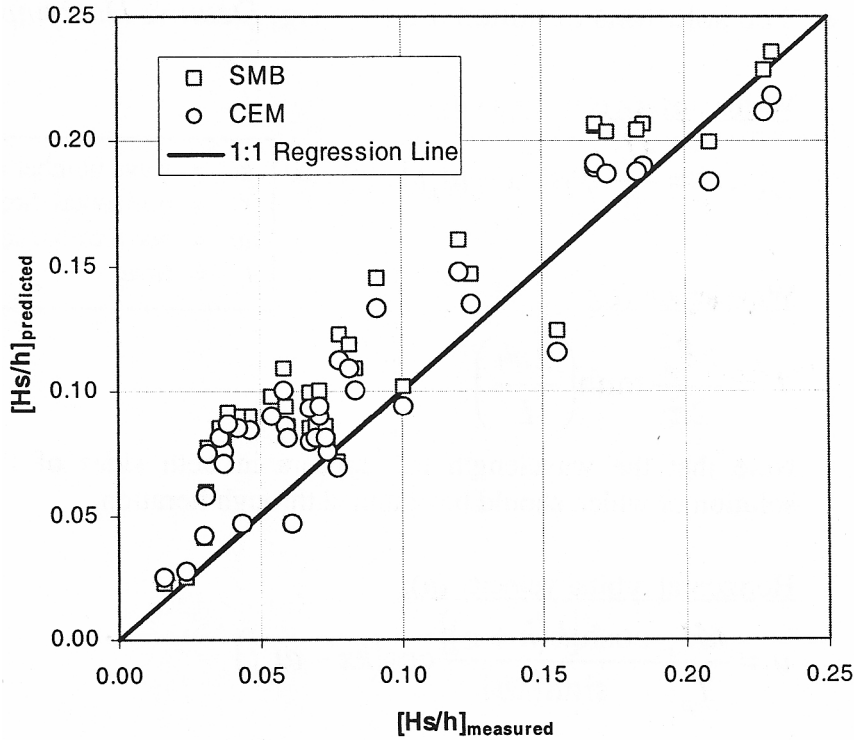


Figure 2.3 Comparison of wave heights predicted by SMB and CEM methods with measured data (Samad and Yanful 2005)

either of the SMB or the CEM approach, the bed shear stress can be computed by applying any of the existing theories of wave propagation, such as (i) the linear wave theory (Dean and Dalrymple 1984), (ii) Stokes wave theory, and (iii) cnoidal and solitary wave theory (Komar 1998). The most widely used of these is the linear wave theory, which assumes irrotational motion of an incompressible fluid, neglects frictional effects and considers wave heights much smaller than the wavelength and water depth (Dean and Dalrymple 1984). The SMB method along with the linear wave theory has been used in the subsequent chapters of this thesis for the determination of wave bed shear stress. The governing equations and

corresponding details of obtaining wind wave induced bed shear stress have been provided in chapter 3 of this thesis and also in Samad and Yanful (2005).

2.4.1.2 Return Current Action

Wind action at the water surface generates shear induced drift currents in the direction of the wind. Baines and Knapp (1965), Wu (1975), Tsuruya et al. (1983), and Yang (2001) predicted that the generated current produces pressure driven reverse or counter-current flow at the bottom, which maintains the mass balance in the vertical column. A schematic diagram of vertical velocity profile with counter current flow is shown in Figure 2.2.

The bed current velocity is a useful parameter in the estimation of wind induced bed shear stress. When direct measurements of current velocity are not possible, it can be estimated empirically using methodologies such as those described by Vlag (1992), Wu and Tsanis (1995), and Whitehouse et al. (1999). Wu and Tsanis (1995) developed a methodology for the estimation of counter-current flow induced bed shear stress. In this approach it was assumed that vertical velocity distribution follows a double logarithmic structure. The simplified form of Wu and Tsanis (1995) approach along with Yang (2001) laboratory determined parameters has been used in this thesis and governing equations of this methodology have been provided in Chapter 3 and also in Samad and Yanful (2005).

2.4.1.3 Total Bed Shear Stress

Wind induced bed shear stress in a closed water body is made of two parts (i) bed shear stress due to waves and (ii) bed shear stress due to circulatory currents. However it is not clear from published literature how the waves and currents should be handled in enclosed shallow water conditions to obtain the total bed shear stress exerted on the bed surface by wind action, which is required for analyzing resuspension and sediment transport processes. In many studies the current induced bed shear stress in shallow water is either considered too small to contribute to resuspension (Luettich et al. 1990; Bailey and Hamilton 1996; Cozar et al. 2005) or estimated using theoretical and empirical approaches developed under laboratory conditions such as those developed by Wu and Tsanis (1995) and Yang (2001).

Cozar et al. (2005) studied wind induced turbidity in the shallow lake of Esteros del Ibera, Argentina by taking into account only wind induced orbital waves. The bed shear stress associated with horizontal currents was assumed to be too small to influence the suspended solids concentration. The horizontal currents were assumed to be having a secondary role of advection and distribution of sediments suspended by more energetic orbital waves. A model equation was developed to predict the suspended solids concentration for known wind speeds:

$$C_{SSC} (mg / L) = \frac{3.48}{h} \alpha (W + (2.3 - W_0))^\beta \delta(W, W_0) \quad (2.12)$$

where, C_{SSC} is suspended solids concentration, h is depth of water cover (m), α and β are the coefficients depend on the characteristics of the process of remobilization of the

particles from the bottom, W is the wind speed (m/s), W_0 is the wind speed necessary for the wind waves to reach the bottom or bed (m/s), which occurs when wavelength (L) exceeds twice the water depth ($L \geq 2h$), $\delta (W, W_0)$ is a step-function that determines when the wind-induced waves begin to resuspend sediments, $\delta = 0$ if $W < W_0$ and $\delta = 1$ if $W \geq W_0$. The wavelength (L) of wind-induced wave is a function of wind speed (W), and fetch length (F) and it was determined using following empirical equation:

$$L = 1.56 \left[0.77 W \tanh \left[0.077 \left(\frac{9.8F}{W^2} \right)^{0.25} \right] \right]^2 \quad (2.13)$$

Cozar et al. (2005) observed that field measured turbidity data had a good agreement with model predictions. The procedure for water depth calculation described in MEND (2001) completely ignores the contribution of current bed shear stress while in some modeling studies, the currents are assumed as counter currents in the opposite direction to winds and the total bed shear stress is taken as a simple linear addition of the shear stress contributions from waves and currents (Wu and Tsanis 1995; Yang 2001; Catalan and Yanful 2002; Samad and Yanful 2005).

Rodney and Stefan (1987) considered both current and wave components of shear stresses and added them numerically. The total bed shear stress (τ_b) was given by:

$$\tau_b = \tau_w + \tau_c + \tau_s \quad (2.14)$$

where, τ_s is the shear stress due to seiche motion and the other variables are as previously defined. Seiche motion is standing wave phenomenon generated in a basin by the

reflection of a travelling wave at the shore of basin (Rodney and Stefan 1987). The periodic seiche motion is a function of lake geometry (or fetch length F) and wind speed. Assuming a flat bottom, the wave period for the seiche motion to occur can be given as $T = \frac{2F}{\sqrt{gh}}$, where F is fetch length, h is water cover depth and g is gravitational acceleration (Niedda and Greppi 2007). Using a typical value of fetch length $F = 1000$ m, and water cover depth $h = 1.5$ m for a tailings pond, the period of a seiche wave is about 9 minutes. The wind generated waves in the tailings pond are mostly short waves of small wave periods typically less than 1 minute and possibly would not generate significant seiche motion (Yanful and Catalan 2002; Samad and Yanful 2005). In most tailings pond studies the effect of seiche motion has been ignored.

Whitehouse et al. (1999) proposed an approach for determining the total bed shear stress generated by wind induced waves and currents. The total bed shear stress can be calculated by Equations 2.15 and 2.16.

$$\tau_b = \sqrt{(\tau_m^2 + 0.5 \tau_w^2)} \quad (2.15)$$

$$\tau_m = \tau_c \left[1 + 9 \left(\frac{\tau_w}{\tau_c + \tau_w} \right)^9 \right] \quad (2.16)$$

Where, τ_m is the mean shear stress, which can be determined by Equation 2.16 for hydraulically smooth bed conditions, and the other parameters are as previously defined.

Quick et al. (1987) noted that linear addition of wave and current parts of the total bed shear stresses is a simplification of a rather complex process. In other studies, it has

been reported that the wave and currents should not be treated separately and that their interaction may increase the total bed shear stress (Grant and Madsen 1979; Jing and Ridd 1996; Jin and Ji 2004). In order to include wave-current interaction in the total bed shear stress calculations, actual field measured current data is needed. In most tailings pond studies, information about actual currents data have been missing and currents were empirically calculated as counter currents.

2.4.2 Erosion Characteristics

The erosion characteristics of sediments include critical shear stress and erosion rate parameters. In the Samad and Yanful (2005) model, information about the critical bed shear stress and erosion rate parameters of bed material is required to obtain the water depth needed to minimize resuspension and predicting the amount of resuspension when bed shear stress exceeds the critical shear stress. The critical shear stress is the minimum shear stress required to initiate erosion of bed material. For non-cohesive materials critical shear stress or resistance to erosion is mainly due to inter-particle friction which is controlled by weight of individual particles, while in cohesive and especially finer materials, critical shear stress is mainly controlled by inter-particle chemical and electrostatic bonding. Erosion rate parameters are the calibration constants of the erosion rate equation which describes the relation between erosion rate and excess shear stress (see Equation 2.17). The erosion of bed material generally can be quantified by erosion rate equations. There are several erosion rate equations developed for different field scenarios available in literature as described by Mehta et al. (1989). The most generalized

form of erosion rate equation was developed by Ariathurai–Partheniades (Ariathurai and Arulanandan 1978; Partheniades 1986; Samad and Yanful 2005) assuming that the depth of erosion is small and that the critical bed shear stress for erosion does not vary with depth. This erosion rate equation was developed for mainly cohesive materials and has been applied in most tailings resuspension studies. However, a field calibrated erosion rate equation should be applicable for both cohesive and non-cohesive tailings. A generalized power law equation for erosion rate can be written as follows.

$$E = \begin{cases} \alpha \left(\frac{\tau_b}{\tau_{cr}} - 1 \right)^M & \text{if } \tau_b > \tau_{cr} \\ 0 & \text{if } \tau_b \leq \tau_{cr} \end{cases} \quad (2.17)$$

where, coefficient α , and exponent M are commonly called erosion rate parameters and are characteristic of the sediment. These parameters can be determined by calibration of Equation 2.17 for known values of erosion rate (E), applied bed shear stress (τ_b), and critical shear stress (τ_{cr}) for site specific sediments. These characteristic parameters of sediments are governed by many factors including tailings mineralogy, composition of pore water and eroding fluid (saline or brackish), consolidation of material, sand and silt content, bio-film, organic content (Kamphuis and Hall 1983; Mian 2004). In a tailings pond, erosion occurs when wind induced total bed shear stress exceeds the critical shear stress of the bed tailings (Yanful and Catalan 2002; Samad and Yanful 2005). In published studies so far, the erosion characteristics were calculated by using different approaches described in the next sections.

2.4.2.1 Empirical Approaches

Some of the empirical approaches used to determine the critical shear stress of the bed sediments include the Shields Criterion (Shields 1936); Fischenich (2001) equation, and the Chien and Wan (1998) equation. Shield (1936) was one of the first researchers who attempted to develop an analytical approach to predict sediment erosion under wave and current actions, especially in rivers. He defined a dimensionless parameter and established a criterion (Shield's Criterion) of incipient motion. According to this criterion, the factors important for the determination of incipient motion are shear stress (τ), difference in density between sediment and water ($\rho_s - \rho_w$), particle diameter (D), kinematic viscosity (ν), and gravitational acceleration (g). Two dimensionless parameters used to develop the well known Shield's diagram (Figure 2.4) were obtained using Equations 2.18 and 2.19.

$$\frac{Du_*}{\nu} = \frac{D \left(\frac{\tau}{\rho_w} \right)^{1/2}}{\nu} \quad (2.18)$$

$$\frac{\tau}{D(\rho_s - \rho_w)g} = \frac{\tau}{D\gamma_w \left(\frac{\rho_s}{\rho_w} - 1 \right)} \quad (2.19)$$

where, u_* is the shear velocity and γ_w is the specific weight of water. The Shield's diagram has been used as a criterion for determining sediment incipient motion by many engineers and researchers (Yang 1977; Kennedy 1995).

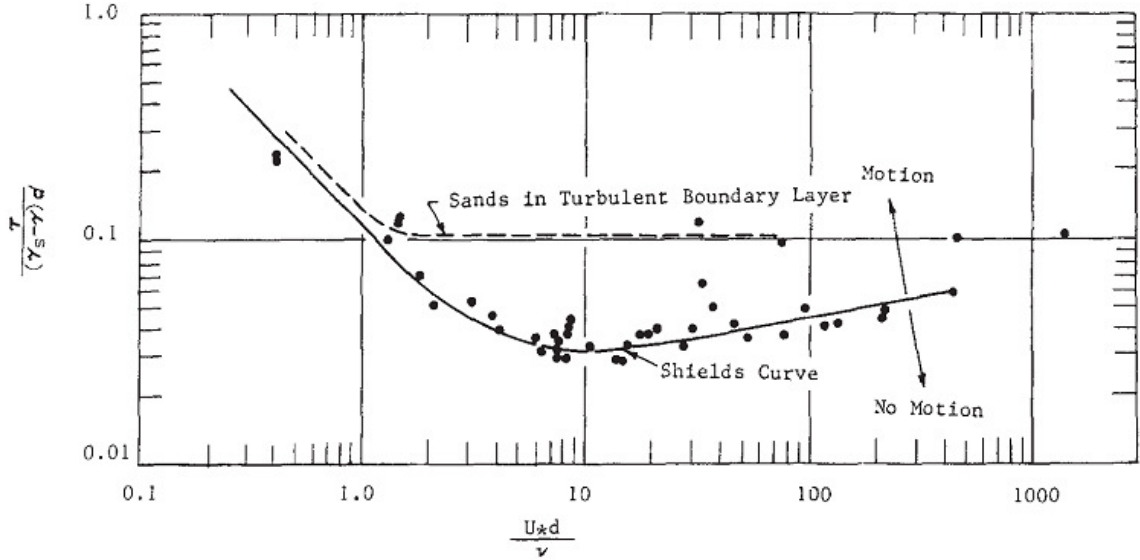


Figure 2.4 Shield's diagram: the relationship between dimensionless critical shear stress and shear velocity Reynolds number (Yang 1977)

Adu-Wusu et al. (2001) used the Chien and Wan (1998) empirical equation (Equation 2.20) to estimate the critical shear stress of bed tailings at the Quirke Waste Management Area (Cell 14):

$$\tau_{cr} = \frac{1}{77.5} \left[3.2(\gamma_s - \gamma_w)D + \left(\frac{\gamma_b}{\gamma_{bo}} \right)^{10} \frac{k}{D} \right] \quad (2.20)$$

where, γ_s and γ_w are the unit weights of the sediment and water, respectively, γ_b is the unit weight of sediment on the bed, γ_{bo} is the unit weight of consolidated sediment, k is a constant ($= 2.9 \times 10^{-4}$ N/m), and D is the sediment particles diameter. The unit weight of sediment bed (γ_b), and that of consolidated sediment (γ_{bo}) were assumed to be equal for compacted tailings at the time of deposition. The critical shear stress obtained was in the range of 0.12 to 0.22 Pa with an average value of 0.17 Pa. These values were reported to

be similar to the critical shear stress (0.12-0.17 Pa) of Heath Steele mine tailings, where the critical shear stress was obtained in a laboratory rotating circular flume using a disturbed sample of bed tailings (Yanful and Catalan 2002).

Fischenich (2001) provided a set of three empirical equations to determine the critical shear stress of different bed sediments. According to Fischenich (2001) the critical shear stress can be obtained by equating the applied forces to the resisting forces. For sediments of diameter, D , and angle of repose, ϕ , on a flat bed, the following equations were developed to approximate the critical shear stress of various sizes of sediment:

$$\tau_{cr} = 0.5(\gamma_s - \gamma_w)D \tan \phi \quad \text{For Clays} \quad (2.21)$$

$$\tau_{cr} = 0.25 D_*^{-0.6} (\gamma_s - \gamma_w)D \tan \phi \quad \text{For Silts and Sands} \quad (2.22)$$

$$\tau_{cr} = 0.06(\gamma_s - \gamma_w)D \tan \phi \quad \text{For Gravels and Cobbles} \quad (2.23)$$

where,

$$D_* = D \left[\frac{(G-1)g}{\nu^2} \right]^{1/3}, \quad (2.24)$$

G is the specific gravity or relative density of the sediment, g is gravitational acceleration, ν is the kinematic viscosity of the water/sediment mixture. The important thing to note is that these equations were developed for non-cohesive and uniform size sediments, but in nature where a mixture of various sized sediments exist, the presence of cohesion,

organic matter, vegetations, and geochemistry can significantly alter the critical shear stress of the bed material. However, Fischenich's (2001) equation has been used in the present study to determine the critical shear stress of bed tailings at the Shebandowan tailings storage facility (Chapter 3). The results for east and west cells of the tailings pond were similar to those reported for tailings from other mining sites such as Quirke and Heath Steele (Adu-Wusu et al. 2001; Yanful et al. 2002). In the case of the finer middle cell tailings at Shebandowan site, the estimated critical shear stress was quite low (0.04 Pa) and could not explain field resuspension results.

2.4.2.2 Laboratory Experiments

Krishnappan (1993) used a circular flume to determine the critical shear stress and erosion rate parameters. In this flume, the critical shear stress was measured by monitoring the concentration of suspended sediments with increasing bed shear stress applied by generating fluid motion with two annular plates rotating in opposite directions. The diameter of the set up was 7.0 m. A bulk sample of approximately 90 kg of tailings and 500 L of tap water were used to prepare slurry used in the flume. The speed of the flume rotation was increased in time steps of 30 min and suspended solids concentration in the water was monitored during each time step. The bed shear stress applied by the flume and suspended solids concentration was plotted to identify the onset of sediment erosion. The detailed procedure has been described in published articles by Krishnappan (1993), Yanful and Verma (1998), and Yanful et al. (2002). Several other authors, including Fukuda (1978), Sheng and Lick (1979), and Mehta et al. (1982) have used

similar annular rotating flumes to obtain critical shear stress of the sediments. Other smaller scale laboratory experiments include column tests such as used by Geremew and Yanful (2010).

In laboratory experimental methods, a known value of shear stress is applied mechanically to packed sample of bed tailings material. However, in the field the presence of benthic organism and bio-films in bed sediments influence the erosion characteristics of bed sediments and disturbed samples used in the laboratory erosion tests may not represent the same physical, chemical and biological sediment characteristics (Krishnappan and Droppo 2006).

2.4.2.3 In situ Experiments

It is necessary to estimate erosion characteristics or parameters in field conditions. There are very limited studies available on the estimation of critical shear stress and erosion rate parameters in the field. Several in-situ instruments are used for determining erosion characteristics. Amos et al. (1992) developed a benthic annular flume in the horizontal plane (Sea Carousel) based on the principle of laboratory developed carousels in which the shear stress is induced by a horizontal circulating flow. A similar principle has been used by Black (1993), who developed the mobile recirculating sea water flume (MORF) for measuring the resuspension of intertidal muds. Maa et al. (1993) developed an annular sea-bed flume (VIMS) which can be deployed under deep water conditions. Similar in-situ benthic circular flumes equipped with more advanced sensors such as

optical backscatter sensor (OBS) were designed and deployed in the field by Moreau et al. (2003), and Krishnappan and Droppo (2006). Straight flumes have also been developed by Young (1976) and Gust and Morris (1989).

Houwing and Rijn (1998) reported that all of the in situ instruments basically work on a similar principle in which a circulating or straight water flow exerts a known amount of shear stress on the bed. The major disadvantage of this technique is the relatively large size of instrument required to ensure a logarithmic distribution of the velocity profile. The average size of these flumes was of the order of 2 m and the size of the test sections was in the range of 0.1 – 1.0 m². Houwing and Rijn (1998) developed an in situ erosion flume (ISEF) to determine the critical shear stress and erosion rate parameters. This relatively small (1.8 m length) and light weight (50 kg) instrument was calibrated and tested under laboratory conditions on a kaolinite bed. The volume of the water in the flume was 100 dm³ and a propeller was rotated to generate the turbulent flow measured by disc-type electromagnetic flow meter (EMF). The suspended solids concentration was recorded by an optical sensor (MEX). The inaccuracy reported by authors in the shear stress was 20%. However, this light weight flume was not tested under field conditions.

Other in situ techniques have been developed for the determination of the erosion characteristics of cohesive sediment bed on a smaller scale, which have not been widely applied. A cohesive strength meter (CSM) was developed by Patterson (1989) in which a generated water jet impacted a sediment surface. Tsai and Lick (1986) developed an instrument called “shaker” in which turbulent motion of water column was generated

above the sediment surface by an oscillating horizontal grid. Schunemann and Kuhl (1991) developed EROMES in which turbulent motions were induced just above a bed surface using a propeller. Williamson (1994) designed an inverted bell-shaped funnel (ISIS) which generates a stream of water at close range above a sediment surface. The test surface of these instruments was very small of the order of 0.01 m^2 , and the results were highly dependent on small scale irregularities of the bed surface and deployment of the instruments on the bed (Houwing and Rijn 1998).

In most of the above mentioned in-situ and laboratory experiments, a known value of shear stress was applied by mechanical means. In nature, bed shear stress applied by wind induced waves and currents are quite unsteady and, rarely, can be simulated by mechanical flumes. Wang (2002) estimated erosion rate parameters for cohesive sediments by measuring field tidal waves and currents and turbidity at Long Island Sound, USA. However, no published literature was found where actual wind induced waves and currents data and corresponding resuspension data have been used to obtain critical shear stress and erosion rate parameters of bed tailings.

2.5 MOTIVATION FOR THE PRESENT RESEARCH

Water cover technology for long term tailings storage has been proven to be effective in the reducing the environmental impacts of reactive mine tailings. Wind plays an important role in determining the required depth of water cover. From the foregoing literature review, it is observed that there are a number of unresolved issues with water

cover technology that must be investigated in order to improve the technology for continuing and wider applications in industry. Some common problems highlighted by the literature review are:

1. The Samad and Yanful (2005) model provided a design approach for shallow water covers, however there were unknown variables such as wind induced currents, critical bed shear stress, erosion rate parameters, wave-current interaction that must be determined prior to using the model.
2. From the published studies it is not clear how currents contribute to the total bed shear stress. The wave-current interaction term, which may enhance the shear stress exerted on the bed by wind action, was ignored in all previous water cover studies. The effect of wave-current interaction on total bed shear stress must be studied for mine tailings ponds.
3. To the best of the author's knowledge, there is no published study available, where actual currents were measured in a mine tailings pond. In most of the studies, currents were empirically determined and linearly added to obtain the total bed shear stress. Knowledge of current speed and direction is necessary in order to incorporate the wave-current interaction term, which can only be obtained by actual field measurement of currents.
4. Accurate knowledge of erosion characteristics, which include the critical shear stress and erosion rate parameters, must be made in order to select the water cover depth. Most of the experimental methods to estimate critical bed shear stress involve disturbed or mechanically packed sample of bed sediments and simulated bed shear stress conditions. Hence the results may not be representative of actual

field values, especially in cohesive bed tailings. No study was found where field measured real time resuspension and wind data were used to determine erosion rate parameters and the critical shear stress of bed material.

In the present thesis, an attempt has been made to resolve above the mentioned issues with water cover technology, based on an extensive field investigation involving a fully equipped weather station, sediment traps, optical backscatter sensors (OBS), and acoustic Doppler current profiler (ADCP).

2.6 REFERENCES

1. Adu-Wusu, C., Yanful, E.K., & Mian, M.H. (2001). Field evidence of resuspension in a mine tailings pond. *Canadian Geotechnical Journal*, 38(4): 796-808.
2. Amos, C.L., Daborn, G.R., & Christian, H.A. (1992). In-situ erosion measurements on fine-grained sediments from the Bay of Fundy. *Marine Geology* 108: 175-196.
3. Ariathurai, R., & Arulanandan, K. (1978). Erosion rates of cohesive soils. *Journal of Hydraulic Division, Proceedings of the American Society of Civil Engineers*, 104(HY2): 279-283.
4. Armienta, M.A., Talavera, O., Morton, O., & Barrera, M. (2003). Geochemistry of metals from mine tailings in Taxco, Mexico. *Bulletin of Environmental Contamination and Toxicology*, 71: 387-393.
5. Bailey, M.C., & Hamilton, D.P. (1997). Wind induced sediment resuspension: a lake-wide model. *Ecological Modelling*, 99:217-228
6. Baines, W.D., & Knapp, D. J. (1965). Wind driven water current. *Journal of the Hydraulic Division, ASCE*, 91(2): 205-221.
7. Bennett, C.V. (2002). Investigation of tailings resuspension under a shallow water cover. Ph.D. dissertation, The University of Western Ontario, London, ON, Canada.
8. Bentzen, T.R., Larsen, T., & Rasmussen, M.R. (2009). Predictions of resuspension of highway detention pond deposits in interrains event periods

- due to wind-induced currents and waves. *Journal of Environmental Engineering*, ASCE, 135(12): 1286-1293.
9. Black, K. (1993). The turbulent resuspension of cohesive intertidal muds: some new concepts and ideas. In: Sterr, H., Hofseide, J., Plag, H.-P. (Eds.), *Proceedings of the International Coastal Congress ICC-Kiel` 92*. Peter Lang, Berlin pp. 223-239.
 10. Bois, D., Benzaazoua, M., Bussiere, B., Kongolo, M., & Poirier, P. (2005). A feasibility study on the use of desulphurized tailings to control acid mine drainage. *Cim Bulletin* 98(1087): 74-82.
 11. Bussiere, B., Benzaazoua, M., Kongolo, M., & Aubertin, M. (2002). *Integration de la desulfuration dans la restauration des sites miniers generateurs de DMA*. Symposium 2002 sur l'environnement et les mines, Rouyn-Noranda, Quebec.
 12. CERC (1984). *Shore protection manual*. U.S. Army Corps of Engineer, Coastal Engineering Research Centre, Vicksburg, M.S.
 13. CERC (2002). *Coastal engineering manual*. U.S. Army Corps of Engineer, Coastal Engineering Research Centre, Vicksburg, M.S.
 14. Changul, C., Sutthirat, C., Padmanabhan, G., & Tongcumpou, C. (2009). Chemical characteristics and acid drainage assessment of mine tailings from Akara Gold Mine Thailand. *Environmental Earth Sciences*, 60: 1583-1595.
 15. Chien, N., & Wan, Z. (1998). *Mechanics of sediment transport*. ASCE press, Virginia.

16. Cozar, A., Galvez, J.A, Hull, V., Garcia, C.M., & Loiselle, S.A. (2005). Sediments resuspension by wind in a shallow lake in Esteros del Ibera (Argentina): a model based on turbidimetry. *Ecological Modelling*, 186: 63-76.
17. Da Silva, E.F., Fonseca, E.C., Matos, J.X., Patinha, C., Reis, P., & Oliveira, J.M.S. (2005). The effect of unconfined mine tailings on the geochemistry of soils, sediments and surface waters of the Lousal area (Iberian Pyrite Belt, Southern Portugal). *Land Degradation and Development* 16: 213-228.
18. Dave, N.K., Lim, T.P., Horne, D., Boucher, Y., & Stuparyk, R. (1997). Water cover on reactive tailings and waste rock: laboratory studies of oxidation and metal release characteristics. *Proceedings 4th International Conference on Acid Rock Drainage*, Vancouver, BC, Canada, May31-June 6, II: 779-794.
19. Demers, I., Bussiere, B., Benzaazoua, M., Mbonimpa, M., & Blier, A. (2008). Column test investigation on the performance of monolayer covers made of desulphurized tailings to prevent acid mine drainage. *Minerals Engineering* 21: 317-329.
20. Environment Canada (2003). Status report on water pollution prevention and control in the Canadian metal mining industry 2001. Environment Canada EPS 1/MM/10-August 2003.
21. Environment Canada (2009). Environmental code of practice for metal mines. Environment Canada 1/MM/77.
22. Evangelou, V.P. (1995). Pyrite oxidation and its control. Boca Raton. CRC Press Inc., Miami, FL.

23. Fischenich, C. (2001). Stability thresholds for stream restoration materials. EMRRP technical notes collection, ERDC TN-EMRRP-SR-29, U.S. Army engineer research center, Vicksburg, M.S.
24. Fukuda, M.K. (1978). The entertainment of cohesive sediments in fresh water. Ph.D. dissertation, Case Western Reserve University, Cleveland, Ohio, USA.
25. Gautam, R., Yanful, E.K., & Karamanev, D.G. (2000). Laboratory scale sulphide tailings oxidation. Proceedings 53rd Canadian Geotechnical Conference, Montreal, Quebec, 1: 649-656.
26. Geremew, A.M., & Yanful, E.K. (2010). The role of fines on the cohesive behavior of mine tailings inferred from the critical shear stress. Canadian Geotechnical Journal. In Press. Accepted October 4, 2010.
27. Grant, W.D., & Madsen, O.S. (1979). Combined wave and current interaction with a rough bottom. Journal of Geophysical Research, 84(C4): 1979-1808.
28. Gust, G., & Morris, M.J. (1989). Erosion thresholds and entrainment rates if undisturbed in situ sediments. Journal of Coastal Research, 5: 87-99.
29. Halfman J.D., & Scholz C.A. (1993). Suspended sediments in Lake Malawi, Africa: a reconnaissance study. Journal of Great Lakes Research, 19(3): 499-511.
30. Herlin, B. (2007). Project case study – composite soil cover for sulphide tailings at mine site in northeastern Ontario, Canada. Diamond Jubilee Canadian Geotechnical Conference, Ottawa, ON, Canada, October 21-24, 2007, 2155-2160.

31. Houwing E.J., & Van Rijn L.C. (1998). In situ erosion flume (ISEF): determination of bed-shear stress and erosion of a kaolinite bed. *Journal of Sea Research* 39: 243-253.
32. Jin, K.-R., & Wang, K.-H. (1998). Wind generated waves in Lake Okeechobee. *Journal of the American Water Resources Association*, 34(5): 1099-1108.
33. Jin, K., & Ji, Z. (2004). Case study: modeling of sediment transport and wind-wave impact in Lake Okeechobee. *Journal of Hydraulic Engineering*, 130:1055-1067.
34. Jing, L., & Ridd, P.V. (1996). Wave-current bottom shear stresses and sediment resuspension in Cleveland Bay, Australia. *Coastal Engineering*, 29:169-186
35. Kennedy, J.F. (1995). The Albert Shields Story. *Journal of Hydraulic Engineering*, 121(11): 766-772.
36. Komar, P.D. (1998). *Beach processes and sedimentation*. 2nd Edition, Prentice-Hall, Inc., NJ, USA.
37. Krishnappan, B.G. (1993). Rotating circular flume. *Journal of Hydraulics Engineering*, 119(6): 758-767.
38. Krishnappan, B.G., & Droppo, I.G. (2006). Use of an in-situ erosion flume for measuring stability of sediment deposits in Hamilton Harbour, Canada. *Water Air and Soil Pollution*, 6: 557-567.

39. Lawrence, G.A., Ward, G.A., & Mckinnon, P.R.B. (1991). Wind-wave induced suspension of mine tailings in disposal ponds: a case study. *Canadian Journal of Civil Engineering*, 18(6), 1047-1053.
40. Li, M.G., Aube, B., & St-Arnaud, L. (1997). Considerations in the use of shallow water covers for decommissioning reactive tailings. *Proceedings 4th International Conference on Acid Rock Drainage, Vancouver, B.C.*, 1, 115-130.
41. Lick, W. (1982). Entrainment, deposition, and transport of fine-grained sediments in lakes. *Hydrobiologia*, 55: 219-228.
42. Ljungberg, J., & Ohlander, B. (2001). The Geochemical dynamics of oxidising mine tailings at Laver, northern Sweden. *Journal of Geochemical Exploration* 74: 57-72.
43. Luettich, R.A., Harleman, D.R.F., & Somlyody, L. (1990). Dynamic behaviour of suspended sediment concentrations in shallow lake perturbed by episodic wind events. *Limnology and Oceanography*, 35:1050-1067
44. Maa, J.P.-Y., Wright, L.D., Lee, C.-H., & Shannon, T.W. (1993). VIMS Sea Carousel: a field instrument for studying sediment transport. *Marine Geology*, 115: 271-287.
45. Mehta, A.J., Parchure, T.M., Dixit, J.G., & Ariathrai, R. (1982). Resuspension potential of the deposited cohesive sediment beds. *Estuarine comparisons*, V.S. Kennedy, ed., Academic, Ney York, 591-609.

46. Mehta, A.J., Hayter, E.J., Parker, W.R., Krone, R.B., & Teeter, A.M. (1989). Cohesive sediment transport. Part I: Process Description. *Journal of Hydraulic Engineering*, 115(8): 1076-1093.
47. MEND Manual (2001). Prevention and control, Volume 4, Energy Mines and Resources Canada.
48. Mian, M.H., & Yanful, E.K. (2003). Tailings erosion and resuspension in two mine tailings ponds due to wind waves. *Advances in Environmental Research*, 7, 745-765.
49. Mian, M.H., & Yanful, E.K. (2004). Optical backscatter measurements of tailings resuspension in a mine tailings pond. *Proceedings 57th Canadian Geotechnical Conference, Session 7D*, 38-45.
50. Mian, M.H. (2004). Erosion and resuspension of cohesive mine tailings. Ph.D. dissertation, The University of Western Ontario, London, ON, Canada.
51. Mining Watch Canada (2009). Two million tonnes a day: a mining waste primer. Mining Watch Canada, December 2009. www.miningwatch.ca.
52. MMER (2002). Metal mining effluent regulations. SOR/2002-222, <http://laws.justice.gc.ca/PDF/Regulation/S/SOR-2002-222.pdf>, Accessed November 10, 2009.
53. Neidda, M., & Greppi, M. (2007). Tidal, seiche and wind dynamics in a small lagoon in the Mediterranean Sea. *Estuarine Coastal and Shelf Science*, 74: 21-30.
54. O’Kane, M., & Wells, C. (2003). Mine waste cover system design – linking predicted performance to groundwater and surface water impacts. *Proceedings*

of the Sixth International Acid Rock Drainage Conference July 14–17, 2003, Cairns, Australia (2003), pp. 341–349.

55. Partheniades, E. (1986). A fundamental framework for cohesive sediment dynamics. In *Estuarine Cohesive Sediment Dynamics*. Ed. Mehta A.J. Springer, Berlin.
56. Patterson, D.M. (1989). Short-term changes in the erodibility of intertidal cohesive sediments related to the migratory behaviour of epipellic diatoms. *Limnology and Oceanography*, 34: 223-234.
57. Philips, O.M. (1957). On the generation of waves by turbulent wind. *Journal of Fluid Mechanics*, 2: 417-445.
58. Quick, M.C., Kingston, K., & Lei, S. (1987). Onset of sediment motion under waves and currents. *Canadian Journal of Civil Engineering*, 14: 196-206.
59. Reid, N.B., & Naeth, M.A. (2005). Establishment of a vegetation cover on Tundra Kimberlite mine tailings: 2. A field study. *Restoration Ecology*, 13(4): 602-608.
60. Renken, K., Yanful, E.K., & Mchaina, D.M. (2005). Field performance evaluation of soil-based cover systems to mitigate ARD for the closure of a potentially acid-generating tailings storage facility. *British Columbia Reclamation Symposium*, Abbotsford, BC. September 19-22, 2005.
61. Ritcey, G.M. (1989). *Tailings management, problems and solutions in the mining*. Elsevier
62. Rodney, M.W., & Stefan, H.G. (1987). Conceptual model for wind generated sediment resuspension in shallow ponds. *Proceedings National Symposium on*

Mining, Hydrology, Sedimentology, and Reclamation. University of Kentucky, 263-269

63. Salomons, W. (1995). Environmental impact of metals derived from mining activities: processes, prediction prevention. *Journal of Geochemical Exploration*, 52: 5-23.
64. Samad, M. A., & Yanful, E.K. (2005). A design approach for selecting the optimum water cover depth for subaqueous disposal of sulfide mine tailings. *Canadian Geotechnical Journal*, 42, 207-228.
65. Schunemann, M., & Kuhl, H. (1991). A device for erosion-measurements on naturally formed, muddy sediments: the EROMES-system. GKSS-Forschungszentrum Geesthacht GmbH, Report GKSS 91/E/18, 28 pp.
66. Sheng, Y.P., & Lick, W. (1979). The transport and resuspension of sediments in a shallow lake. *Journal of Geophysical Research*, 84(C4), 1809-1826.
67. Shields, A. (1936). Application of similarity principles and turbulence research to bed-load movement. *Mitteilunger der Preussischen Versuchsanstalt fur Wasserbau und Schiffbau* 26: 5-24.
68. Simms, P.H., Yanful, E.K., St-Arnaud, L., Aube, B., et al. (2001). A laboratory evaluation of metal release and transport in flooded preoxidized mine tailings. *Applied Geochemistry*, 15, 1245-1263.
69. Tsai, C.-H., & Lick, W. (1986). A portable device for measuring sediment resuspension. *Journal of Great Lakes Research*, 12: 314-321.
70. Tsuruya, H., Nakano, S., Kato, H., Ichinohe, H., et al. (1983). Experimental study of wind driven current in wind-wave tank - effect of return flow on wind

- driven flow, report. Port and Harbour research Institute, In Japanese, 22(2), 127-174.
71. Vigneault, B., Campbell, P.G.C., Tessier, A., & Vitre, R.D. (2001). Geochemical changes in sulfide mine tailings stored under a shallow water cover. *Water Research*, 35(4): 1066-1076.
72. Vlag, D.P. (1992). A model for predicting waves and suspended silt concentration in a shallow lake. *Hydrobiologia*, 235(236): 119-131.
73. Williamson, H.J. (1994). Recent field measurements of erosion shear stress using ISIS. 4th Nearshore and Estuarine Cohesive Sediment Transport Conference INTERCOH' 94. Wallingford, England.
74. Wu, J. (1975). Wind-induced drift currents. *Journal of Fluid Mechanics*, 68(1): 49-70.
75. Wu, J., & Tsanis, I.K. (1995). Numerical study of wind induced water currents. *Journal of Hydraulic Engineering, ASCE*, 121(5), 388-395.
76. Yanful, E.K., & Verma, A. (1998). Predicting resuspension in flooded mine tailings. *Proceedings 51st Canadian Geotechnical Conference, Edmonton, Canada*, 1: 113-121.
77. Yanful, E.K., & Verma, A. (1999). Oxidation of flooded mine tailings due to resuspension. *Canadian Geotechnical Journal*, 36: 826-845.
78. Yanful, E.K., & Catalan, L.J.J. (2002). Predicted and field measured resuspension of flooded mine tailings. *Journal of Environmental Engineering, ASCE*, 128(4), 341-251.

79. Yang, C.T. (1977). The movement of sediment in rivers. *Geophysical Surveys*, 3: 39-68.
80. Yang, Y. (2001). Wind induced countercurrent flow in shallow water. Ph.D. thesis, The University of Western Ontario, London, ON.
81. Young, R.A. (1976). Seaflume: a device for in-situ studies of threshold erosion velocity and erosional behaviour of undisturbed marine muds. *Marine Geology*, 23: 11-18.

CHAPTER 3: WATER COVER TECHNOLOGY FOR REACTIVE TAILINGS MANAGEMENT: A CASE STUDY OF FIELD MEASUREMENT AND MODEL PREDICTIONS

3.1 INTRODUCTION

The long-term disposal of reactive mine tailings with minimal environmental impact is a major challenge facing the mining industry. Many tailings, mostly from metal (for example, Ni, Cu, and Zn) mining operations, contain sulphide minerals like chalcopyrite (CuFeS_2), pyrite (FeS_2), sphalerite (ZnS) and galena (PbS) in abundance. On direct exposure to oxygen and moisture, these sulphide minerals may oxidize, generate acidity and release heavy metals into the environment and adversely impact it.

The placement of tailings under a cover of water has been shown to be an effective method of minimizing acid generation and metal release from tailings. The effectiveness of the water cover technology is based on the fact that oxygen has lower solubility and diffusivity in water (8.6 g/m^3 and $2 \times 10^{-9} \text{ m}^2/\text{s}$ at 25°C , respectively), than in air (285 g/m^3 and $1.78 \times 10^{-5} \text{ m}^2/\text{s}$ at 25°C). These parameters mean that the influx of oxygen to the tailings is low; hence oxidation is significantly reduced (Simms et al. 2001; Adu-Wusu et al. 2001). A water cover also eliminates wind erosion of tailings and, in the long term, provides an anoxic or reducing environment for sulphate reduction and generation of alkalinity for the precipitation of metals.

A major problem with implementing a water cover over tailings is the presence of strong wind induced waves and currents in water. Wind waves deliver energy to the water to generate currents and initiate sediment motion. Wind induced turbulence in water also keeps the dissolved oxygen at saturation level (Li et al. 1997; Samad and Yanful 2005). Strong winds sustained over a long period can cause resuspension of tailings in water that contains dissolved oxygen, and result in a greater potential for tailings to oxidize and change the water quality in the pond and at the outlet.

A number of previous studies have demonstrated the occurrence of wind induced resuspension and oxidation of mine tailings (Adu-Wusu et al. 2001; Yanful and Catalan 2002; Mian and Yanful 2003; Mian and Yanful 2004). Bennett and Yanful (2001), Catalan and Yanful (2001), and Adu-Wusu et al. (2001) showed evidence of tailings resuspension using sediment traps deployed in tailings pond, while Mian and Yanful (2004) used OBS (optical backscatter sensors) to measure wind induced resuspension. Yanful and Verma (1999) showed that the potential for the oxidation of resuspended tailings is greater than for flooded bed tailings under laboratory conditions. Bengtsson and Hellstrom (1992) used sediment traps in Lake Tamnaren, Sweden, to measure wind-induced resuspension. All of these authors noted that resuspension of tailings depends on variables such as wind speed, wind direction, pond geometry or fetch length, water cover depth and also on tailings properties such as particle size distribution and critical shear stress of the bed material. Strong winds of high frequency blowing in the direction of maximum pond fetch for a significantly long period may cause tailings resuspension under shallow water cover depths. Under such conditions, shear stress generated at the

tailings bed generally exceeds the critical shear stress or erosion resistance of the tailings (Adu-Wusu et al. 2001; Yanful and Catalan 2002).

MEND Manual (2001) and MEND Report (1998) contains a procedure for designing subaqueous tailings disposal facilities. Water cover depth is a key parameter that must be known either in the design of a new tailings pond or in the management of an existing facility. A minimum water cover depth must be determined to prevent erosion of bed material from wind-induced wave activity and subsequent resuspension. MEND manual (2001) provides a method to estimate a minimum water cover depth based on the approach by Lawrence et al. (1991). The method is based on the assumption that, to avoid resuspension, wind-wave induced near bed velocity must not exceed the critical velocity for the erosion. The method has a few limitations. First, it is limited to the design of deep-water cover facilities such as deep lakes. It does not provide a solution for intermediate and shallow water covers. Second, it prescribes a single water cover depth for the entire pond, which may be unrealistic because fetch length is not the same everywhere in the pond. Fetch length depends on pond geometry and the direction of predominant winds. Third, the assumption that bed shear stress due to counter currents is only about 10% of the total shear stress may not be valid for cases where strong winds and high water cover depths exist (Lawrence et al. 1991; Samad and Yanful 2005).

Samad and Yanful (2005) have developed a methodology for calculating the minimum water cover depth required to eliminate or minimize resuspension. A key feature of that methodology is discretization of the pond area into a mesh of square grids and calculation of the bed shear stress for each square grid cell taking into account the

fetch length for that grid cell. Input parameters include cell coordinates, wind data, pond geometry, median grain size of bed material, critical shear stress of bed material, erosion test results, and sulphate production rate constants. From the analysis, a specific value of water cover depth is obtained for each square grid cell. The method is based on the premise that erosion and resuspension of bed sediment occur when the total bed shear stress induced by waves and return currents exceeds the critical shear stress of the bed material. Thus the bed shear stress contribution from return currents is not ignored. The required water cover depth is calculated by comparing the total bed shear stress and critical shear stress of the bed tailings. In addition, the method can be used to estimate the concentration of resuspended sediments and sulphate concentrations in the water cover if the water cover depth is below the minimum required value. The Samad and Yanful (2005) approach can also provide optimal water cover depths that allow regulatory acceptable suspended solids or tailings concentrations. In this paper, the method of Samad and Yanful (2005) is used to investigate tailings resuspension at the Shebandowan tailings storage facility and the results are compared to field measured values. The minimum required water cover depth is calculated and compared with existing water cover depth to predict resuspension. The major limitation of the Samad and Yanful (2005) was found to be that it does not take into account sediment transportation and redeposition from one station to other station.

The main objectives of the present work are to investigate resuspension that occurs in a tailings pond subdivided into cells by wave breaks using the Shebandowan tailings storage facility as a study site and to compare field measured data to model predictions using the methodology of Samad and Yanful (2005). At the Shebandowan

tailings site, located 100 km northwest of Thunder Bay, Ontario, tailings have been decommissioned with several perimeter dams and two wave breaks that divide the pond into three cells: east, middle and west cells. Although resuspension of flooded mine tailings has been extensively studied, as indicated by the papers cited above, none of the published work to date has dealt with an assessment of resuspension in a tailings pond subdivided into cells by wave breaks. The wave breaks or internal dykes are generally installed in tailings ponds to decrease the fetch (distance over which wind blows) and eliminate or reduce resuspension to insignificant levels.

Resuspension was measured in the tailings pond using sediment traps and optical backscatter (OBS) sensors. A sediment trap measures the amount of suspended material over a certain period while an OBS sensor gives the time series results of the concentration of resuspended material in water. The use of OBS sensors also allowed relation of wind events to episodic resuspension during the monitoring period, information that would not have been available from sediment trap measurements alone. In previous work and in many published tailings pond studies, this information had been lacking. In this paper, an attempt has also been made to compare measured resuspension to predicted values.

3.2 THE STUDY SITE

The study was conducted at the Shebandowan Mine tailings storage facility, located 100 km west of Thunder Bay, northwestern Ontario, Canada. The site is located along the south shore of Lower Shebandowan Lake. The Shebandowan mine was operated as an

underground nickel and copper mining and milling facility from 1971 to 1998 (with two interim shut down periods from 1986 to 1989 and 1992 to 1995). Figure 3.1 shows the plan view of the tailings storage facility. The tailings storage facility includes six perimeter dams of crest elevation of 482 m and occupies an area of about 115 ha. In 1999 approximately 85,000 m³ of potentially acid generating waste rock from around the mine and mill site were deposited within the tailings basin in a submerged state (Golder Associates 2000). Two wave breaks (internal dykes) were constructed across the tailings facility, which divided the pond into three cells, namely, west cell, middle cell and east cell. The purpose of the wave breaks is to reduce the fetch length and hence eliminate or minimize sediment disturbance and subsequent erosion and resuspension of tailings. The depth of water cover in the pond varies from less than 1 m at some locations to over 2 m at others. On average, the depth of water cover is about 1 m at most locations in the pond.

3.3 METHODS AND MATERIALS

3.3.1 Weather Station

Much research has shown that wind is a very important factor that controls the performance of a tailings pond. The erosion and resuspension of tailings is caused by energy transfer to the bed, and this energy transfer is a function of wind speed, direction, and duration. At the study site, a fully equipped weather station, consisting of a Young Wind Monitor model 05103-10 RM (wind speed and direction), CS500-U (air temperature and relative humidity), NR LITE Kipp and Zonen Net Radiometer sensor

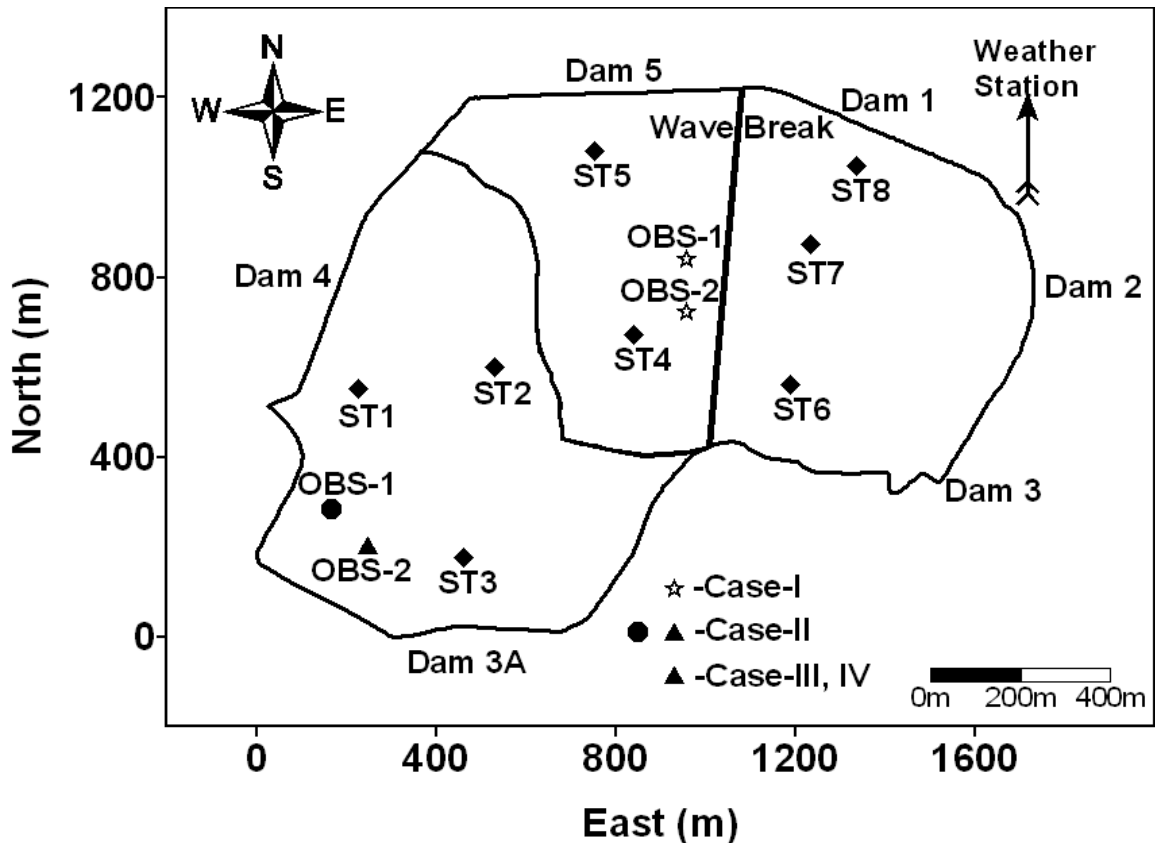


Figure 3.1 Map of Shebandowan Mine tailings storage facility showing the location of sediment traps (ST) and OBS sensors

(Solar radiation), TE525M Texas Electronics Tipping Bucket Metric Rain Gauge (precipitation) linked with a CR10X data logger (Campbell Scientific Canada Corp. Edmonton, Alberta), has been installed. The instruments and sensors were mounted on a tower close to the tailings pond at a height of 10 m from the water surface. Wind measurements must be made at standard 10 m height from the water surface for wind induced waves predictions using wave hindcasting equations mentioned later in section 3.4 (CERC 1984). The variation of weather data within the location area of the tailings pond is likely to be very minimal and therefore one weather station can be considered

representative for the pond. The data logger was programmed to record weather data including wind speed and direction every 15 minutes.

3.3.2 Measurement of Resuspension

3.3.2.1 Sediment traps:

The sediment trap is a widely used device to evaluate the amount of sedimentation in oceans and lakes; however, in shallow and turbulent water, these traps also collect secondary sedimentation or resuspended material and hence can overestimate sedimentation (Rosa 1994; Kozerski 1994). Sediment traps can be used to quantify resuspension by measuring the secondary sedimentation (Kozerski 1994). In a tailings pond where water is shallow and there is no primary sedimentation, sediment traps are used to measure the near bed cumulative resuspension and redeposition of tailings over a certain period of deployment.

The sediment traps used in this study are exactly the same as those used and described by Adu-Wusu et al. (2001) and Catalan (2002). The whole sediment trap assembly consists of two parts. The metallic sediment trap holder and cylindrical sediment trap made of clear polycarbonate with a diameter of 10 cm and a height of 40 cm as shown in Figure 3.2. The top part of the sediment trap is a hexagonal polycarbonate plate with slots at ends to facilitate sliding of the trap into its metal holder. The sediment trap can be pulled out and put back in the holder by means of two ropes attached to the hexagonal plate. The third rope is attached to the lid provided on the hexagonal plate. This rope is used to close and open the inlet of sediment trap whenever

required. The sediment trap can be easily sampled by means of a valve provided at the bottom of the trap; this valve was closed during operation. The metallic sediment trap holder is used to keep the sediment trap in place and maintain a vertical position. The trap holder is made of stainless steel with a diameter of 13 cm and depth of 53 cm, and is welded to stainless steel rods of about 1 m length.

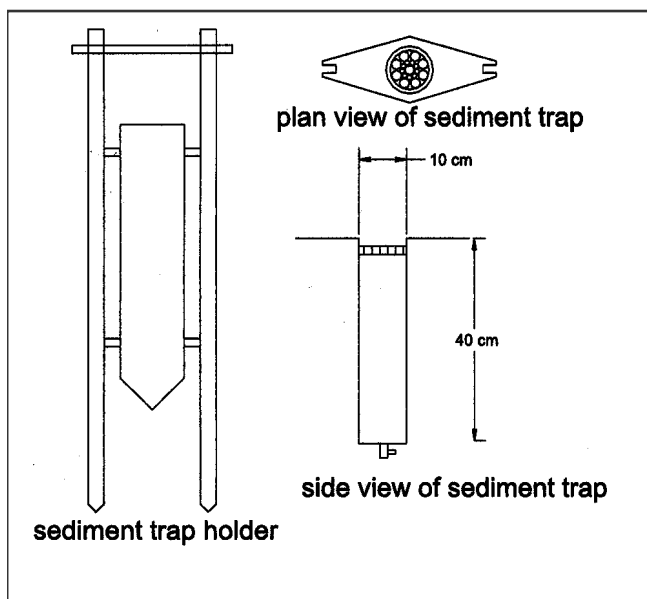


Figure 3.2 Schematic diagram of sediment trap (Adu-Wusu et al. 2001)

During installation the trap was hammered down into the tailings at the bottom of the pond. An extra pair of stainless steel rods was screwed onto the welded rods to provide extension. A polycarbonate slab was used to hold the rods in place. The sediment trap was placed in the holder by sliding it onto the steel rods and ropes attached to the sediment trap were tied to the slab to keep them visible out of the water.

Eight sediment traps were installed at selected locations in the tailings pond first time on July 26, 2006 to collect suspended and redeposited material in the water cover. Three sediments traps were installed in the east and west cells of the pond and two in the middle cell. The exact locations of the traps were recorded in terms of latitude and longitude using a handheld GPS device. The locations were selected to provide a good coverage of the tailings pond and to allow a comparison of the amount of resuspended material at different depths. The locations were assigned the identification numbers of ST-1 to ST-8 as shown in Figure 3.1. All sediment traps were sampled on August 30 and October 06, 2006, called Trip-1 and Trip-2 respectively in this paper.

The sediment traps were again installed on May 29, 2007 at the same locations (within GPS accuracy) using GPS data. The lids of the traps were opened two days after installation on May 31, 2007. First sampling was done on July 19, 2007 (Trip-3) and second on October 03, 2007 (Trip-4). Unfortunately, the top hexagonal plate of sediment trap ST-2 came off during sampling and the sample was lost.

3.3.2.2 OBS sensors:

The optical backscatter sensor or OBS sensor has been used extensively to record time dependent resuspension activity in coastal areas, lakes, streams and tailings pond. Osborne and Greenwood (1993) used an array of OBS sensors in the field to measure near bed sediment resuspension due to waves and currents. Malcolm and Boon (1993) used OBS in the laboratory to investigate the resuspension of non-homogeneous

sediments like silt/sand mixtures. OBS sensors have also been used to measure in situ erosion rate or sediment flux (Debnath et al. 2007; Bass et al. 2007).

In the present study, two OBS3+ sensors (Campbell Scientific Canada Corp., Edmonton, Alberta), also known as turbidity sensors, were used to measure the concentration of suspended sediments. The sensors must be installed at least 10 cm above the tailings bed to avoid scouring of sediments during period of strong flow. The OBS sensor consists of a high intensity infrared emitting diode (IRED) and an optical sensor that measures turbidity and suspended solids concentration by detecting infrared (IR) radiation scattered from suspended material in water. The IRED emits an infrared beam with half-power points at 50° in the axial plane of the sensor and 30° in the radial plane. The optical detector integrates the IR scattered between 140° and 160° . A filter absorbs visible light incident on the sensor. These sensors were connected to a CR10X datalogger (Campbell Scientific, Edmonton, Alberta, Canada) and programmed to measure the total suspended solids concentration every 5 minutes. The output was recorded in millivolts.

The response of an OBS sensor depends on the size, composition, and shape of suspended particles. For this reason, the OBS sensors must be calibrated with suspended solids from the water to be monitored. The two OBS sensors used in the study were calibrated in the laboratory using bed tailings from the west and middle cell of the site. Sensor readings in millivolts and gravimetric suspended solids concentrations in mg/L were recorded for distilled water alone (zero suspended solids) and then for known amounts of tailings added to distilled water to form suspensions. The calibration curves (mg/L versus millivolts) were all found to be linear ($R^2 = 0.9903$ to 0.9968) as shown in

Figure 3.3. The equations of the straight lines were then used to convert voltage outputs from the OBS sensors to total suspended solids concentration, recorded in the tailings pond. The detailed OBS calibration procedure is provided in the Appendix-I of the thesis.

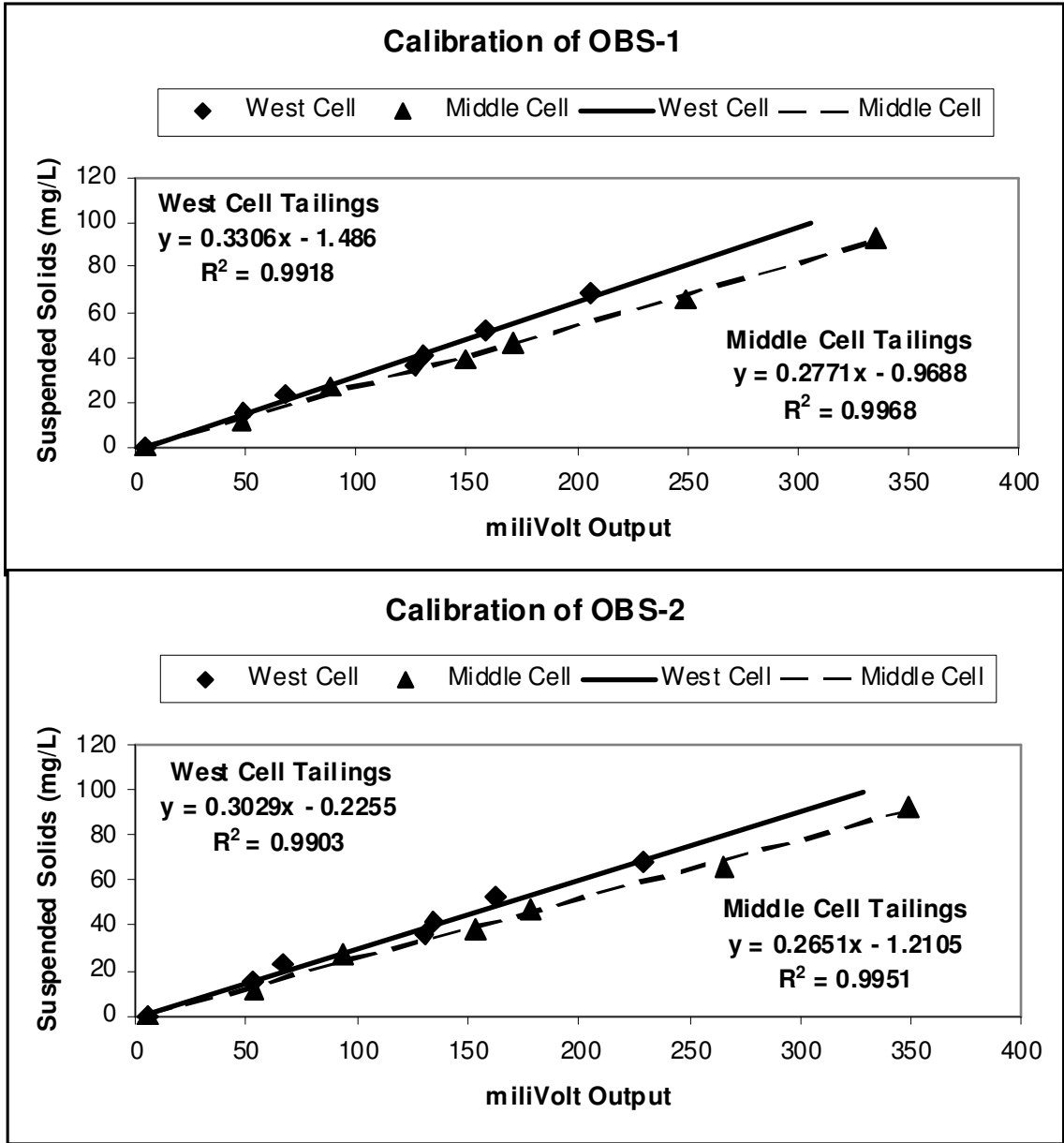


Figure 3.3 Field calibration curves of OBS sensors for West and Middle cell tailings

3.3.3 Characteristics of Bed Tailings

The particle size distributions of bed tailings collected near the location of each sediment trap were determined by sieve and hydrometer analysis and results are presented in Figure 3.4. The results show that bed tailings at all locations vary in particle size distribution. Bed tailings located between the wave break (ST 4 and ST 5) were finer than those at other locations. With the exception of tailings at ST8, all tailings fall in the silt to medium sand range (0.002-0.25 mm) with very small amounts ($\leq 5\%$) of clay size (< 0.002 mm) material. Bed tailings near ST8 contain a high amount of gravel. Given their finer sizes, bed tailings near ST4 and ST5 could be cohesive. The median grain size D_{50} (particle size below which 50% of the material is finer) is used as the representative particle size in subsequent computational analysis in the rest of this paper (Soulsby and Whitehouse 1997; Pohl 2004; Kubicki 2008). Some basic index and geotechnical properties of bed tailings determined by laboratory experiments are provided in Table 3.1.

3.3.4 A New Approach to Predicting Resuspension

Samad and Yanful (2005) developed a new approach to the design of a water cover for mine tailings. The method can calculate a minimum water cover depth to eliminate resuspension as well as an optimized cover water depth that allows tailings resuspension to a prescribed limit. During the analysis, the entire tailings pond is discretized into a mesh of square grids and the water depth is computed for each grid cell. The bed shear

stress is calculated for each grid cell accounting for the difference in fetch length for the particular square grid spacing. Input parameters include grid cell coordinates, wind data, pond geometry, median grain size of bed material, critical shear stress of bed material, and erosion test data (erosion coefficient and exponent) (see, Samad and Yanful (2005)).

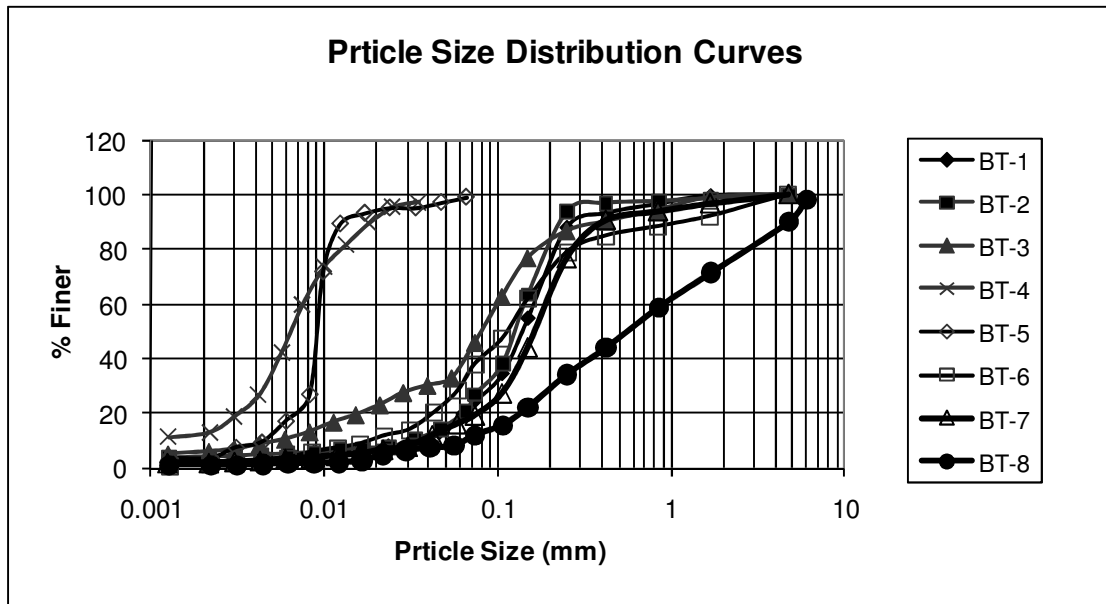


Figure 3.4 Particle size distribution curve of bed tailings samples collected from location of each sediment trap

The key computational steps used in the present study are summarized below.

1. Long-term (51 years for the present study) wind speed and wind direction data were analyzed statistically to determine wind speed for a design return period. A wind speed of 19.57 m/s was obtained for a 20-year return period. The tailings pond area was divided into a mesh of square grids of 50 m design spacing

interval. A value of fetch length (F) was calculated for each square grid cell according to the wind direction frequency distribution.

Table 3.1 Some basic characteristics properties of bed tailings

Sample No.	Colour	D ₅₀ (50% finer), mm	Specific Gravity, (G _s)	Friction Angle (ϕ), Degrees	Cohesion (c), Pa
BT-1	Black	0.15	2.71	35	0
BT-2	Black	0.14	2.71	38	0
BT-3	Black	0.08	2.73	38	0
BT-4	Grey	0.0064	2.78	34	11
BT-5	Grey	0.009	2.75	37	8
BT-6	Black	0.12	2.73	38	0
BT-7	Black	0.18	2.71	38	0
BT-8	Black	0.55	2.70	38	0

- Total bed shear stress was calculated at each square grid spacing using the calculated wind speed and fetch length from step one. Previous resuspension studies have indicated erosion and entrainment of sediments at the bottom of a water body is initiated when the shear stress exerted on a bed material exceeds its critical shear stress. Wind that blows over the water surface in the pond generates waves in the direction of the wind and return currents or countercurrents near the

bed (Wu and Tsanis 1995; Yang et al. 2002). The maximum total bed shear stress (τ_b) is assumed to have two parts: bed shear stress due to waves (τ_w), which is maximum shear stress over a complete wave period and bed shear stress due to countercurrents (τ_c). The total bed shear stress is given by following equation:

$$\tau_b = \tau_w + \tau_c \quad (3.1)$$

Resuspension occurs in a closed water body when the total bottom shear stress exerted by wind waves and currents exceeds the critical shear stress of the bed material (Partheniades 1965; Bengtsson et al. 1990). The rate of resuspension increases with wind speed in the direction of longest fetch (Mian and Yanful 2003). The erosion and resuspension of bed material for given wind conditions can be predicted by comparing the calculated bed shear stress to the estimated critical shear stress.

In the present study, the maximum bed shear stress exerted by wind waves was calculated using the SMB (Sverdrup-Munk-Bretschneider) method of wave characteristics (CERC 1984) and linear wave theory. Assuming shallow water wave conditions ($h/L < 0.5$), wave parameters, significant wave height, H and significant wave period T may be calculated using the following equations:

$$H_s = 0.283 \frac{U_a^2}{g} \tanh \left[0.530 \left(\frac{gh}{U_a^2} \right)^{3/4} \right] \tanh \left\{ \frac{0.00565 \left(\frac{gF}{U_a^2} \right)^{1/2}}{\tanh \left[0.530 \left(\frac{gh}{U_a^2} \right)^{3/4} \right]} \right\} \quad (3.2)$$

and,

$$T_s = 7.54 \frac{U_a}{g} \tanh \left[0.833 \left(\frac{gh}{U_a^2} \right)^{3/8} \right] \tanh \left\{ \frac{0.0379 \left(\frac{gF}{U_a^2} \right)^{1/3}}{\tanh \left[0.833 \left(\frac{gh}{U_a^2} \right)^{3/8} \right]} \right\} \quad (3.3)$$

where, U_A is wind stress factor ($= 0.71 U^{1.23}$, where U is wind speed (in m/s) measured at height of 10 m from water surface), h is water cover depth, F is the fetch length, g is the acceleration due to gravity and L is the significant wavelength (m) which can be calculated using the following equation:

$$L = \frac{gT^2}{2\pi} \sqrt{\tanh \left[\frac{4\pi^2 h}{T^2 g} \right]} \quad (3.4)$$

The maximum horizontal bottom velocity in shallow water is calculated using equation:

$$u_{bm} = \frac{\pi H}{T} \left[\frac{1}{\sinh \left(\frac{2\pi h}{L} \right)} \right] \quad (3.5)$$

The maximum displacement of fluid particles corresponding to maximum bottom velocity can be obtained as:

$$a_m = \frac{H}{2 \sinh\left(\frac{2\pi h}{L}\right)} \quad (3.6)$$

Using the above parameters, the bed shear stress due to wind induced waves can be calculated as (Jonsson 1966):

$$\tau_w = \frac{1}{2} f_w \rho u_{bm}^2 \quad (3.7)$$

where, $f_w = \frac{2}{\sqrt{R_w}}$ is the wave friction factor for laminar wave boundary;

$R_w = \frac{u_{bm} a_m}{\nu}$ is the wave Reynolds number and ν is kinematic viscosity of fluid

(m²/s). The value of wave Reynolds number R_w for the onset of turbulent flow is about 10⁵ for smooth bed conditions and varies from 10³ to 10⁵ for relatively rough bed conditions (Jonsson 1966; Samad and Yanful 2005). In most tailings pond studies including present study, wave Reynolds number was in the range of laminar wave boundary ($R_w < 10^5$) (Yanful and Catalan 2002; Samad and Yanful 2005). Jonsson (1966) calculated $R_w \geq 1.26 \times 10^4$ at the onset of turbulence.

Wind induced countercurrent flow in a water column has been studied experimentally by Baines and Knapp (1965), Tsuruya et al. (1983) and Yang (2000). Wu and Tsanis (1995) developed a numerical model for wind-induced counter current flow and verified it with laboratory experimental results. Shear stress at the bed due to currents can be calculated using the following equations

derived by Samad and Yanful (2005) based on the Wu and Tsanis (1995) approach of counter-currents and equation parameters determined by Yang et al. (2000) based on laboratory experiments:

$$\tau_c = \rho_w u_{*s}^2 \lambda z_{bh} (z_{sh} + 1) \times \left(\frac{A}{z_{bh}} - \frac{B}{z_{sh} + 1} \right) \quad (3.8)$$

The variables A and B in the above equation are given as:

$$A = \frac{q_2}{p_1 q_2 - p_2 q_1} \quad \text{and} \quad B = \frac{-q_1}{p_1 q_2 - p_2 q_1} \quad (3.9)$$

where,

$$\begin{aligned} p_1 &= \lambda z_{sh}; \\ p_2 &= \lambda z_{sh} / z_{bh}; \\ q_1 &= (1 + z_{sh}) \ln \left(1 + \frac{1}{z_{sh}} \right) - 1; \text{ and} \\ q_2 &= z_{sh} \ln \left(1 + \frac{1}{z_{bh}} \right) - 1; \end{aligned}$$

The variables z_{sh} ($=2.2 \times 10^{-4}$) and z_{bh} ($=1.4 \times 10^{-4}$) are the surface and bottom characteristic lengths, respectively, and are calculated based on experimental data (Yang et al. 2000). The parameter λ is a constant that depends on the intensity of turbulence in water. It varies from 0.2 to 0.5 with an average value of about 0.35. The variation in the values of these parameters affects mainly the near surface shear stress but has little influence on the bed shear stress (Yang 2002; Samad and Yanful 2005). The surface shear velocity of water u_{*s} is given by

$$u_{*s} = 0.035U \sqrt{\frac{\rho_a}{\rho_w}} \quad (3.10)$$

Where U is the wind speed (m/s), ρ_a is the density of air (kg/m^3) and ρ_w is the density of water (kg/m^3). The countercurrent induced bed shear stress calculated using the above equations depends on wind speed and water cover depth.

3. The required minimum water cover depth was calculated by comparing the total bed shear stress at each square grid cell and the critical shear stress of the bed material. To eliminate resuspension total bed shear stress must theoretically be less than the critical shear stress of bed material. For the present study, critical shear stress was calculated using Fischenich's (2001) method as mentioned in the section 3.5 of this paper.
4. Finally, the suspended tailings concentration was calculated using a generalized power law relationship (Equation 3.11) for erosion.

$$E = \alpha \left(\frac{\tau_b - \tau_{cr}}{\tau_{cr}} \right)^M \quad (3.11)$$

Here, E is the erosion rate ($\text{kg/m}^2 \cdot \text{s}$), τ_b and τ_{cr} are the total bed and critical shear stress, respectively, coefficient (α) and exponent (M) are erosion rate parameters and can be determined by laboratory erosion test results. In the present study coefficient (α) and exponent (M) for the west cell tailings obtained from Geremew

and Yanful (2010) were used to predict resuspension in the west cell. The suspended solids concentration (mg/L) can be calculated from $c_i = E_i/h_i$, assuming an even distribution of resuspended material in the entire column of water depth. In addition to the aspects covered in the present study, the method of Samad and Yanful (2005) can also predict the sulphate production in the tailings pond, provided the site-specific oxidation rate of bed tailings is known.

3.3.5 Critical Shear Stress

The critical shear stress is the minimum mobilized bed shear stress required to initiate sediment motion. It is a characteristic property of bed material and depends on physical and chemical properties of material such as particle size, cohesiveness, cementation, and degree of consolidation. Apart from measurement using various experimental methods, the critical shear stress of tailings can also be approximately calculated using empirical equations.

Fischenich (2001) proposed the following equation to approximate the critical shear stress of silt and sand sized particles:

$$\tau_{cr} = 0.25d_*^{-0.6} (\gamma_s - \gamma_w)d \tan \phi \quad (3.12)$$

where,

$$d_* = d \left[\frac{(G-1)g}{\nu^2} \right]^{1/3} \quad (3.13)$$

Here, ϕ is the angle of repose of particle, G is the specific gravity of bed material, g is the acceleration due to gravity, γ_s is the unit weight of sediment, γ_w is the unit weight of water, ν is the kinematic viscosity, d is the particle size of sediment. The median grain size D_{50} (particle size below which 50% of the material is finer) was used as the representative particle size of the bed tailings sample in the calculation of the critical shear stress (Soulsby and Whitehouse 1997; Pohl 2004; Kubicki 2008). The value of angle of repose ϕ , specific gravity (G) and median grain size D_{50} of bed tailings were used as tabulated in Table 3.1.

The critical shear stress (τ_{cr}) was estimated using the approach by Fischenich (2001) and D_{50} as the representative particle size. The critical shear stress varies from 0.04 Pa at station 4 to 0.25 Pa at station 8. The critical shear stress is very small (0.04 Pa) for middle cell bed tailings at station 4 and 5 due to the fine particle size (D_{50} 0.0065 and 0.009 mm respectively). For the east and west cells, the critical shear stress is almost similar except at station 8 where the bed material is coarser. The average value of the critical shear stress of 0.13 Pa for east and west cells can be used in the analysis. Experimentally measured values of critical shear stress of tailings from other sites in Canada show almost similar values, for example, 0.12 Pa for the Heath Steele upper cell, New Brunswick (Yanful and Catalan 2002); and 0.09 Pa for the Falconbridge site, Ontario (Bennett 2002). Adu-Wusu (2001) estimated the critical shear stress of bed tailings and reported values in the range of 0.12 to 0.22 Pa. The critical shear stress values calculated for the Shebandowan site are of similar order of magnitude as compared to other sites.

Fischenich's (2001) equation does not account for cohesive properties of fine particles. The presence of binding cohesive forces in fine particles can increase the resistance to erosion and resuspension. The critical shear stress for the middle cell particles may be higher than calculated by Fischenich's (2001) method due to the presence of cohesion.

3.4 RESULTS AND DISCUSSION

3.4.1 Wind Data Analysis

At the Shebandowan site, the period May-November is the only time when both strong wind storm events and unfrozen tailings pond water conditions may be expected. Thus analysis was carried out only for this 7-month period in the 2006 and 2007 years. Wind speed (in m/s) and wind direction (degrees from North) data recorded and averaged every 15 minutes were used in the analysis. The observed maximum wind speed for each month was above 10 m/s for both years. The average maximum wind speed was 12.57 m/s for year 2006 (May to November) and 12.00 m/s for year 2007. Long-term wind data of the last 51 years recorded at Thunder Bay airport were obtained from Environment Canada. The wind direction frequency distribution for data recorded on site during years 2006 and 2007 and long-term wind data are presented in Figure 3.5. The data show that the most dominant wind direction at the site is 270° to 315° from the north (that is, northwest). This would explain the design (location and orientation) of the wave breaks shown in Figure 3.1. Without the breaks, the fetch in the direction of the dominant winds would

have been quite long (up to 1650 m) resulting in significant tailings erosion and resuspension.

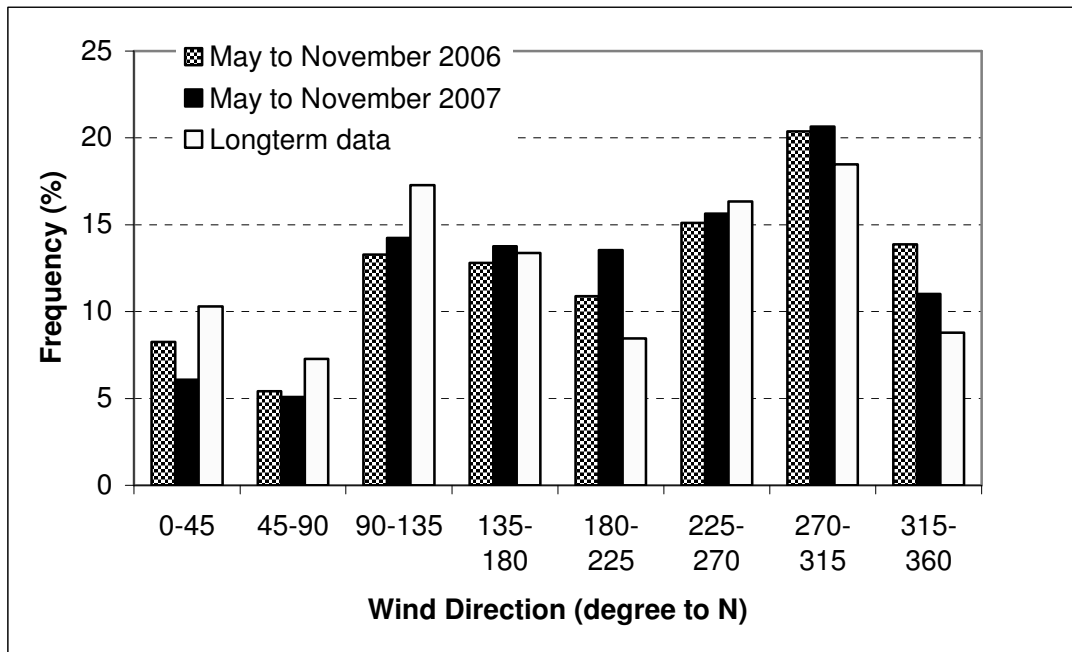


Figure 3.5 Wind direction frequency distribution plotted for summer (May to November) months of year 2006, 2007 and for long-term wind data

3.4.2 Evaporation and Precipitation

Knowledge of onsite evaporation and precipitation gives an indication of the total water demand required to provide a certain water cover depth. The total evaporation during each Trip in the study was calculated using the following method. Total evaporation consists of evaporation from radiation and evaporation from mass transfer/aerodynamics and is given by the following equation (Thomson 1999).

Total Evaporation = Evaporation from radiation + Evaporation from mass transfer/aerodynamics

$$E_0 = \frac{\Delta}{\Delta + \gamma} E_n + \frac{\gamma}{\Delta + \gamma} E_a \quad (3.14)$$

where,

Δ = Rate of change in saturation vapor pressure with temperature = de_s/dT

$$= (0.000815T + 0.8912)^7$$

γ = Psychometric constant ($\cong 0.66 \text{ mb}^0\text{C}^{-1}$)

E_a = Mass transfer/aerodynamic evaporation = $(0.013 + 0.00016U) * (e_s - e_a)$

U = Wind speed (km/day)

e_s = Saturation vapor pressure of air (mb) = vapor pressure of water surface $e_a =$

e_a = Vapor pressure of air = $f * e_s$

f = Relative humidity (%)

E_n = Net evaporation due to radiation = $Q_n / \rho L_v$

Q_n = Net radiation ($\text{cal cm}^{-2} \text{ day}^{-1}$) ($1\text{W/m}^2 = 2.016 \text{ cal cm}^{-2} \text{ day}^{-1}$)

L_v = Latent heat of vaporization (cal/g) = $597.3 - 0.564T$

ρ = Density of water (1 g/cm³)

The input data in the above evaporation formula, for example, temperature (T), radiation (Q_n), relative humidity (f), and wind speed (U) were recorded by the weather station installed at the site. Evaporation was calculated for two scenarios. First, maximum evaporation was calculated using daily measured maximum wind speed, maximum temperature, maximum radiation, and minimum relative humidity. In the second case, evaporation was calculated using daily measured averaged values of wind speed, temperature, relative humidity and radiation. The precipitation at Shebandowan site was recorded by a rain gauge installed at the weather station. Evaporation calculated for each Trip is tabulated below in Table 3.2.

Table 3.2 On site recorded precipitation and calculated evaporation during different trips

Trip	I	II	III	IV
Period of Deployment (days)	32	34	49	72
Total Precipitation (cm)	10	6	16	23
Total Maximum Evaporation (cm)	84	75	138	169
Total Average Evaporation (cm)	23	21	65	49
Daily Maximum Evaporation (cm/day)	2.63	2.21	2.82	2.35
Daily Average Evaporation (cm/day)	0.72	0.62	1.32	0.68

The calculated average evaporation was significantly higher than the recorded precipitation during sediment trap deployment periods (Trips) as shown in Figure 3.6. The data show the need for additional water to be pumped into the tailings pond to provide sufficient water depths to eliminate or decrease tailings resuspension. Seepage losses from the pond add to water demand.

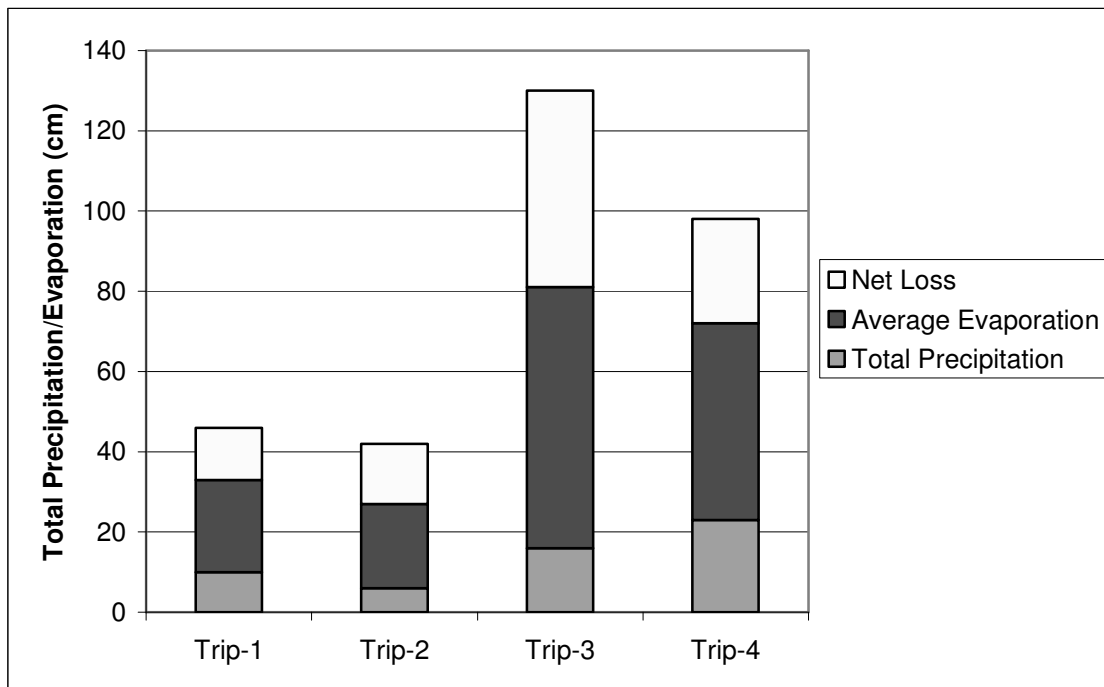


Figure 3.6 Total precipitation and total average evaporation during each Trip

3.4.3 Water Cover Depth to Eliminate Resuspension

The minimum water depth required to protect the tailings bed and resuspension at each grid was calculated. The computation was performed for the whole pond neglecting the

presence of wave breaks (internal dykes) and for each cell of the pond (in the presence of wave breaks) separately. The whole pond area and each cell area were discretized into a grid of 50 m intervals, as shown in Figure 3.7. The fetch length for each grid cell was determined according to pond geometry and wind direction distribution. Contour plots of the fetch length for the whole pond and for the east and west cell are shown in Figure 3.8. The presence of wave breaks in the pond significantly decreases the fetch length considerably, which could result in none or reduced erosion of bed depending on the water cover depth.

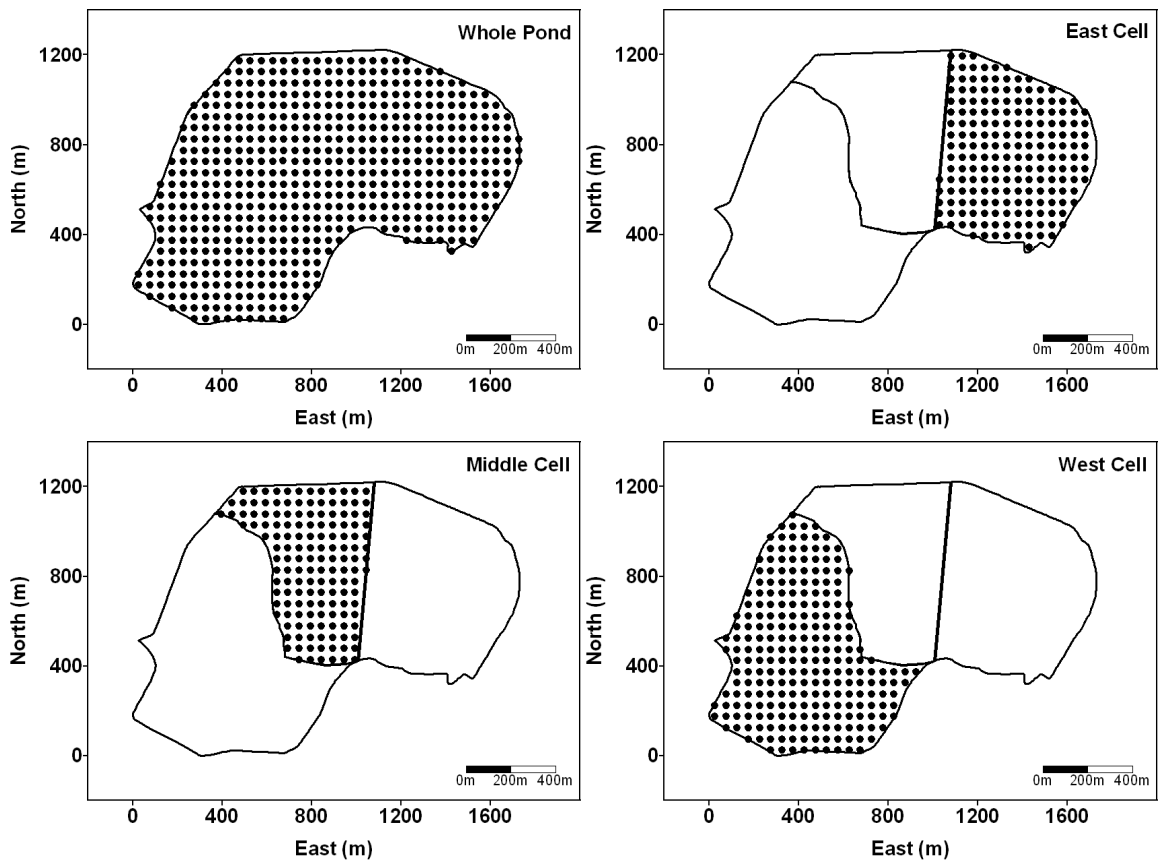


Figure 3.7 Shebandowan mine tailings pond boundary and location of square grids of 50 m interval for whole pond and west, middle and east cells

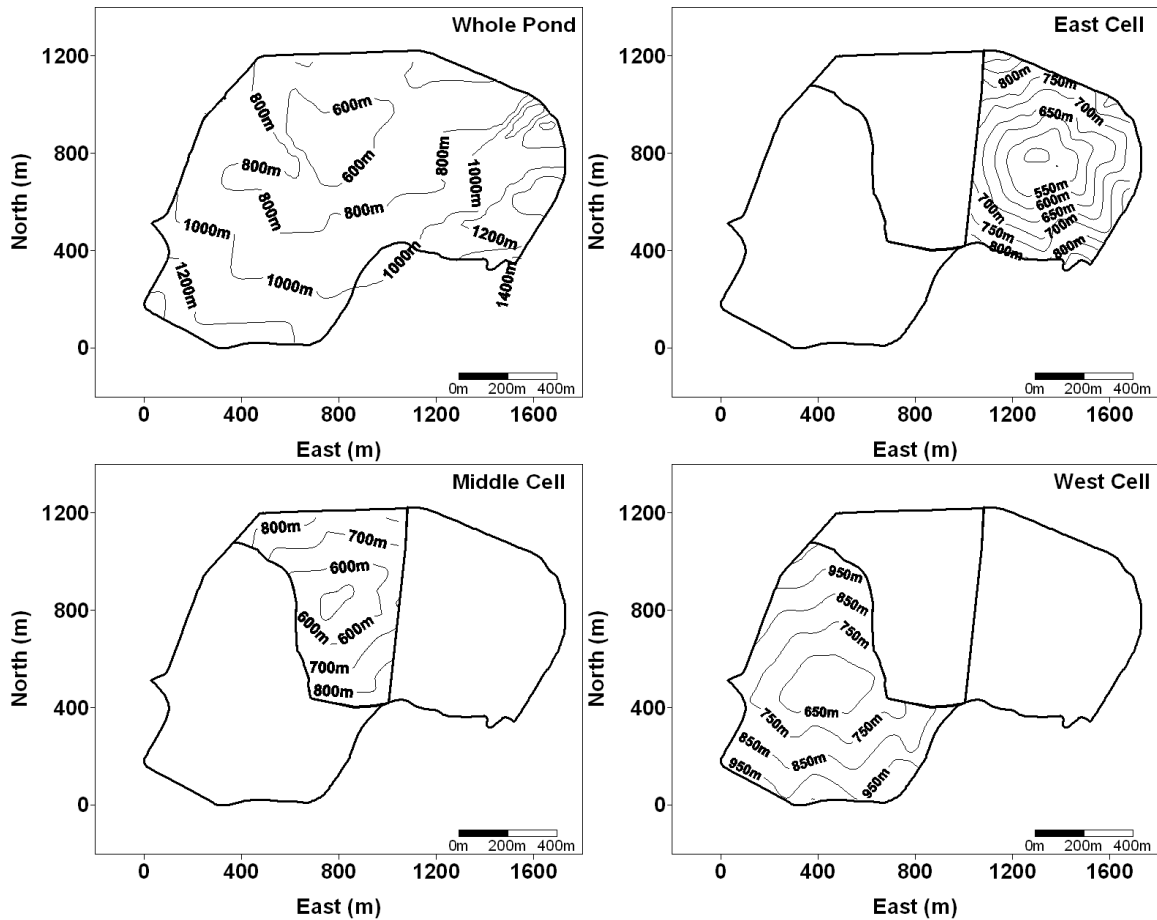


Figure 3.8 Contour plots of fetch length (in m) for whole pond (without wave breaks) and each cell (with wave breaks)

The minimum water cover depth for each grid was determined by comparing the total bed shear stress (Equation 3.1) with the critical shear stress of bed material and by assuming that, there is no resuspension for a specific water depth when the total bed stress is less than the critical shear stress. Figure 3.9 presents contour plots of required minimum water depth computed for the whole pond (without wave breaks) and for each cell (with wave breaks) separately. To see the effect of wave breaks, a uniform 0.12 Pa value of critical shear stress was used throughout the pond including the middle cell where actual calculated critical shear stress was equal to 0.04 Pa.

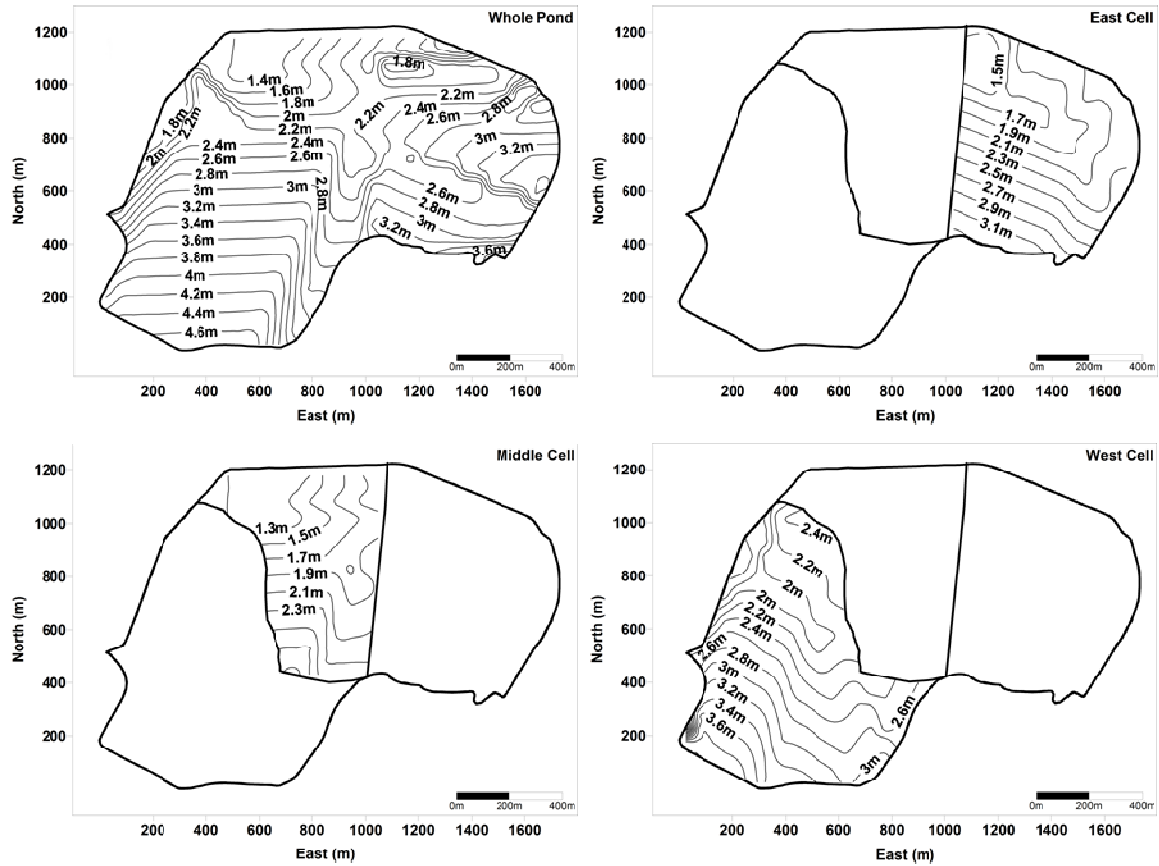


Figure 3.9 Contours of minimum required water cover depth to completely eliminate resuspension for whole pond and each cell

In the absence of wave breaks, the minimum required depth of water cover for the whole pond varies between 1.23 m to 4.74 m. The contour plot (Figure 3.9) shows that the maximum water depth of the whole pond is required in the southwest section. In the presence of wave breaks or dykes, each cell of the pond can be treated as a separate water body. Water cover requirements depend on the size and geometry of each cell. The required water depth for the east cell varies from 1.3 m to 3.3 m and, for the west cell, from 1.4 m to 3.6 m and for the middle cell, from 1.1 m to 2.8 m. These results show that

the wave breaks have significantly reduced the water cover depth requirements at the Shebandowan tailings storage facility.

Particle size distribution of middle cell tailings showed that bed tailings are very fine in nature and therefore actual predicted minimum water cover depth is 5.0 m in the entire middle cell area, due to the very small value of the critical shear stress (0.04Pa) of the tailings. The Fischenich's empirical formula for estimating the critical shear stress does not account for cohesive properties of fine particles and may have underestimated the critical shear stress.

3.4.4 Resuspension Measured with Sediment Traps

The sediment trap data are presented in Table 3.3. As indicated, the dry mass of collected suspended material varied from 0.18 g in sediment trap 4 during Trip-2 to 6.50 g in sediment trap 3 during Trip-3. An exceptionally high amount of 31.82 g was recovered from sediment trap 6 during Trip-1, but this high amount was not repeated and was therefore considered an outlier.

These observed amounts of resuspension are not as high as those reported for the Heath Steele Mines tailings pond located in New Brunswick, Canada, where up to 54 g of suspended material was collected at some locations (Catalan and Yanful 2001). However they are comparable to resuspended tailings amounts observed at the Quirke Cell 14 tailings site, near Elliot Lake, Ontario (Adu-Wusu et al. 2001; Yanful and Catalan 2002). The difference in the amount of resuspended tailings may be attributed to the different

particle size distributions. Finer particles have low critical shear stress as previously mentioned in this paper and hence can be resuspended more easily than coarser particles. The Heath Steele tailings had a finer nature than the Quirke tailings. With the exception of locations 4 and 5 (ST4 and ST5), the bed tailings at the Shebandowan site (present study) were sandy and coarse, similar to tailings from the Quirke site. At locations 4 and 5 of Shebandowan, bed tailings were finer and likely, of cohesive nature.

Table 3.3 Total suspended solids (TSS) collected in sediment traps and corresponding water cover depth

Sediment Trap No.	Trip-1 (32 days ¹)		Trip-2 (34 days)		Trip-3 (49 days)		Trip-4 (72 days)	
	TSS (g)	Depth of water (cm)	TSS (g)	Depth of water (cm)	TSS (g)	Depth of water (cm)	TSS (g)	Depth of water (cm)
ST-1	1.80	99	0.31	86	1.03	86	1.44	88
ST-2	6.03	91	0.47	81	Broken	--	Broken	--
ST-3	1.78	93	3.21	91	4.60	89	1.70	95
ST-4	2.22	150	0.18	152	4.30	142	1.89	152
ST-5	4.00	211	0.72	213	6.50	130	2.10	140
ST-6	31.82 ²	95	0.52	97	1.01	91	1.65	93
ST-7	1.46	241	0.31	117	1.14	136	1.84	144
ST-8	3.95	93	0.36	104	0.8	124	0.96	137

Notes: TSS = Total Suspended Solids, ¹ = Period over which sediments traps were deployed, ² = Outlier

However, no correlation was found between water cover depth and amount of suspended material during each trip (Figure 3.10). This could be a result of sediment transport of tailings from one station to the other due to waves and currents following erosion. During the period that it is deployed, a sediment trap would collect not only eroded material at particular location, but also material that has been eroded and transported from a different location and re-deposited at the location of the trap. Thus water cover depths may not always correlate with amount of material collected in sediment traps especially if there is significant bed movement.

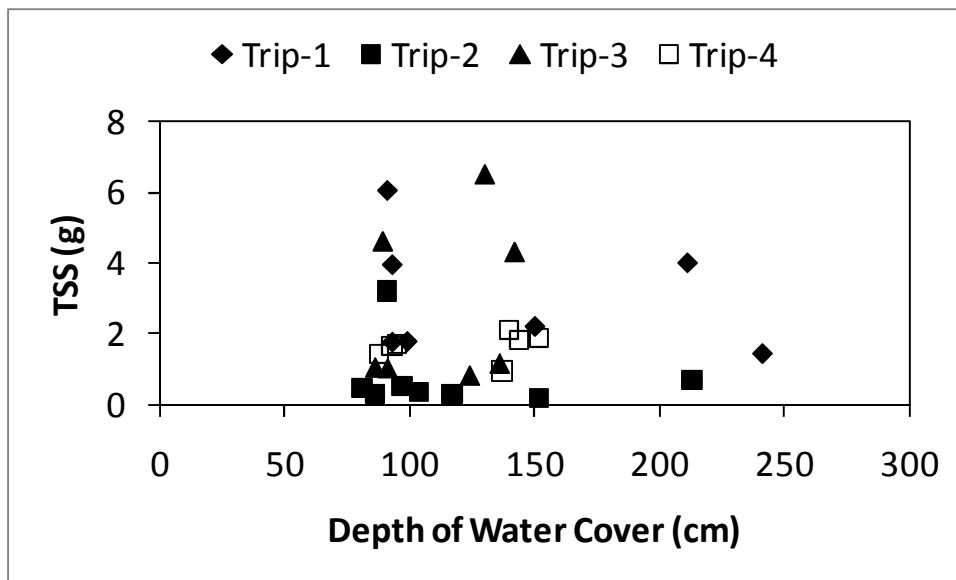


Figure 3.10 Total suspended solids collected in sediment traps versus depth of water cover

These results are similar to those observed for the Heath Steele site (Catalan and Yanful 2001). Bed shear stress may decrease with increasing water cover depth at a

specific wind speed but wind direction or fetch length is also a major factor that can influence the amount of resuspension. Sediment trap data represent the cumulative effect of several wind events each of which may have a different direction or fetch length and hence different bed shear stress for each sediment trap location. Thus a simple correlation between depth and resuspended amount (measured by sediment traps) may not always exist.

3.4.5 Mineralogical and Elemental Analysis of Suspended and Bed Material

Bed tailings sampled from the same locations as the sediment traps and resuspended material collected in the sediment traps were vacuum dried to perform mineralogical and elemental analyses. X-ray diffractograms showed that both bed and resuspended tailings do not contain much clay mineral (Figure 3.11). This was later verified by clay fractionation of the samples. The only clay mineral identified in X-ray powder analysis was chlorite. Non-clay minerals identified in the diffractograms are quartz, pyrite, pyrrhotite, feldspar, calcite and dolomite. X-ray diffractograms of bed and resuspended materials show similar peaks but of different heights or intensities. Figure 3.11 shows, that the chlorite peak intensity for the bed tailings at ST-5 in the middle cell is slightly higher than at ST-2, suggesting higher clay content at ST-5 as indicated in the grain size curves. Resuspended material shows reduced intensity of pyrrhotite and pyrite peaks relative to those of the bed material. This could be because of the oxidation of pyrrhotite and pyrite in resuspended tailings. X-ray diffractograms of remaining resuspended and bed tailings samples are provided in the Appendix-II at the end of this thesis.

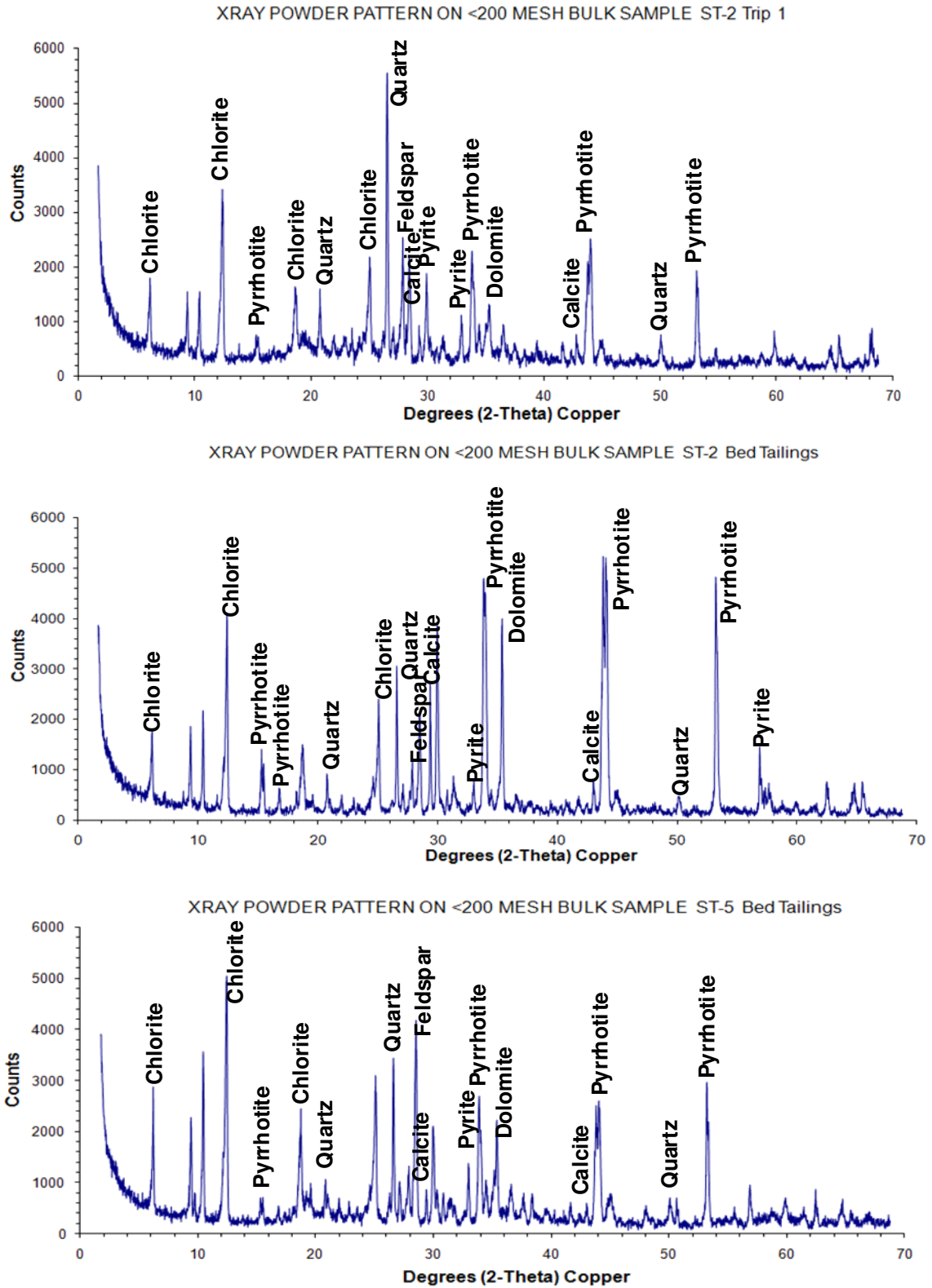


Figure 3.11 X-ray diffractograms of resuspended material collected at ST2 during Trip-1 and bed tailings at ST-2 and ST-5

Elemental analysis showed that both bed and resuspended tailings are rich in iron and sulphur. Iron concentration in bed tailings vary from 10.23 % to 45.16% (by weight) and in resuspended tailings from 9.90% to 22.66% (by weight) while sulphur concentration vary in bed material from 0.28 % to 36.40% (by weight) and in resuspended tailings from 1.05 % to 35.20% (by weight). Other major elements are Si, Cu and Ni (Tables 3.4 and 3.5). A comparison of selected elemental composition of bed tailings and resuspended tailings with typical crustal composition has presented in Table 3.6. The elemental composition of resuspended tailings (collected in sediment traps) showed much higher amount of elements such as S, Fe, Cu, Ni, Pb, and Zn than the typical crustal composition (Wedepohl 1995). Since the Shebandowan site has been remediated and all tailings have been collected and deposited in the tailings pond under water cover. Natural soil material at the site would not be expected to contain Fe, S, Cu, Ni, Pb, and Zn at concentrations similar to those of the bed tailings. It is clear that the sediment trap samples (ST-1 to ST-8) in Tables 3.4 and 3.5 were derived from mine tailings because of their relatively high sulphur (S) and heavy metal concentrations.

The mineralogy and elemental analysis results strongly indicate that material collected in the sediment traps come from bed tailings and not from outside the tailings pond. This would indicate that wind-induced erosion of bed tailings and entrainment into the water cover may be occurring at the Shebandowan site. However, elemental concentrations of bed and resuspended tailings were not correlated because of possible sediment transportation and redeposition from one station to other.

Table 3.4 Composition of Tailings: Major Oxides in wt% by XRF (BT = Bed tailings & ST = Suspended Tailings)

Sample ID	SiO ₂	TiO ₂	Al ₂ O ₃	Fe ₂ O ₃	MgO	MnO	CaO	K ₂ O	Na ₂ O	P ₂ O ₅
BT-1	10.66	0.21	0.01	65.21	4.53	0.11	1.83	0.01	0.01	0.04
ST-1	30.95	0.21	0.01	18.89	5.22	0.18	7.26	0.36	0.38	0.16
BT-3	43.16	0.32	9.71	14.62	16.75	0.18	4.50	0.42	0.59	0.07
ST-3	36.21	0.31	3.80	26.02	11.71	0.16	4.64	0.30	0.75	0.10
BT-5	42.13	0.29	8.44	15.37	17.09	0.19	4.77	0.50	0.69	0.01
ST-5	34.14	0.32	3.32	32.40	11.44	0.18	3.13	0.30	0.57	0.09
BT-6	27.09	0.34	0.01	43.57	8.87	0.16	4.06	0.25	0.32	0.07
ST-6	25.92	0.19	0.01	14.16	5.23	0.50	17.04	0.35	0.48	0.14
BT-7	19.53	0.29	0.01	50.60	7.21	0.11	2.15	0.13	0.01	0.07
ST-7	28.77	0.19	2.18	22.79	5.58	0.72	4.33	0.38	0.41	0.39
BT-8	49.68	0.70	8.92	19.06	4.32	0.10	4.78	1.05	2.06	0.13
ST-8	34.57	0.25	4.52	20.40	6.05	0.50	6.81	0.55	0.91	0.01
ST-4	43.57	0.36	6.99	14.50	14.57	0.23	6.34	0.32	0.93	0.10

Table 3.5 Tailings Composition: Trace elements in µg/g by ICP-AES (BT = Bed Tailings & ST = Suspended Tailings)

Sample ID	Ag	As	Cd	Cu	Ni	Pb	S	Zn	U	Th
BT1	< 0.01	< 0.01	70.5	566	3950	367	18.70%	58	< 0.01	4.56
ST1	< 0.01	12.70	20.7	596	2200	179	35.20%	116	< 0.01	< 0.01
BT3	< 0.01	3.76	12.2	684	2400	176	0.28%	118	< 0.01	< 0.01
ST3	< 0.01	< 0.01	26.6	698	2540	139	5.70%	110	< 0.01	< 0.01
BT5	< 0.01	8.96	13.1	671	3160	145	0.67%	137	< 0.01	< 0.01
ST5	< 0.01	9.86	33.4	803	2070	167	7.35%	94	< 0.01	3.94
BT6	< 0.01	7.28	41.8	1060	4170	215	11.10%	116	< 0.01	0.49
ST6	< 0.01	14.60	15.6	441	1750	111	2.31%	103	< 0.01	< 0.01
BT7	< 0.01	< 0.01	50.9	1130	3090	232	12.80%	71	< 0.01	2.13
ST7	< 0.01	36.30	24.2	541	2250	176	2.08%	139	< 0.01	1.57
BT8	< 0.01	< 0.01	16.5	1030	1570	120	36.40%	50	< 0.01	0.91
ST8	< 0.01	9.37	23.8	570	2210	167	2.75%	97	< 0.01	< 0.0
ST4	< 0.01	2.11	11.8	787	1280	82	1.05%	117	< 0.01	< 0.01

Table 3.6 Concentration of selected elements in tailings compared to typical crustal composition^a (Fe is in weight % as oxide and other elements in µg/g)

Sample	Cu	Ni	Pb	Zn	S	Fe ₂ O ₃ (as
Location	(µg/g)	(µg/g)	(µg/g)	(µg/g)	(µg/g)	Oxide in wt %)
BT-1	566	3950	367	58	18.7x10 ⁴	65.21%
ST-1	596	2200	179	116	35.2x10 ⁴	18.89%
BT-5	671	3160	145	137	6700	15.37%
ST-5	803	2070	167	94	73500	32.40%
Crustal Composition ^a	14.3	18.6	17	52	953	4.32%

Notes: ^a = Wedepohl (1995)

3.4.6 Resuspension Data from OBS Sensors

As previously mentioned, two OBS sensors were installed in the tailings pond to identify temporal variations in resuspension and possible correlation with wind activity. The output from the OBS sensors was recorded every 5 minutes and then averaged every 15 minutes for comparison with corresponding wind data. The main limitation in selecting the location of the OBS in the pond was the length of cable connecting the OBS sensor to the datalogger. As the cable for each sensor was only 30 m, the distance from sensor to shore was only approximately 24-27 m. The locations of OBS sensors in the west and middle cells of the pond are shown in Figure 3.1. The OBS data and relations to wind events at the site are discussed in the sections that follow.

Case I: OBS in middle cell, July 19 to 21, 2007:

During this period both OBS sensors were installed in the middle cell of the pond near the wave break dyke dividing the east and middle cells. The sensors were located 15 m from each other and 10 cm above the tailings bed. The depth of water cover at the locations of both sensors was approximately the same (71 cm). During this period (July 19-21, 2007) both wind direction and speed changed rapidly and wind speed was quite low (maximum of 4 m/s). The most favoured wind direction for resuspension to occur in the middle cell was 270-360 degrees to north (northwest). Wind blowing in this direction had the longest fetch in the middle cell.

Initially, the wind blew along $0-45^{\circ}$ to north (northeast direction) with a speed of approximately 3 m/s. Results from both OBS sensors show that the suspended solids concentration in the water was negligible. Wind blowing in the northeast direction had negligible fetch length to initiate resuspension at both OBS locations. At approximately 08:15 PM (July 19, 2007) and after, wind was slowing down and also changing direction. At this time, even though the wind speed was relatively low (approximately 2 to 2.5 m/s), the changing direction allowed wind to blow over the longer fetch of the tailings pond. This likely resulted in resuspension, as indicated by the peaks of suspended solids concentration in water (Figure 3.12). The suspended solids concentration reached up to a maximum value of 25.1 mg/L for OBS-1 and 37.5 mg/L for OBS-2 sensor. Considering the slow wind, this is a significant value of resuspension. At approximately 9:45 PM (July 20, 2007), when wind speed was 3.5 m/s and wind direction changed from

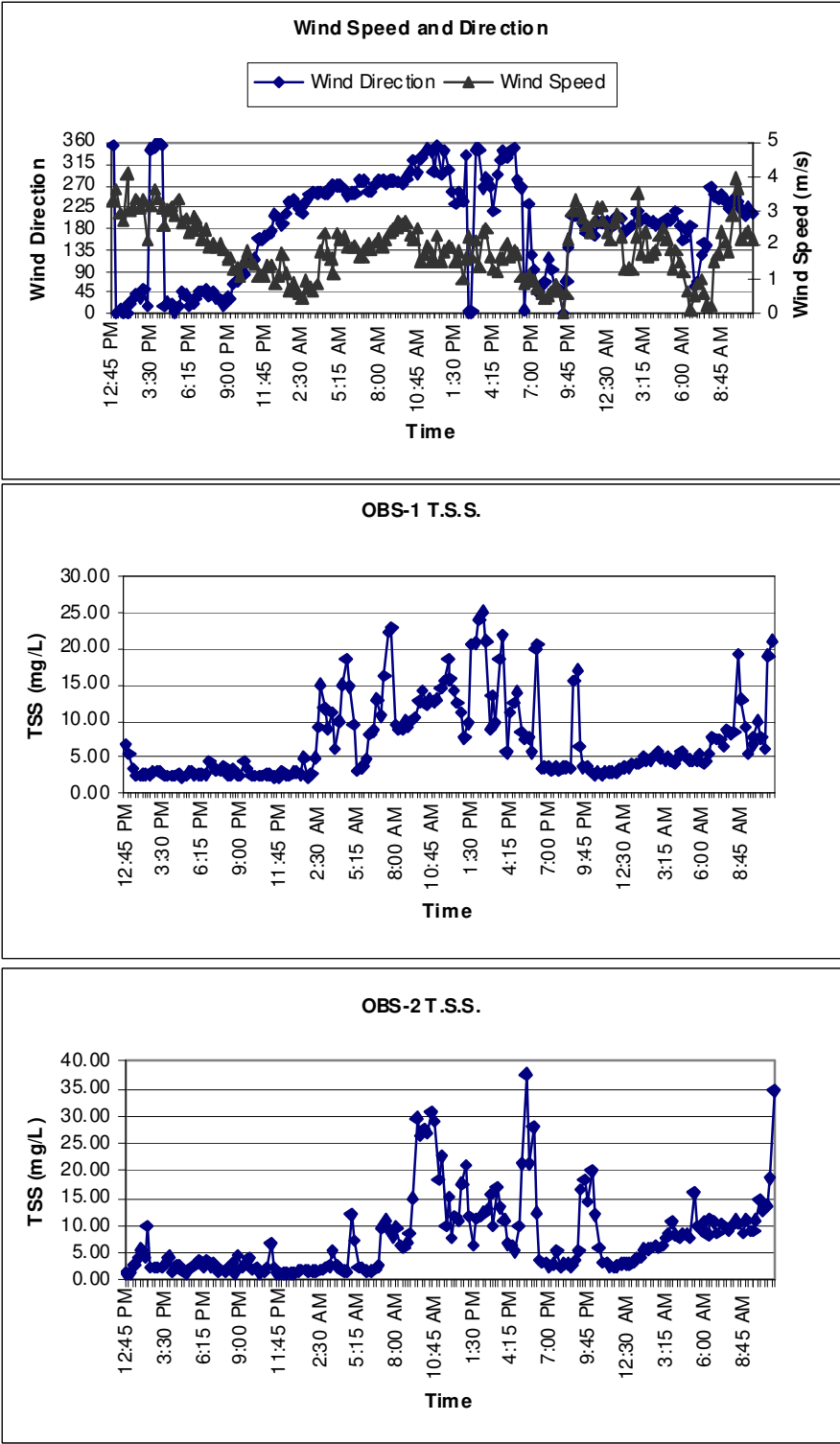


Figure 3.12 Case I: Time series results of total suspended solids concentration (TSS) measured by OBS-1 and OBS-2 on July19 to 21, 2007 in the middle cell with corresponding wind data

southeast to southwest direction (180-225 degree to North), a higher value of suspended solids concentration of 17 mg/L for OBS-1 and 20 mg/L for OBS-2 resulted.

Case II: OBS in West cell, July 21 to 23, 2007:

On July 21, 2007 the two OBS sensors were removed from the middle cell and installed in the west cell at approximately 20 m from each other and 10 cm above the tailings bed. The water cover depth was approximately 0.51 m at the location of OBS-1 sensor and 0.42 m at OBS-2 sensor. The sensors recorded suspended solids concentrations till 12:00 noon of July 23, 2007. At the locations of the OBS sensors, the most important wind direction that covered the longest fetch length and caused resuspension of tailings was northeast. Winds blowing from 45-180 degrees to the north also likely contributed significantly to resuspension.

The suspended solids concentration recorded by OBS-1 was quite low in comparison with the records from OBS-2. The main reason for the difference could be the greater water depth at OBS-1. It can be seen that the dominant wind direction that can produce the most amount of resuspension was not present during the entire monitoring period. As indicated in Figure 3.13, peaks of suspended solids concentration for both sensors occur, when wind was in the southerly direction (180° from North). During this time the maximum wind speed was approximately 5 m/s and the maximum recorded suspended solids concentration was 7.5 mg/L for OBS-1 and 18 mg/L for OBS-2. Again

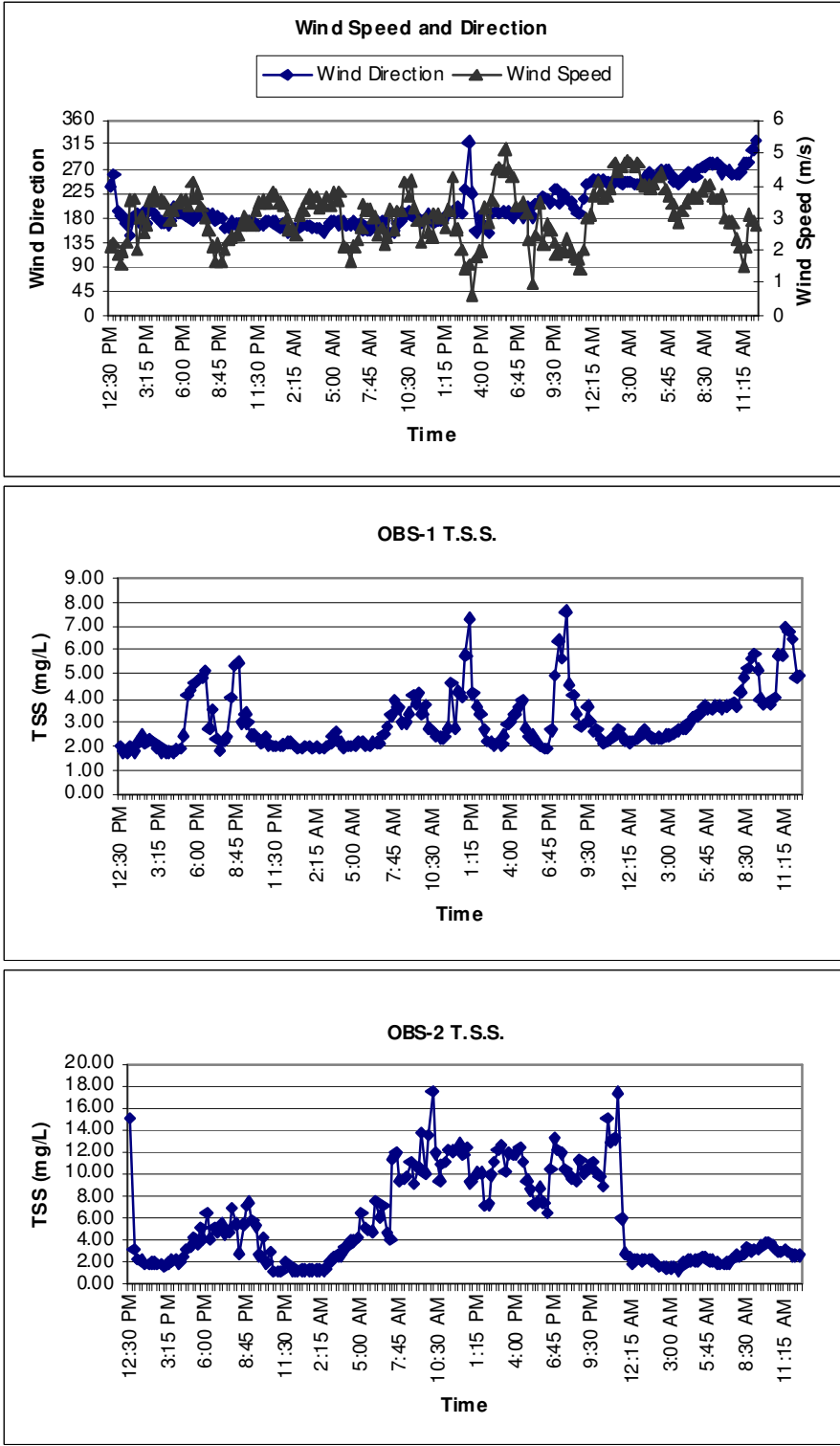


Figure 3.13 Case II: Time series results of total suspended solids concentration (TSS) measured by OBS-1 and OBS-2 on July21 to 23, 2007 in the west cell with corresponding wind data

the difference may be attributed to the slightly deeper water cover at OBS-1, which meant that wind-wave activity was relatively less at that location.

Case III: OBS in West cell, October 04, 2007:

OBS records obtained on October 04, 2007 for the west cell are presented in Figure 3.14. The selected location was the same as it was for OBS-1 in Case II, but at different heights from the tailings bed. OBS-1 was at a height of 25 cm while OBS-2 was 10 cm above the bed. As expected, the amount of suspended solids concentration recorded from OBS-2 was higher than from OBS-1. The depth of water cover at this location was about 0.70 m. As discussed in Case II, the most important wind directions at this location were 0-45⁰ to north (northeast to southwest) and 45-180⁰ to north (east to west) and could contribute to significant resuspension.

The wind data show that wind direction was consistently 200⁰ to 300⁰, which is not at all the direction that covers the longest fetch over pond water. Even if the wind speed was approximately 5 m/s and above for most of the time, the data from both sensors showed almost no resuspension. Most of the time, the suspended solids concentration in water was below 6 mg/L. There are some sudden peaks in the OBS data (max up to 16 mg/L) in Figure 3.14, but not consistent and may not be related to wind data.

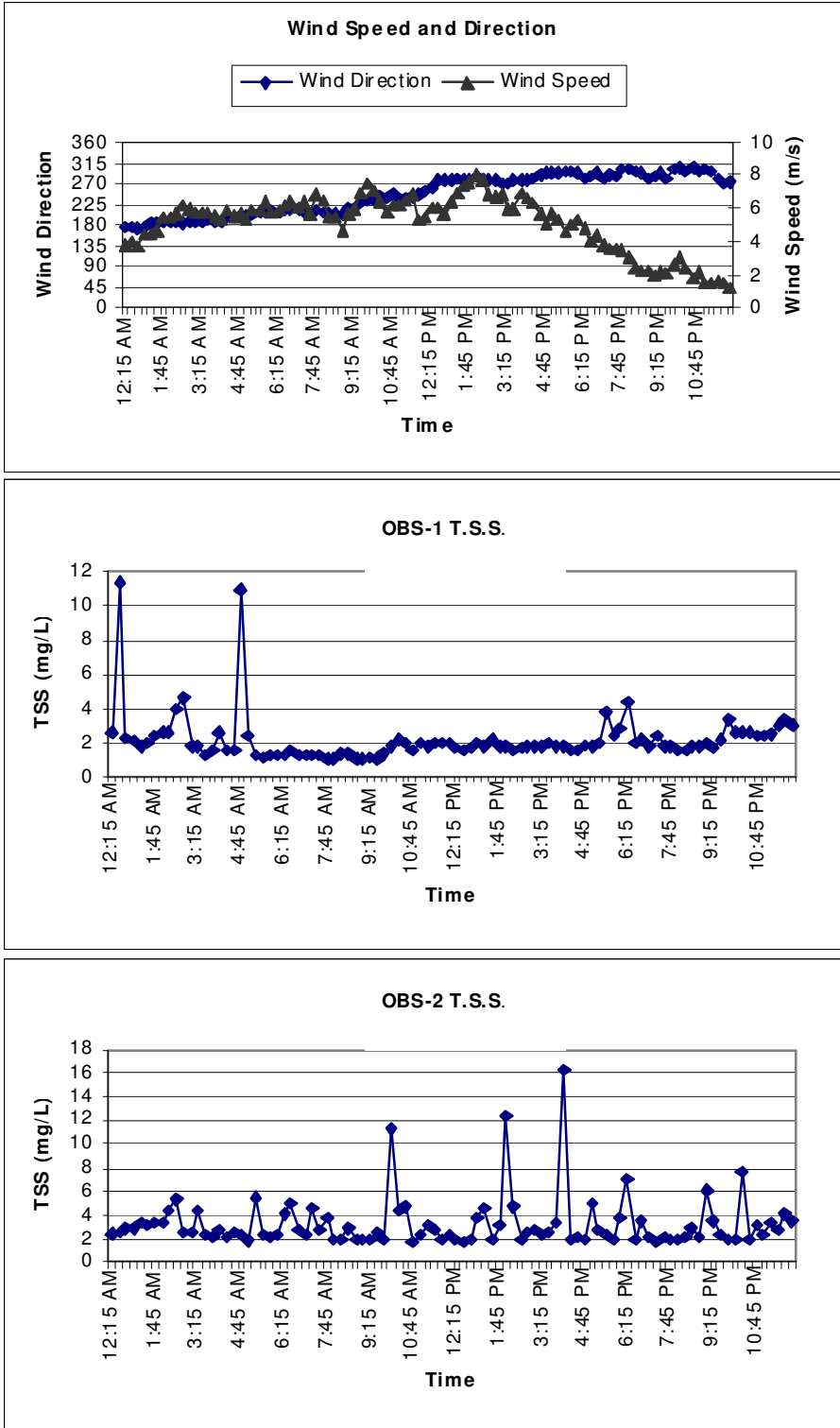


Figure 3.14 *Case III*: Time series results of total suspended solids concentration (TSS) measured by OBS-1 and OBS-2 on October 04, 2007 in the west cell with corresponding wind data

Case IV: OBS in West cell, October 09, 2007:

The method of sensor installation, sensor location in the pond, water cover depth, preferred wind direction for resuspension and all other conditions were exactly same here as in Case III. From the observed results we can see that at approximately 8:00 AM and after, the wind speed was relatively high (around 6 m/s) (Figure 3.15). Wind direction also contributed to resuspension as indicated by much higher values of suspended solids concentration. The maximum amount of resuspension was 25 mg/L for OBS-1 and 80 mg/L for OBS-2. The difference in resuspended concentration is due to the height of the sensors from the bed. The sensor closer to the bed shows higher value of resuspension than the other one.

These OBS results from four cases (Case-I, II, III and IV) of different wind and deployment conditions confirm the contribution of strong winds and wind directions to resuspension. If wind direction covers a long fetch, then a high wind speed can result in high resuspension. During strong wind events, there will always be some resuspension because strong winds do not allow the resuspended material to settle back and, instead, add to the suspended solids concentration. Settling velocity depends on the nature of resuspended particles. Large particles settle immediately after the wind ceases while finer particle may remain in suspension for longer periods. Once a sediment load is in suspension in water, currents generated by long duration storm events can carry it to the outlet.

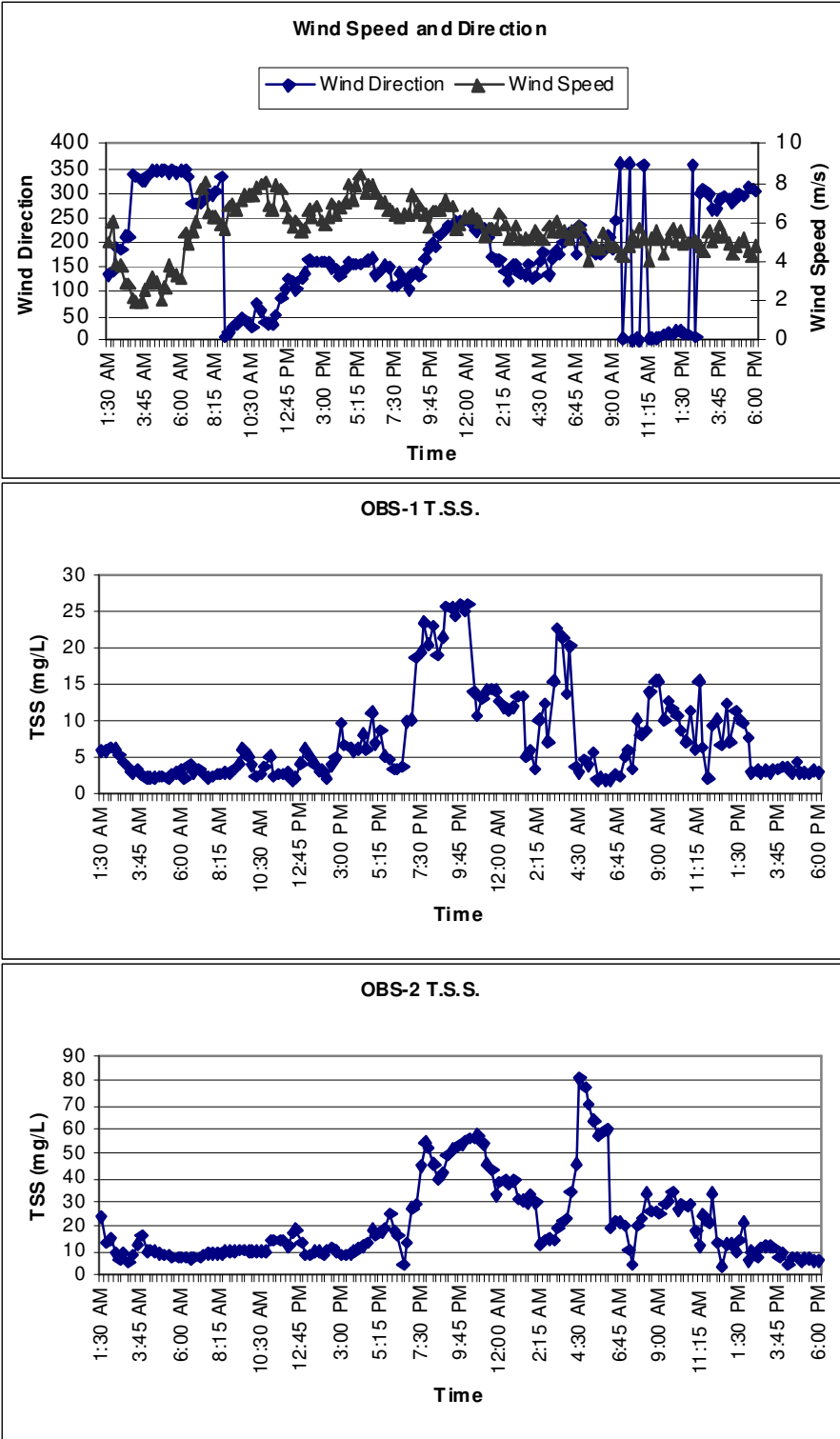


Figure 3.15 Case IV: Time series results of total suspended solids concentration (TSS) measured by OBS-1 and OBS-2 on October 09, 2007 in the west cell with corresponding wind data

3.4.7 Predicted and Measured Resuspension

The predicted water cover depths presented in the earlier section of the paper were to completely eliminate resuspension. However, the existing water cover depths in each cell of the pond were measured at all sediment trap locations during each trip, as shown in Table 3.3 and OBS sensor locations. The existing water depths in the tailings pond at all locations were smaller than the minimum required water depth. This might be the main reason for sediment resuspension recorded by sediment traps and OBS sensors.

Using the method developed by Samad and Yanful (2005), depth restriction was applied to predict the resuspended sediment concentration. The restricted water depth was chosen close to the existing or operating average depth in the tailings pond. Sediment resuspension was determined for each square grid cell using the power law erosion equation (Equation 3.14). The coefficient ($\alpha = 0.0025$) and exponent ($M = 1.121$) in Equation 3.14 were calculated from laboratory erosion tests using tailings from the west cell of the Shebandowan Mine site (Geremew and Yanful 2010). The Samad and Yanful (2005) model is an erosion model and it does not account possible sediment transportation and redeposition to one station to another in the tailings pond.

Figure 3.16 shows the contours of total bed shear stress (Pa) and predicted resuspended tailings concentration (mg/L) in the west cell with the water depth restricted to 0.9 m. The value of 0.9 m is also the average existing water cover depth in the west cell. For the restricted water cover depth of 0.9 m, the total bed shear stress calculated from the model was 0.35 Pa to 0.75 Pa, which is much higher than the critical shear stress of bed tailings (0.12 Pa) in the west cell. The fact that the calculated mobilized bed shear

stress is higher than the critical shear stress of the tailings may explain the occurrence of resuspension in the west cell. For the water depth of 0.9 m., the calculated resuspended tailings concentration is 6.5 mg/L to 22.7 mg/L with an average value of 15.0 mg/L. Thus, for this water depth, sediment resuspension on the average may not exceed the regulatory limit of 15 mg/L (MMER 2002).

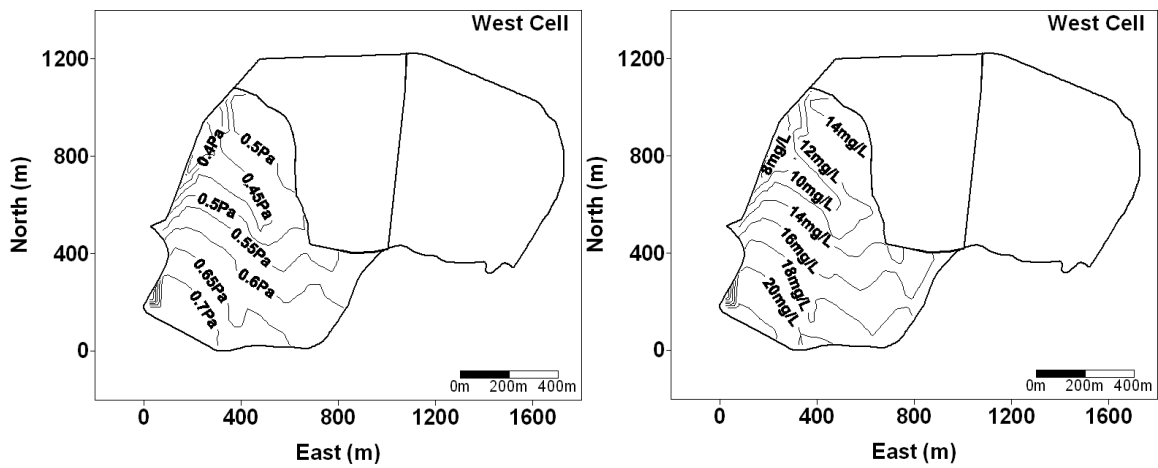


Figure 3.16 Contours of total bed shear stress (Pa) and predicted resuspension concentration (mg/L) in the west cell after applying depth restriction of 0.9 m

The OBS measured resuspension and model predicted resuspension were compared. The two OBS sensors installed in the west cell during October 2007 (Case-IV) showed resuspended tailings concentration up to 80 mg/L. As already mentioned, in this case (Case-IV) the OBS-1 sensor was 25 cm above the bed, while OBS-2 sensor was 10 cm above the bed. By virtue of its location from the bed OBS-1 would record resuspended tailings concentrations more representative to the water column than OBS-2, which would record resuspension close to the bed. The OBS-1 sensor recorded

resuspended tailings concentrations of 3 to 25 mg/L. These values are similar to the range of values calculated from Samad and Yanful (2005). Thus the model was able to reasonably predict the field resuspension tailings concentration in the west cell. The suspended solids concentration recorded during Case-II and Case-III were also within the range of model prediction. During Case-II, both OBS recorded concentration 7-18 mg/L and during Case-III, it was 12-16 mg/L.

Figure 3.17 presents a plot of calculated maximum total bed shear stress versus water cover depth for the west cell. As indicated, an increase in water cover depth decreases the bed shear stress. Figure 3.18 shows the predicted maximum concentration of resuspended material for different water depths using the Samad and Yanful (2005) model. The data show that a water depth of 0.9 m results in a resuspension tailings concentration of approximately 22 mg/L under strong wind conditions. The corresponding calculated total bed shear stress was 0.75 Pa compared to the value of 0.12 Pa for the critical shear stress of the tailings. As shown, a maximum water depth of 4.0 m may be required to completely eliminate resuspension in the west cell. Most importantly, the data show that even a water depth of 2.0 m can substantially reduce the resuspended tailings concentration to approximately 2.0 mg/L.

In the same way, results were obtained for the east cell, where bed tailings have similar texture, color and particle size distribution (except at sediment trap location 8, where bed tailings are coarser) as was the case for the west cell bed tailings. The erosion coefficient ($\alpha = 0.0025$) and exponent ($M = 1.121$) experimentally obtained for the west cell tailings can be used for the east cell as well. As a result of a restricted water depth to

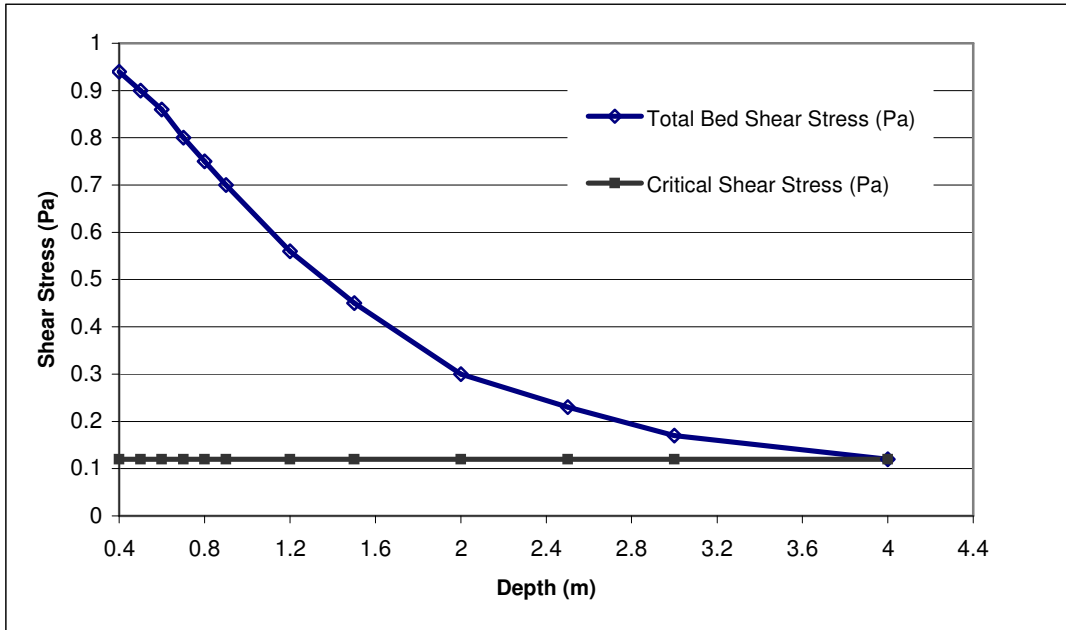


Figure 3.17 Change in total bed shear stress (Pa) with increasing water cover depth (m)

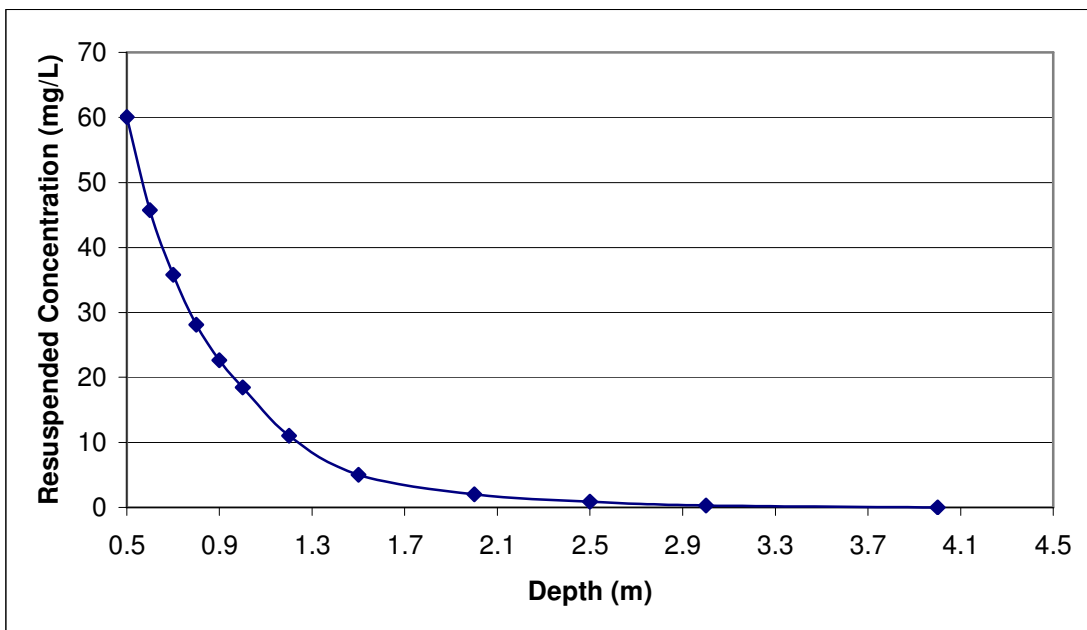


Figure 3.18 Change in resuspended solids concentration (mg/L) with water cover depth

1.0 m (average of existing water cover depth) in the east cell, the suspended tailings concentration was calculated to be 1.0 mg/L to 10.9 mg/L with an average value of 6.0 mg/L. These values are again within regulatory limits and may not raise any concerns. However, for the east cell, OBS data were not available to be compared with model predicted values. The application of the methodology by Samad and Yanful (2005) to both the east and west cell of the tailings pond indicated a small amount of resuspension with the existing water cover depths. The sediment trap data (Table 3.3) obtained during year 2006 and 2007 supports this finding however the sediment trap results were cumulative effect of sediment erosion and transportation by waves and currents and redeposition from one station to another station. The model predicted results may not be correlated with sediment trap results.

The particle size distribution of tailings in the middle cell showed that bed tailings are very fine (0.0065 mm) in nature and have a very low critical shear stress. Due to this low critical shear stress and the existing shallow water depth (average 1 m) relative to the minimum limit (5 m), the middle cell tailings can resuspend more easily. The sediment trap and OBS results did not show any unusual amount of resuspension in the middle cell. The actual critical shear stress of the middle cell tailings may be higher than the estimated value probably because of the existence of cohesiveness in the tailings.

The model predicted and field measured results indicate a small amount of resuspension occurring in the west cell of the pond with existing water depths. This resuspension does not raise an immediate concern because of the existing discharge monitoring and management strategies adopted at the site. In the long term though, the

water cover depth in the west cell of the pond may need to be managed (say, by dredging when necessary) to maintain an acceptable level of resuspension. Dredged tailings from shallow depths may be relocated to deeper areas. It is quite possible that disturbing the bed tailings by relocating dredged tailings may increase the degree of resuspension, but this would be the case in the short term only. In the long term, however, dredging has shown to eliminate resuspension.

The model calculations are performed ignoring the presence of any other natural and structural variables that might affect resuspension, such as the presence of vegetation and rocks in the bed tailings. Patches of dense vegetation were observed in parts of the Shebandowan mine tailings pond during multiple field visits especially in the west and east cells. At the present time, the model is not able to account for vegetation effects. The values of erosion rate constants used in the analysis were obtained from laboratory test results from Geremew and Yanful (2010). The location and sampling conditions of bed tailings in the west cell in the present study may be different from where Geremew and Yanful (2010) obtained their sample. Thus the values may be not representative of the whole site. The results of sediment resuspension directly depend on these values and a slight difference in these values can change the predicted values. The predicted sediment resuspension depends on the values of coefficient and exponent used in the erosion equation.

3.5 CONCLUSIONS

An attempt has been made in this paper to examine water cover technology and wind-induced erosion and resuspension of bed tailings at a tailings storage facility at the Shebandowan mine where reactive sulphide tailings have been deposited under water. The idea of discretizing the pond into grid cells and solving for bed shear stress and required water depths using the method developed by Samad and Yanful (2005) gave reasonable estimates of resuspended tailings concentrations similar to field measured values. The approach provides an economic solution for managing subaqueous tailings storage facilities by optimizing water cover depths. The model results and field measurements show that a small amount of resuspension is occurring under the existing conditions at the site. The following are key conclusions from the study:

1. The minimum water cover depth was significantly reduced by the presence of the wave breaks. The existing water depths in all cells were found to be less than the required values. This would explain the occurrence of resuspension. However for existing water cover depths, the resuspended tailings concentration for west cell and east cell was predicted to be within regulatory limits. The middle cell bed tailings are finer and representative erosion test results are required to predict the resuspension.
2. Combining sediment traps and optical back scatter (OBS) data provides a reliable assessment of resuspension.
3. Sediment trap results helped to quantify the amount of resuspension over a certain period of time. Resuspension did not directly correlate with water cover depth.

Sediment trap data are a cumulative effect of wind events of different speeds and directions or fetch lengths, duration of wind events, water cover depth, erosion, sediment transportation and redeposition processes. Mineralogical and chemical analysis of bed tailings and resuspended tailings collected by sediment traps showed similarity between the two tailings which confirms erosion and subsequent resuspension of bed tailings.

4. The optical back scatter (OBS) results support the fact that some wind-induced resuspension may be occurring at the site and that resuspension depends on wind speed, direction and water cover depth. Strong winds that do not blow in directions that develop long fetches have minimal effect on resuspension.
5. The Samad and Yanful (2005) method is probably more rigorous than other tailings resuspension models (for example, MEND Manual (2001)) as it is able to predict both minimum and optimum water cover depths and resulting resuspended tailings concentrations.

The wave breaks appear to be working well at the Shebandowan site. There is some amount of resuspension, but, overall, it is within acceptable limits. One can always design the water cover to eliminate resuspension by using a deeper water cover. However, at the Shebandowan site where wave breaks have been implemented, this is not necessary. Increasing water depth to eliminate resuspension may not always be preferable. The design and stability of perimeter dams and other site-specific constraints must be taken into account. Depending on the severity of the impact, proper management of the tailings pond, such as dredging of tailings at locations with shallow water cover, can be undertaken. The calculation method outlined in this paper can be used to assess

the effectiveness of the dredging operation. The method can also be used in a preliminary design of new tailings facilities where very little data initially exists and no in-situ measurements can be conducted.

3.6 REFERENCES

1. Adu-Wusu, C., Yanful, E.K., & Mian, M.H. (2001). Field evidence of resuspension in a mine tailings pond. *Canadian Geotechnical Journal*, 38(4): 796-808.
2. Baines, W.D., & Knapp, D.J. (1965). Wind driven water currents. *Journal of the Hydraulics Division, ASCE*, 91(HY2): 205-221.
3. Bass, S.J., McCave, I.N., Rees, J.M., Vincent, C.E., et al. (2007). Sand and mud flux estimates using acoustic and optical back scatter sensors: measurements seaward of the Wash, southern North Sea, Geological Society, London, special publications, 274: 25-35.
4. Bengtsson, L., Hellstrom, T., & Rakoczi, L. (1990). Redistribution of sediments in three Swedish lakes. *Hydrobiologia*, 192: 167-181.
5. Bengtsson, L., & Hellstrom, T. (1992). Wind-induced resuspension in a small shallow lake. *Hydrobiologia*, 241: 163-172.
6. Bennett, C.V., & Yanful, E.K. (2001). Investigation of tailings resuspension under a shallow water cover, Proc. 54th Canadian Geotechnical Conference, 3, pp. 1596-1603.
7. Bennett, C.V. (2002). Investigations of tailings resuspension under a shallow water cover. M.E.Sc. thesis, The University of Western Ontario, London, ON.
8. Catalan, L.J.J., & Yanful, E.K. (2002). Sediment trap measurement of suspended mine tailings in a shallow water cover. *Journal of Environmental Engineering Division, ASCE*, 128(1): 19-30.

9. CERC (1984). Shore protection manual. U.S. Army Corps of Engineers, Coastal Engineering Research Centre, Vicksburg, M.S.
10. Debnath, K., Nikora, V., & Elliott, A. (2007). Stream bank erosion: In situ flume tests. *Journal of Irrigation and Drainage Engineering*, ASCE, 133(3): 256-264.
11. Fischenich, C. (2001). Stability thresholds for stream restoration materials. EMRRP technical notes collection, ERDC TN-EMRRP-SR-29, U.S. Army engineer research center, Vicksburg, M.S.
12. Geremew, A.M., & Yanful, E.K. (2010). The role of fines on the cohesive behavior of mine tailings inferred from the critical shear stress. *Canadian Geotechnical Journal*. In Press. Accepted October 4, 2010.
13. Golder Associates (2000). A report on Shebandowan tailings facility. Annual inspection-August 2000.
14. Green, M.O., & Boon, J.D. (1993). The measurement of constituent concentrations in non-homogenous sediment suspensions using optical back scatter sensors, *Marine Geology*, 110: 73-81.
15. Jonsson, I.G. (1966). Wave boundary layers and friction factors, Proc. 10th Conference on Coastal Engineering, Tokyo, Japan, ASCE, 1, pp. 127-148.
16. Lawrence, G.A., Ward, G.A., & MacKinnon, P.R.B. (1991). Wind wave-induced suspension of mine tailings in disposal ponds: a case study. *Canadian Journal of Civil Engineering*, 18(6): 1047-1053.
17. Li, M.G., Aube, B., & St-Arnaud, L. (1997). Considerations in the use of shallow water covers for decommissioning reactive tailings. Proc. 4th

- International Conference on Acid Rock Drainage, Vancouver, B.C., 1, pp. 115-130.
18. Kozerski, H.-P. (1994). Possibilities and limitations of sediment traps to measure sedimentation and resuspension, *Hydrobiologia*, 284: 93-100.
 19. Kubicki, A. (2008). Large and very large subaqueous dunes on the continental shelf of southern Vietnam, South China Sea. *Geo-Marine Letters*, 28: 229-338.
 20. MEND Manual (2001). Prevention and control, Volume 4, Energy Mines and Resources Canada.
 21. MEND Report. (1998). Design guide for the sub-aqueous disposal of reactive tailings in constructed impoundments, MEND 2.11.9.
 22. MMER. (2002). Metal mining effluent regulations. SOR/2002-222, <http://laws.justice.gc.ca/PDF/Regulation/S/SOR-2002-222.pdf>, Accessed November 10, 2009.
 23. Mian, M.H., & Yanful, E.K. (2003). Tailings erosion and resuspension in two mine tailings ponds due to wind waves. *Advances in Environmental Research*, 7: 745-765.
 24. Mian, M.H., & Yanful, E.K. (2004). Optical backscatter measurements of tailings resuspension in a mine tailings pond. Proc. 57th Canadian Geotechnical Conference, Session 7D, pp. 38-45.
 25. Osborne, P.D., & Greenwood, B. (1993). Sediment suspension under waves and currents: time scales and vertical structure, *Sedimentology*, 40(4): 599-622.

26. Partheniades, E. (1965). Erosion and deposition of cohesive soils. *Journal of the Hydraulics Division, ASCE*, 91(HY1): 105-139.
27. Pohl, M. (2004). Channel bed mobility downstream from the Elwha dams, Washington. *The Professional Geographer*, 56(3), 422-431.
28. Rosa, F., Bloesch, J., & Rathke, D.E. (1994). Sampling the settling and suspended matter (SPM), In Mudroch, A. & Macknight, S.D. (editors), *Handbook of techniques for aquatic sediment sampling*, second ed., CRC Press, Florida, USA.
29. Samad, M. A., & Yanful, E.K. (2005). A design approach for selecting the optimum water cover depth for subaqueous disposal of sulphide mine tailings. *Canadian Geotechnical Journal*, 42: 207-228.
30. Simms, P.H., Yanful, E.K., St-Arnaud, L., Aube, B., et al. (2001). A laboratory evaluation of metal release and transport in flooded preoxidized mine tailings. *Applied Geochemistry*, 15: 1245-1263.
31. Soulsby, R.L., & Whitehouse, R.J.S (1997). Threshold of sediment motion in coastal environments. *Proc. Pacific Coasts and Ports Conference*, University of Canterbury, Christchurch, NewZealand, pp. 149–154
32. Thomson, S.A. (1999). *Hydrology for water management*, A.A. Balkema Publication, Rotterdam, Netherlands.
33. Tsuruya, H., Nakano, S., Kato, H., Ichinohe, H., et al. (1983). Experimental study of wind driven current in wind-wave tank - effect of return flow on wind driven flow, report. Port and Harbour research Institute, In Japanese, 22(2): 127-174.

34. Wedepohl, K.H. (1995). The composition of the continental crust. *Geochimica et Cosmochimica Acta*, 59(7): 1217-1232.
35. Wu, J., & Tsanis, I.K. (1995). Numerical study of wind induced water currents. *Journal of Hydraulic Engineering, ASCE*, 121(5): 388-395.
36. Yanful, E.K., & Catalan, L.J.J. (2002). Predicted and field measured resuspension of flooded mine tailings. *Journal of Environmental Engineering, ASCE*, 128(4): 341-251.
37. Yanful, E.K., & Verma, A. (1999). Oxidation of flooded mine tailings due to resuspension. *Canadian Geotechnical Journal*, 36: 826-845.
38. Yang, Y., Straatman, A.G., Yanful, E.K., et al. (2000). Experimental study on wind induced motions and sediment resuspension in shallow waters, Proc. 6th Environmental Engineering Speciality Conference of the CSCE and 2nd Spring Conference of the Geoenvironmental Division of the Canadian Geotechnical Society, London, ON, Canada, pp. 177-182.
39. Yang, Y. (2001). Wind induced countercurrent flow in shallow water. Ph.D. thesis, The University of Western Ontario, London, ON.

CHAPTER 4: A SEMI-EMPIRICAL APPROACH FOR ESTIMATION OF BED SHEAR STRESS IN A TAILINGS POND

4.1 INTRODUCTION

In a pond where sulphide rich reactive mine tailings are submerged under water, erosion and resuspension of the bed tailings can potentially alter the water quality and adversely affect the environment by releasing acid and metals. The only driving force available to initiate sediment motion in such a tailings pond is wind blowing over the water surface. Wind induced waves and currents exert shear stress on the tailings bed. The importance of knowledge of the wind induced bed shear stress in a tailings pond has been pointed out by several researchers (e.g., Yanful and Catalan 2002; Samad and Yanful 2005). The bed shear stress can be used to assess tailings erosion and resuspension, which further helps in the design and management of a tailings pond.

Wind induced total bed shear stress has two components: that due to waves and that due to current velocities. However it is not clear from published literature how the waves and currents should be handled in shallow water conditions to analyze resuspension and sediment transport processes. In many studies the current induced bed shear stress in shallow water is either considered too small to contribute to resuspension (Luettich et al. 1990; Bailey and Hamilton 1996) or estimated using theoretical and empirical approaches such as those developed by Wu and Tsanis (1995) and Yang (2001). Luettich et al. (1990) concluded that the bed shear stresses due to horizontal

currents are generally too small to contribute to sediment motion in shallow waters, however these circulatory currents are known to play an important role in the redistribution of material eroded and resuspended by wave action. In previous modeling studies the currents were assumed as counter currents in opposite direction to winds while waves in the direction of the wind and the total bed shear stress were taken as a simple linear addition of the shear stress contributions from waves and currents (Wu and Tsanis 1995; Yang 2001; Catalan and Yanful 2002; Samad and Yanful 2005; Kachhwal et al. 2010).

It has been reported in other studies that wave-current interaction in shallow waters enhances the bed turbulence and causes an increase in the bed shear stress (Grant and Madsen 1979; Jing and Ridd 1996; Jin and Ji 2004). In most tailings pond studies, even though pure wave induced flow was found to be in laminar range, however in reality the wave motion near bed is turbulent because it is superimposed on a current which might be turbulent. According to Grant and Madsen (1979) near bed unsteady oscillatory wave motion will generate significant turbulence at the bed which may significantly affect the current motion in the case of combined wave and current flows. In the immediate vicinity of bed the shear stress and turbulent intensities are due to combined effect of both the wave and the current, which are coupled non-linearly (Grant and Madsen 1979). Jing and Ridd (1996) used a wave-current interaction model developed by Grant and Madsen (1979) to investigate resuspended sediment concentrations in Cleveland Bay, Australia. They found high correlation ($R^2 = 0.83$) between wave-current bed shear stresses and suspended solids concentration. In their study, Jing and Ridd (1996) found that the maximum total bed shear stress estimated by the wave-current

interaction model was greater than that estimated by waves alone. Grant and Madsen (1979) predicted that currents actually contribute to the total bed shear stress, and that waves and current motions should not be treated separately. They developed a model based on non-linear interaction between waves and currents responsible for sediment erosion and transportation. Signell et al. (1990) showed that wave-current interaction significantly affects the wind driven current circulation in shallow embayment. The non-linear wave-current interaction model of Grant and Madsen (1979) has been adopted by many other researchers to estimate the total bed shear stress and to model the flow pattern in shallow waters (Jones and Davies 2001; Liang and Li 2008; Dufois et al. 2008). Rennie et al. (2002) found a strong correlation between apparent bed load velocity and current bed shear stress which indicates that the current induced bed shear stress was sufficient to initiate sediment motion. Jin and Ji (2004) found that wind induced currents contribute significantly to both the total bed shear stress and sediment redistribution in shallow lake Okkechobee, Florida, USA.

In most studies so far conducted on tailings ponds, the total bed shear stress was taken as a simple linear addition of the shear stress contributions from waves and currents (Catalan and Yanful 2002; Samad and Yanful 2005; Kachhwal et al. 2010). In these studies near bed currents were assumed as counter current flow in opposite direction to wind based on the Wu and Tsanis (1995) theoretical model developed for pure currents in absence of waves. In presence of both waves and currents, linear addition may not be accurate especially for strong currents and may underestimate the total bed shear stress. The empirical approaches used to estimate wind induced currents in these tailings pond studies do not provide any information on current directions and circulation patterns. The

lack of field measured wind induced current data in small tailings pond is a constraint. The main objectives of the present study were to measure real time wind induced currents in a tailings pond and study the effect of wave-current interaction on total bed shear stress.

The presents study was conducted in a tailings pond where an Acoustic Doppler Current Profiler (ADCP) was used to measure circulatory currents near the bed. To the best of the authors' knowledge, this is the first study in which an ADCP has been used to measure wind induced small magnitude currents in a mine tailings pond. In the study, a semi empirical approach is employed to estimate the total bed shear stress due to wind induced waves and currents. The approach is based on the wave-current interaction model of Grant and Madsen (1979). The bed shear stress due to circulatory currents is calculated from field measured vertical current profiles obtained using an ADCP and the well-known Log-Law relation (Wilcock 1996; Rennie et al. 2002; Yu and Tan 2006; Garcia 2007). The bed shear stress due to wave orbital velocities was calculated using shallow water wave hindcasting equations as provided in CERC (1984) and discussed in Samad and Yanful (2005). The total bed shear stress was calculated using the Grant and Madsen (1984) model considering non-linear wave-current interaction. The ADCP results were also used to visualize the three-dimensional complex current flow circulation in the tailings pond. The results showed that the concept of counter currents near the bed opposite to the wind direction (Wu and Tsanis 1995; Yang 2001; Samad and Yanful 2005) could be augmented by one of circulatory currents under wave-current interactions in field conditions.

4.1 STUDY SITE

The study was conducted at the Shebandowan Mine tailings storage facility, located 100 km west of Thunder Bay, northwestern Ontario, Canada. The Shebandowan mine was operated as an underground nickel and copper mining and milling facility from 1971 to 1998. Figure 4.1 shows the map of the Shebandowan tailings storage facility. Two wave breaks (internal dykes) divide the tailings storage facility into three cells, namely, the West cell, Middle cell and East cell. In 1999 approximately 85000 m³ of sulphide rich mine tailings were deposited in the Shebandowan tailings storage facility. The present study was conducted in the Middle cell. Figure 4.1 shows the middle cell and the locations of ADCP stationary data collection points. The depths of water cover in this particular cell varied from less than 1 m at some locations to over 3.4 m at others. The bathymetry of the pond showed an abrupt depression (3.4 m depth) in the bed close to the east dyke. The average median grain size of the bed tailings was of the order of 0.007 mm. The grain size of the tailings in this cell was finer than those in the other two cells and was likely to be of cohesive nature (Kachhwal et al. 2010).

4.2 METHODS AND MATERIALS

4.2.1 The Acoustic Doppler Current Profiler (ADCP) Data Collection

For the present study, a 1200 kHz Workhorse Rio Grande ADCP (Teledyne, RD Instruments, CA, USA) was used. An Acoustic Doppler Current Profiler (ADCP) can be used to measure real time currents in a water body. The ADCP uses ultrasonic sound

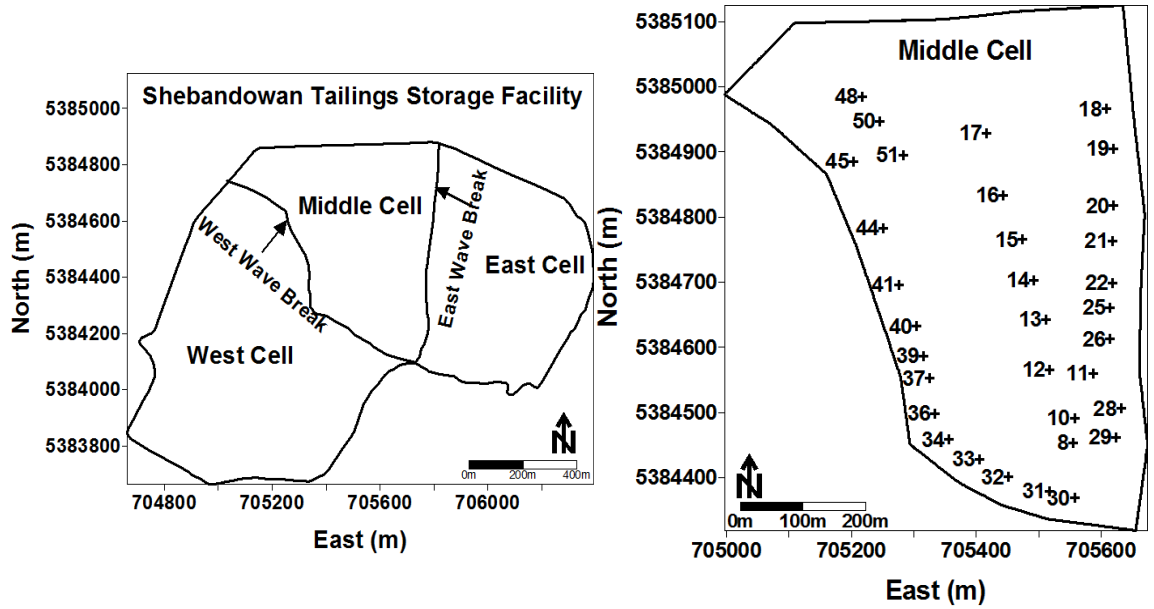


Figure 4.1 The map of Shebandowan tailings storage facility, the Middle cell, and ADCP data collection locations in the Middle cell

waves with Doppler’s principle, which relates the change in frequency of a source to the relative velocities of the source and the observer. The ADCP transmits an acoustic pulse, or “ping”, into the water column and then receives the return echo backscattered off small suspended material present in the water, which is assumed to be moving at the same velocity as the water. The ADCP’s onboard signal processing unit compares the frequencies of the initial transmitted and received signals and calculates the Doppler shift in the frequency. As the time after transmission of the initial ultrasonic pulse increases, the returned signal comes from successively more distant sample volumes known as range bins. Backscattered energy from each range bin arrives at the transducer with a Doppler shift proportional to the average speed of many scatterers within the sampled volume. This ADCP has four independently working acoustic beams angled at a specific angle (20^0) from vertical axis (Janus configuration) to measure three dimensional velocity

components. The 1200 kHz Workhorse Rio Grande ADCP used in the present study can measure water velocities with an accuracy of ± 0.25 cm/s ($\pm 0.25\%$) (Teledyne RD Instruments 2009). A Differential Global Positioning System (DGPS) is generally linked with the ADCP to measure absolute current velocities and avoid errors associated with relative boat velocities. The additional information on the ADCP's working principles and related terminology can be found in Simpson (2001).

In the present study, bottom tracking ADCP data were collected in the Middle cell of the Shebandowan tailings pond on September 19, 2008 using the 1200 kHz Workhorse Rio Grande ADCP linked to a DGPS. As shown in Figure 4.2, the ADCP was mounted on a boat looking downward using a steel fabricated mounting assembly. Stationary boat current profiles were recorded at different locations in the Middle cell as shown in Figure 4.1. The stationary boat profiling was chosen because very small current velocities were expected. Stationary boat measurements of current velocities and depths have greater

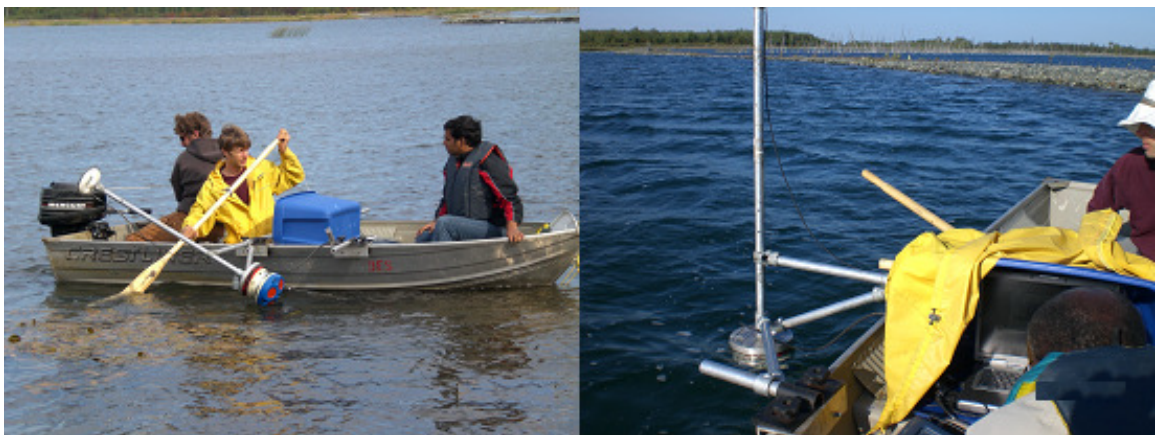


Figure 4.2 Boat mounted Workhorse Rio Grande 1200 kHz ADCP with mounting assembly

accuracy due to increased temporal averaging than those measured from a moving boat, especially in the case where current velocities were expected to be very small (Muste et al. 2004). The bottom tracking, water velocity profile in columns and depth of each ensemble at several locations in the pond were recorded for approximately 180 seconds at each location. Current velocities were recorded along three beams in depth cells or bins vertically spaced 5 cm apart, using pulse coherent water mode 11. The use of pulse coherent processing increased the accuracy and resolution of the velocity data, and was appropriate for the shallow and low velocity conditions of the site (Teledyne RD Instruments, 2009). A MATLAB code was developed to process and filter raw data to obtain mean current velocity and direction at different depth cells in a column. ADCP data in the tailings pond were useful for quantification and visualization of circulatory currents near the bed. However the major limitation of the boat mounted ADCP was that it could not measure velocities in the top 0.35 m of water due to instrument size and blanking distance. Moving boat data were also collected and used only to develop the approximate bathymetry of the middle cell.

4.2.2 Estimation of Bed Shear Stress

In a tailings pond, erosion and resuspension occur when the wind induced bed shear stress exceeds the critical shear stress of the bed tailings (Samad and Yanful 2005). The critical shear stress is a characteristic property of bed material and depends on its physical and chemical composition. Accurate estimation of total bed shear stress due to wind induced waves and circulatory currents is not always easy. In the present study we used a

semi-empirical approach based on the Grant and Madsen (1979) model of wave-current interaction with the well-known “Log-Law” and ADCP measured current profiles in the tailings pond. The total bed shear stress due to waves and currents (τ_b) can be written as a tensor addition:

$$\tau_b = \tau_w + \tau_c \quad (4.1)$$

where, τ_c is the shear stress due to currents and τ_w is the maximum shear stress due to waves calculated over one wave period.

In the Grant and Madsen (1979) model, waves and currents are not treated separately. The waves influence the drag felt by currents at a reference level and this enhancement of drag is a function of wave orbital velocities, current velocities at reference level, wave period, bottom roughness and the angle between waves and currents. The combined wave-current bed shear velocities can be obtained by:

$$u_{*cw} = \left(u_{*c}^2 + u_{*w}^2 + 2u_{*c}u_{*w} \cos\theta_c \right)^{1/2} \quad (4.2)$$

where, u_{*w} and u_{*c} are wave and current bed shear velocities, respectively and θ_c is the angle between the direction of wave propagation and current, ranged between 0 to 90⁰ considering the simple harmonic motion of waves in linear wave theory.

Using Equation 4.2, and the definition that $\tau = \rho u_*^2$ in general, we can write the combined total bed shear stress under wave-current interaction as:

$$\tau_b = \rho u_{*cw}^2 = \tau_c + \tau_w + 2\sqrt{\tau_c \tau_w} \cos\theta_c \quad (4.3)$$

The bed shear stress due to wind induced wave orbital velocities τ_w can be calculated using the empirical wave hindcasting equations provided in CERC (1984) based on linear wave theory. These equations have been applied in tailings resuspension studies by several researchers (Samad and Yanful 2005; Kachhwal et al. 2010). The input data required in this process are wind speed, direction, pond geometry or fetch length, and water cover depth.

$$\tau_w = \rho u_{*w}^2 = \frac{1}{2} \rho f_w U_w^2 \quad (4.4)$$

$$U_w = \frac{\pi H}{T \sinh(2\pi h/L)} \quad (4.5)$$

Where, ρ is fluid (water) density, f_w is the wave friction factor, U_w is the near-bed wave orbital velocity, H is the significant wave height, T is the significant wave period.

The well-known “Log-Law” (Wilcock 1996; Rennie et al. 2002; Garcia 2007) describes a methodology for the estimation of bed shear stress due to currents by assuming a log linear velocity profile for both smooth and rough bed boundary conditions. The relationship between the current bed shear velocity u_{*c} and variation of near-bed velocity u with elevation above the bed z can be written as:

$$\frac{u}{u_{*c}} = \frac{1}{\kappa} \ln \left(\frac{z}{z_0} \right) \quad (4.6)$$

Where, κ is von Karman’s constant (~ 0.40), z_0 is the bed roughness length corresponding to $u = 0$.

The near bed shear velocity u_{*c} can be estimated as the slope of the log linear near bed velocity profile multiplied by κ , von Karman's constant. The bed shear stress due to currents can thereby be obtained by using measured horizontal current velocities at different elevation above the bed in a vertical column. In a tailing pond, the bottom boundary can be assumed sufficiently smooth, the currents will be suppressed drastically in an extremely thin layer (viscous sub-layer) near bed, where velocity distribution holds a linear profile. For a hydraulically smooth bottom boundary, the bed roughness length $z_0 = \nu/9u_{*c}$, where ν is kinematic viscosity of water. The advantage of this method is that knowledge of bed roughness length z_0 is not required. However, z_0 values can be used as acceptability criteria for the field measured current results as discussed in section 4.3.2. Detailed explanation on the use of log-law in hydraulically smooth and rough flow conditions is available in Garcia (2007). The bed shear stress due to currents can be calculated using bed shear velocity u_* as follows:

$$\tau_c = \rho u_{*c}^2 \quad (4.7)$$

4.3 RESULTS AND DISCUSSION

4.3.1 ADCP Measured Flow

In a tailings pond where only wind driven flow exists, accurate knowledge of wind data becomes necessary and important. In the present study, on-site wind data were collected with a Young wind monitor installed at standard 10 m height above the water surface along with a weather station. During the ADCP data collection on September 19, 2008

wind was quite consistent both in speed and direction as shown in Figure 4.3. The average wind speed was about 6.5 m/s and the direction was 250° from North. The wind direction varied within 10 degrees during the period of data collection.

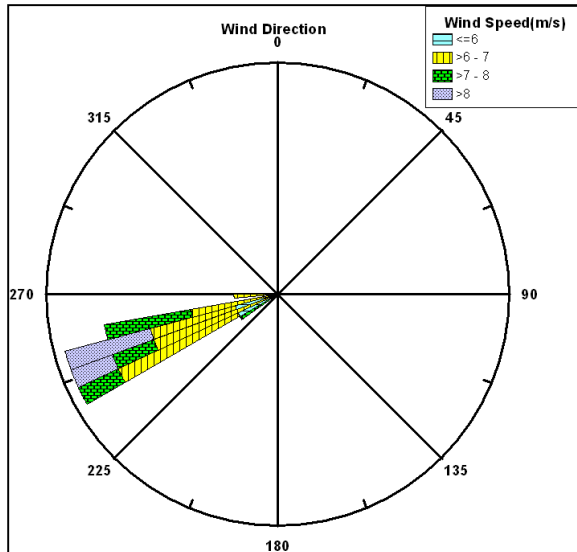


Figure 4.3 Plot of wind data during ADCP data collection

Figure 4.4 shows the contour maps of water cover depth or bathymetry of the middle cell. Water cover depth near east dyke was as high as 3.5 m due to abrupt depression in the bed. Three-dimensional vector plots of the time-averaged circulatory horizontal current velocities along with approximate bathymetry are shown in Figure 4.5. The group of figures show flow patterns in the middle cell of the tailings pond viewed from different angles for enhanced visualization. The X and Y-axis represent the East and North directions respectively while the Z-axis represents the depth of the pond. These results showed a complex pattern of near bed circulation of flow. The magnitude of

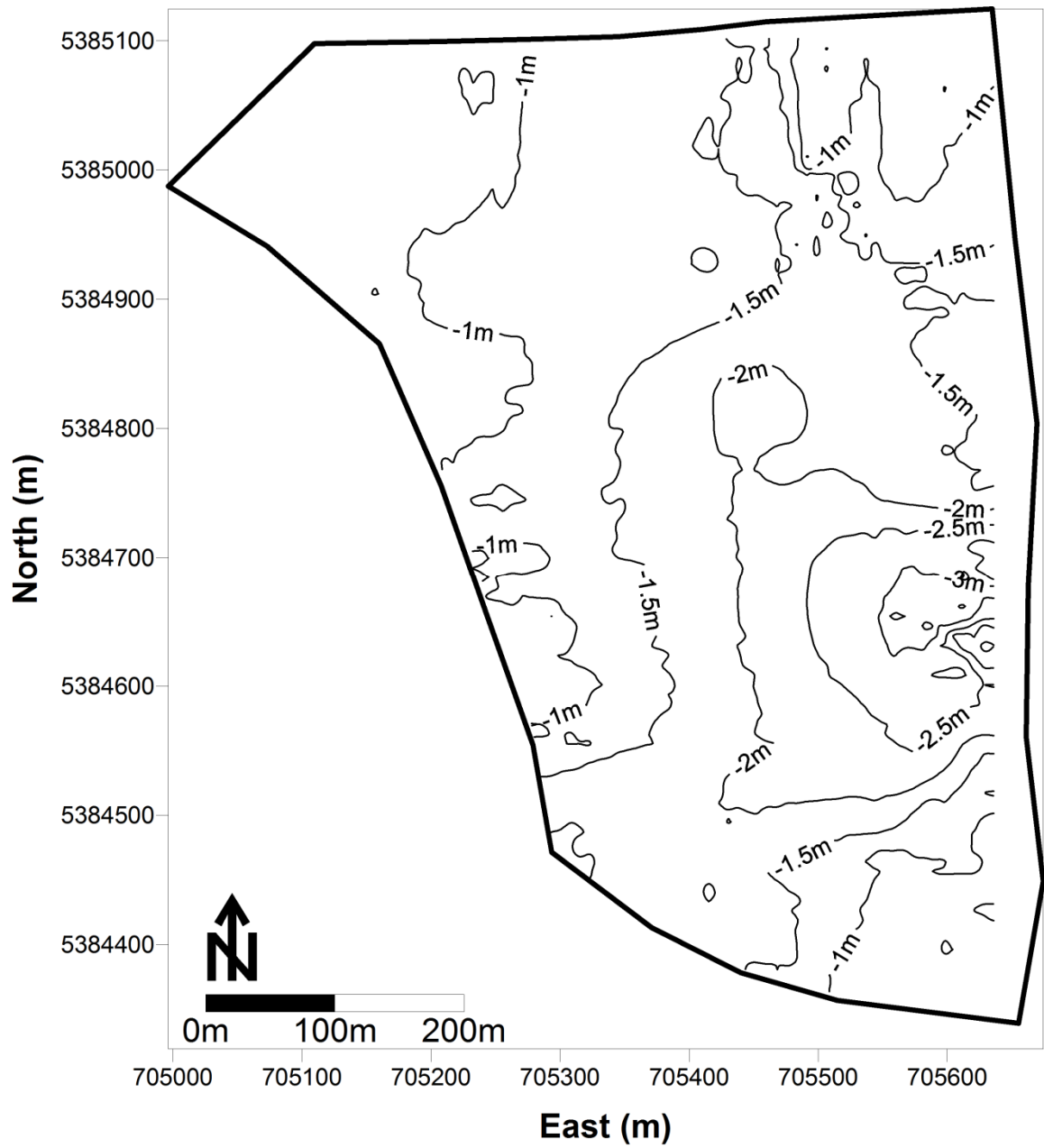


Figure 4.4 Contour map of water cover depth or bathymetry of the middle cell

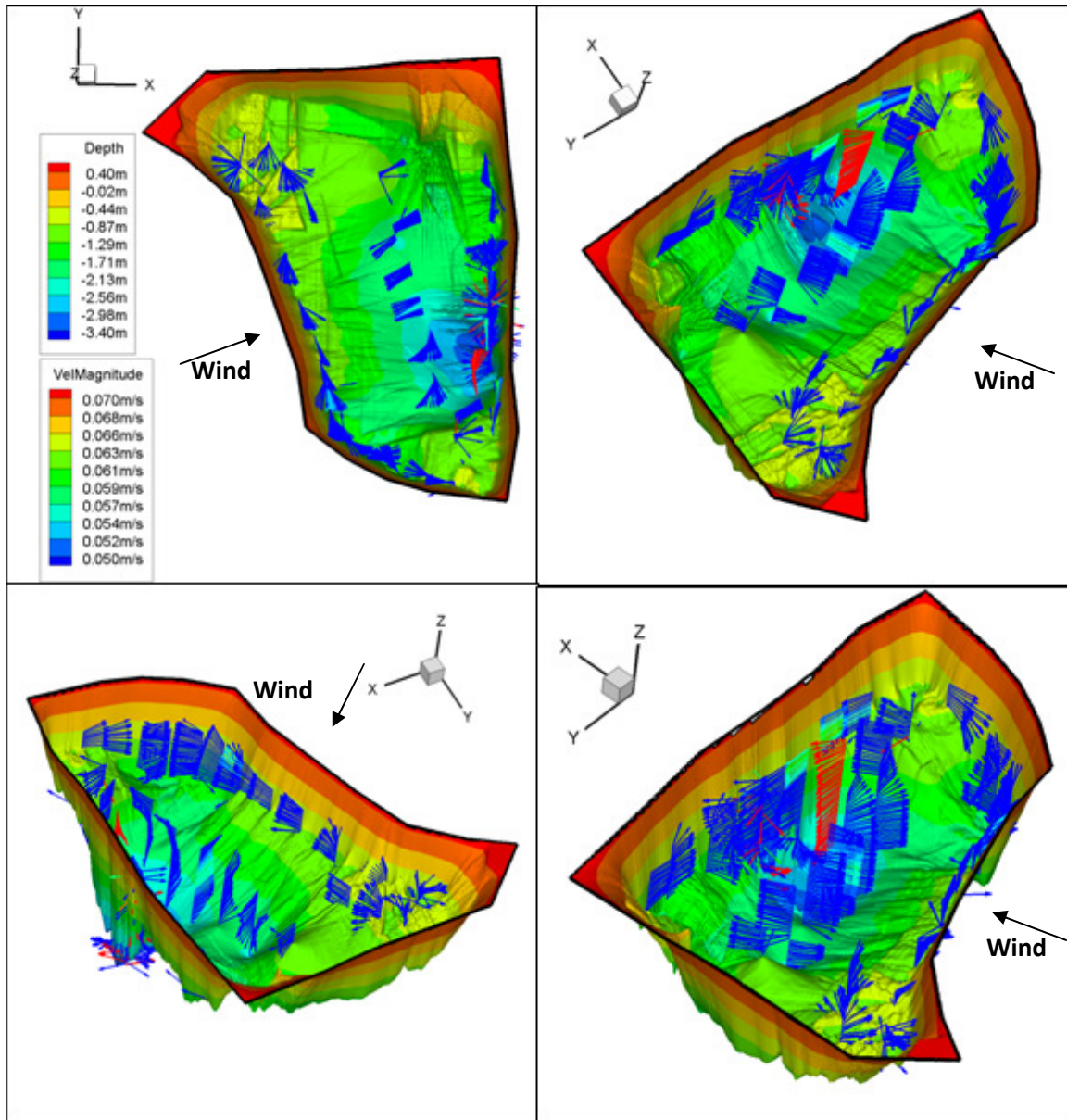


Figure 4.5 Three-dimensional visualization of current flow pattern with bathymetry in the Middle cell viewed from different angles (Note: Vector color represents velocity magnitude and pond color represents depths as shown in color scale legends for both)

measured velocities was of the order of 5 cm/s. The standard error in the ADCP measured horizontal velocities at all profile locations were less than 0.1 cm/s. Jin and Ji (2004) reported wind induced current velocities typically ranging from 1 to 10 cm/s in Lake Okeechobee, Florida, USA. The mean depth of this lake was 2.7 m. The current velocities measured in the present study were within the same order of measured values in Lake Okeechobee.

At most locations in the Middle Cell, current velocities consistently varied in both magnitude and direction throughout the profile except at locations close to the east wall of the pond where an abrupt depression in the bed produced anomalies in flow. The measured velocities were small but the pattern of circulation currents is remarkably visible. The depth-averaged data of horizontal current velocities were plotted on an interpolated grid using Surfer. The two dimensional view is shown in Figure 4.6, which shows the complex near bed flow circulation pattern in the pond. It was evident that wave-current interaction, irregular bathymetry, abrupt depression and pond geometry were causing this complex flow pattern.

A number of researchers have discussed wind induced flow patterns in lakes or ponds in terms of flow in the direction of wind at the top surface and near bed counter current flow in the opposite direction to maintain energy or mass conservation based on laboratory experimental results (Wu and Tsanis 1995; Yang 2001). This flow pattern would occur where the influence of surface waves is negligible and counter current flow conditions are fully developed. Non-linear interaction between waves and currents is responsible for generating complex current circulation (Signell et al. 1990). The present

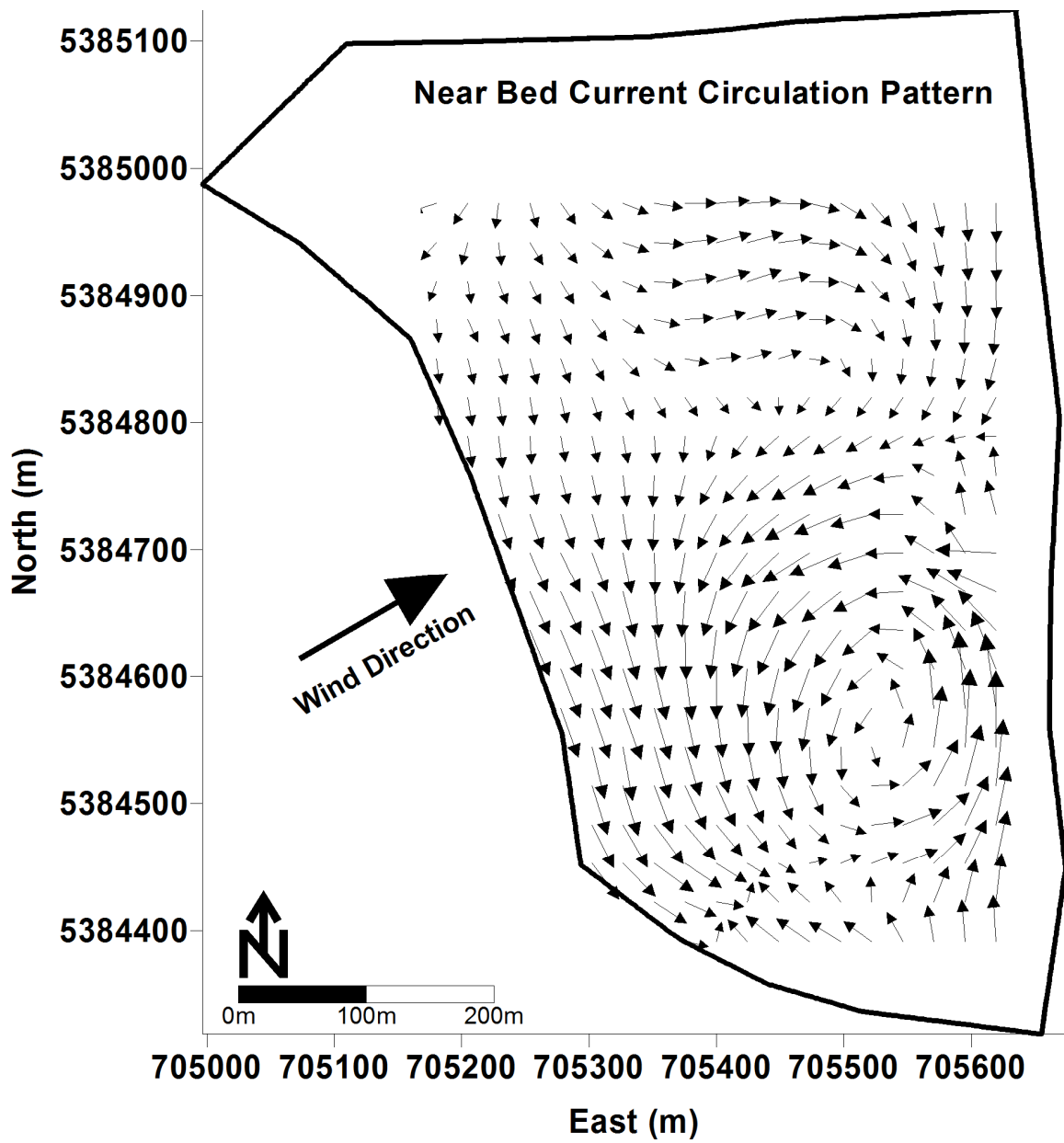


Figure 4.6 Two-dimensional near bed currents flow circulation pattern

ADCP results show the complex flow pattern near the tailings bed. The near bed counter current flow opposite in direction to the wind was seen in only a few profiles, for example at locations 16 and 18, in the present study (Figure 4.5, and Appendix-III), and flow reversal within these profiles appeared to be related to the complicated pattern of flow circulation within the entire pond. In the field where irregular bathymetry is present and wave and current interaction cannot be neglected, the concept of counter currents can be replaced with circulatory currents.

4.3.2 The Bed Shear Stress

The bed shear stress due to wind waves is a function of fetch length and water cover depth. The estimated bed shear stress due to wind waves in general was very small because of slow winds and minimal fetch length available for the wind waves to grow. The wind-wave induced bed shear stress varied from almost zero along the west dyke locations to 0.02 Pa close to the east dyke in the northeast corner of the pond. The fetch available for locations along the west dyke of the Middle cell was negligible. The variation was also associated with depth. At locations close to the east dyke where there was a depression in the bed and the depth was approximately 3.4 m, the estimated bed shear stress was still close to zero even though some fetch was available for the waves to grow. The estimated results for all locations were plotted in the form of a contour map as shown in Figure 4.7. The zero bed shear stress contour essentially divided the cell into two parts. On the west side of the Middle cell, there was no effect of wind waves whereas on the east side some stress was exerted on the bed. However these results were estimated

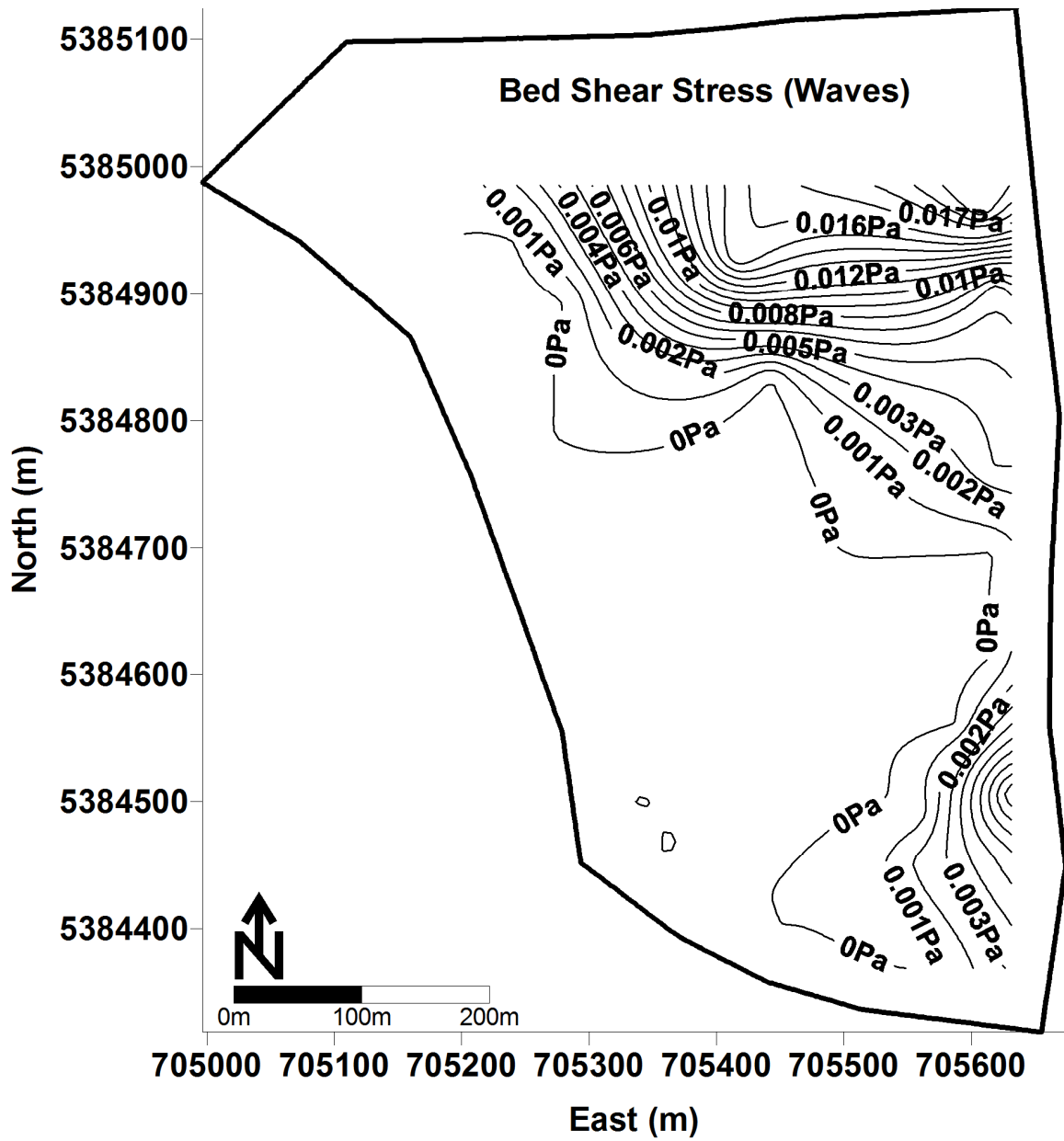


Figure 4.7 Contour map of estimated bed shear stress due to wind induced wave orbital velocities

for observed winds blowing at low speed along the shorter axis of the Middle cell. These bed shear stress conditions would be different in the case of stronger wind events and longer fetch lengths.

The current bed shear velocity (u_{*c}) was calculated by measuring the slope of a least-square line fitted to ADCP measured velocities in each depth cell and calculating the log of elevation above the bed of that particular depth cell. The intercept of the linear regression line provides an estimate of the bed roughness coefficient (k_{*c}), depending on whether smooth or fully rough turbulent flow conditions (Garcia 2007). Figures 4.8(a) and 4.8(b) show typical time-averaged velocity profiles at locations 10 and 14 (Figure 4.1), respectively, plotted with elevation above the bed on a log scale. Only the portion of the data that showed a linear trend near the bed was used to fit the least-square line to obtain a velocity profile slope for that particular location. For example, for the log profile shown in Figure 4.8(a) a linear profile was fitted to seven data points, while in Figure 4.8(b), twenty-six data points were fitted (see Appendix-III for remaining current velocity profiles). The advantage of this method was that knowledge of the bed roughness length, z_0 , is not required because u_{*c} depends only on the slope of the velocity profile. Results thus obtained for bed shear velocity (u_{*c}) due to bed currents were weakly filtered to exclude unrealistic bed roughness (k_s) values, considering smooth bed conditions. All the profiles with bed roughness values of more than 1.0 m were excluded from further calculations.

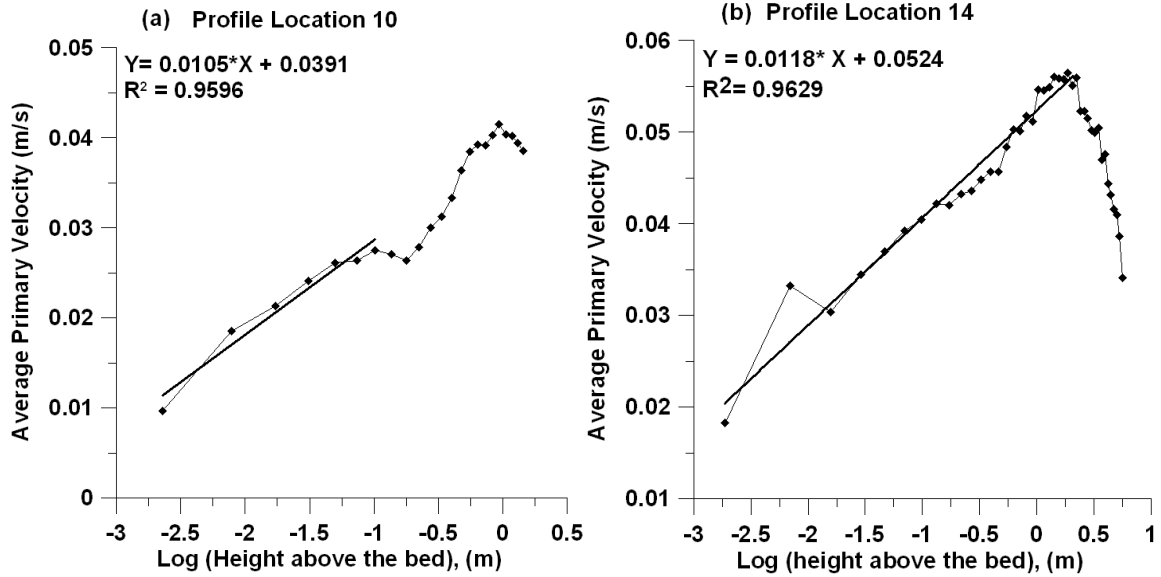


Figure 4.8 (a), (b) Log linear current velocity profile for locations 10 and 14

Figure 4.9 shows a contour map of the bed shear stress due to circulatory currents obtained for each ADCP profiling location. The ADCP measured current profiles at all locations were almost of the same order of magnitude, hence variation in current induced bed shear stress was localized. The bed shear stress due to currents is not a function of fetch length and thus variation is not related to location in the pond. At the location of abrupt depression higher current velocities were recorded, which would explain the relatively higher bed shear stress at that location.

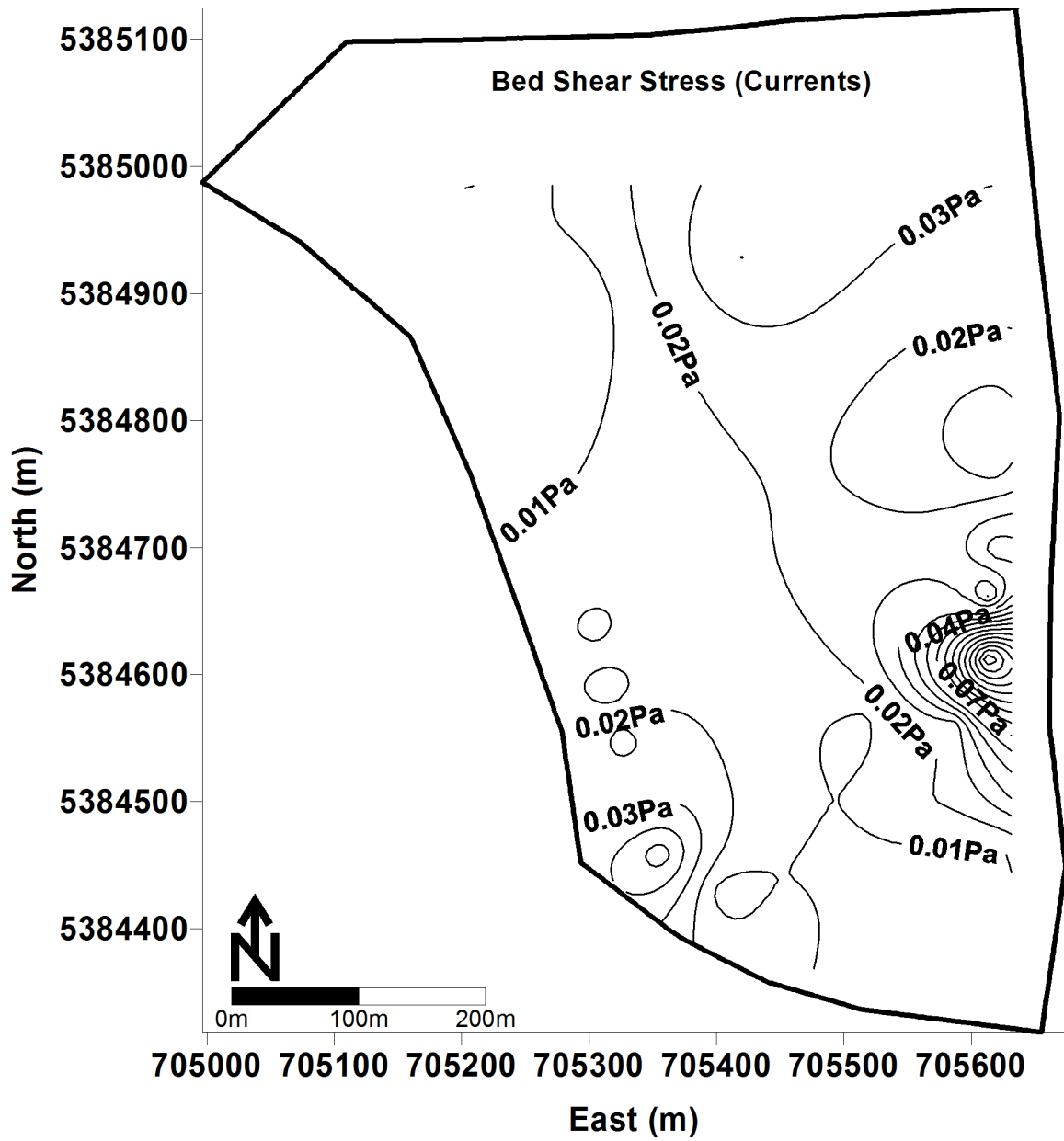


Figure 4.9 Contour map of estimated bed shear stress due to wind induced circulatory current velocities

The direction of current vectors measured by ADCP was from East in the counter-clockwise direction while wind direction was measured clockwise direction from the North. In order to find the angle between waves and currents, the current direction was first transformed in the same reference system. It can be assumed from the field observations that surface waves propagate in the same direction as the wind and this assumption is reasonable because wind is the only driving force available for the waves in tailings pond. The angle between the wave propagation direction and depth averaged current direction was obtained for each location and used in Equations 4.2 and 4.3 to obtain combined wave-current bed shear stress. Figure 4.10 presents the contour plot for combined bed shear stress under wave-current interaction. The estimated combined wave-current bed shear stress varied from 0.001 Pa at location 51 to 0.160 Pa at location 26 (see Figure 4.1 for location numbers). Location 26 was at the depression where relatively strong currents were recorded. The average value of total bed shear stress in the pond was 0.028 Pa. It was evident that on the west side of the zero wave-induced bed shear stress contour line (shown in Figure 4.7), the bed shear stress was mostly due to circulatory currents, while on the east side it was the result of combined wave-current interaction. From the results it may be concluded that circulatory currents greatly affect bed shear stress in a tailings pond and they cannot be ignored. It also should be noted that maximum bed shear stress was the location of deepest water cover. It was due to stronger currents recorded at the locations of abrupt depression in the pond. In general, magnitude of currents is not a function of water depth and depends on topography of bed.

Previous studies (Catalan and Yanful 2002) ignored current induced bed shear stress in a tailings pond, assuming it to be only 10% of the total bed shear stress.

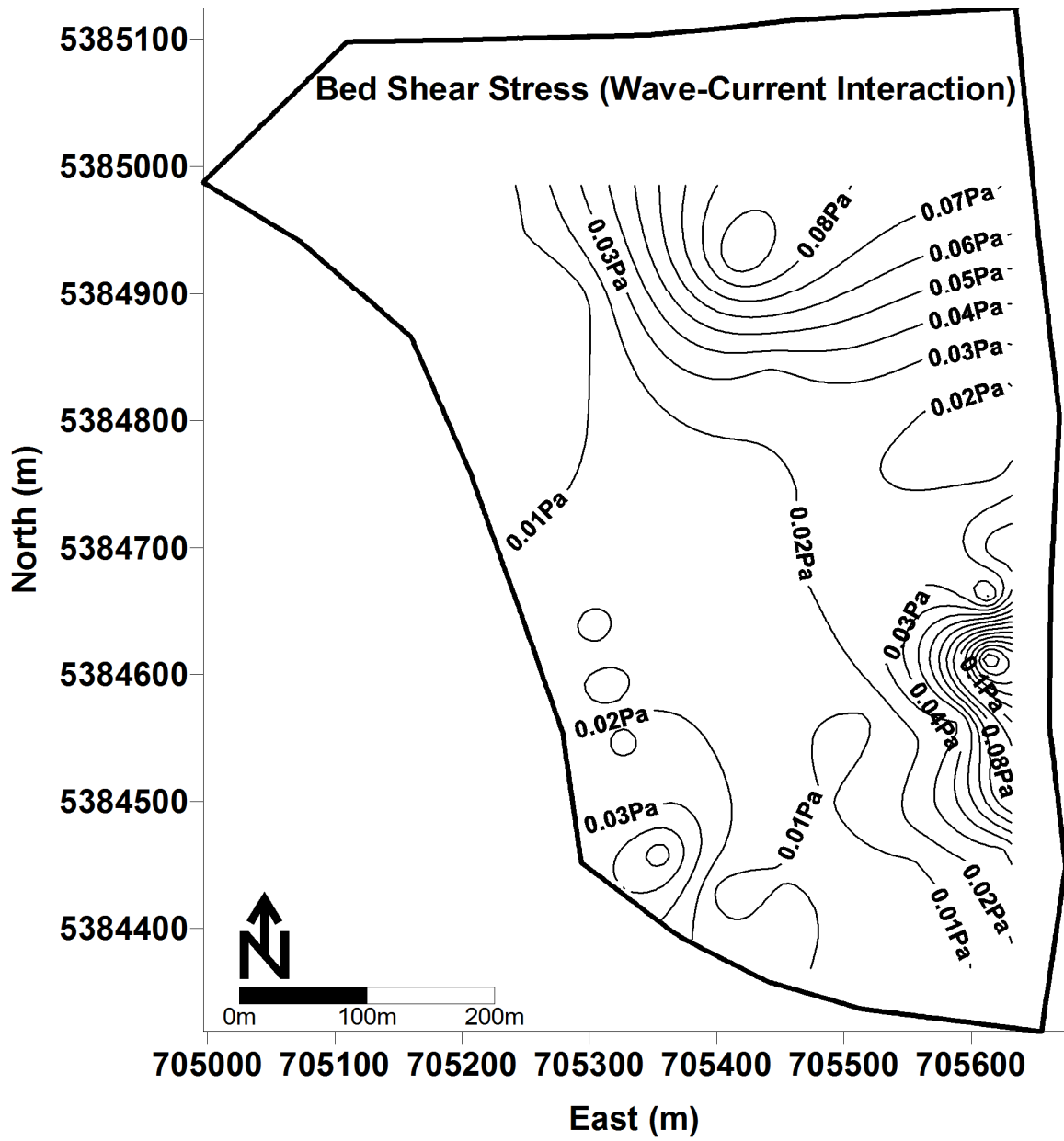


Figure 4.10 Contour map of estimated bed shear stress due to combined wave current interaction

However, Samad and Yanful (2005) later found that bed shear stress due to currents often exceeded 20% of the total bed shear stress. In their study Samad and Yanful (2005) also calculated total bed shear stress as a linear addition of both wave and current induced bed shear stresses. They ignored any possible wave-current interaction. In the present study, an attempt has been made to compare linear versus non-linear addition of wave and current bed shear stresses as shown in Figure 4.11. The ratio of pure current bed shear stress (τ_c) to non-linear total wave-current bed shear stress (τ_{cw}) was found to be up to 0.97 (97%) and ratio of non linear wave-current total bed shear stress (τ_{cw}) to linearly added wave-current bed shear stress was found up to 1.97. In Figure 4.11, the total bed shear stresses obtained from linear and non-linear additions of wave and current bed shear stress were almost equal at locations where wind wave induced bed shear stress was negligibly small, especially westward of the zero bed shear stress (wave-induced) contour line shown in Figure 4.7, and the total bed shear stress was mainly due to currents. But at locations where wave induced bed shear stress is higher, the non-linear total bed shear stress is greater than that obtained by linear addition of wave and current shear stresses. It is clear from these results that currents significantly contribute to total bed shear stresses and they cannot be ignored. Also non-linear wave-current interaction enhances the total bed shear stress as predicted by Jing and Ridd (1996).

Resuspension occurs when bed shear stress exceeds the critical shear stress of the bed tailings. The critical shear stress is a characteristic property of bed tailings and depends on the physical and chemical properties of tailings, such as grain size distribution, degree of consolidation, mineral composition, and cohesiveness. The empirically estimated average value of the critical shear stress of bed tailings in the East

and West cells of the Shebandowan tailings pond were of the order of 0.12 Pa while in the Middle cell it was estimated to be 0.04 Pa (Kachhwal et al. 2010). The median particle size (D_{50}) was 0.08-0.55 mm in the east and west cell while in the middle cell it was 0.007 mm. The bed tailings in the Middle cell were comparatively finer than bed tailings in the other two cells. In the present study the total bed shear stress in the Middle cell was calculated to be 0.16 Pa, which was higher than the empirically estimated critical shear stress of 0.04 Pa. However for finer sediment particles that are likely to be cohesive, such as the bed tailings in the Middle cell, empirical approaches may not reliably predict the critical shear stress (Blake et al. 2004).

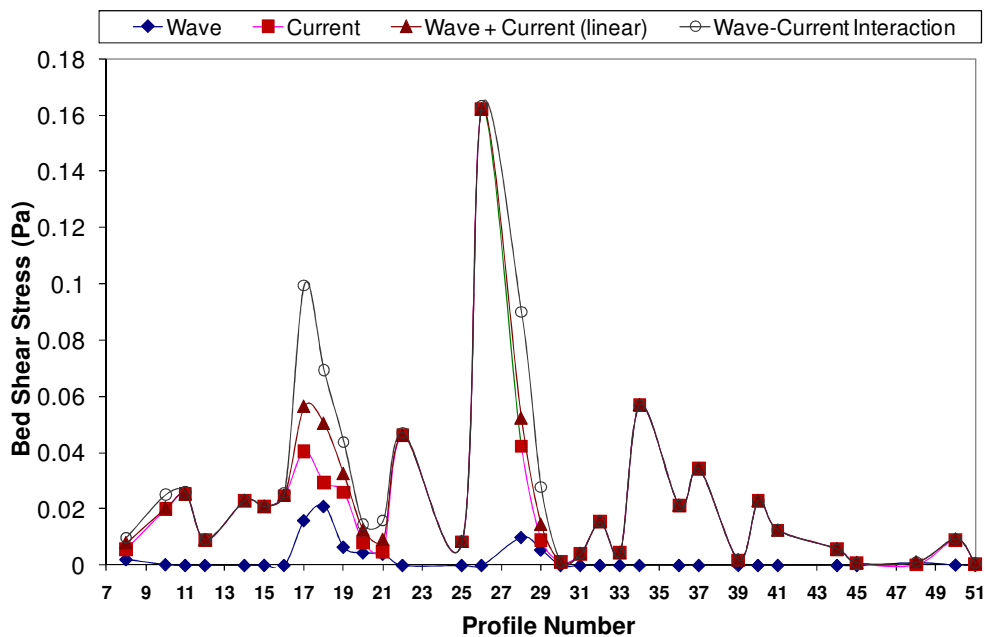


Figure 4.11 Comparison of wind wave and current induced bed shear stresses

4.3.3 Sources of Error

Apart from possible field measurement and instrumental limitations, the following are the major sources of error that could have affected the estimation of bed shear stress under wave-current interaction.

1. The empirical wave hindcasting equations used in the calculation of wave induced bed shear stress are simplified solutions of complex wave growth and propagation phenomena (CERC 2002). The amount of error introduced in using these equations can be measured only if the actual wave parameters could be measured in the field. The ADCP that was used in this study was capable of measuring only currents and not waves. Other ADCPs are capable of measuring both waves and currents simultaneously. This could be considered in future studies.
2. In complex flow conditions when the current velocity profile is not completely log linear, only the portion of profile near the bed that can be fitted to a least-square regression line should be used for current induced bed shear stress estimation. The manual selection of this linear portion depends on visible deviation of the velocity profile from log linearity. This may introduce some error in the calculated current induced bed shear stress. A typical shape of log velocity profile was shown in Figure 4.8(a) for location number 10, where seven measurement points from the bed were chosen to calculate the slope. Here we will repeat the calculation of bed shear stress by taking only three measurement points near the bed and taking the complete velocity profile (Figure 4.12). The results are presented in Table 4.1. If we consider the seven-point measurement accurate

then the three-point measurement overestimates the bed shear stress by 48% while the full profile measurement underestimates it by only 6%. However the amount of error depends on the shape of log velocity profile, which was different for each measurement location.

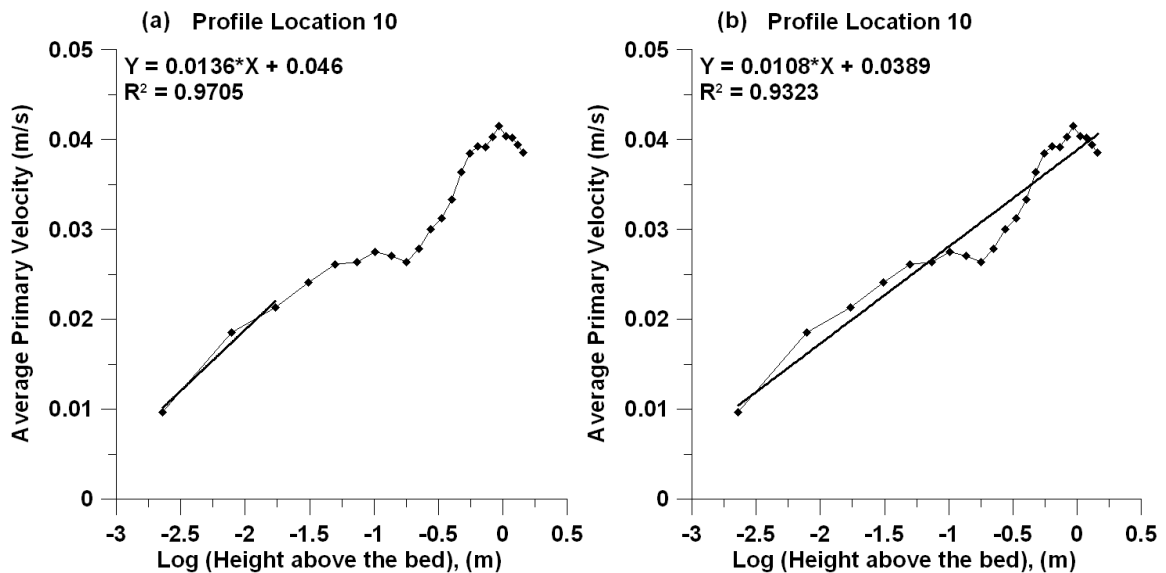


Figure 4.12 Log current velocity profile at location 10 with linear regression line fitted for three points and for full profile

Table 4.1 Comparison of log linear profile fitted with different number of measurement points at location 10

# Points	Bed shear velocity (m/s)	Bed shear stress (Pa)	% Difference
3	5.44×10^{-3}	0.029	48% (over)
7	4.46×10^{-3}	0.019	
Full profile	4.32×10^{-3}	0.018	6% (under)

4.4 CONCLUSIONS

Wind-induced currents in a tailings pond were measured using an ADCP. An intricate pattern of flow circulation was observed in the pond, which was more complex than the near-bed flow reversal that is typically assumed. Knowledge of the total bed shear stress induced by wind waves and currents is an important parameter in the management of a tailings pond. A semi-empirical approach of bed shear stress calculation was used that considered non-linear wave-current interactions. The ADCP measured circulatory currents were used to estimate the bed shear stress due to currents. A major finding of the study was that linear addition of wave and current bed shear stresses can underestimate the total bed shear stresses and that a non-linear approach accounting for wave-current interaction should be used. Given knowledge of the bed tailings characteristics, such as critical shear stress and erosion rate constants, accurate estimation of bed shear stress can help in the prediction of resuspended concentrations, and hence provide a useful tool for tailings pond management.

4.5 REFERENCES

1. Bailey, M.C., & Hamilton, D.P. (1997). Wind induced sediment resuspension: a lake-wide model. *Ecological Modelling*, Vol. 99, pp. 217-228.
2. Blake, A.C., Chadwick, D.B., White, P.J., & Jones, C.A. (2004). Interim guide for assessing sediment transport at Navy facilities. Spawar System Center, San Diego, CA, USA.
3. CERC (1984). Shore protection manual. U.S. Army Corps of Engineers, Coastal Engineering Research Centre, Vicksburg, M.S.
4. Dufois, F., Garreau, P., Hir, P.L., & Forget, P. (2008). Wave- and current-induced bottom shear stress distribution in the Gulf of Lions. *Continental Shelf Research*, Vol. 28, pp. 1920-1934.
5. Garcìa, M. H. (2007). "Sediment transport and morphodynamics", in Garcìa, M. H. (ed.), *Sedimentation Engineering, Processes, Measurements, Modeling and Practice, ASCE Manuals and Reports on Engineering Practice, No. 110*, American Society of Civil Engineers, Reston, VA.
6. Grant, W.D., & Madsen, O.S. (1979). Combined wave and current interaction with a rough bottom. *Journal of Geophysical Research*, 84(C4): 1979-1808.
7. Jin, K., & Ji, Z. (2004). Case study: modeling of sediment transport and wind-wave impact in Lake Okeechobee. *Journal of Hydraulic Engineering*, 130:1055-1067.
8. Jing, L., & Ridd, P.V. (1996). Wave-current bottom shear stresses and sediment resuspension in Cleveland Bay, Australia. *Coastal Engineering*, Vol. 29, pp. 169-186.

9. Jones, J.E., & Davies A.M. (2001). Influence of wave-current interaction, and high frequency forcing upon storm induced currents and elevations. *Estuarine, Coastal and Shelf Science*, Vol. 53, pp. 397-413.
10. Kachhwal, L.K., Yanful, E.K., & Lanteigne, L. (2010). Water cover technology for tailings management: a case study of field measurement and model predictions. *Water, Air and Soil Pollution*, 214 (1-4): 357-382.
11. Liang, B., & Li, H. (2008). Bottom shear stress under wave-current interaction. *Journal of Hydrodynamics*, Vol. 20(1), pp. 88-95.
12. Luettich, R.A., Harleman, D.R.F., & Somlyódy, L. (1990). Dynamic behaviour of suspended sediment concentrations in shallow lake perturbed by episodic wind events. *Limnology and Oceanography*, 35:1050-1067.
13. Muste, M., Yu, K., Pratt, T., & Abraham, D. (2004). Practical aspects of ADCP data use for quantification of mean river flow characteristics; Part II: fixed-vessel measurements. *Flow Measurement and Instrumentation*, Vol. 15, pp. 17-28.
14. Teledyne RD Instruments (2009): Workhorse Rio Grande high accuracy ADCP. Teledyne RD Instruments, San Diego, CA, USA.
15. Rennie, C.D., Miller, R.G., & Church, M.A. (2002). Measurement of bedload velocity using an Acoustic Doppler Current Profiler. *Journal of Hydraulic Engineering*, Vol. 128(5), pp. 473-483.
16. Samad, M.A., & Yanful, E.K. (2005). A design approach for selecting the optimum water cover depth for subaqueous disposal of sulfide mine tailings. *Canadian Geotechnical Journal*, Vol. 42, pp. 207-228.

17. Signell, R. P., Beardsley, R.C., Graber, H.C., & Capotondi, A. (1990). Effect of wave-current interaction on wind-driven circulation in narrow, shallow embayments. *Journal of Geophysical Research*, Vol. 95(C6), pp. 9671-9678.
18. Wilcock, P.R. (1996). Estimating local bed shear stress from velocity observations. *Water Resources Research*, Vol. 32(11), pp. 3361-3366.
19. Wu, J., & Tsanis, I.K. (1995). Numerical study of wind induced water currents. *Journal of Hydraulic Engineering*, Vol. 121(5), pp. 388-395.
20. Yanful, E.K., & Catalan, L.J.J. (2002). Predicted and field measured resuspension of flooded mine tailings. *Journal of Environmental Engineering*, Vol. 128(4), pp. 341-251.
21. Yang, Y. (2001). Wind induced countercurrent flow in shallow water. Ph.D. thesis, The University of Western Ontario, London, ON.
22. Yu, G., & Tan, S.-K. (2006). Errors in the bed shear stress as estimated from vertical velocity profile. *Journal of Irrigation and Drainage Engineering*, Vol. 132(5), pp. 490-497.

CHAPTER 5: ESTIMATING THE EROSION CHARACTERISTICS OF TAILINGS USING FIELD RESUSPENSION DATA

5.1 INTRODUCTION

Sulphide rich mine tailings are frequently deposited under shallow water cover to minimize the ingress of oxygen. Tailings entrained into the overlying water have a greater potential to oxidize from contact with dissolved oxygen in the near surface water than tailings at rest (Catalan and Yanful 2000). Oxidized tailings can generate acidity and release heavy metals, which can adversely affect the water quality and surrounding environment. Wind induced resuspension of bed tailings deposited under shallow water covers pose a significant environmental threat as discussed by many researchers (Adu-Wusu et al. 2001; Yanful and Catalan 2002; Mian and Yanful 2003, 2004). There is, therefore, the need to develop a simple method for predicting resuspension and suspended solids concentration in water.

In water bodies of closed boundary, such as tailings pond, erosion and subsequent resuspension of bed material occurs when bed shear stress induced by wind waves and currents exceeds the critical shear stress of bed material. The erosion of bed material is, in general, quantified by erosion rate equations. In most resuspension studies, suspended solids concentration in water has been predicted using various erosion rate equations (Partheniades 1986; Maa et al. 1998; Mehta et al. 1993; Sanford et al. 1991; Samad and Yanful 2005). In these equations, erosion rate is defined as a function of the excess bed

shear stress over the critical shear stress. Mehta et al. (1993) reviewed and listed some common erosion rate equations. The most generalized form of erosion rate equation was developed assuming the depth of erosion is small and that the critical bed shear stress for erosion does not vary with depth (Partheniades 1986; Samad and Yanful 2005). The generalized power law equation for erosion rate can be written as follows:

$$E = \begin{cases} \alpha \left(\frac{\tau_b}{\tau_{cr}} - 1 \right)^M & \text{if } \tau_b > \tau_{cr} \\ 0 & \text{if } \tau_b \leq \tau_{cr} \end{cases} \quad (5.1)$$

where, E is erosion rate (in g/m².s), τ_b is total bed shear stress (in N/m² or Pa), and τ_{cr} is critical shear stress of bed material for erosion (in N/m² or Pa). The coefficient (α) and exponent (M), generally known as erosion rate parameters, are typically obtained from laboratory erosion tests such as the rotating annular flume test and column tests (Krishnappan 1993; Geremew and Yanful 2010; Samad and Yanful 2005). In typical laboratory experiments, a disturbed bulk sample of bed material is subjected to known values of shear stresses by mechanical means and the amount of eroded material is obtained. The results obtained in this way are plotted using Equation 5.1 and the best fit erosion rate parameters are obtained for that sample.

The two major drawbacks of using laboratory experiments to estimate erosion rates are that: (i) considerable effort and time are required to conduct such experiments, which also include the collection and transportation of representative bed material sample from the field, and (ii) in most cases the laboratory experiments are conducted on disturbed bed samples and the results may not be representative of actual field conditions.

In most cases, field conditions of bed materials are completely different from those imposed in the laboratory experiments. The bed material in the field generally has two layers. The top layer is made of loose sediment of high water content while the bottom layer contains consolidated sediments. The top layer, also commonly called the “fluffy layer”, is a result of exposure to frequent erosion and re-deposition processes occurring in the field. The bed materials in the two layers have different erosion characteristics. In general, the top layer bed material has lower critical shear stress than the bottom consolidated material and can be easily resuspended by combined wave-current bed shear stresses (Wang 2002). In the field, the presence of benthic organisms and bio-films in bed sediments influence the erosion characteristics of cohesive sediments and disturbed samples used in the laboratory erosion tests may not represent the same physical, chemical and biological sediment characteristics (Krishnappan and Droppo 2006).

In field applications, it is important to estimate the critical shear stress and erosion rate parameters from field measured resuspension data. There are limited published studies available on the estimation of erosion rate parameters from field experiments. Wang (2002) estimated erosion rate parameters of cohesive sediments by field measurement of tidal waves and currents and turbidity at the Long Island Sound, USA. In that study, a two term power law was applied between erosion rate and bed shear stress. Moreau et al. (2003) obtained in-situ measured sediment erosion parameters using a benthic flume at Saguenay Fjord, Quebec, Canada. The rotating flume was mechanically powered to exert known amounts of bed shear stresses at the bed and a pre calibrated OBS sensor was attached to measure the corresponding suspended solids concentration. Krishnappan and Droppo (2006) used an in-situ erosion flume to measure erosion

parameters at Hamilton Harbour, Ontario, Canada. In most cases, the nature of the bed shear stresses applied by mechanical flume and wind induced waves and currents are totally different. The bed shear stresses generated in mechanical flumes are steady in nature while bed shear stresses generated by wind induced waves and currents are mostly unsteady.

The main objectives of the present study were to obtain erosion rate parameters using field measured wind induced resuspension obtained in an engineered tailings storage facility, and to develop a simplified approach to predict resuspension using field measured wind and depth data. In this study, the critical shear stress and erosion rate parameters of bed tailings were determined using OBS measured suspended solids concentration data along with wind data. A simplified equation was derived and used to estimate the total bed shear stress in shallow water conditions using wind and water depth data. Once the site specific erosion rate parameters have been determined, the erosion rate Equation 5.1 can be used to predict field resuspension for known wind and water depth conditions. A major limitation of the present approach is that the erosion equation cannot predict the instantaneous suspended solids concentrations. For example, it does not take into account the changes in the suspended solids concentration with time due to varying settling velocities after the wind conditions have changed. The role of settling velocity and its impact on the suspended solids concentration was not considered. However if settling is significant it would result in a reduction in the amount of suspended tailings and hence the oxidation rate. Consequently it is conservative to assume that settling is not important when predicting oxidation due to resuspension. In tailings pond studies, knowledge of accumulated suspended solids concentrations is more

important than the settling velocity. The suspended bed tailings are prone to oxidation through contact with high dissolved oxygen in the water cover. This paper differs from the work of Samad and Yanful (2005) and Kachhwal et al. (2010) in the sense that it proposes a method for estimating the critical shear stress and erosion parameters from field measured OBS data. Previous papers, such as Mian et al. (2007), Geremew and Yanful (2010) estimated critical shear stress and erosion parameters from laboratory column and flume experiments, which may not always be feasible because of cost or other limitations.

5.2 STUDY SITE

The study was conducted at the Shebandowan Mine tailings storage facility, located 100 km west of Thunder Bay, northwestern Ontario, Canada. The site is located along the south shore of Lower Shebandowan Lake. The Shebandowan mine was operated as an underground nickel and copper mining and milling facility from 1971 to 1998. Figure 5.1 shows the plan view of the tailings storage facility. The tailings storage facility occupies an area of about 115 ha. In 1999 approximately 85,000 m³ of potentially acid generating mine tailings were deposited under shallow water cover (Golder Associates 2000). Two engineered wave breaks (internal dykes) were constructed across the tailings facility, which divided the pond into three cells, namely, west cell, middle cell and east cell. The purpose of the wave breaks was to reduce the fetch length and hence eliminate or minimize sediment disturbance and subsequent erosion and resuspension of tailings. The depth of water cover in the pond varies from less than 1 m at some locations to over 3 m

at others. On average, the depth of water cover is about 1 m at most locations in the pond. The present study resuspension data were collected at locations in the west and middle cells of the tailings storage facility as shown in Figure 5.1.

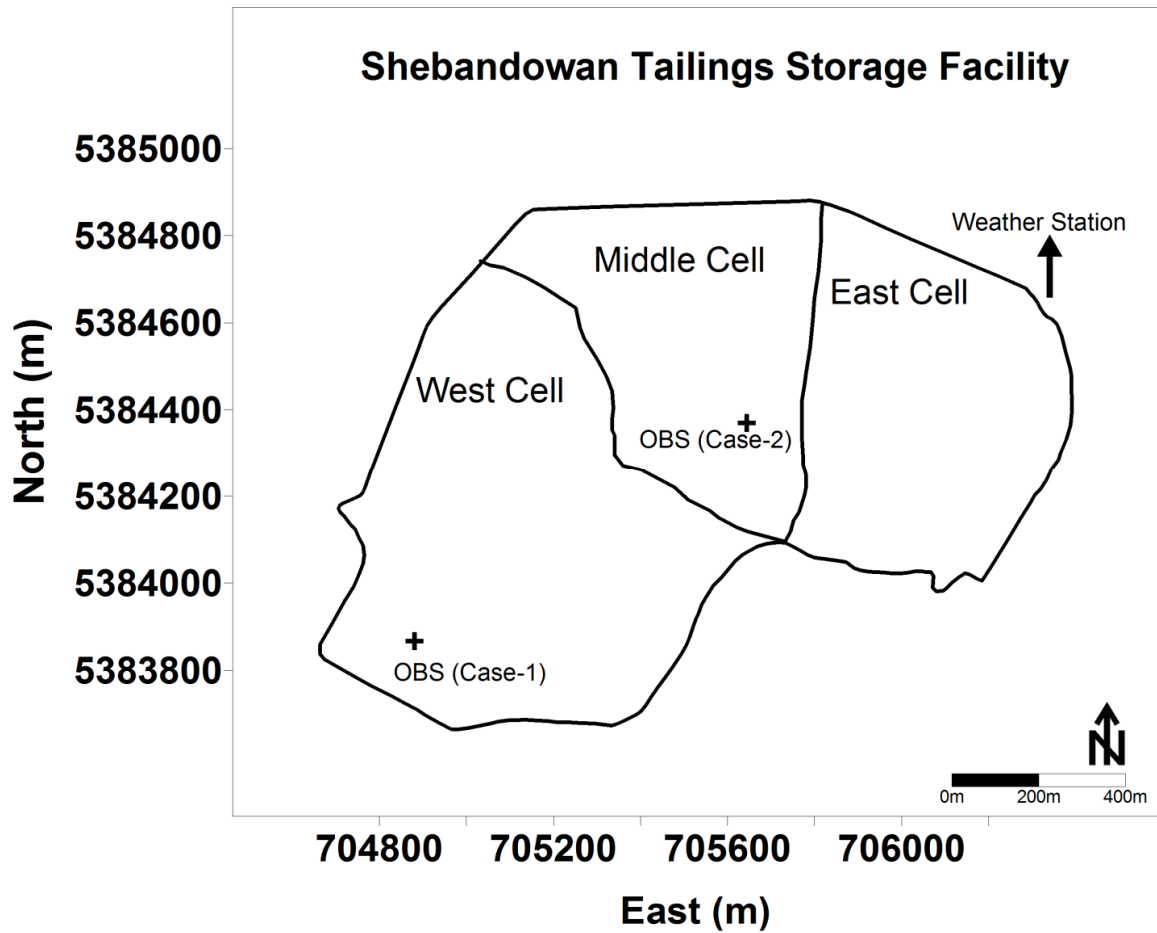


Figure 5.1 Map of Shebandowan tailings storage facility showing the OBS data collection locations in the west and middle cells and location of weather station

5.3 METHODS AND MATERIALS

Wind induced erosion and subsequent resuspension of bed material in a closed water body is a function of wind velocity (U), wind direction or fetch length (F), that is, the length of water surface over which wind blows in a particular direction, water cover depth (h), and erosion characteristics of bed material (K) which include the critical shear stress and erosion rate parameters (Kachhwal et al. 2010).

$$E = f(U, F, h, K) \quad (5.2)$$

In tailings ponds with shallow water cover, erosion and subsequent resuspension of bed material occurs when bed shear stress exerted by wind induced waves and currents exceeds the critical shear stress of bed material (Partheniades 1965; Bengtsson et al. 1990; Samad and Yanful 2005). The erosion of bed material generally can be quantified by erosion rate equations. As mentioned in the previous section, the most generalized form of erosion rate equation was developed assuming that the depth of erosion is small and that the critical bed shear stress for erosion does not vary with depth (Partheniades 1986; Samad and Yanful 2005).

The main objective of the present study is to obtain erosion rate parameters in equation (1), the coefficient (α) and exponent (M) by calibration of Equation 5.2 to field measured resuspension data. In order to calibrate Equation 5.2, the erosion rate (E) was determined using OBS recorded suspended solids concentrations (SSC) and total bed shear stress (τ_b) can be calculated using corresponding wind data. In this study, simultaneously recorded, suspended solids concentrations (SSC) by OBS sensors and

wind data were used to derive erosion rate parameters and critical shear stress of bed material as outlined below.

(1) Estimation of Erosion Rate (E)

The erosion rate, E , can be estimated for various wind conditions in the field using OBS recorded suspended solids concentration data. Suspended solids concentration (C_{ssc}) for a particular time can be converted to erosion rate (E) assuming equal distribution of eroded sediment in the water column depth (h) (Samad and Yanful 2005). This assumption is valid for depth averaged suspended solids concentration at any location in the tailings pond.

$$C_{ssc} = \frac{E}{h} \text{ or } E = C_{ssc} * h \quad (5.3)$$

(2) Estimation of Total Bed Shear Stress (τ_b)

Wind that blows over the water surface in the pond generates waves and currents by transferring its energy to the water surface in the direction of the wind. The waves grow during their travel over the water surface and along the available fetch length. These waves start to feel the bed of the pond when they are grown enough to exert shear stress on the bed. The strength of wind generated currents does not depend on fetch length, but on the intensity of turbulence generated in the water by waves. The total bed shear stress exerted by wind-induced waves and currents at the bottom of the pond is made of three components: pure wave bed shear stress, pure currents bed shear stress and a third term

due to wave-current interaction (Kachhwal et al. 2011). In most studies the total bed shear stress can be calculated as a linear addition of bed shear stress due to waves and currents. Previous research based on the Grant and Madsen (1979) theory showed that the non-linear wave-current interaction may enhance the bed shear stress (Kachhwal et al. 2011). The total bed shear stress from non-linear wave-current interaction can be given by following equation:

$$\tau_b = \tau_c + \tau_w + 2\sqrt{\tau_c \tau_w} \cos\theta_c \quad (5.4)$$

where, τ_w and τ_c are the bed shear stress due to waves and currents, respectively; θ is the angle between waves and currents which varies between 0 to 90^0 , assuming simple harmonic motion of waves. The third term in Equation 5.4 is due to non-linear wave current interaction. The value of this term is maximum when the angle between wave and current is zero or they are collinear, while it is zero when wave and currents are perpendicular to each other. The angle, θ , between waves and currents mostly needs to be determined from field experiments.

The total bed shear stress can be calculated using wind speed U (m/s) measured at 10 m above the water surface, fetch length F (m) measured in the direction of the wind, and water cover depth h (m). The following Equation 5.5 has been derived by combining wind waves and currents bed shear stress estimation methods discussed in Samad and Yanful (2005) and Kachhwal et al. (2010) to obtain total bed shear stress using wind speed (U), Fetch length (F), and water cover depth (h).

$$\tau_b = \frac{0.2182 * U^{0.613}}{\sinh \left[\frac{1541.5 * h}{U^{0.820} * F^{0.667}} \right]} + 3.734 \times 10^{-4} * U^2 + \frac{0.0180 * U^{1.307}}{\sqrt{\sinh \left[\frac{1541.5 * h}{U^{0.820} * F^{0.667}} \right]}} \quad (5.5)$$

In the Equation 5.5, the first term on the right-hand-side is the bed shear stress due solely to wind waves. It was obtained by simplifying the shallow water wave hindcasting equations used in the SMB method (CERC 1984). The second term defines the bed shear stress due to currents and was obtained by using the approach adopted by Wu and Tsanis (1995) and Yang (2001). The third term shows the enhancement in bed shear stress due to non-linear wave-current interaction based on the Grant and Madsen (1979) model. As discussed later in section 6.3.2 of Chapter 6 that Wu and Tsanis (1995) approach can predict the magnitude of currents shear velocities similar to those measured in the field using ADCP for the similar conditions. However, the theoretical approach used for calculating the bed shear stress due to currents did not provide any information on current direction (Wu and Tsanis 1995; Yang 2001). In this equation, the waves and currents were assumed collinear (Angle $\theta = 0$ or 180 degrees) to obtain maximum total bed shear stress. Detailed derivation of the simplified Equation 5.5 of the total bed shear stress estimation is provided in Appendix-IV of this thesis.

(3) *Estimation of Critical Shear Stress*

Once the erosion rate (E) and total bed shear stress (τ_b) have been obtained for different wind conditions, the critical shear stress can be estimated by assuming that (i) erosion rate E is zero if total bed shear stress is less than the critical shear stress of bed material

and, (ii) if the bed shear stress is greater than the critical stress, then erosion rate is directly proportional to total bed shear stress. The critical bed shear stress can be determined by plotting erosion rate versus total bed shear stress and fitting the data to a linear regression line. The critical shear stress of bed material would be equal to value of total bed shear stress obtained by extrapolating the regression line to intercept the x-axis, which corresponds to zero erosion rate ($E = 0$).

(4) Estimation of Erosion Rate Parameters

Once the erosion rate, E , estimated from field measured resuspension data and total bed shear stress obtained from wind and water depth data are known, erosion rate parameters, such as the coefficient (α) and exponent (M), can be determined as follows:

$$\text{Log}(E) = \text{Log}(\alpha) + M * \text{Log}\left(\frac{\tau_b}{\tau_{cr}} - 1\right) \quad (5.6)$$

Erosion rate parameters, coefficient (α) and exponent (M) can be obtained as the intercept and slope of a linear plot between the logarithms of erosion rate (E) and $\left(\frac{\tau_b}{\tau_{cr}} - 1\right)$.

5.4 DATA COLLECTION

In the present study, resuspension data were collected in the west and middle cells of the pond using two optical backscatter sensors or OBS sensors (OBS-3+, Campbell Scientific

Canada Corp., Edmonton, Alberta). These sensors have been used reliably to measure wind induced resuspension and results were fairly correlated with wind data (Kachhwal et al. 2010). The wind data, wind speed and wind direction were recorded from a Young Wind Monitor installed close to the tailings pond at 10 m height above the water surface. The locations of OBS sensors in the middle and west cells and weather station are shown in Figure 5.1.

The OBS sensor works on the principle of emission of infrared light signal and reception of light backscattered by suspended particulates in water. The intensity of backscattered light can be directly correlated with the concentration of suspended solids in water. However, the interaction of emitted light with particulate material depends on the size, shape and composition of material and, therefore, varies between different materials. The two OBS sensors used in the present study were calibrated in the laboratory for bed tailings from the west and middle cells (Kachhwal et al. 2010). One OBS sensor was installed at a height of 10 cm above the bed and the other at 25 cm above the bed. However, the variation in the suspended solids concentrations in the water column with respect to their locations above the bed was not used, and only the depth averaged OBS results were used in the calculations. Details of OBS data collected in the west and middle cells along with corresponding wind data are presented below for two cases:

Case- 1: OBS in West Cell on October 09-10, 2007:

OBS results recorded in the west cell on October 09-10, 2007 and corresponding wind data are shown in Figure 5.2. The longest fetch at the location of the OBS sensors was

1055 m for winds blowing in the direction of northeast (0° - 45°). A significant fetch length was also available for the winds blowing in the direction 45° to 180° , that is, northeast to southwest. Winds of relatively high speed, up to 6 m/s, and in the direction of longer fetch length were available periodically to resuspend the bed tailings. The depth averaged suspended solids concentration was up to 40 mg/L.

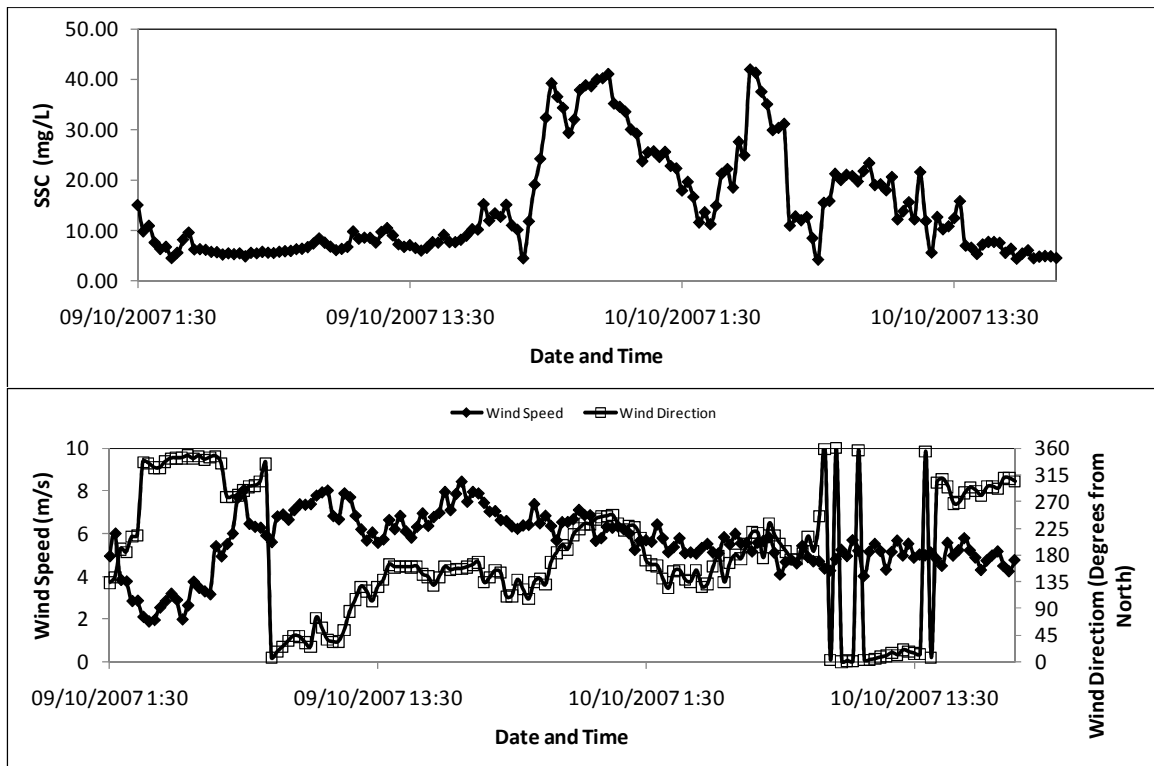


Figure 5.2 OBS recorded suspended solids concentration (SSC) and corresponding wind data in the west cell of the tailings pond on October 09-10, 2007

Case- 2: OBS in Middle Cell on July 25-26, 2008:

OBS sensors deployed in the middle cell during July 19-21, 2007 showed small peaks of suspended solids concentration (Kachhwal et al. 2010). However, for the middle cell bed tailings, the empirically calculated critical shear stress was small (0.04 Pa) in comparison with the wind induced total bed shear stress and the total bed shear stress always exceeded the critical value, which should have resulted in a relatively larger amount of suspended solids concentration than those recorded in the field by two OBS sensors. The authors pointed out that the bed tailings in the middle cell were likely to be cohesive and the critical shear stress of the bed tailings in the middle cell could be higher than the empirically determined value. In that study, the erosion rate parameters for the middle cell bed tailings were not available and due to that the Samad and Yanful (2005) model predicted and field measured resuspension results could not be compared. During the summer of 2008, OBS sensors were installed in the middle cell using a specially fabricated steel platform. The sensors were deployed to record long term episodic resuspension events. As the sensors are prone to fouling by deposition of suspended material, only data from the first few days of monitoring were used in the present study.

Figure 5.3 shows the time series variation in depth averaged suspended solids concentration recorded in the middle cell on July 25-26, 2008 and the corresponding wind data. Wind conditions during this period were favourable to induce high bed shear stress. Wind direction was mostly northwest (270° - 360°), which was also the direction of the longest axis of the middle cell. Thus this direction provided a relatively long fetch length for the wind-waves to grow. Wind speed varied periodically. The maximum wind

speed recorded was above 9 m/s. The high wind speed and long fetch mobilized sufficient bed shear stress to resuspend the tailings and depth averaged suspended solids concentration was up to 60 mg/L.

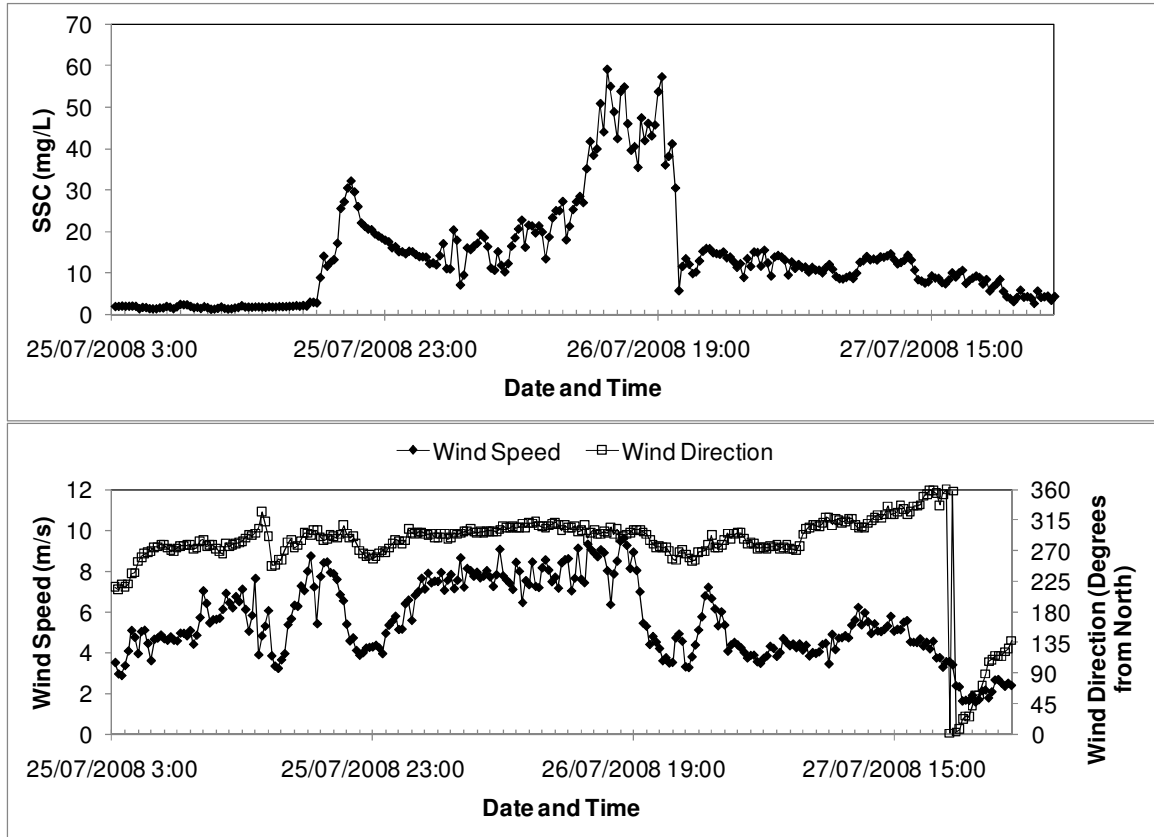


Figure 5.3 OBS recorded suspended solids concentration (SSC) and corresponding wind data in the middle cell of the tailings pond on July 25-27, 2008

5.5 DATA ANALYSIS

Erosion of bed tailings occurs when wind induced total bed shear stress exceeds the critical shear stress of the bed material. The erosion rate of the bed material is directly related to the total bed shear stress. The total bed shear stress and hence the erosion rate change with wind speed and direction. It can be assumed that eroded material stays in suspended state in the water until the bed shear stress exceeds the critical shear stress, which means there will be no settling of the suspended material and increasing suspended solids concentration between two time steps is the result of net erosion. The time series of depth averaged concentrations of suspended solids obtained from OBS data can be converted into erosion rates using the following steps.

1. First, not all the SSC values in Figures 5.2 and 5.3 are due to erosion. The SSC values increasing with time, that is, the values on the ascending side of peak, should be used in the calculations. Values on the descending side of the peak, where SSC is decreasing with time, should be avoided. These values show the effect of settling velocities after the wind conditions have changed and the total bed shear stress is below the critical shear stress under new wind conditions.
2. Once the bed shear stress is higher than the critical shear stress of bed material, continuous erosion of bed material adds to the suspended solids concentration until the wind condition changes to lower the bed shear stress. It can be assumed that during the period when bed shear stress is greater than the critical shear stress, there will be no settling of resuspended material. In order to obtain the net concentration of material eroded between two successive measurements, the

difference between SSC values should be taken into account for the estimation of erosion rates.

3. The OBS results were recorded as the average concentration of suspended solids concentration every 15 minutes. The net concentration obtained in step two was the increase in suspended solids concentration over 15 minutes. From this, the net increase in concentration per second was calculated. The erosion rate ($\text{g/m}^2\cdot\text{s}$) was calculated using Equation 5.3 by multiplying the net suspended solids concentration by water cover depth. Prior to that, suspended solids concentrations were converted from mg/L to g/m^3 .

5.6 RESULTS AND DISCUSSION

The total wind induced bed shear stress is a function of wind speed (U), fetch length (F) and water cover depth (h). A simplified equation was developed in terms of these three parameters to obtain total bed shear stress in shallow water conditions. The time series of total bed shear stress was obtained from field measured wind data using simplified Equation 5.3. At any moment, the fetch length (F) was determined at the location of OBS sensors in the direction of wind and water cover depth (h) was measured at the time of OBS sensors deployment in the pond. Figure 5.4 shows the variation in wind induced total bed shear stress with time corresponding to OBS results presented in Case-1 and Case-2 in the west and middle cells respectively.

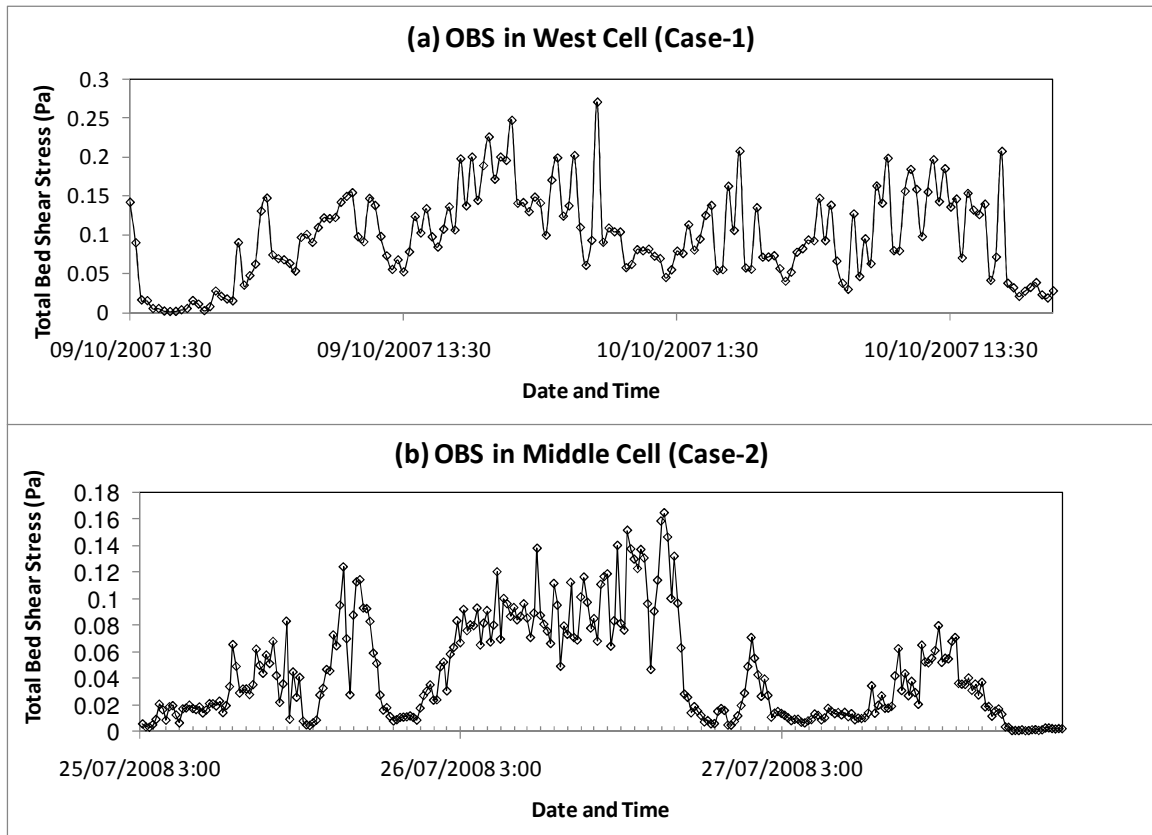


Figure 5.4 Time series of total bed shear stress (in Pa) calculated from wind data corresponding to OBS data collected in (a) the west cell or Case-1 and (b) the middle cell or Case-2

The critical shear stress was calculated assuming there would be no erosion ($E = 0$) when bed shear stress is equal to or less than the critical shear stress. Graphs of estimated erosion rates (from OBS data) versus calculated total bed shear stresses for the west and middle cells were plotted as shown in Figure 5.5. The fitted regression line was extrapolated back to the x-axis to yield the critical shear stress (corresponding to erosion rate, E , of zero) of the bed material. The graphically calculated critical shear stress for the west cell bed tailings was 0.10 Pa. This value was slightly less than the empirically calculated value of 0.12 Pa obtained by Kachhwal et al. (2010). The empirical approach

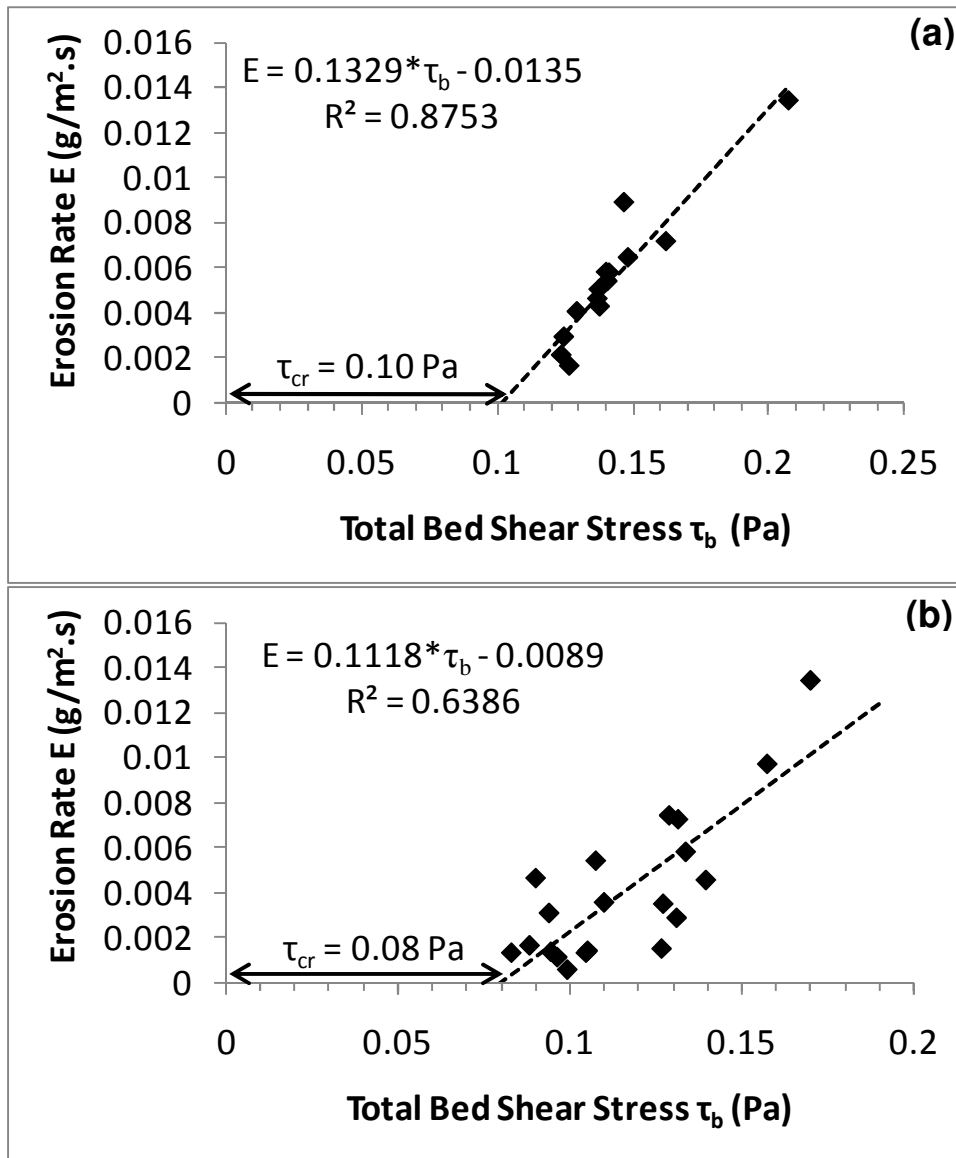


Figure 5.5 Plot of calculated erosion rates versus total bed shear stress data to obtain critical shear stress values for the (a) west cell and (b) middle cell

used to calculate shear stress was based on the median grain size (D_{50}) and specific gravity (G_s) as input values. The slight difference may be attributed to less dense top layer (fluffy layer) of bed sediments which is subjected to frequent erosion and re-deposition processes (Wang 2002). In the same graphical approach, the critical bed shear

stress was estimated for the middle cell bed tailings to be 0.08 Pa. The bed tailings in the middle cell were finer than the west cell bed tailings and, therefore, in our previous study, the empirically calculated critical shear stress of the middle cell bed tailings was 0.04 Pa (Kachhwal et al. 2010). It was found that, field measured resuspension with sediment traps and OBS sensors did not agree with such a low critical shear stress value and it was predicted that the critical shear stress of the middle cell tailings might actually be higher than the empirically calculated value due to the presence of binding cohesive forces in the finer middle cell bed tailings. The higher value of critical shear stress of the middle cell bed tailings obtained in the present study supports that finding.

The erosion rate parameters were obtained by plotting the graph between logarithm of calculated erosion rate ($\text{Log}_{10}(E)$) (in $\text{g}/\text{m}^2.\text{s}$) and logarithm of ratio of total bed shear stress to critical shear stress minus one ($\text{Log}_{10}(\tau_b/\tau_{cr} - 1)$) as per Equation 5.6. The data were fitted to a linear regression line and from the equation of the straight line, the slope and intercept were used to obtain erosion rate parameters. Figure 5.6 shows the graphs plotted for the west cell and middle cell results. The results fitted with a linear regression line, showed good correlation with $R^2 = 0.86$ and $R^2 = 0.54$ for the west and middle cell results respectively. A higher correlation was found between the west cell data than the middle cell data. It may be attributed to the complex nature of binding cohesive forces in the finer middle cell bed tailings. These binding forces provide additional strength to the bed material for erosion but finer bed tailings will resuspend with a higher erosion rate once these binding forces have been broken by applied bed shear stress. For the west cell, the slope of linear regression line provided the value of erosion rate exponent $M = 0.6145$, while the intercept was equivalent to $\text{Log}_{10}(\alpha) = -$

1.7943, which results in an erosion rate coefficient, $\alpha = 0.0161$. Using the similar approach, for the middle cell erosion rate parameters, the exponent $M = 0.6121$ and the coefficient $\alpha = 0.0069$ were obtained. For the west cell bed tailings at the Shebandowan

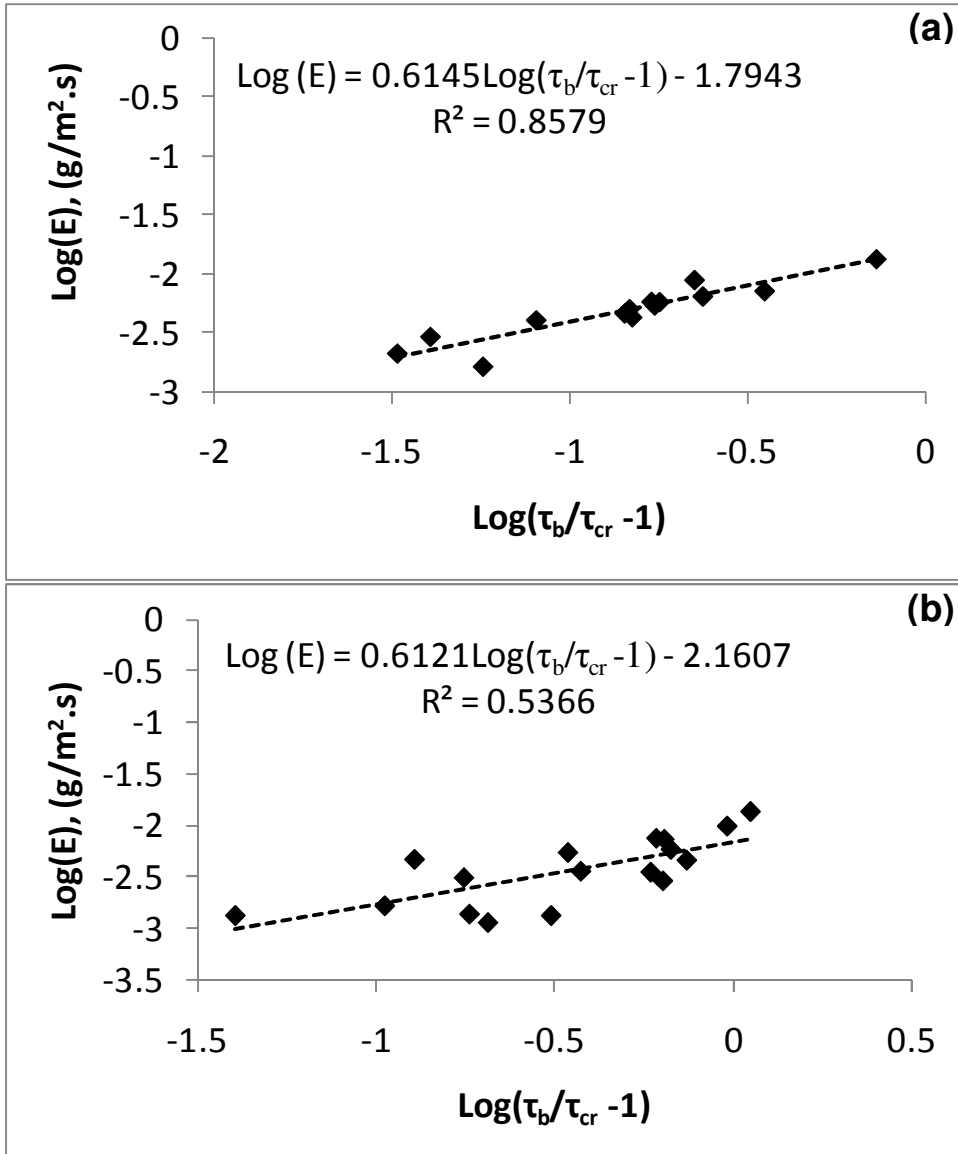


Figure 5.6 Plot of logarithm of erosion rate versus logarithm of bed shear stress over the critical shear stress to obtain erosion rate parameters of the bed tailings in the (a) west cell and (b) middle cell

site, values of erosion rate parameters, exponent (M) and coefficient (α) were calculated to be 1.121 and 0.0025, respectively, through laboratory column experiments by Geremew and Yanful (2010).

For mine tailings, Samad and Yanful (2005) predicted typical values of erosion parameters, exponent $M = 1.333$ and coefficient $\alpha = 0.1667$. The erosion rate parameters obtained in this study were of the same order of magnitude but at the same time were quite different from those obtained by Geremew and Yanful (2010). These values may be different because of two reasons. First, the location and sampling conditions of bed tailings collected by Geremew and Yanful (2010) may be different from the location of the OBS sensors used in the present study. Second, as discussed earlier, erosion and resuspension occurs mostly in the surface layer of the bed material and due to frequent erosion and redeposition, the erosion characteristics of the material in the surface layer will be different from those of the disturbed bulk sample of bed material. The erosion rate parameters calculated in this study was for actual resuspended material in water and can be considered more representative.

5.7 CONCLUSIONS

Time series suspended solids concentrations of bed tailings were obtained using optical backscatter sensors (OBS) in the west cell and middle cell of the Shebandowan tailings storage facility. A simplified equation was derived for calculating the total bed shear stress under shallow water conditions using wind and water depth data. The critical shear

stress and erosion rate parameters of bed tailings were obtained using field measured resuspension and wind data. These results were found to be more reliable and representative of actual field conditions than data obtained mathematically and using laboratory-derived erosion characteristics. Field-derived erosion characteristics of the bed material can be used with the simplified equation developed in the present paper to estimate the wind induced bed shear stress for the prediction and evaluation of erosion and resuspension in engineered mine tailings storage facilities.

5.8 REFERENCES

1. Adu-Wusu, C., Yanful, E.K., & Mian, M.H. (2001). Field evidence of resuspension in a mine tailings pond. *Canadian Geotechnical Journal*, 38(4): 796-808.
2. Geremew, A.M., & Yanful, E.K. (2010). The role of fines on the cohesive behavior of mine tailings inferred from the critical shear stress. *Canadian Geotechnical Journal*. In Press. Accepted October 4, 2010.
3. Golder Associates (2000). A report on Shebandowan tailings facility. Annual inspection-August 2000.
4. Grant, W.D., & Madsen, O.S. (1979). Combined wave and current interaction with a rough bottom. *Journal of Geophysical Research*, 84(C4): 1979-1808.
5. Kachhwal, L.K., Yanful, E.K., & Lanteigne, L. (2010). Water cover technology for tailings management: a case study of field measurement and model predictions. *Water Air Soil Pollution*, 214(1-4): 357-382.
6. Kachhwal, L.K., Yanful, E.K., & Rennie, C.D. (2011). A semi-empirical approach for estimation of bed shear stress in a tailings pond. *Journal of Environmental Earth Sciences*, under review.
7. Krishnappan, B.G. (1993). Rotating circular flume. *Journal of Hydraulics Engineering*, 119(6): 758-767.
8. Krishnappan, B.G., & Droppo, I.G. (2006). Use of an in-situ erosion flume for measuring stability of sediment deposits in Hamilton Harbour, Canada. *Water Air and Soil Pollution*, 6: 557-567.

9. Maa, J.P.-Y., Wright, L.D., Lee, C.-H., & Shannon, T.W. (1993). VIMS Sea Carousel: a field instrument for studying sediment transport. *Marine Geology*, 115: 271-287.
10. Mehta, A.J., Parchure, T.M., Dixit, J.G., & Ariathrai, R. (1982). Resuspension potential of the deposited cohesive sediment beds. *Estuarine comparisons*, V.S. Kennedy, ed., Academic, New York, 591-609.
11. Mehta, A.J. (1993). Hydraulic behaviour of fine sediment. In: Abbot, M.B. Price, W.A. (Eds.). *Coastal, Estuarine, and Harbour Engineer's Reference Book*. Chapman and Hall, London, UK, 557-584.
12. Mian, M.H., & Yanful, E.K. (2003). Tailings erosion and resuspension in two mine tailings ponds due to wind waves. *Advances in Environmental Research*, 7: 745-765.
13. Mian, M.H., & Yanful, E.K. (2004). Optical backscatter measurements of tailings resuspension in a mine tailings pond. *Proc. 57th Canadian Geotechnical Conference, Session 7D*: 38-45.
14. Mian, M.H., Yanful, E.K., & Martinuzzi, R. (2007). Measuring the onset of mine tailings erosion. *Canadian Geotechnical Journal*, 44: 473-489.
15. Moreau, A.-L., Locat, J., Hill, P., Long, B., & Ouellet, Y. (2003). In situ flume measurements of sediment erodability in Saguenay Fjord (Quebec, Canada). In: Locat, J., Galvez-Cloutier, R., Chaney, R.C., Demars, K. (Eds.), *Contaminated Sediments: Characterization, Evaluation, Mitigation/Restoration, and Management Strategy Performance*, ASTM STP 1442. ASTM International, West Conshohocken, PA, pp. 119– 138.

16. Partheniades, E. (1986). A fundamental framework for cohesive sediment dynamics. In *Estuarine Cohesive Sediment Dynamics*. Ed. Mehta A.J. Springer, Berlin.
17. Samad, M. A., & Yanful, E.K. (2005). A design approach for selecting the optimum water cover depth for subaqueous disposal of sulphide mine tailings. *Canadian Geotechnical Journal*, 42: 207-228.
18. Sanford, L.P., Panageotou, W., & Halka, J.P. (1991). Tidal resuspension of sediments in northern Chesapeake Bay. *Marine Geology*, 97: 87-103.
19. Wang, Y.H. (2002). The intertidal erosion rate of cohesive sediment: a case study from Long Island Sound. *Estuarine, Coastal, and Shelf Science* 56: 891-896.
20. Wu, J., & Tsanis, I.K. (1995). Numerical study of wind induced water currents. *Journal of Hydraulic Engineering, ASCE*, 121(5): 388-395.
21. Yanful, E.K., & Catalan, L.J.J. (2002). Predicted and field measured resuspension of flooded mine tailings. *Journal of Environmental Engineering, ASCE*, 128(4): 341-251.
22. Yang, Y. (2001). Wind induced countercurrent flow in shallow water. Ph.D. thesis, The University of Western Ontario, London, ON.

CHAPTER 6: AN IMPROVED MODEL FOR THE DESIGN OF WATER COVER FOR REACTIVE MINE TAILINGS

6.1 INTRODUCTION

Water cover technology is one of the most effective methods for the long-term storage of reactive mine tailings with potential environmental impacts strongly dependent on the structural integrity and safety of the impoundments (dams and dykes). A reliable resuspension model can play an important role in designing and managing a water cover over reactive mine tailings, where wind induced erosion and resuspension of bed tailings pose a major threat to the effectiveness of the cover. However, resuspension models available to design water cover over mine tailings are very limited. Samad and Yanful (2005) reviewed existing methods, such as those by Lawrence et al. (1991), Mohamed et al. (1996) and MEND (2001) used in the design of water covers. Major limitations with these models include the assumptions that return currents are too weak to contribute to the total bed shear stress; the restriction that selected water depths must always eliminate resuspension completely which sometimes result in uneconomical water depths; the use of the threshold bed velocity to identify incipient motion of the bed instead of the critical shear strength, which is a tailings material property.

Other than those mentioned above, another common limitation of these models is that only one water cover depth can be calculated for the entire tailings pond. However, in a tailings pond where wind is the only driving force causing bed erosion and

resuspension, wave parameters are a function of fetch length which is the distance over the water covered by the waves in the direction of the wind. Greater fetch length will provide more distance available for wind waves to grow and a greater chance for bed erosion to occur. Samad and Yanful (2005) developed a model that takes fetch length into consideration in order to calculate the design water cover depth for a particular grid station or location in the pond. In this model, the total pond area is discretized into a mesh of grids of fixed design interval or spacing and a fetch length and hence a water cover depth is obtained for each of the square grid cell in the pond area. Circulation currents, which were ignored in previous models, are incorporated into the Samad and Yanful (2005) model considering them as counter-currents in the opposite direction to the wind based on the Wu and Tsanis (1995) and Yang (2001) models. Details of the Samad and Yanful (2005) model are available in two foundational papers by Samad and Yanful (2005) and Kachhwal et al. (2010).

Kachhwal et al. (2010) used the existing Samad and Yanful (2005) model to compare field measured and model predicted results for the Shebandowan tailings storage facility, located near Thunder Bay, ON, Canada. In general, the results showed that model predicted and field measured suspended tailings concentrations were in agreement. Although the Samad and Yanful (2005) model advanced the design of water covers for reactive mine tailings, there are still some limitations, some of which outlined below:

1. The lack of field representative data such as return currents, critical shear stress and erosion rate parameters limits the use of the model. Erosion rate parameters can be estimated from laboratory experiments using empirical relations available

in literature, but the accuracy of the results is questionable without actual field data for verification.

2. The return currents computational scheme used in the model is based on theoretical equations developed by Wu and Tsanis (1995) and Yang (2001). The parameters used were obtained from laboratory water tank studies and were not verified under field conditions.
3. Linear addition of wave and current bed shear stresses adopted in the model cannot be justified (Kachhwal et al. 2011). In field conditions, where waves and currents are both present, the interaction between them should not be ignored (Grant and Madsen 1979).
4. Accurate knowledge of bed material characteristics such as the critical shear stress and erosion rate parameters is necessary for obtaining reliable results. Existing methods for the estimation of these parameters include either laboratory erosion tests or empirical relations, which may not be representative as pointed out by Kachhwal and Yanful (2011b).
5. The Samad and Yanful (2005) model calculates the resuspended solids concentrations in the water cover at each grid point for a single water cover depth restricted over the entire area of the pond. The fetch length is different for each grid point; therefore, a single water cover depth for the entire area of the pond would not be economical. This approach needs to be improved by providing an optimized water depth for each grid cell.

An attempt was made in the present study to resolve the above limitations in the Samad and Yanful (2005) model. The main objective of the study was to improve the

resuspension prediction model developed by Samad and Yanful (2005) by incorporating the results of field studies and new approaches to the computation of the wave-current interactions. In order to achieve this objective the following four main improvements in the existing model were made:

1. The field measured currents were compared with currents predicted using the Wu and Tsanis (1995) model.
2. Wave-current interaction was incorporated into the model. An interaction term was included in the estimation of total bed shear stress, instead of the linear addition of wave and current induced bed shear stresses.
3. The critical shear stress and erosion rate parameters were determined using field recorded wind induced resuspension instead of empirical equations. A graphical technique developed by Kachhwal and Yanful (2011b) based on the field recorded real-time resuspension data using optical backscatter sensors (OBS sensors) was used.
4. Instead of a single optimized water cover depth over the entire area of the pond, a different water cover depth was obtained at each grid cell in the discretized pond area for known regulatory limits of the suspended solids concentration in the water.

In the present paper, wherever the term “existing model” is used, it refers to the existing Samad and Yanful (2005) model.

6.2 METHODS AND MATERIALS

6.2.1 The Total Bed Shear Stress

In the existing Samad and Yanful (2005) model, the total bed shear stress τ_b is calculated as linear addition of empirically determined bed shear stresses due to waves and currents.

$$\tau_b = \tau_w + \tau_c \quad (6.1)$$

where, τ_w is the shear stress due to waves and τ_c is the shear stress due to currents. The bed shear stress due entirely to waves, τ_w , was determined by wave hindcasting equations, also known as the SMB method (CERC 1984) and linear wave theory. This method provides a set of equations that can be used to calculate the bed shear stress (Kachhwal et al. 2010). The input parameters needed are wind data, pond geometry and fetch length. The bed shear stress due to circulation currents was estimated using equations derived by Samad and Yanful (2005) based on the Wu and Tsanis (1995) approach of counter-currents and equation parameters determined by Yang et al. (2001) from laboratory experiments. More details on the SMB method of wave predictions and the method of Wu and Tsanis (1995) can be found in summaries provided in Samad and Yanful (2005) and Kachhwal et al. (2010).

Grant and Madsen (1979) noted that under conditions where both waves and currents are present in water simultaneously, neither of them can be treated separately and wave-current interaction must be taken into account. It has also been reported in other studies that wave-current interaction in shallow waters enhances bed turbulence and causes an increase in the bed shear stress (Grant and Madsen 1979; Jing and Ridd 1996;

Jin and Ji 2004). Since SMB method predicts bed shear stress due to pure currents while Wu and Tsanis (1995) model for pure currents, the interaction between wave-currents should be included in calculations. Therefore Kachhwal et al. (2011) proposed a relationship to determine the total bed shear stress under wave-current interaction derived from the Grant and Madsen (1979) model.

$$\tau_b = \tau_c + \tau_w + 2\sqrt{\tau_c \tau_w} \cos \theta_c \quad (6.2)$$

where, θ_c is the angle between wind induced waves and circulation currents at any location. In order to improve the Samad and Yanful (2005) model, wave-current interaction must be considered and this requires knowledge of the angle, θ_c , between wind-induced waves and circulation currents.

6.2.2 Prediction of Currents

The wind induced currents can either be predicted by mathematical modeling or be measured in the field using instruments such as an acoustic Doppler current profiler (ADCP). In this section, details are provided of two approaches used to obtain bed shear velocities due to currents, which will later be used to compare predicted and field measured circulation currents. Kachhwal et al. (2011) used an ADCP to obtain field current data, which were then used to evaluate the effect of wave-current interaction on the total bed shear stress. In that study, the bed shear velocities were obtained by fitting the current profile to the Log- Law. The near bed shear velocity was estimated as the slope of the log linear bed velocity profile. The relationship between the current bed

shear velocity u_{*c} and the variation of the near-bed velocity u with elevation above the bed z can be written as:

$$\frac{u}{u_{*c}} = \frac{1}{\kappa} \ln \left(\frac{z}{z_0} \right) \quad (6.3)$$

where, κ is von Karman's constant (~ 0.40), z_0 is the bed roughness length corresponding to $u = 0$.

The Wu and Tsanis (1995) approach of near bed counter-current flow was used in the existing Samad and Yanful (2005) model to obtain the bed shear stress due to currents. In this approach, the surface shear velocity of water u_{*s} is given by:

$$u_{*s} = 0.035U \sqrt{\frac{\rho_a}{\rho_w}} \quad (6.4)$$

where, U is the wind speed (m/s), ρ_a is the density of air (kg/m^3) and ρ_w is the density of water (kg/m^3). The bed shear stress due to currents can be written as:

$$\tau_c = \rho_w u_{*s}^2 \lambda_{z_{bh}} (z_{sh} + 1) \times \left(\frac{A}{z_{bh}} - \frac{B}{z_{sh} + 1} \right) \quad (6.5)$$

The variables A and B in the above equation are defined as:

$$A = \frac{q_2}{p_1 q_2 - p_2 q_1} \quad \text{and} \quad B = \frac{-q_1}{p_1 q_2 - p_2 q_1} \quad (6.6)$$

where,

$$\begin{aligned}
p_1 &= \lambda z_{sh}; \\
p_2 &= \lambda z_{sh} / z_{bh}; \\
q_1 &= (1 + z_{sh}) \ln\left(1 + \frac{1}{z_{sh}}\right) - 1; \text{ and} \\
q_2 &= z_{sh} \ln\left(1 + \frac{1}{z_{bh}}\right) - 1;
\end{aligned}$$

The variables z_{sh} ($=2.2 \times 10^{-4}$) and z_{bh} ($=1.4 \times 10^{-4}$) are the surface and bottom characteristic lengths, respectively, and are calculated based on experimental data (Wu and Tsanis 1995; Yang 2001). The parameter λ is a constant that depends on the intensity of turbulence in water. It varies from 0.2 to 0.5 with an average value of about 0.35. The variation in the values of these parameters affects mainly the near surface shear stress but has little influence on the bed shear stress (Yang 2001; Samad and Yanful 2005). The current bed shear velocity u_{*c} can be obtained using the following relationship:

$$u_{*c} = \sqrt{\frac{\tau_c}{\rho_w}} \quad (6.7)$$

The Wu and Tsanis (1995) model gives one value of current induced bed shear stress corresponding to input wind speed regardless of the location and water depth in the pond. However, this model cannot predict the direction of currents; consequently, it was assumed to be in the opposite direction to the wind.

6.2.3 Erosion Characteristics of Bed Material

Another challenge encountered in the use of the existing Samad and Yanful (2005) model is the availability of characteristic erosion parameters for the bed material, namely, the critical shear stress and erosion rate constants. Any resuspension prediction model is quite sensitive to these parameters. The existing model depends on the prior knowledge of these values. In most cases, these parameters are either determined empirically or through laboratory experiments on a disturbed bulk sample of the bed material which may not be representative of actual field conditions such as tailings pore water and the presence of bio film and organic matter (Adu-Wusu et al. 2001; Krishnappan 1993; Geremew and Yanful 2010). Kachhwal and Yanful (2011b) recently developed a graphical method to estimate these parameters using real time field resuspension data obtained with optical backscatter (OBS) sensors and the corresponding wind data. Details of the method can be found in Kachhwal and Yanful (2011b).

6.3 RESULTS AND DISCUSSION

6.3.1 Results from Existing Samad and Yanful (2005) Model

Table 6.1 presents erosion characteristics of bed tailings used in the Samad and Yanful (2005) model and predicted results. The critical shear stress of bed tailings was estimated using Fischenich's (2001) empirical equation and D_{50} as the representative tailings particle size. Average critical shear stress values of 0.12 Pa for the west and east

Table 6.1 Input data and results of water cover depth predictions using the existing Samad and Yanful (2005) model

Location	Fetch length		Erosion characteristics			Water cover depth		
	Minimum	Maximum	Critical shear	Coefficient	Exponent	Minimum	Maximum	Average
	(m)	(m)	stress (Pa)	(α)	(M)	(m)	(m)	(m)
West Cell	553	1067	0.12	0.0025	1.121	1.4	3.6	2.9
Middle Cell	470	870	0.04	NA*	NA*	Greater than 5.0 m		5.0
East Cell	482	938	0.12	0.0025	1.121	1.3	3.3	2.2
Whole pond**	887	1827	0.12	0.0025	1.121	1.2	4.7	2.8

*NA = not available, ** Whole pond without wave breaks

cells and 0.04 Pa for the middle cell tailings were used in the analysis. The empirically determined critical shear stress of the middle cell bed tailings was very small due to their fine particle size (average D_{50} 0.007 mm). The Fischenich's (2001) empirical approach did not take presence of cohesiveness into account for the determination of the critical shear stress of fine tailings, which otherwise can increase the resistance to erosion and hence the critical shear stress. Erosion rate parameters, coefficient (α) and exponent (β), used in the model were 0.0025 and 1.121 respectively. These values were obtained in laboratory erosion tests by Geremew and Yanful (2010) for the west cell bed tailings. The same values were used in the model to predict resuspension in the west and east cells due to the similar geotechnical characteristics of bed tailings in the two cells (Kachhwal et al. 2010). However, the same values of erosion parameters could not be used for the middle cell because bed tailings in the middle cell were much finer and likely to be cohesive (Kachhwal et al. 2010).

The required minimum water cover depths to eliminate resuspension were up to 3.6 m in the west cell and 3.3 m in the east cell (Table 6.1). For the middle cell, the required water cover depth was greater than 5.0 m. The rather deep water cover was due to the very small critical shear stress determined empirically. The existing water depths observed during sediment trap sampling and OBS sensor installation were found to be smaller than the minimum required to eliminate resuspension. In the case of the middle cell, existing average water depth was 1 m, which was much smaller than the model predicted minimum water depth of 5 m. However, the sediment traps and OBS did not record any unusually high amount of resuspension in the middle cell. The reason could be the cohesive nature of fine bed tailings in the middle cell. The presence of binding

cohesive forces in fine particles can increase the resistance to erosion and resuspension. The critical shear stress for the fine middle cell tailings material may be higher than the value calculated from Fischenich's (2001) method due to the presence of cohesion.

6.3.2 Comparison of Model Predicted and Field Measured Currents

Kachhwal et al. (2011) made measurements of wind induced circulation currents at 32 locations in the middle cell of the Shebandowan tailings storage facility using the ADCP. The ADCP data provided evidence of increase in the total bed shear stress due to wave-current interactions. However, the currents were measured only for a small range of wind speed of 5-8 m/s blowing in the direction 250° to the North. In order to incorporate the wave-current interactions into the existing Samad and Yanful (2005) model, a tool for the prediction of currents under various wind conditions, such as the Wu and Tsanis (1995) model, is needed.

A comparison was made between the magnitude of bed shear velocities due to currents obtained from field measured current profiles at 32 different stations in the middle cell and those predicted by the Wu and Tsanis (1995) model under similar wind conditions. The results are presented in Table 6.2. The bed shear velocities obtained from field measured currents ranged from 0.0001 m/s to 0.0226 m/s. The ADCP recorded currents showed that the magnitude of the bed shear velocities were not constant but almost of the same order at most of the locations. However, the direction of the currents varied between different locations (Kachhwal et al. 2011). Only 5 out of the 32 stations showed measured results that were either much lower or higher than the model

Table 6.2 Comparison of field measured and model predicted bed shear velocities under similar wind conditions

Current bed shear velocities			
Field measured		Wu and Tsanis (1995) model prediction	
Profile ID	Bed shear velocity (m/s)	Wind speed (m/s)	Bed shear velocity (m/s)
8	0.0024	5.0	0.0028
10	0.0045	5.2	0.0029
11	0.0050	5.5	0.0031
12	0.0030	5.8	0.0033
14	0.0048	6.0	0.0034
15	0.0046	6.2	0.0035
16	0.0050	6.5	0.0037
29	0.0030	6.8	0.0038
30	0.0010	7.0	0.0040
31	0.0020	7.2	0.0041
32	0.0039	7.5	0.0043
40	0.0048	7.8	0.0044
41	0.0035	8.0	0.0045

predictions. After excluding these five stations, the magnitude of field recorded bed shear velocities for the remaining stations ranged from 0.002 m/s to 0.007 m/s. In comparison, the Wu and Tsanis (1995) model predicted current bed shear velocities for wind speeds of 5-8 m/s of the order of 0.0028 m/s to 0.0045 m/s. Thus most of the bed shear velocities obtained from field measured currents were very close to those predicted by the model. Statistical analysis was performed comparing the two data sets using the single factor analysis of variance (ANOVA) method. The results gave a P value of 0.71, which indicated that the two data sets were comparable to each other.

The foregoing results show that the Wu and Tsanis (1995) model can give the currents of the same order of magnitude as those measured in the field. However, the direction of the currents could not be predicted by this model. It is possible to incorporate the wave-current interaction into the existing Samad and Yanful (2005) model by introducing an additional term in Equation 6.1 to determine the total wind induced bed shear stress. The angle between waves and currents, which is generally not easily measured, can be assumed to be either 0° or 180° in order to maximize (Cosine of 0° and $180^{\circ} = 1$) the total bed shear stress, considering the worst case scenarios. This assumption will result in slightly higher water depths than those predicted if the actual angle was known.

6.3.3 Wave-Current Interactions

In order to improve or enhance the resuspension model of Samad and Yanful (2005), the Wu and Tsanis (1995) model of circulatory currents prediction was used with an added

term for wave-current interaction. Total bed shear stresses were obtained for two conditions: (i) without wave-current interaction, which is similar to the existing Samad and Yanful (2005) model, and (ii) with wave-current interactions, assuming collinear waves and currents, which maximizes the total bed shear stress. The critical shear stress and erosion rate parameters were determined through a graphical technique developed by Kachhwal and Yanful (2011b) using field recorded resuspension data. The characteristics parameters of the bed tailings are listed in Table 6.3. Long term wind data (50 years) with a return period of 10 years were used in analysis. Water cover depths required to eliminate resuspension and the magnitude of resuspension were determined.

The minimum required water cover depth to completely eliminate resuspension predicted by the modified Samad and Yanful (2005) model are presented in Figures 6.1 and 6.2. The results show that wave-current interaction significantly increased the minimum water cover depth required to eliminate resuspension. For example, in the west cell, without considering the wave-current interaction, the model predicted water cover depth varied from 1.5 m to 3.5 m with an average value of 2.5 m. When wave-current interaction was considered, the model predicted water depths ranged between 2.5 and 6.0 m. Wave-current interaction only increased the total bed shear stress which resulted in greater required water cover depths, however it did not affect the pattern of water cover distribution over the area of the pond. The results also show that a relatively deep water cover was required in the southwest area of the pond.

Analysis was also carried out for the whole pond area without the wave breaks. The results are presented in Figures 6.3 and 6.4 for the cases without wave-current

Table 6.3 Erosion characteristics derived from field measured resuspension data and model predicted water cover depth with and without wave-current interactions

Location	Erosion parameters			Water cover depth to eliminate resuspension					
	Critical shear stress (Pa)	Erosion Rate		Without interaction			With interaction		
		Coefficient	Exponent	Max.	Min.	Avg.	Max.	Min.	Avg.
		(α)	(M)	(m)	(m)	(m)	(m)	(m)	(m)
West Cell	0.10	0.0161	0.6145	3.9	1.5	2.6	6.3	2.1	4.0
Middle Cell	0.08	0.0069	0.6121	3.1	1.0	1.8	5.2	1.6	3.0
East Cell	0.10	0.0161	0.6145	3.2	1.3	2.2	5.3	1.9	3.4
Whole Pond**	0.10	0.0161	0.6145	4.7	2.2	3.3	7.5	3.2	5.1

** Whole pond without wave breaks

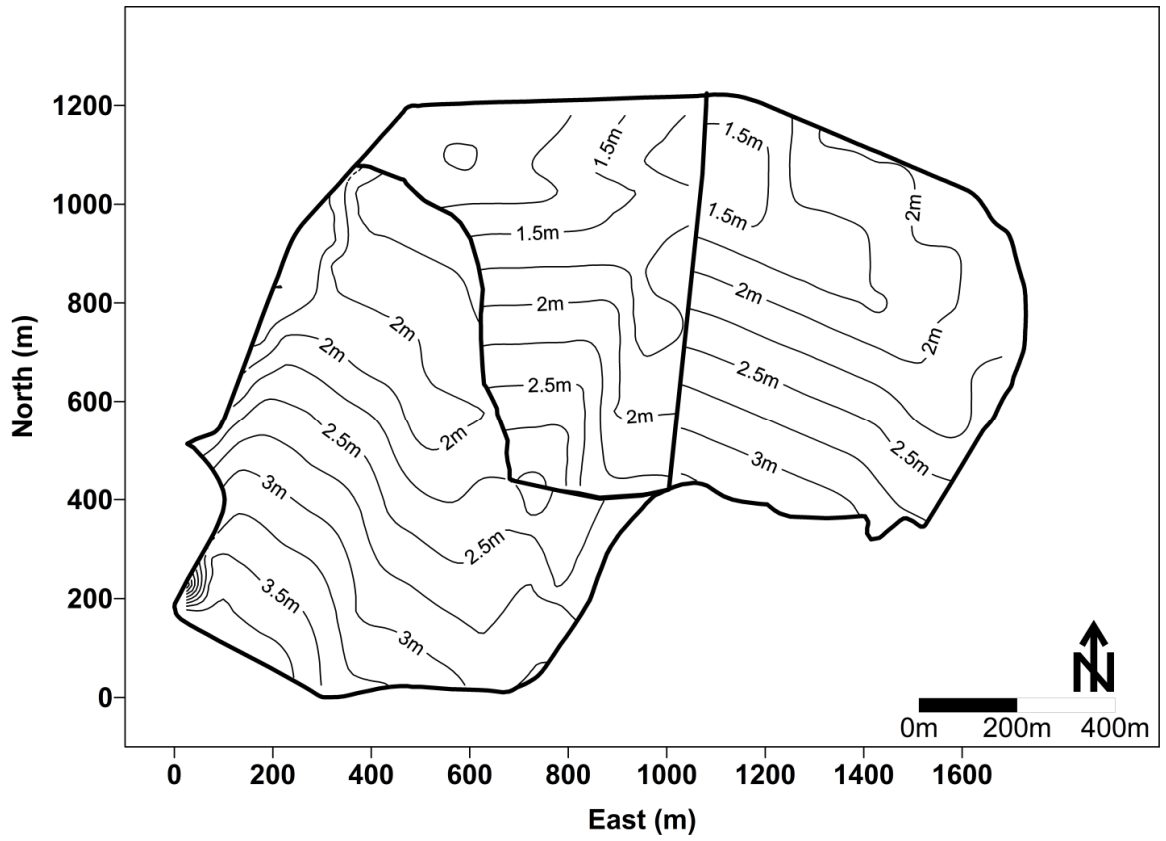


Figure 6.1 Contour map of minimum required water cover depth without wave-current interaction in the each cell of tailings pond

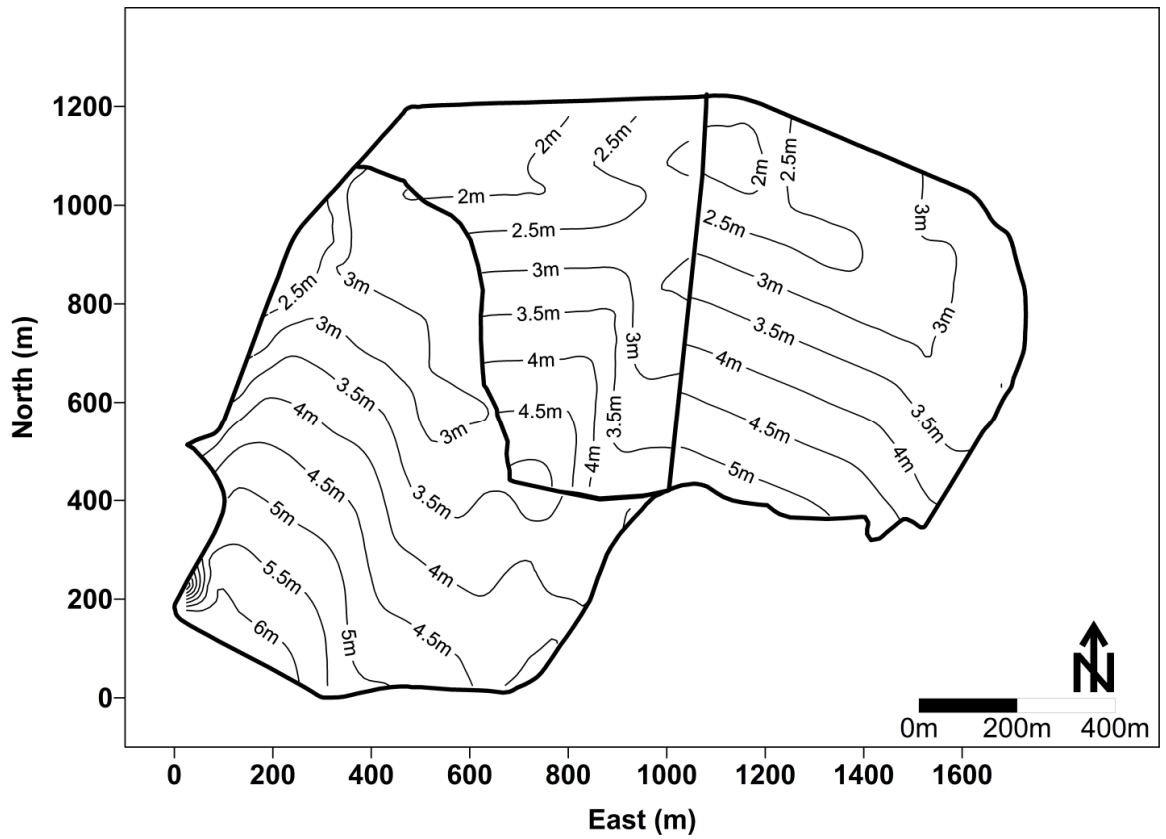


Figure 6.2 Contour map of minimum required water cover depth with wave-current interaction in the each cell of tailings pond

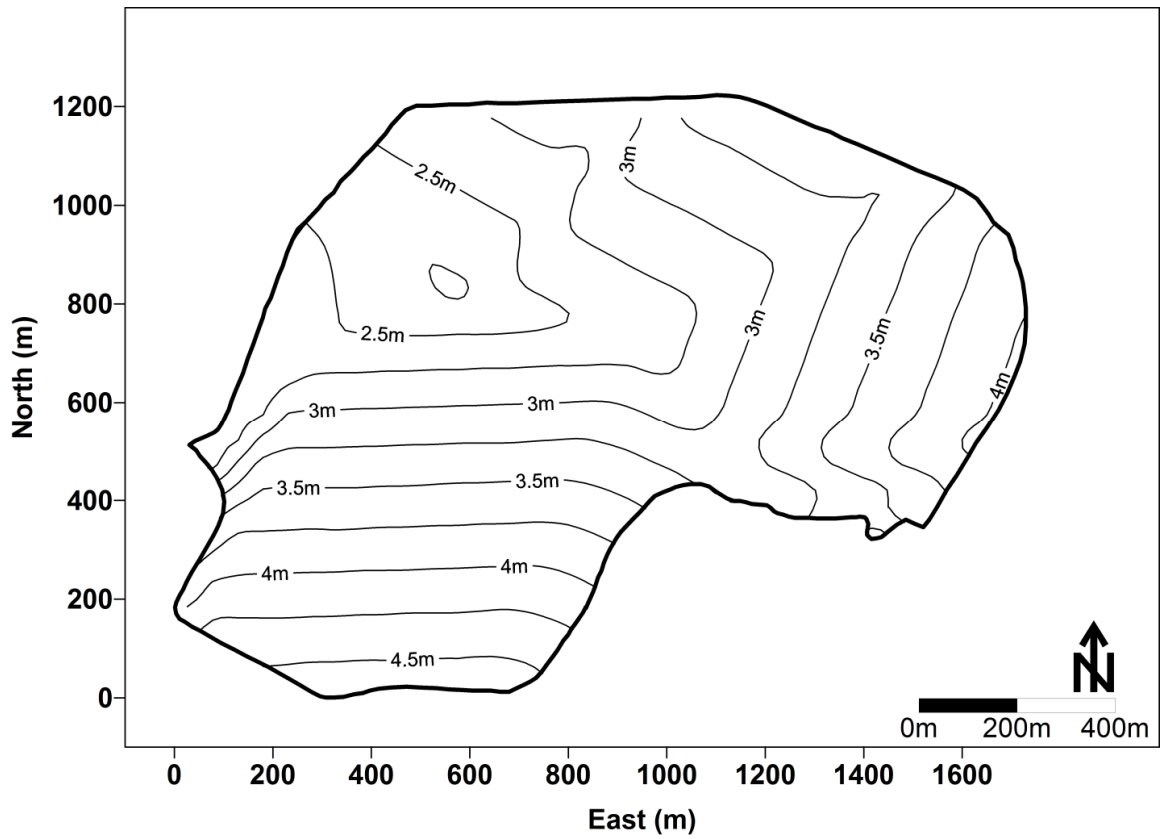


Figure 6.3 Contour map of minimum required water cover depth without wave-current interaction in the whole pond in absence of wave breaks

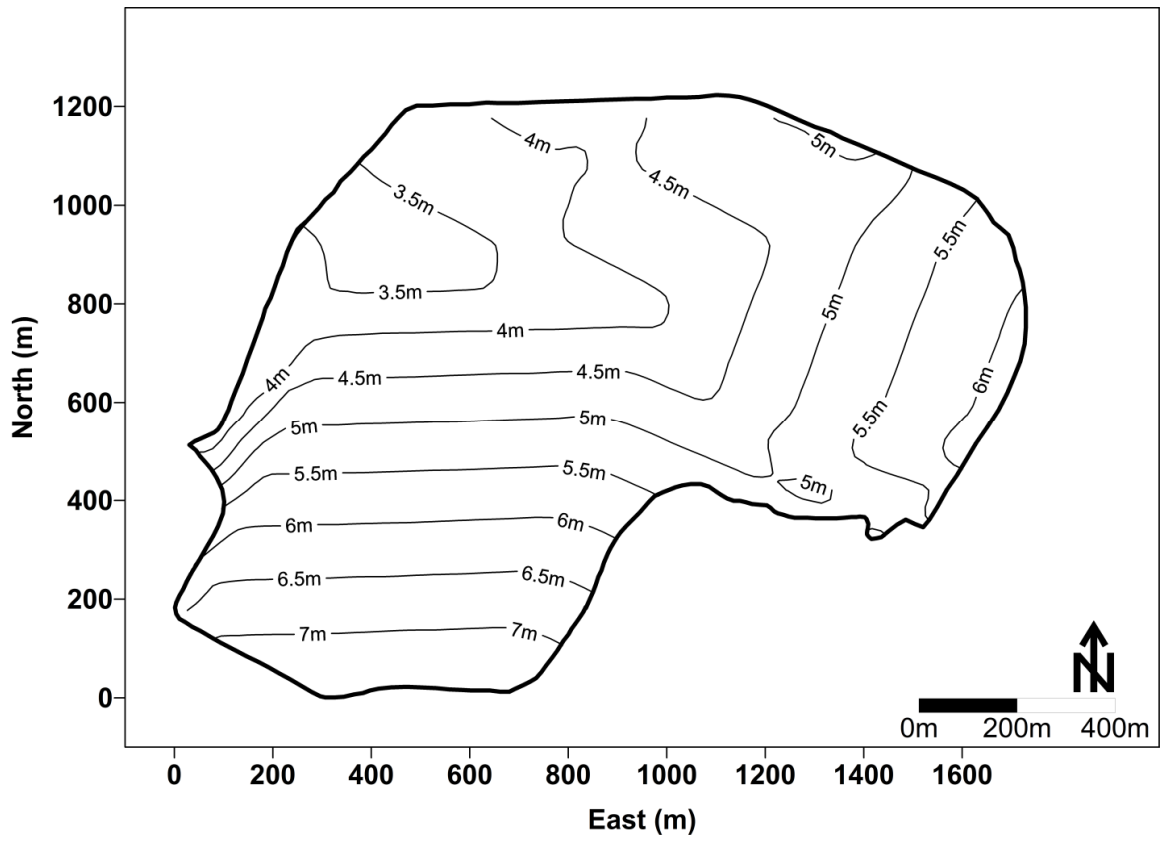


Figure 6.4 Contour map of minimum required water cover depth with wave-current interaction in the whole pond in absence of wave breaks

interactions and with wave current interaction, respectively. In the absence of the two wave breaks, the required water depth to eliminate resuspension of bed tailings would be quite high. In the absence of wave-current interaction, the maximum required water depth was 4.5 m in the southwest area of the pond, while in the presence of wave-current interaction; it increased to a maximum value of 7.0 m. Similar results obtained for the west cell, middle cell, east cell, and the entire pond (in the absence of the wave breaks) and with and without wave-current interactions are presented in Table 6.3. It is evident from these results that the presence of the two wave breaks significantly reduced the water depth required to eliminate resuspension. However in the presence of the wave breaks, the water cover requirement for the west cell is still quite high (up to 6.3 m) and over 5 m for the middle and east cells. The greater fetch length available in the west cell is responsible for this higher water depth requirement, while the relatively small fetch length of the middle cell helped to reduce the water depth requirement in that cell.

In the next step of the analysis, the effect of water depth restriction on resuspended tailings concentrations was studied. Results were obtained for water cover depths restricted to 1 m and 2 m over the entire tailings pond using the erosion rate parameters determined from Kachhwal and Yanful (2011b) (also provided in Table 6.3). Figures 6.5 and 6.6 show contour maps of model predicted suspended solids concentration with the water depth restricted to 1 m for the cases of with and without wave-current interactions respectively. The minimum, maximum, and average model predicted suspended tailings concentrations are listed in Table 6.4. The maximum suspended tailings concentrations predicted were 42.4 mg/L for the west cell, 10.9 mg/L

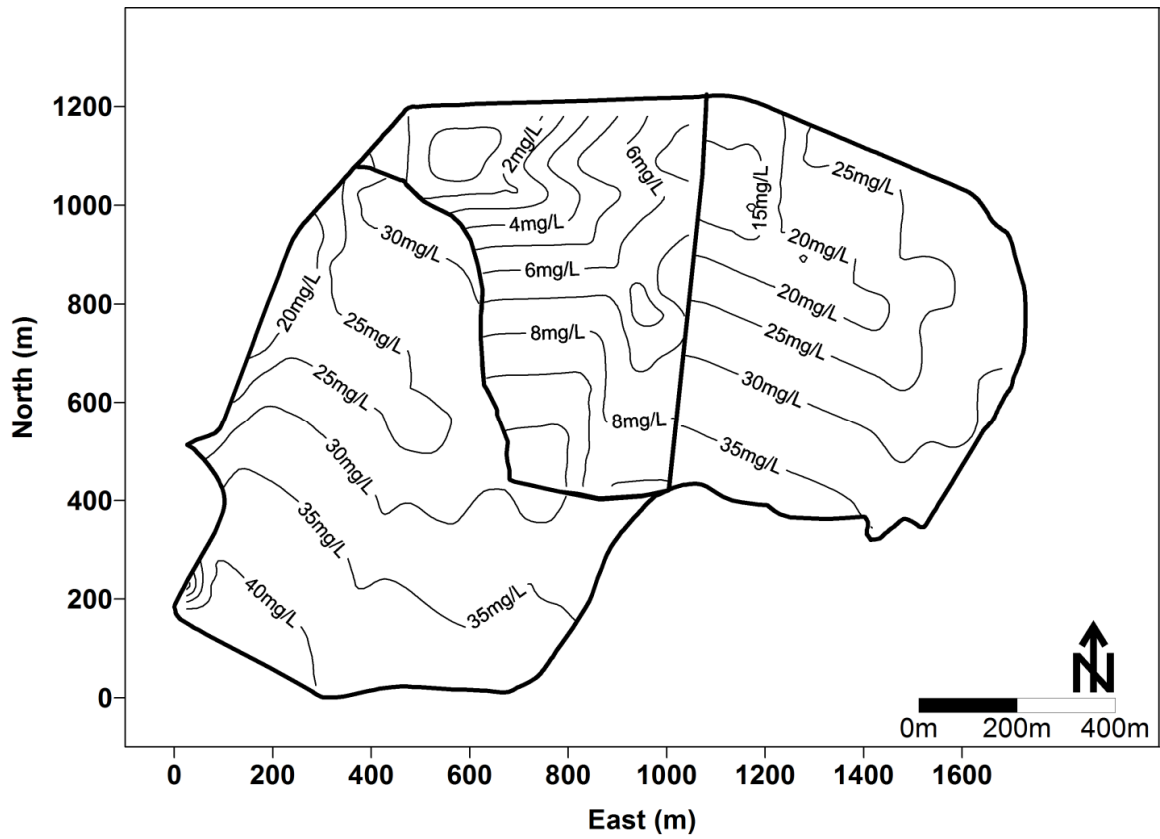


Figure 6.5 Contour map of predicted resuspension without wave-current interaction for restricted depth of 1.0 m over the entire tailings pond area

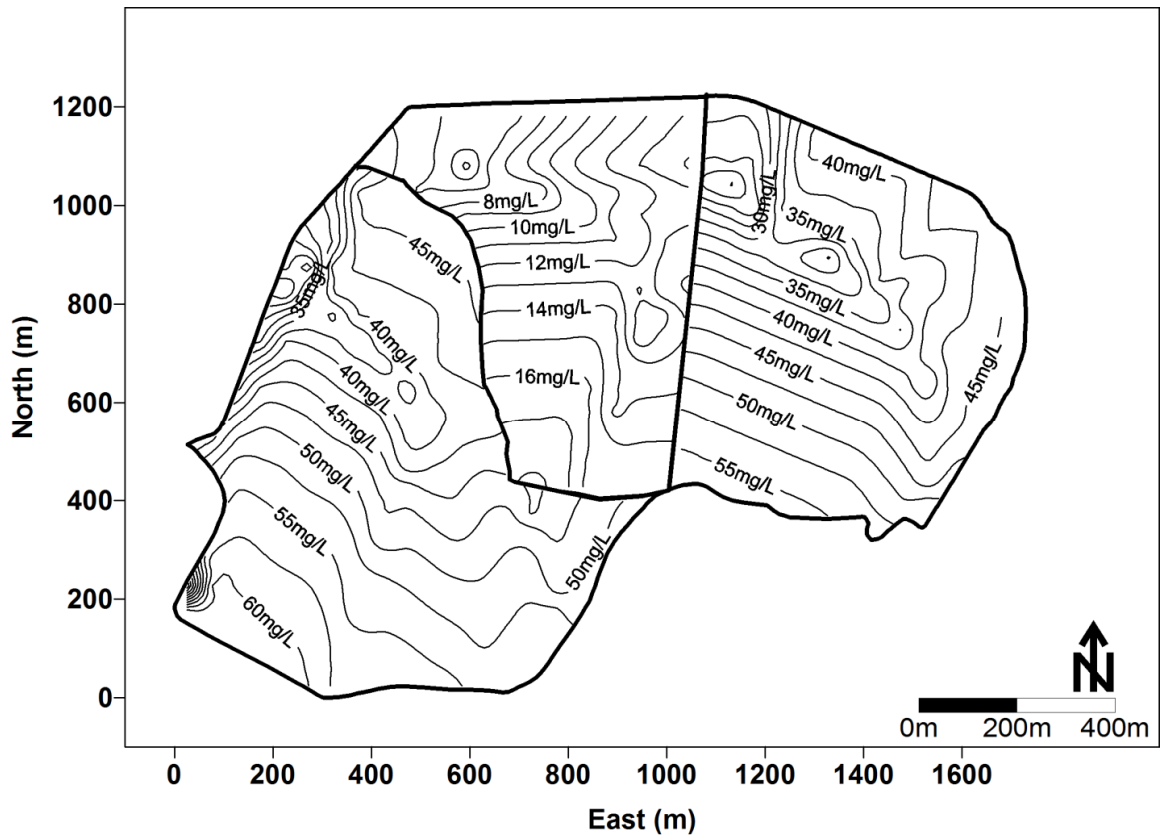


Figure 6.6 Contour map of predicted resuspension with wave-current interaction for restricted depth of 1.0 m over the entire tailings pond area

Table 6.4 Model predicted resuspended tailings concentrations after applying depth restrictions under conditions of with and without wave-current interactions

Location	Resuspended tailings concentration with applied depth restrictions											
	1.0 m over the entire area						2.0 m over the entire area					
	Without interaction			With interaction			Without interaction			With interaction		
	Max.	Min.	Avg.	Max.	Min.	Avg.	Max.	Min.	Avg.	Max.	Min.	Avg.
(mg/L)	(mg/L)	(mg/L)	(mg/L)	(mg/L)	(mg/L)	(mg/L)	(mg/L)	(mg/L)	(mg/L)	(mg/L)	(mg/L)	(mg/L)
West	42.4	16.0	31.4	62.0	22.1	48.1	10.51	0.0	4.6	18.7	1.0	11.5
Cell												
Middle	10.9	0.0	6.1	18.2	4.6	12.4	2.3	0.0	0.4	5.3	0.0	2.2
Cell												
East	37.6	9.3	26	56.6	19.4	41.9	8.0	0.0	2.3	15.7	0.0	8.3
Cell												

for the middle cell and 37.6 mg/L for the east cell, ignoring the wave-current interactions. When wave-current interactions were taken into consideration, the predicted maximum suspended tailings concentrations were 62.0 mg/L, 18.2 mg/L, and 56.6 mg/L for the west, middle and east cells respectively. Figures 6.7 and 6.8 show contour maps of model predicted suspended solids concentration with the water depth restricted to 2 m for the cases of with and without wave-current interactions respectively. For a water depth restriction of 2 m over the tailings pond, the model predicted maximum suspended tailings concentrations were 10.6 mg/L for the west cell, 2.3 mg/L for the middle cell and 8.0 mg/L for the east cell ignoring wave-current interactions, and 18.7 mg/L, 5.3 mg/L, and 15.7 mg/L respectively, taking wave-current interactions into consideration.

From the foregoing results, it is evident that a water cover depth of 1.0 m, which was close to the observed or existing water depths at most locations in the pond, was not sufficient to eliminate the wind-induced resuspension of bed tailings at the Shebandowan tailings storage facility. However, the results showed that a uniform water cover of 2 m over the entire tailings pond was sufficient to reduce the suspended tailings concentrations under the regulatory limit of 15 mg/L (MMER 2002) even when wave-current interactions are considered. These results suggest that tailings at locations where the water cover is significantly shallower than 2 m would have to be dredged and move to deeper areas to ensure an overall water cover depth of 2 m or deeper, which will ensure that erosion-induced suspended tailings concentrations meet effluent discharge limits (15 mg/L).

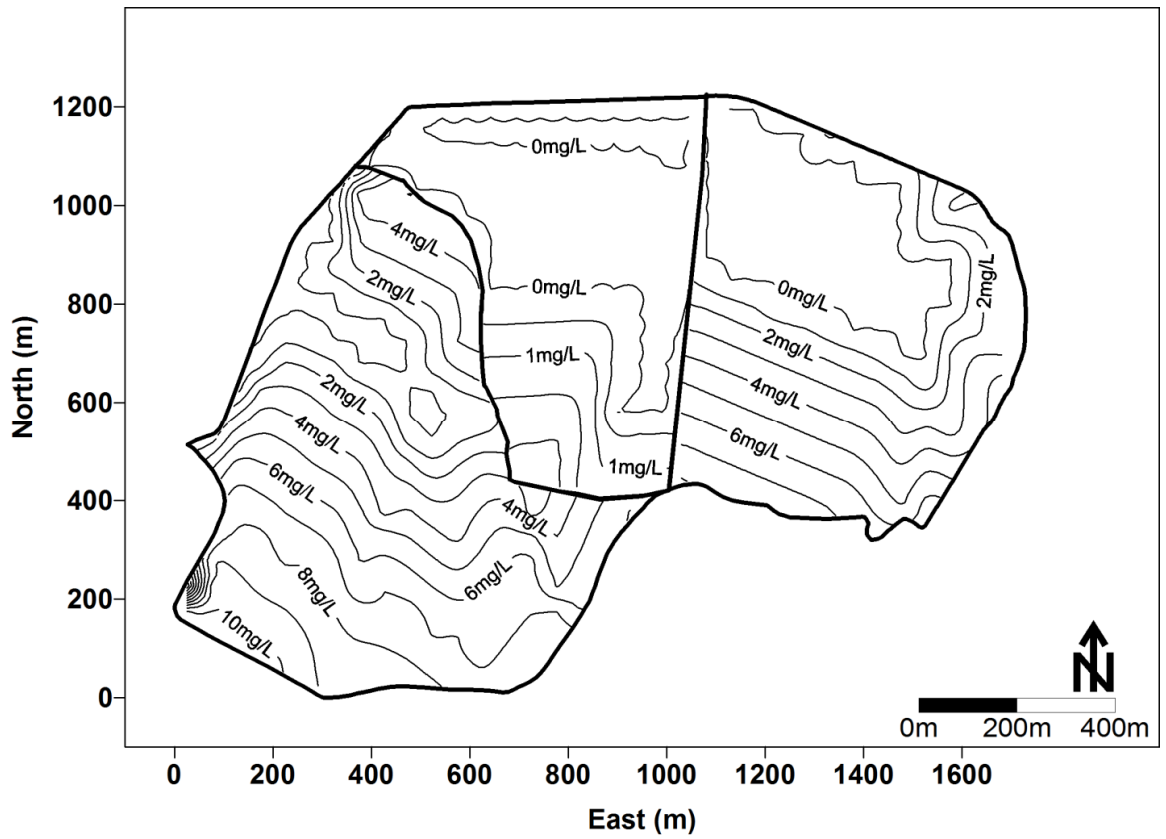


Figure 6.7 Contour map of predicted resuspension without wave-current interaction for restricted depth of 2.0 m over the entire tailings pond area

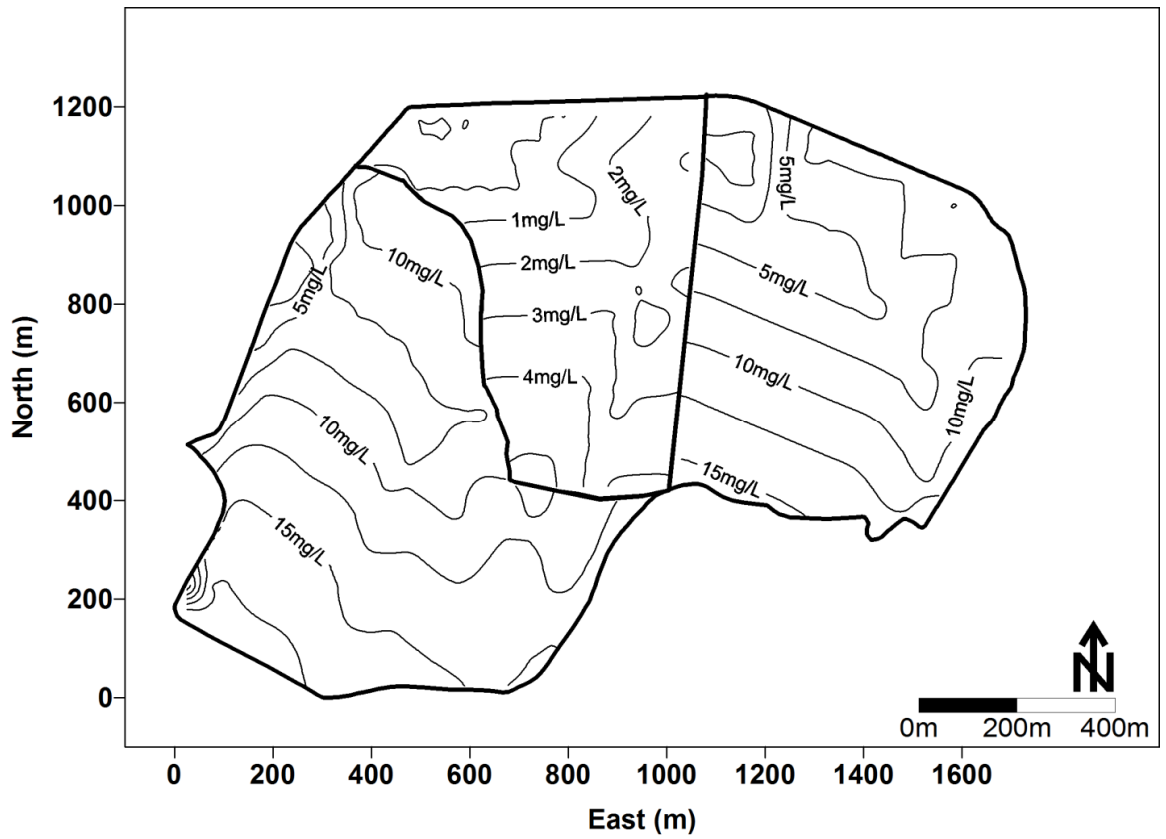


Figure 6.8 Contour map of predicted resuspension with wave-current interaction for restricted depth of 2.0 m over the entire tailings pond area

6.3.4 Optimized Water Cover Depths

The minimum water depth required to completely eliminate resuspension was as high as 6 m. Obviously, implementing this water cover in the field would not be economically feasible due to high cost of construction of dams to store that much water. The long-term stability of high dams is also matter of concern. However, the results of depth restriction showed that a water depth of 2.0 m over the entire tailings pond was able to reduce the resuspension of bed tailings substantially. It would be economically and technically preferable if the model can determine the water depth that would allow resuspension to occur within the regulatory limits at the center of each square grid cell in the pond, instead of adopting a single water cover depth of 2 m for the entire tailings pond area. Since fetch length is different for each grid station, a separate optimized water cover depth can be assigned for each grid station.

If the regulatory limit of suspended solids concentration in the water is known, e.g. 15 mg/L for metal mining effluents in Ontario, Canada (MMER 2002), an optimized water cover depth can be obtained for each grid station allowing resuspension to occur under the regulatory limit. A contour map of optimized water depths for a regulatory suspended solids concentration limit of 15 mg/L is shown in Figure 6.9 taking wave-current interactions into account. From these results, which are also summarised in Table 6.5, it can be shown that a maximum water depth of 2.2 m in the west cell, 2.0 m in the east cell and 1.1 m in the middle cell would be sufficient to reduce the resuspension of bed tailings to values below the regulatory limit of 15 mg/L.

Table 6.5 Optimized water cover depths for allowed maximum resuspended tailings concentrations of 15 mg/L

Location	Optimized water cover depths for allowed resuspension up to 15 mg/L		
	Maximum	Minimum	Average
	(m)	(m)	(m)
West Cell	2.2	1.2	1.8
Middle Cell	1.1	0.7	0.9
East Cell	2.0	1.1	1.6

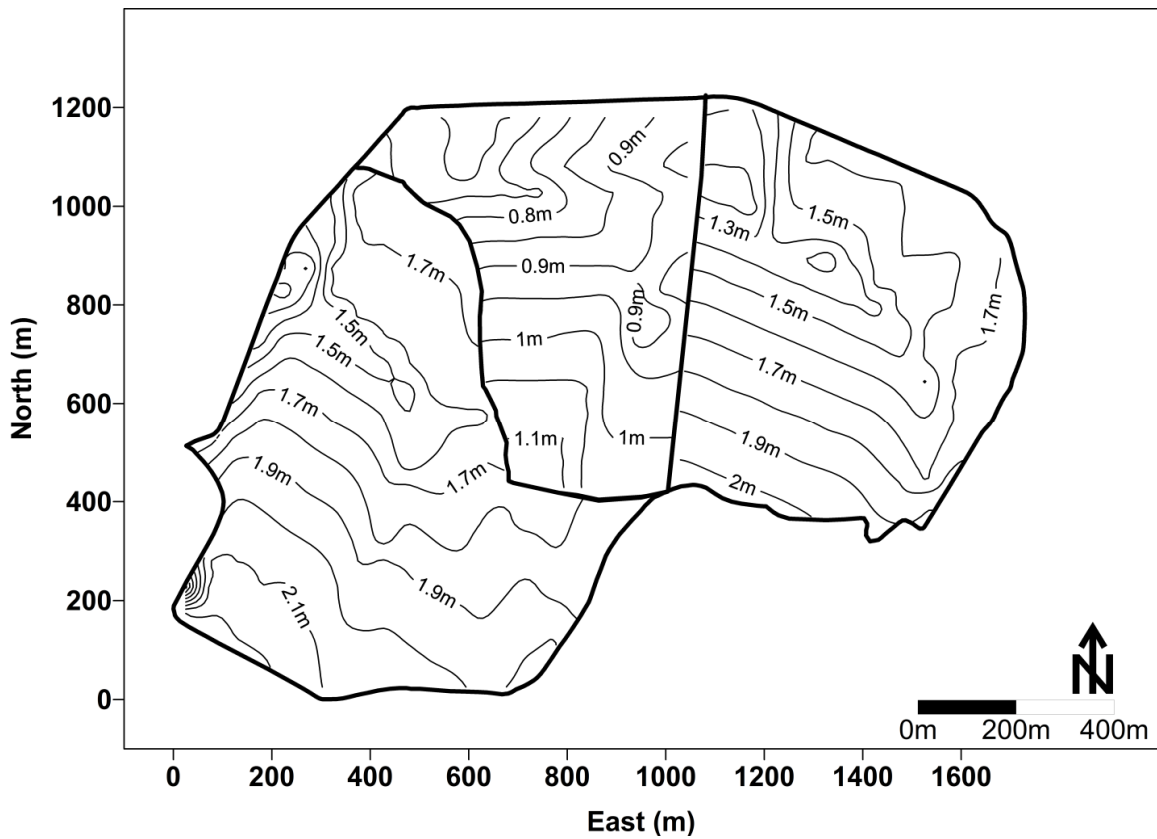


Figure 6.9 Contour map of optimized water cover depths in the each cell with allowed resuspension of under 15 mg/L

6.4 CONCLUSIONS

The present work makes three major improvements to the existing Samad and Yanful (2005) resuspension model based on the results of our previous field studies. The improvements are:

1. The addition of a wave-current interaction term to the model.
2. The critical shear stress and erosion rate parameters were obtained from field results and used in the model to more accurately predict resuspension.
3. The addition of an option to estimate the optimized water cover depths at any location in the pond for a known regulatory limit of suspended solids concentration in the water.

The main outcome of the above improvement was that the overall requirement for the water cover depth was increased due to the added term of wave-current interaction in the total bed shear stress. In the west and east cells, the required water depth was increased due to the relatively small critical shear stress obtained graphically in relation to the one computed empirically, while in the middle cell the minimum required water depth was lower than those predicted by the existing Samad and Yanful (2005) model . The reason was that the critical shear stress obtained graphically was higher than the one computed empirically for fine middle cell bed tailings. In the end, the optimized water depth was obtained for each cell of the Shebandowan tailings storage facility. A maximum water depth of 2.2 m in the west cell, 2.0 m in the east cell and 1.1 m in the middle cell would be sufficient to reduce the resuspension of bed tailings below the regulatory limit of 15 mg/L.

6.5 REFERENCES

1. Adu-Wusu, C., Yanful, E.K., & Mian, M.H. (2001). Field evidence of resuspension in a mine tailings pond. *Canadian Geotechnical Journal*, 38(4): 796-808.
2. CERC (1984). Shore protection manual. U.S. Army Corps of Engineers, Coastal Engineering Research Centre, Vicksburg, M.S.
3. Fischenich, C. (2001). Stability thresholds for stream restoration materials. EMRRP technical notes collection, ERDC TN-EMRRP-SR-29, U.S. Army engineer research center, Vicksburg, M.S.
4. Geremew, A.M., & Yanful, E.K. (2010). The role of fines on the cohesive behavior of mine tailings inferred from the critical shear stress. *Canadian Geotechnical Journal*. In Press. Accepted October 4, 2010.
5. Grant, W.D., & Madsen, O.S. (1979). Combined wave and current interaction with a rough bottom. *Journal of Geophysical Research*, 84(C4): 1979-1808.
6. Jin, K., & Ji, Z. (2004). Case study: modeling of sediment transport and wind-wave impact in Lake Okeechobee. *Journal of Hydraulic Engineering*, 130:1055-1067.
7. Jing, L., & Ridd, P.V. (1996). Wave-current bottom shear stresses and sediment resuspension in Cleveland Bay, Australia. *Coastal Engineering*, 29:169-186.
8. Kachhwal, L.K., Yanful, E.K., & Lanteigne, L. (2010). Water cover technology for tailings management: a case study of field measurement and model predictions. *Water Air Soil Pollution*, 214(1-4): 357-382.

9. Kachhwal, L.K., Yanful, E.K., & Rennie, C.D. (2011). A semi-empirical approach for estimation of bed shear stress in a tailings pond. *Journal of Environmental Earth Sciences*, under review.
10. Kachhwal, L.K., & Yanful, E.K. (2011b). Estimating erosion characteristics of tailings from field measured resuspension data. *Marine Geology*, submitted.
11. Krishnappan, B.G. (1993). Rotating circular flume. *Journal of Hydraulic Engineering*, 119(6): 758-767.
12. Lawrence, G.A., Ward, G.A., & MacKinnon, P.R.B. (1991). Wind wave-induced suspension of mine tailings in disposal ponds: a case study. *Canadian Journal of Civil Engineering*, 18(6): 1047-1053.
13. MEND Manual (2001). Prevention and control, Volume 4, Energy Mines and Resources Canada.
14. MMER. (2002). Metal mining effluent regulations. SOR/2002-222, <http://laws.justice.gc.ca/PDF/Regulation/S/SOR-2002-222.pdf>, Accessed November 10, 2009.
15. Mohamed, A.M.O., Yong, R.N., Coporuscio, F., & Li, R. (1996). Flooding of a mine tailings site: Suspension of solids-impact and prevention. *International Journal of Surface Mine Reclamation Environment*, 10(3): 117-126.
16. Samad, M. A., & Yanful, E.K. (2005). A design approach for selecting the optimum water cover depth for subaqueous disposal of sulphide mine tailings. *Canadian Geotechnical Journal*, 42: 207-228.
17. Yang, Y. (2001). Wind induced countercurrent flow in shallow water. Ph.D. thesis, The University of Western Ontario, London, ON.

18. Wu, J., & Tsanis, I.K. (1995). Numerical study of wind induced water currents. *Journal of Hydraulic Engineering, ASCE*, 121(5): 388-395.

CHAPTER 7: CONCLUSIONS AND SCOPE FOR FUTURE WORK

7.1 CONCLUSIONS

An evaluation of wind induced resuspension of mine tailings was performed at an existing tailings storage facility at the decommissioned Shebandowan Mine, located near Thunder Bay, Ontario, Canada. Extensive field investigations by means of sediment traps, OBS sensors, and acoustic Doppler current profiler (ADCP) surveys and laboratory analysis and theoretical modeling were done to achieve the objectives set at the beginning of the research. The main conclusions from the research are summarized below:

1. The most dominant wind direction at the site is 270° - 315° to North, that is, southwest direction. This justified the design, which includes the locations and orientations of the two existing wave breaks in the tailings pond.
2. Evaporation determined from weather data was higher than the recorded precipitation during the periods of sediment trap deployment in the summers of year 2006 and 2007. These results showed that it may be necessary to pump additional water into the tailings pond in order to maintain a certain water level to eliminate or decrease tailings resuspension.
3. Under existing conditions of water depths, small amount of tailings resuspension (up to 80 mg/L) was recorded in all three cells of the tailings pond by the sediment traps and OBS sensors. At the time of the study, the amount of resuspension was not a matter of concern, because all the discharge from the pond

was collected and managed before it reports to the final effluent. However, in a long-term disposal plan even this small amount of resuspension should be considered.

4. The mineralogical and elemental analyses were performed on samples of resuspended tailings collected by sediment traps on samples of bed tailings collected from the location of the sediment traps. The major non-clay minerals identified in x-ray diffractograms were pyrite, pyrrhotite, quartz, feldspar, calcite, and dolomite. The only clay mineral identified was chlorite. Resuspended tailings showed reduced intensity of pyrite and pyrrhotite peaks relative to those of the bed material. This indicated oxidation of pyrite and pyrrhotite in the suspended tailings.
5. Elemental analysis showed that both bed and resuspended tailings are rich in iron and sulphur. Iron concentration in bed tailings varies from 10.23 % to 45.16% (by weight) and in resuspended tailings from 9.90% to 22.66% (by weight) while sulfur concentration in bed material varies from 0.28 % to 36.40% (by weight) and in resuspended tailings from 1.05 % to 35.20% (by weight). Other major elements identified in the tailings were Si, Cu, Ni, Pb, and Zn. The concentrations of iron, sulphur, and other major metals in the tailings were much higher than the typical crustal composition.
6. The mineralogical and elemental analysis of the resuspended and bed tailings samples showed compositional similarity, which supports the claim that material collected in sediment traps was mostly resuspended tailings and that little or no

foreign material was deposited in the sediment traps. It added to the evidence that some amount of resuspension was occurring at the study site.

7. The average critical shear was 0.13 Pa for the west and east cells and 0.04 Pa for the middle cell bed tailings due to the finer particle size (average D_{50} 0.008 mm) of the latter. Fischenich's (2001) equation does not account for the cohesive properties of finer particles. The presence of binding cohesive forces in the fine particles can increase the resistance to erosion and resuspension and hence the critical shear stress. The field measured resuspension data (from sediment traps and OBS sensor measurements) did not confirm such a low critical shear stress value. The finer bed tailings in the middle cell could be of cohesive nature, an inference which was supported by higher content of clay minerals in the middle cell bed tailings.
8. The OBS sensor installed at a depth of 25 cm above the bed recorded suspended tailings concentrations of 3 to 25 mg/L, values that were more representative of the average concentration in the water column than the up to 80 mg/L measured by the OBS sensor installed close to the bed (10 cm above the bed). The Samad and Yanful (2005) model prediction of suspended tailings concentrations in the west cell under the existing water depth was 6.5 to 22.7 mg/L. The field measured and model predicted values were found to be in the same range. The field recorded suspended solids concentration using OBS sensors during two other events of the study were also within the range of model predictions.
9. Wind induced circulation currents were recorded using an ADCP in the middle cell of the Shebandowan tailings storage facility. This was the first ever attempt

where actual currents have been recorded in a tailings pond. From the recorded currents, an intricate pattern of flow circulation was observed, which was found to be depending on wind direction and field geometry and more complex than the near-bed flow reversal that was typically assumed in previous tailings pond studies.

10. The magnitude and direction of current velocities were also found to be varying from one location to another in the pond. This finding is somewhat contradictory to observations from counter-current flow models (Wu and Tsanis 1995), in which a single current velocity is predicted over the entire tailings area. However, the order of magnitudes of current velocities was found to be similar to model predicted values at most locations in the pond.
11. An important contribution from the ADCP recorded current data was that it allowed the effect of wave-current interaction on the total bed shear stress to be studied. A semi-empirical approach was developed to estimate the total bed shear stress, where the bed shear stress due to circulatory currents was determined by fitting a log linear profile to near bed measured currents. The results showed that wave-current interaction enhances the total bed shear stress and that linear addition of the wave and current bed shear stresses may underestimate the total bed shear stress.
12. The bed shear stress due to circulation currents is not a function of fetch length and thus its variation is not related to location in the pond. At locations where the fetch length was negligible, depending on the direction of wind and hence the wave induced bed shear stress, the total bed shear stress was mostly due to

circulatory currents. These results showed that circulatory currents significantly contributes to total bed shear stress and cannot be ignored.

13. A simplified equation was derived to estimate the total bed shear stress under shallow water conditions for known values of wind speed (m/s), water depth (m), and fetch length (m). The multiple equations of SMB method of wave parameter prediction, linear wave theory, Wu and Tsanis (1995) model of current prediction, and wave-current interaction were reduced into a single equation. This simplified equation provides a relatively easy approach to estimate the total bed shear stress under shallow water conditions, such as exists in tailings ponds.
14. As an another major outcome of this research, a graphical approach was developed to estimate the critical shear stress and erosion rate parameters using real-time field recorded wind-induced resuspension and wind data. The critical shear stress obtained from this graphical technique was 0.10 Pa for the west cell tailings and 0.08 Pa for the middle cell tailings.
15. For the west cell, slightly lower value of the critical shear stress than empirically determined value of 0.12 Pa may be attributed to less dense top layer (fluffy layer) of bed sediments which is subjected to frequent erosion and re-deposition processes. However, in the case of the middle cell, a higher value of the critical shear stress than the empirically calculated value of 0.04 Pa was obtained. The higher value of the critical shear stress supported the previous claim that the finer tailings in the middle cell might be cohesive.
16. A major improvement was made in the Samad and Yanful (2005) resuspension model by incorporating the term of wave-current interactions in determination of

total bed shear stress. Current directions were assumed to be collinear to wind induced waves, which would maximize the total bed shear stress and result in slightly higher water cover depth requirements. This is probably a conservative approach to the design of water covers.

17. The improved Samad and Yanful model showed that wave-current interactions significantly increased the required depth of water from 3.9 m in the absence of wave-current interaction to 6.3 m to completely eliminate tailings resuspension in the west cell of the Shebandowan tailings pond and similar results were obtained for the middle and east cells of the tailings pond.
18. The minimum water depth required to completely eliminate resuspension was as high as 6.3 m. Obviously, implementing this water cover in the field would not be economically feasible due to high cost of constructing large dams to store that much water. The long-term stability of high dams is also matter of concern. It would be economically and mechanically preferable if the model can determine the water depth that would allow resuspension to occur within the regulatory limits at the center of each square grid cell in the pond. Another major improvement was made in the Samad and Yanful (2005) model by the addition of an option to optimize the water cover depth at the center of each square grid cell for known regulatory limits. The model showed the optimized water depths less than 2.2 m for the west cell, 1.1 m for the middle cell and 2.0 m for the east cell were sufficient to reduce the resuspension within regulatory limits of 15 mg/L.

7.2 APPLICATIONS

The overall results of this research will help in understanding the process of wind-induced resuspension of mine tailings deposited under shallow water covers. Equation (5.5) in chapter 5, derived to determine the total bed shear stress and the graphical approach developed to estimate the erosion characteristics using field measured resuspension, reduce the time and effort required to obtain the same parameters using previous, published methods. The use of this approach and the improved model can be useful either in designing a new tailings storage facility or managing an existing one. The most obvious benefit of the research is significant improvement in the development of a design, management and validation tool for tailings storage facilities. The findings and approaches presented in the present thesis can also be applied to other sediment erosion and resuspension practices e.g. prediction of resuspension in highway detention ponds (Bentzen et al. 2009) or in waterways.

7.3 RECOMMENDATIONS FOR FUTURE WORK

From the observations made and results obtained through the present research, the following recommendations are suggested for future work:

1. The OBS sensors used in present study were subject to fouling during long-term deployments and this limited their use for recording resuspension during storm events. The use of self-cleaning OBS sensors can eliminate this problem and provide a better picture of resuspension.

2. The graphical technique developed in this model to estimate the erosion characteristics of bed sediments should be applied to different sites and verified with other field experiments.
3. Simultaneous field measurements of the wind-induced waves and currents must be made in order to evaluate their contribution to the total bed shear stress. Advanced acoustic Doppler current profilers (ADCPs) capable of measuring both waves and currents simultaneously in shallow waters should be used for measurements at tailings storage facilities.
4. The improved model should be verified in field measurements of resuspension under different site conditions.
5. Hydrology of the storage facility, which includes the water balance, should be incorporated into the model. This requires knowledge of seepage losses from runoff in the tailings pond. This will help to determine the net water required to be pumped into the pond to maintain a certain water cover depth.

7.4 REFERENCES

1. Bentzen, T.R., Larsen, T., & Rasmussen, M.R. (2009). Predictions of resuspension of highway detention pond deposits in interrain event periods due to wind-induced currents and waves. *Journal of Environmental Engineering, ASCE*, 135(12): 1286-1293.
2. Fischenich, C. (2001). Stability thresholds for stream restoration materials. EMRRP technical notes collection, ERDC TN-EMRRP-SR-29, U.S. Army engineer research center, Vicksburg, M.S.
3. Samad, M. A., & Yanful, E.K. (2005). A design approach for selecting the optimum water cover depth for subaqueous disposal of sulphide mine tailings. *Canadian Geotechnical Journal*, 42: 207-228.
4. Wu, J., & Tsanis, I.K. (1995). Numerical study of wind induced water currents. *Journal of Hydraulic Engineering, ASCE*, 121(5): 388-395.

APPENDIX-I: CALIBRATION OF OBS SENSORS

In the present study, two OBS-3+ sensors (Manufactured by D&A Instrument Company, USA) purchased from Campbell Scientific Canada were used. The OBS (Optical Back Scatter) sensors are also known as turbidity sensors. It consists of a high intensity infrared emitting diode (IRED) and an optical sensor that measures turbidity and suspended solids concentration by detecting infrared (IR) radiation scattered from suspended material in water. The IRED emits an infrared beam with half-power points at 50° in the axial plane of the sensor and 30° in the radial plane. The optical detector integrates the IR scattered between 140° and 160° . Visible light incident on sensor is absorbed by a filter. These sensors were connected with CR10X datalogger (Manufactured by Campbell Scientific Canada Corp.) and programmed to measure the total suspended concentration every 5 minutes. Basic operational details of the OBS-3+ sensors are presented in Table I-1.

The response of the OBS sensors to turbidity and suspended solids concentrations can be shown by Figure I-1 which has been divided in three regions A, B and C. In region A, the voltage output of the sensor is proportional to backscatter intensity and backscatter intensity is proportional to turbidity levels or suspended solids concentrations. The OBS sensors, in general, should be calibrated and used in this linear range.

Table I-1 Basic operational properties of OBS-3+ sensor (D&A Instrument Company, USA)

OBS-3+

(D&A Instrument Company)



Range

SSC Mud	0-5000 mg/L
SSC Sand	0-50 g/L
Turbidity	0-4000 NTU

Accuracy

SSC Mud	0.5 mg/L (1% of reading)
SSC Sand	0.25 g/L (1% of reading)
Turbidity	0.25 NTU (1% of reading)

Operational Data

Voltage output	0-1.25 V, 0-2.50 V, or 0-5.00 V
Current output	4-20 mA (optional)
Maximum data rate	10 Hz
Maximum depth	500 m
Daylight rejection	-28 dB (48 mV/cm ²)
Drift	< 2% per year
Housing Material	316 stainless steel
Connector	MCBH-5-FS (wet pluggable)

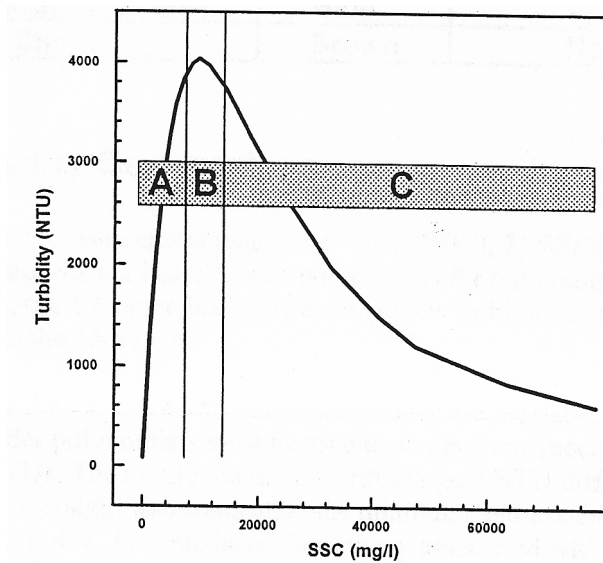


Figure I-1 response of OBS sensors with increasing turbidity and suspended solids concentration

The two OBS sensors were factory calibrated by the manufacturer (D & A Instrument Company, Washington, USA) using Formazin standards for nominal and high range turbidity measurements. The factory calibration certificates are provided in Figures I-2 and I-3. The turbidity calibration shows that the each OBS sensor has its own measurement characteristics and they are not interchangeable. Turbidity and suspended solids concentration of water is directly proportional to each other. But it is not possible to find a universal conversion equation. Measurement of suspended solids concentrations with optical instruments depend greatly upon variety of parameters such as particle size, composition and shape, as well as environmental characteristics. Calibration for suspended solids is a local phenomenon and calibration coefficients change with characteristics of sediments. Calibration of OBS sensors for field sediments is most important part prior to using them on site.

OBS-3+ AMCO Clear Calibration Certificate

Serial Number: S7299

Nominal Low Range: 500 NTU

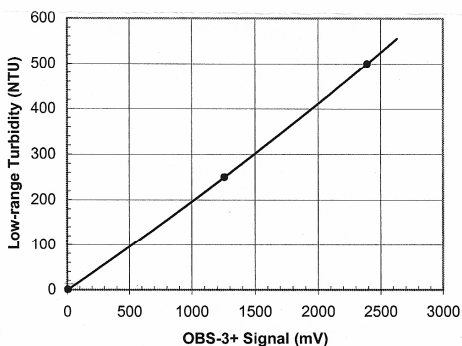
Customer: CSI

Nominal High Range: 2000 NTU

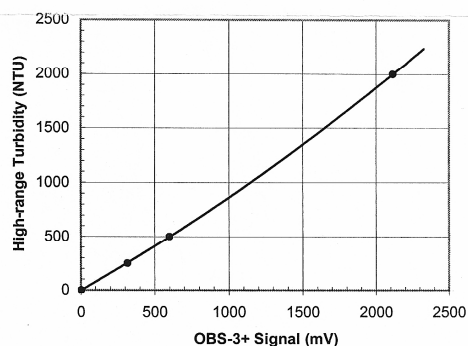
Measurement: Auto Calibrator S/N: 001

Coefficients			
Degree	A	B	C
Low	-0.7170529	0.1877786	9.00E-06
High	-1.9078922	0.7896598	7.40E-05

SN: S7299 Low



SN: S7299 High



Date: October 02, 2006

Performed by: *R. Hatch*



© D&A Instrument Company

Version 2.4

8/2006

Figure I-2 Factory calibration certificate of OBS-1 sensor for turbidity measurements (Serial Number S7299)

OBS-3+ AMCO Clear Calibration Certificate

Serial Number: S7300

Nominal Low Range: 500 NTU

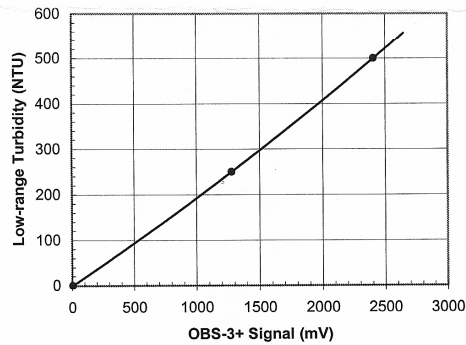
Customer: CSI

Nominal High Range: 2000 NTU

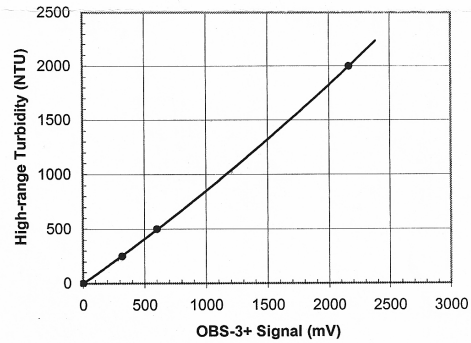
Measurement: Auto Calibrator S/N: 001

Coefficients			
Degree	A	B	C
Low	-0.6725742	0.1822616	1.07E-05
High	-1.8637514	0.787835	6.28E-05

SN: S7300 Low



SN: S7300 High



Date: **October 02, 2006**

Performed by: *Rebecca*



© D&A Instrument Company

Version 2.4

8/2006

Figure I-3 Factory calibration certificate of OBS-2 sensor for turbidity measurements (Serial Number S7300)

The calibration was done in laboratory using the bottom tailings samples collected at site. Both sensors were immersed in a black color bucket full of distilled water. Black color of the bucket was chosen to minimize the effect of other light sources present in the laboratory room. Sensors were oriented in such a way that they don't interfere with each other and also remain submerged at least 10cm in water at all times. Now readings from both sensors for mili-volts and turbidity units (NTU) were recorded for distilled water or zero suspended solids through the datalogger attached to the two sensors. In the next step a little amount of tailings material was mixed thoroughly and after mixing suspended solids concentration was again recorded. Also a 100 ml water sample preserved to measure suspended solids concentration gravimetrically. In the same way tailings material was added in the water in increasing amount and each time water sample was collected to measure suspended solids concentration. The water samples collected during each step were oven dried and weight of the net suspended material was obtained. The volume of each water sample was fixed 150 ml and the concentrations of suspended solids (in mg/L) in water were obtained by dividing the weight of suspended tailings to the volume of water sample.

The mili-volts output from each sensor was plotted against corresponding suspended solids concentration or SSC value (mg/L) and fitted for a straight line. The equation of this straight line is further used to convert voltage outputs from the OBS sensors to total suspended solids concentration, recorded at site. For example, data obtained from the OBS calibration for the west cell bed tailings are provided in Table I-2. Figure I-4 shows the calibration curves plotted for the two OBS sensors. The data were

fitted to linear regression line with very good correlation coefficient $R^2 = 0.99$ for both OBS sensors.

Table I-2 Laboratory calibration data of two OBS sensors for suspended solids concentrations (SSC) using the west cell bed tailings

	OBS 1 Output (mili-volts)	OBS 1 Output (mili-volts)	SSC (mg/L)
Step 1	4.61	4.91	0
Step 2	49.10	52.32	15
Step 3	67.33	66.70	23
Step 4	126.00	130.12	36
Step 5	130.77	135.00	41
Step 6	158.75	163.05	52
Step 7	205.80	228.90	68

Two OBS sensors were also calibrated for the middle cell bed tailings using the similar process. The calibration data for the middle cell bed tailings were fitted to linear regression lines with correlation coefficient $R^2 = 0.99$ for both OBS sensors. The calibration curves for the middle cell bed tailings have been already provided in Figure 3.3 of chapter 3. Bed tailings in the east cell were of the similar geotechnical properties as of the west cell and hence the same calibration curves were used for the suspended solids concentration measurements in the each cell. From all these calibration curves following

equations were obtained and used in the conversion of miliVolts output of the OBS sensors to the suspended solids concentrations or SSC (mg/L).

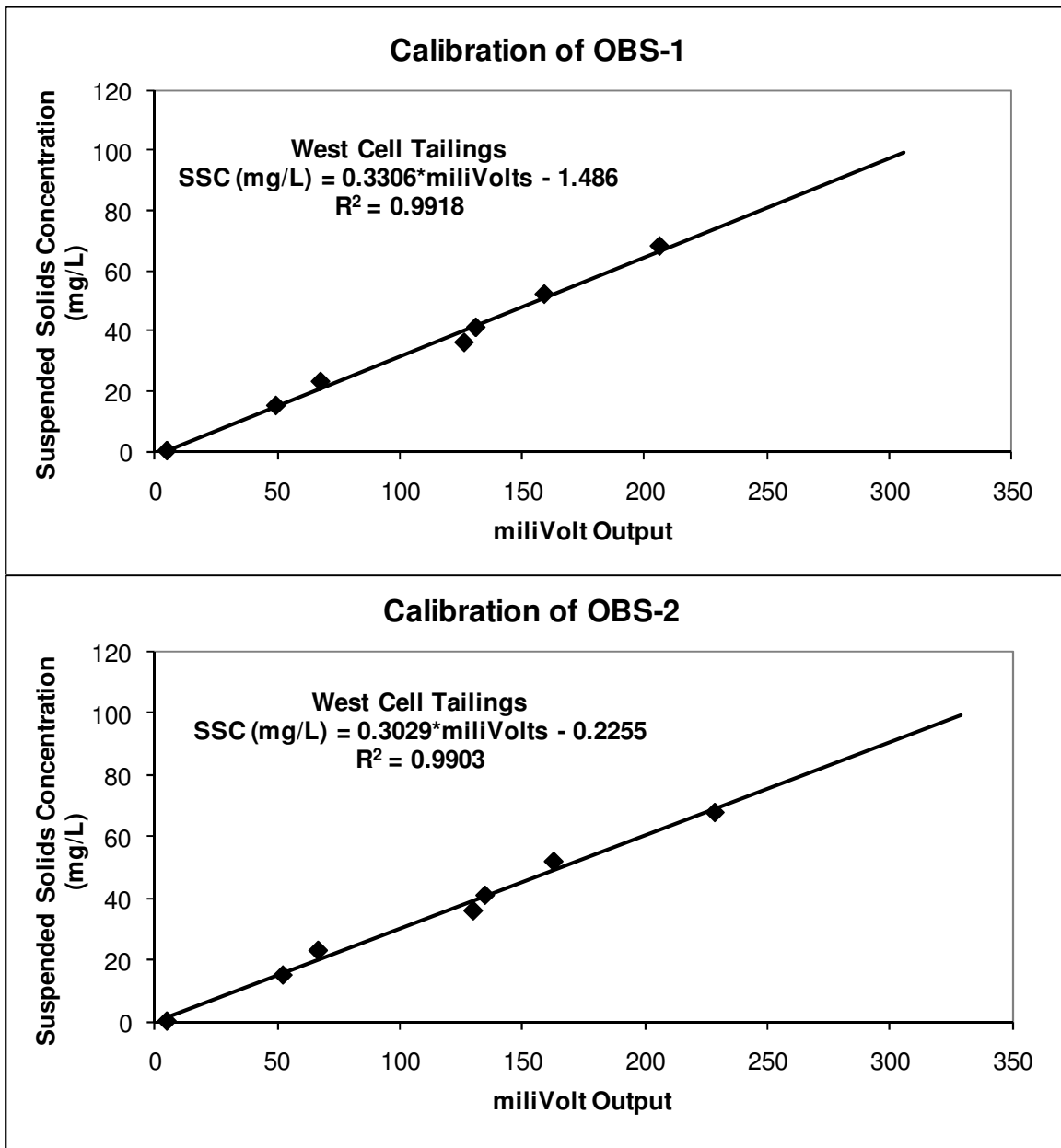


Figure I-4 Laboratory calibration curves of two OBS sensors for suspended solids concentrations (SSC) measurement in the west cell of the tailings pond.

- **West and East Cell**

OBS-1 (Serial Number S7299)

$$SSC\left(\frac{mg}{L}\right)=0.3306 * \text{miliVolts} - 1.486$$

OBS-2 (serial Number S7300)

$$SSC\left(\frac{mg}{L}\right)=0.3029 * \text{miliVolts} - 0.2255$$

- **Middle Cell**

OBS-1 (Serial Number S7299)

$$SSC\left(\frac{mg}{L}\right)=0.2771 * \text{miliVolts} - 0.9688$$

OBS-2 (serial Number S7300)

$$SSC\left(\frac{mg}{L}\right)=0.2651 * \text{miliVolts} - 1.2105$$

APPENDIX-II: MINEROLOGY OF BED TAILINGS

Total eight sediment traps were installed in the Shebandowan tailings storage facility such as sediment trap number 1, 2 and 3 in the west cell, 4 and 5 in the middle cell, and 6, 7, and 8 in the east cell of the tailings pond as already mentioned in section 3.3 of chapter 3. Resuspended tailings were collected in the eight sediment traps for a certain time period and samples were named ST-1 to ST-8. Eight bed tailings samples were collected from the deployment location of each sediment trap and named BT-1 to BT-8. These samples were vacuum dried in desiccators using desiccant silica gel. After completely drying, samples were grounded using a rubber pastel and passed through number 200 sieve. The material passed through the sieve was used to obtain the X-ray powder pattern diffractograms. The detailed diffractograms of suspended tailings collected in each sediment traps and corresponding bed tailings and identified clay and non-clay minerals are shown in Figures II-1 to II-8.

All of these samples showed almost similar mineralogy but of different peak intensities, which suggest difference in the content of minerals. In all of these samples, the non-clay minerals identified were quartz, pyrite, pyrrhotite, feldspar, calcite, and dolomite. The only clay mineral identified was chlorite.

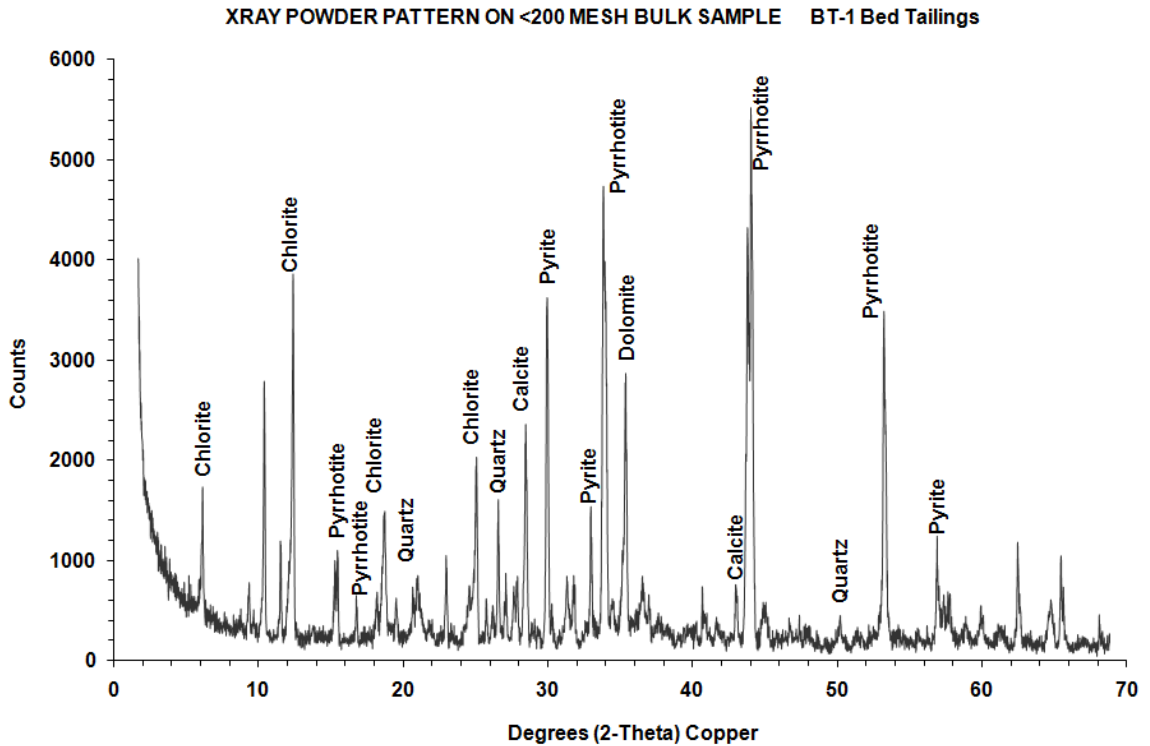
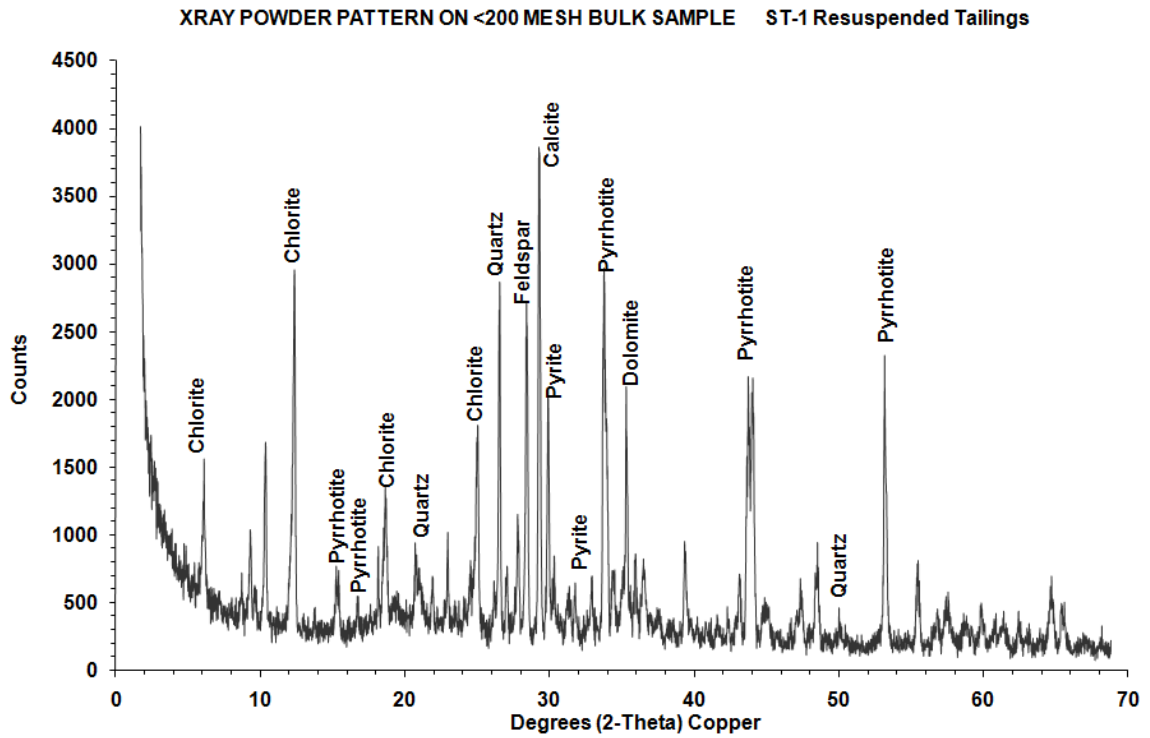


Figure II-1 X-ray diffractograms of resuspended and corresponding bed tailings collected at sediment trap location ST-1

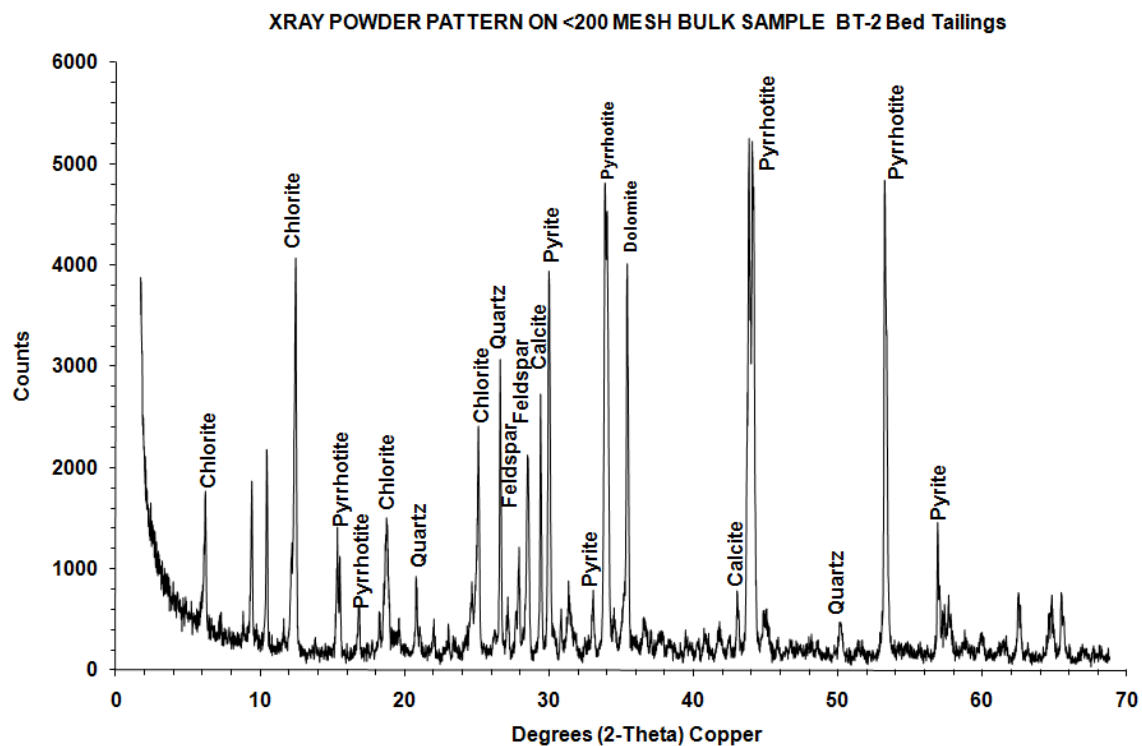
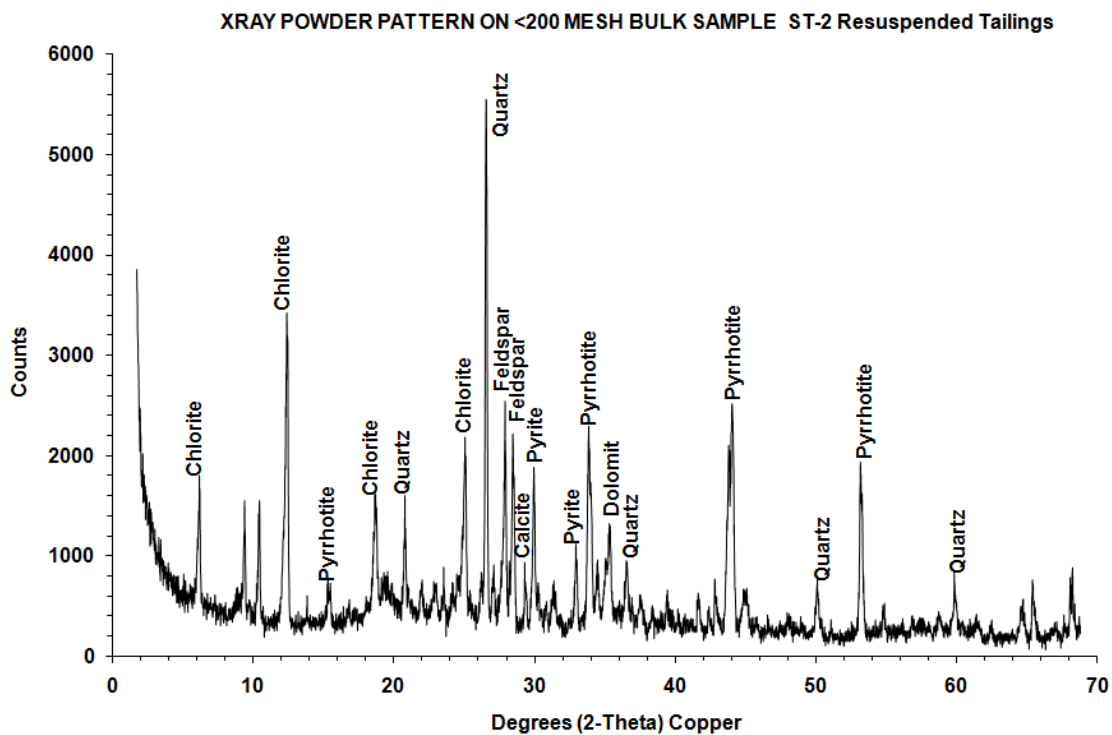


Figure II-2 X-ray diffractograms of resuspended and corresponding bed tailings collected at sediment trap location ST-2

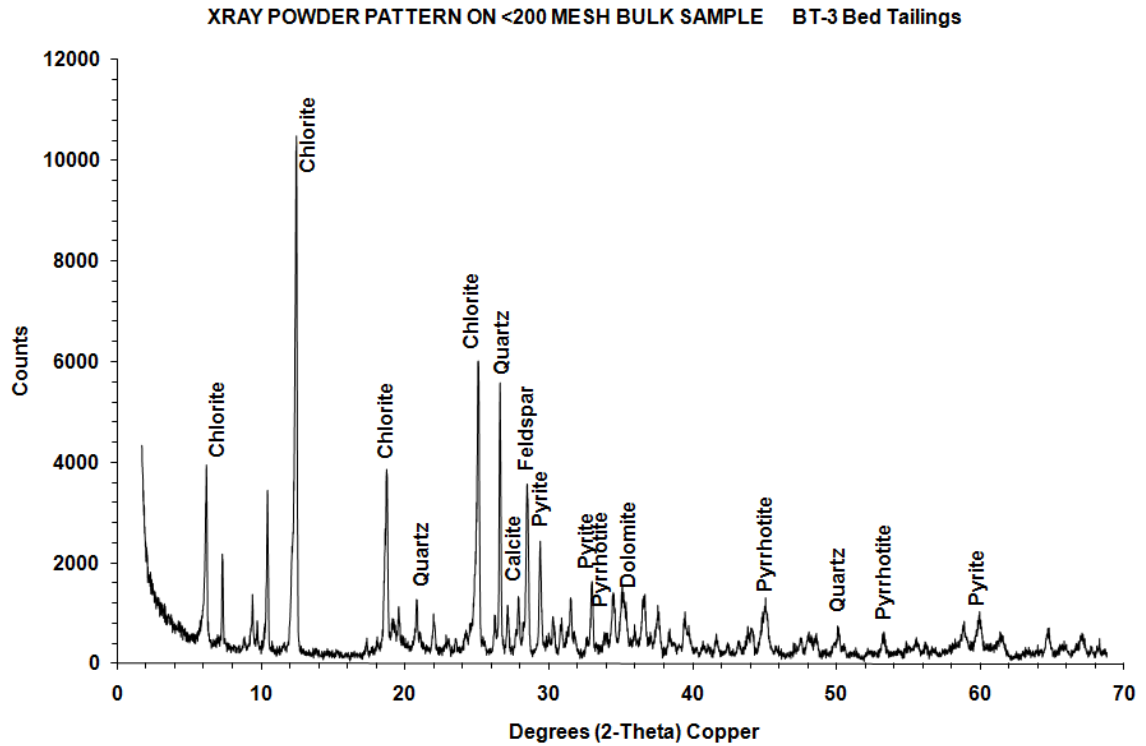
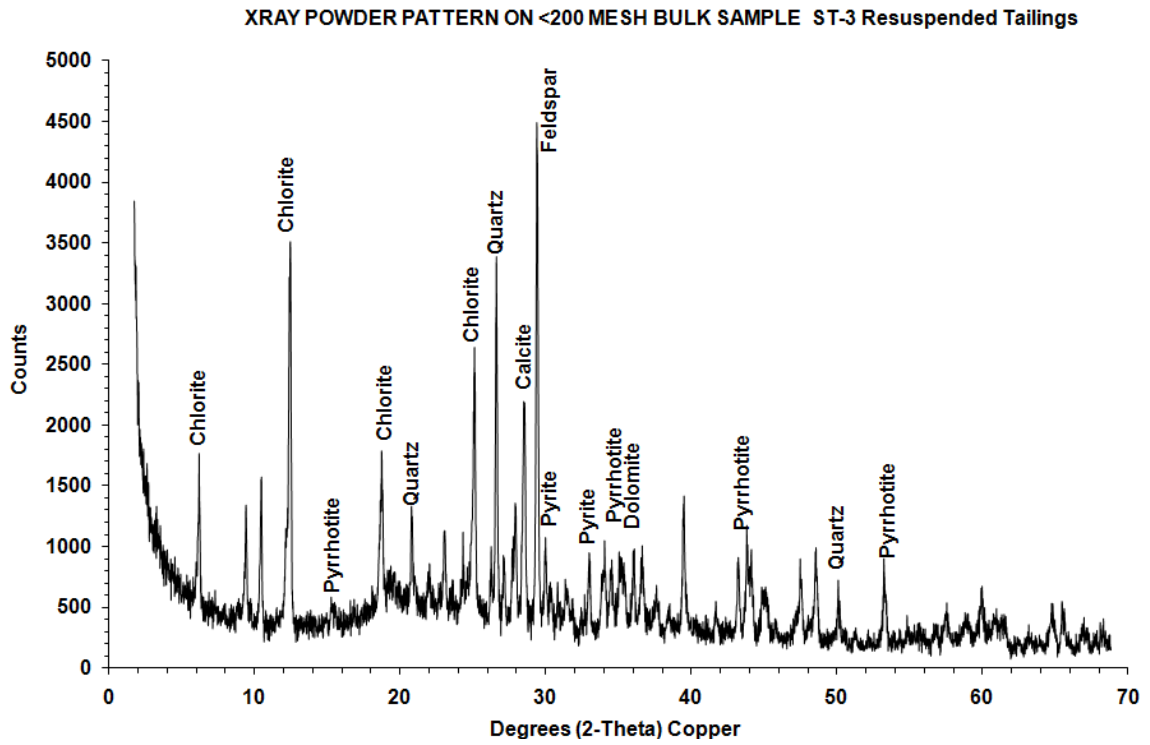


Figure II-3 X-ray diffractograms of resuspended and corresponding bed tailings collected at sediment trap location ST-3

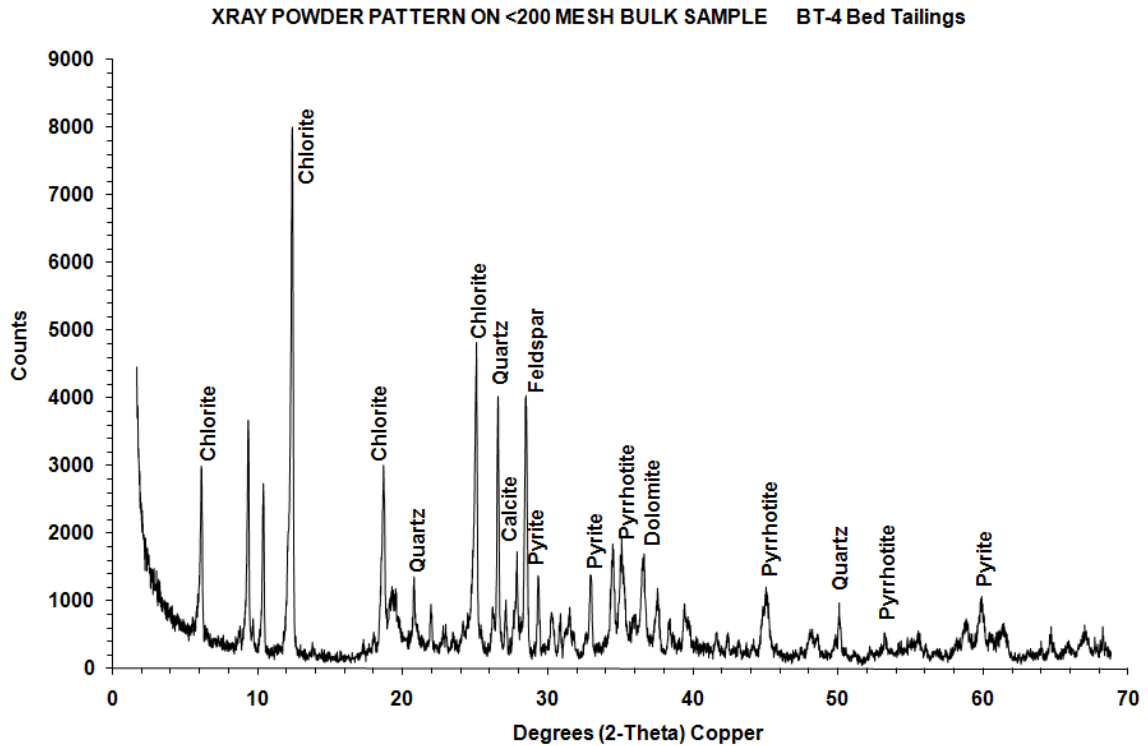
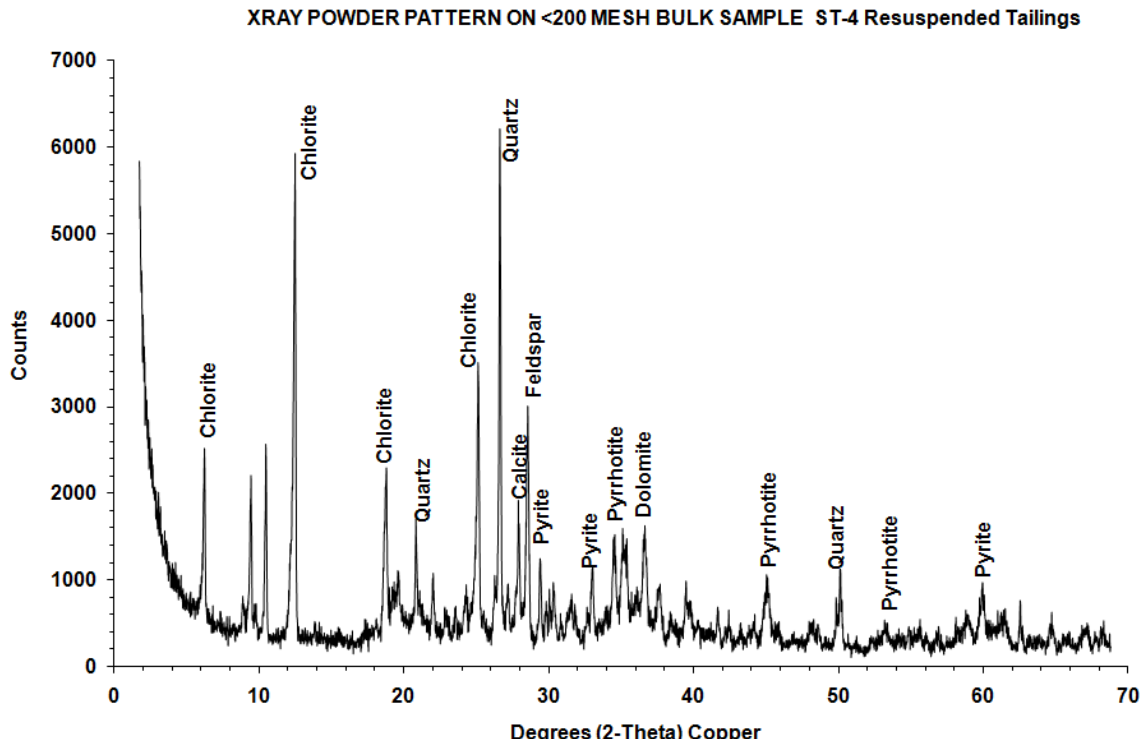


Figure II-4 X-ray diffractograms of resuspended and corresponding bed tailings collected at sediment trap location ST-4

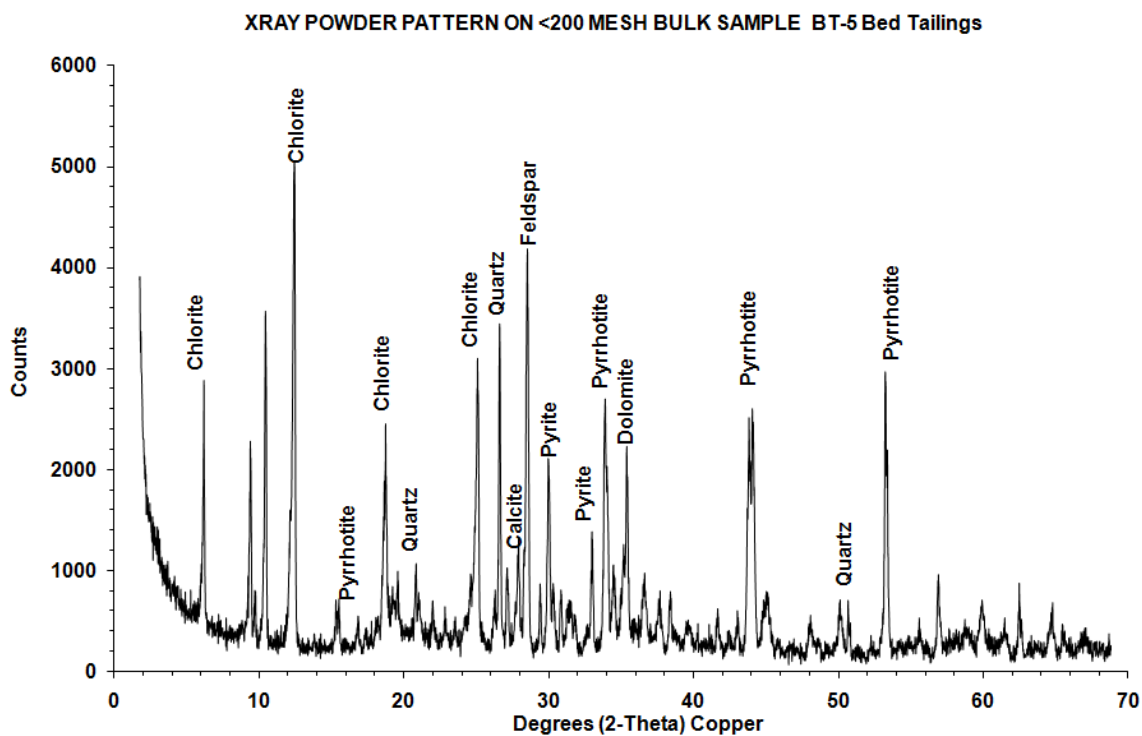
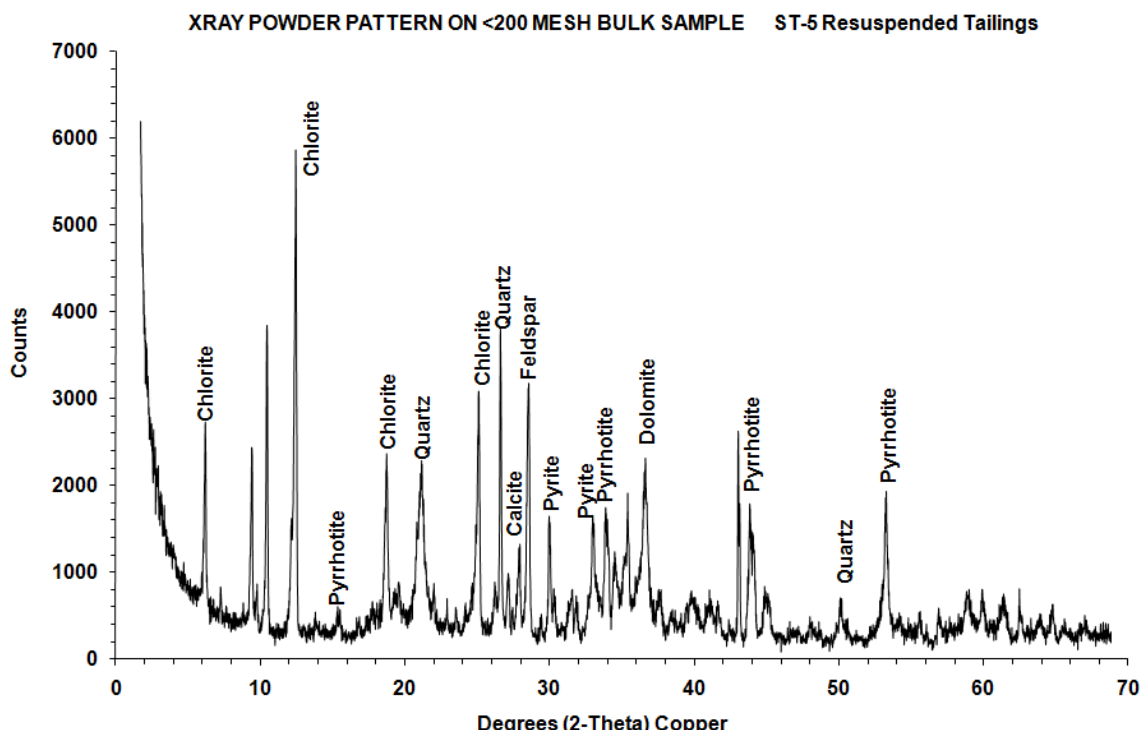


Figure II-5 X-ray diffractograms of resuspended and corresponding bed tailings collected at sediment trap location ST-5

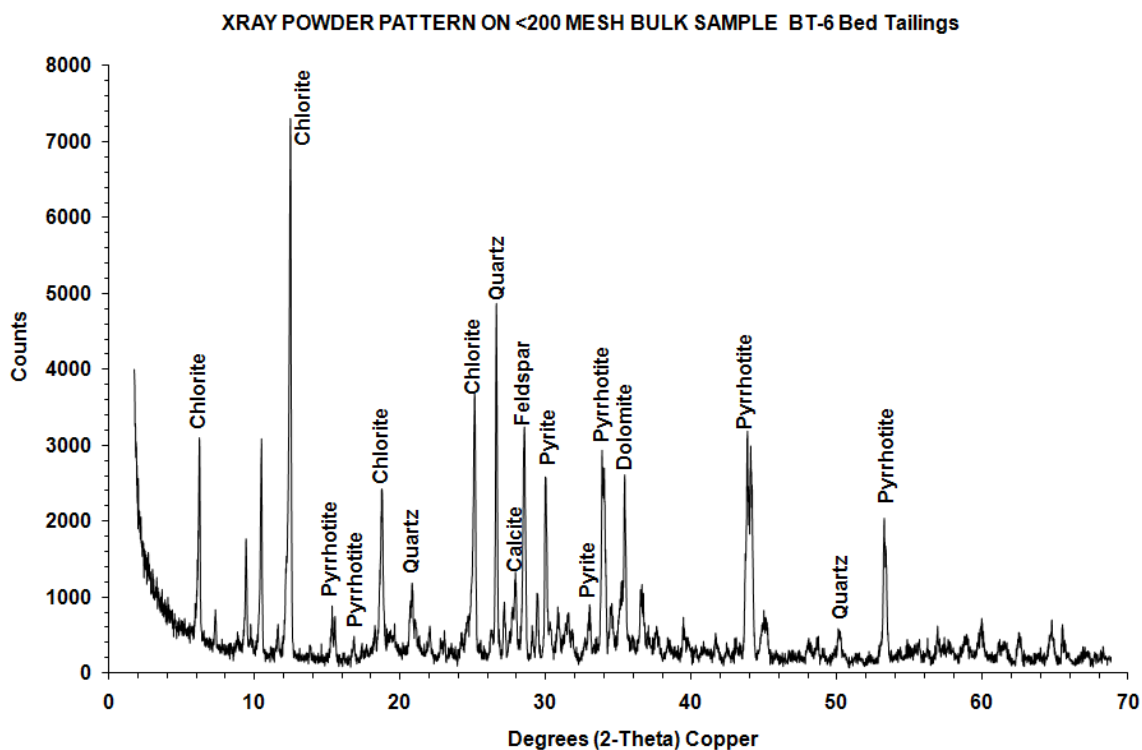
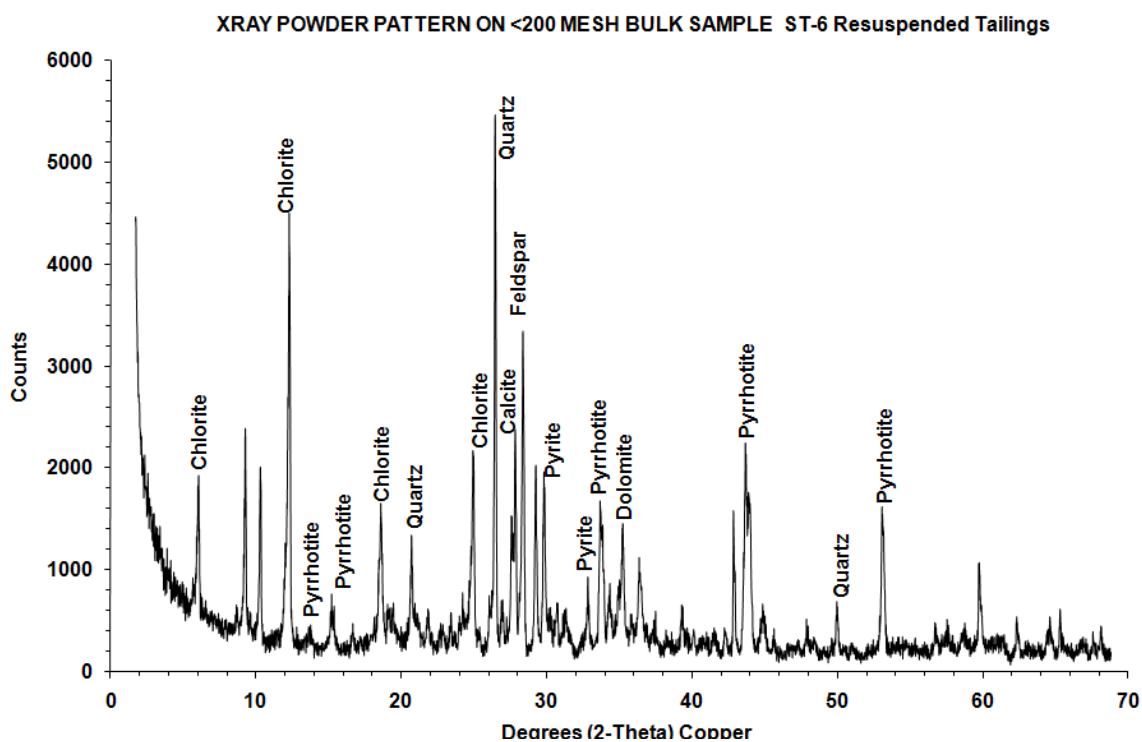


Figure II-6 X-ray diffractograms of resuspended and corresponding bed tailings collected at sediment trap location ST-6

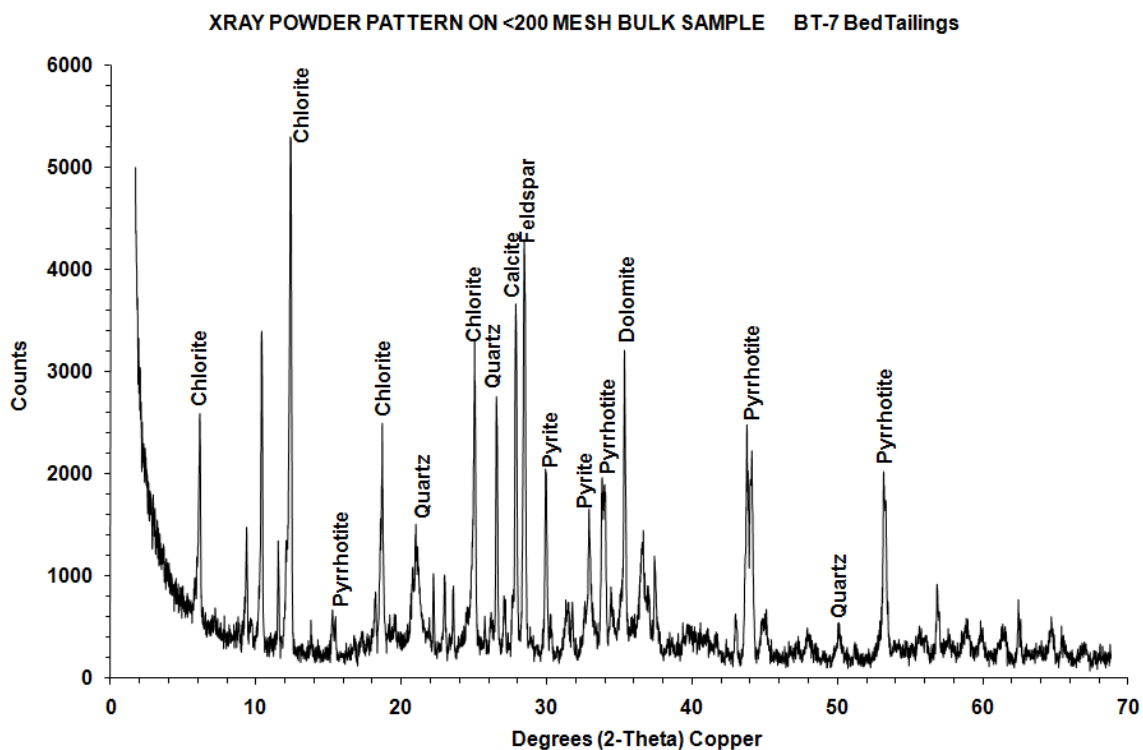
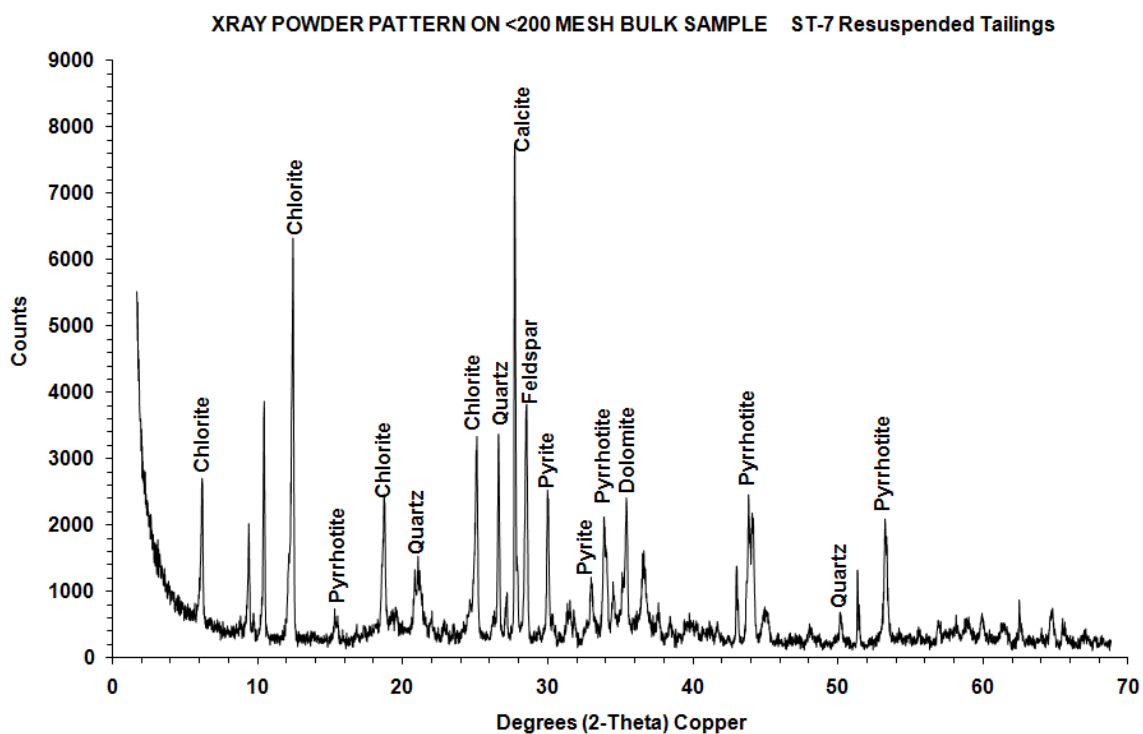


Figure II-7 X-ray diffractograms of resuspended and corresponding bed tailings collected at sediment trap location ST-7

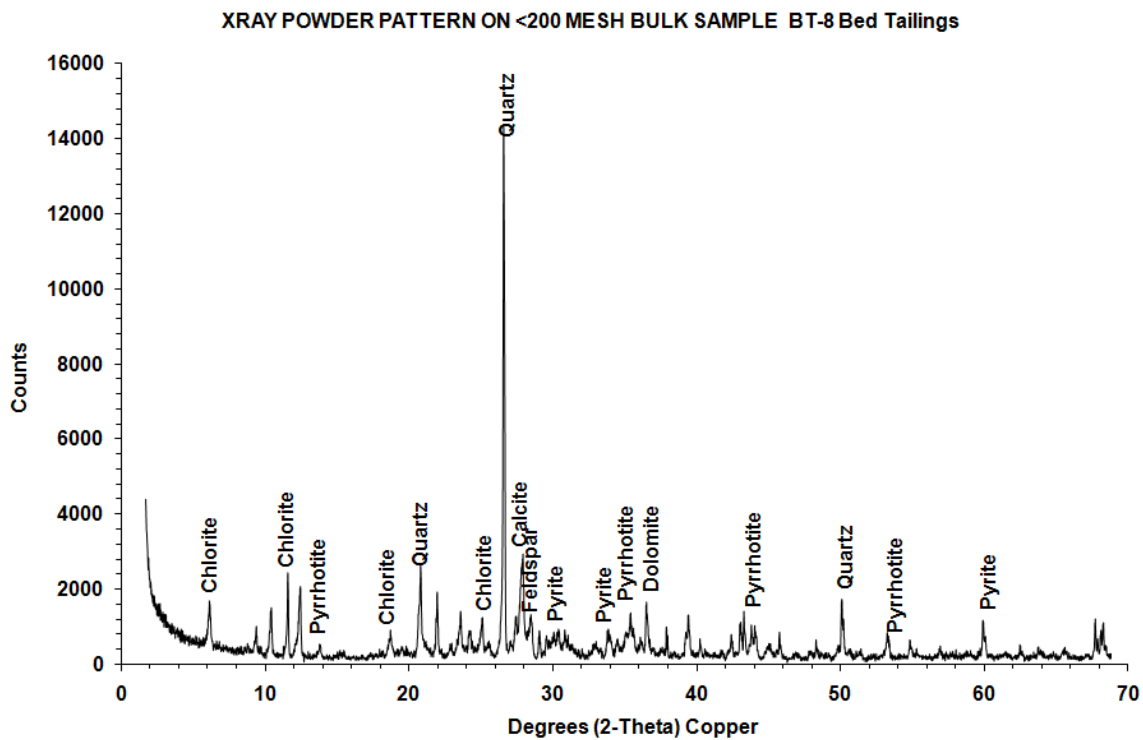
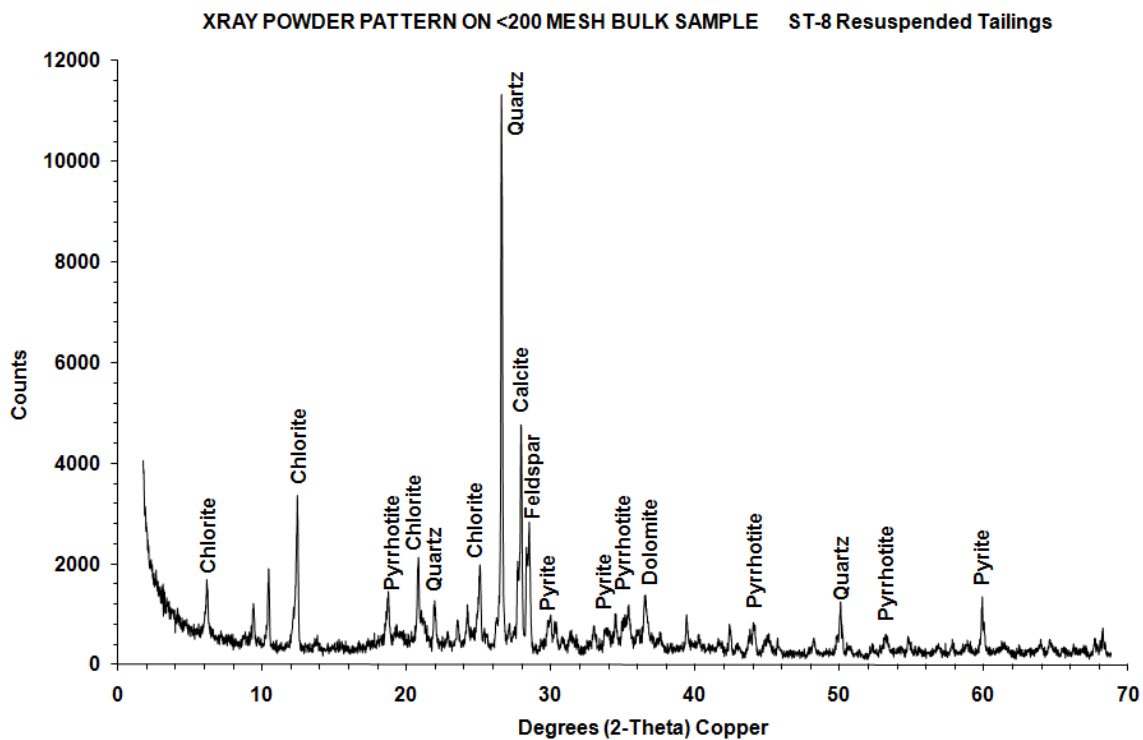


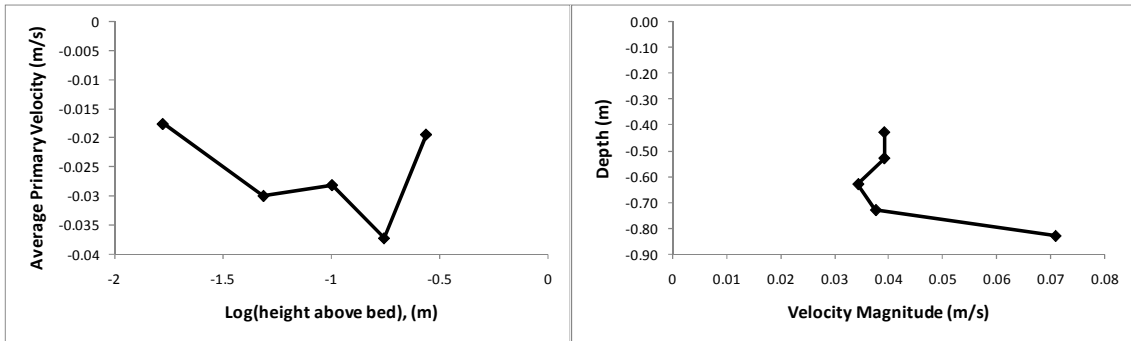
Figure II-8 X-ray diffractograms of resuspended and corresponding bed tailings collected at sediment trap location ST-8

APPENDIX-III: FIELD MEASURED CURRENT VELOCITY PROFILES

Following are the current velocity distributions in water column measured at different stationary locations in the middle cell of the Shebandowan tailings storage facility (Figure 4.1). Velocity data was fitted to log-law to obtain near bed current shear velocity. Current directions were measured in counter-clockwise direction from east in radians.

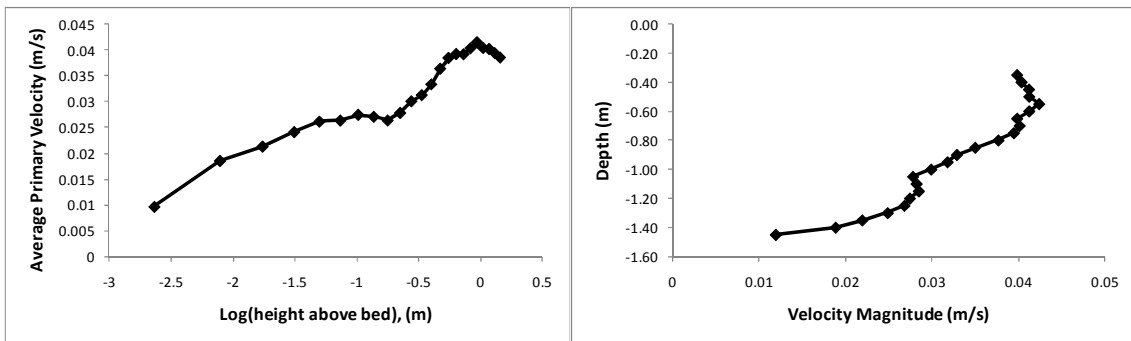
Profile Location# 8

Water cover depth = 0.99 m, and average current direction = 3.26 radians



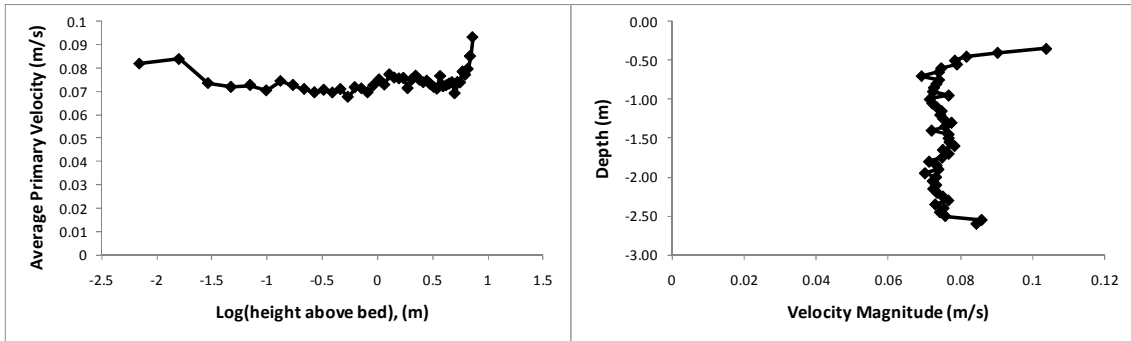
Profile Location# 10

Water cover depth = 1.52 m, and average current direction = 0.78 radians



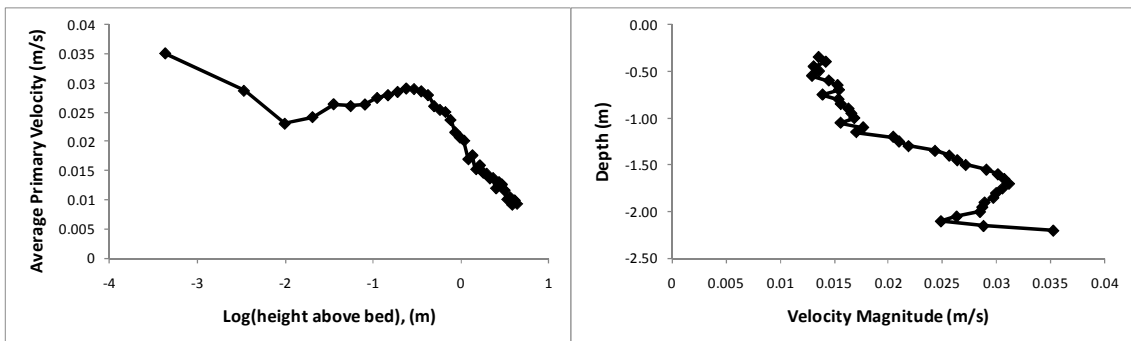
Profile Location# 11

Water cover depth = 2.72 m, and average current direction = 1.44 radians



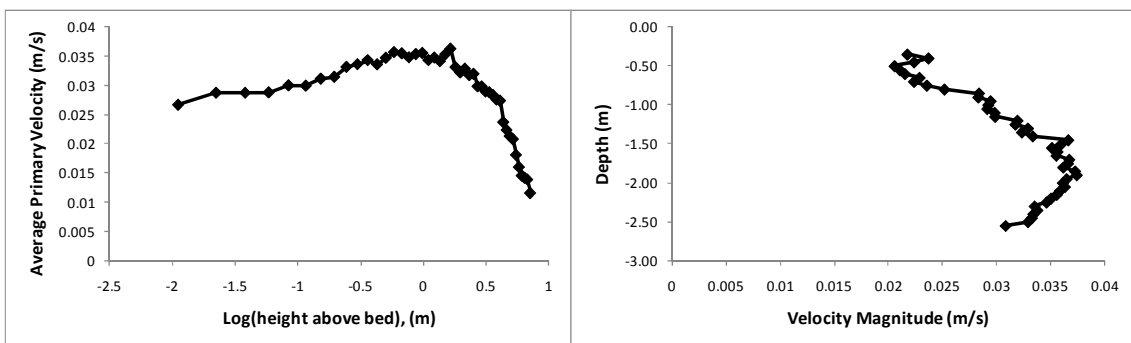
Profile Location# 12

Water cover depth = 2.23 m, and average current direction = 4.39 radians



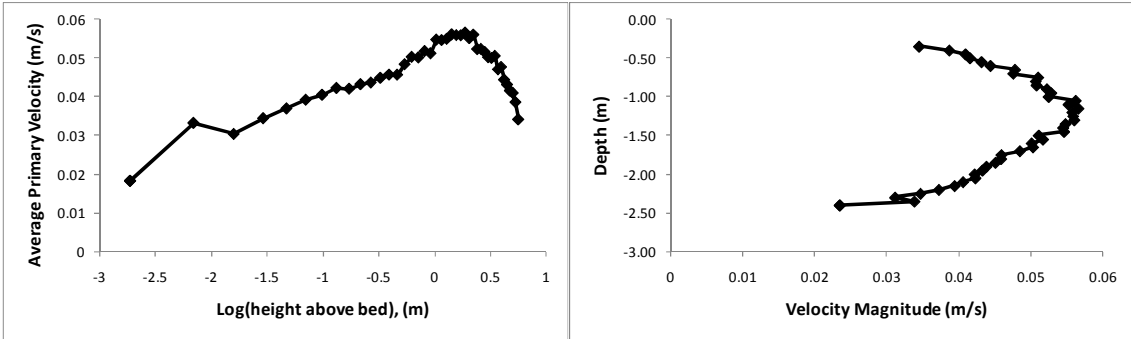
Profile Location# 13

Water cover depth = 2.69 m, and average current direction = 4.12 radians



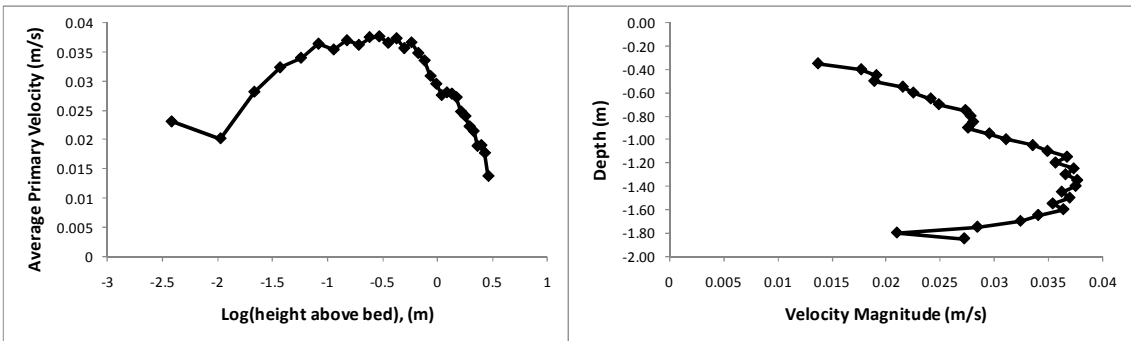
Profile Location# 14

Water cover depth = 2.47 m, and average current direction = 3.55 radians



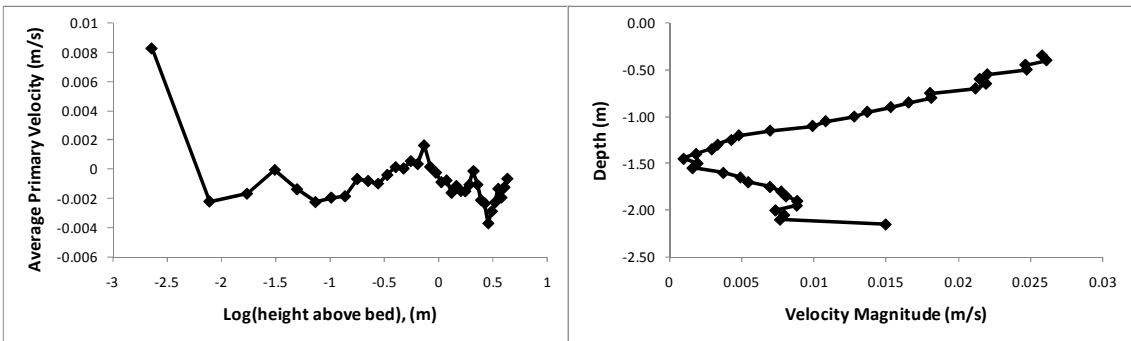
Profile Location# 15

Water cover depth = 1.94 m, and average current direction = 3.78 radians



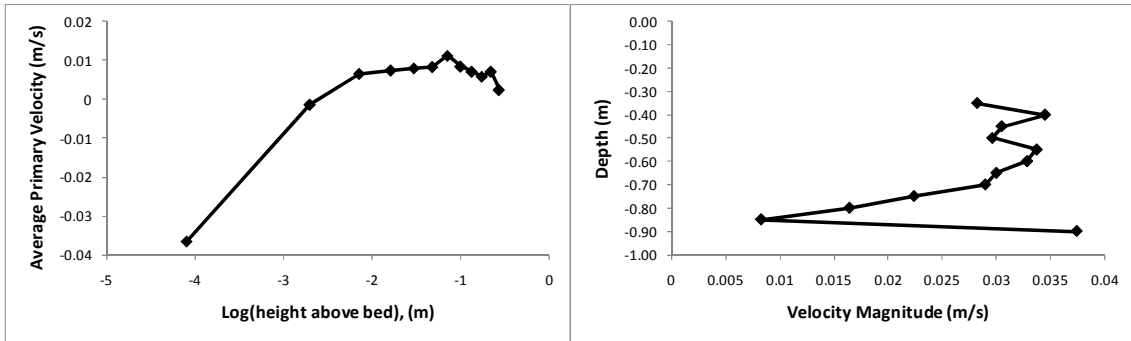
Profile Location# 16

Water cover depth = 2.22 m, and average current direction = 1.45 radians



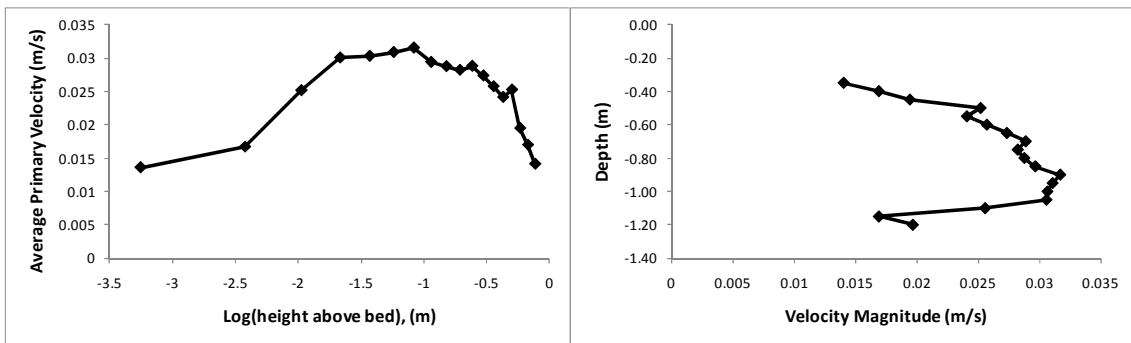
Profile Location# 17

Water cover depth = 0.92 m, and average current direction = 1.80 radians



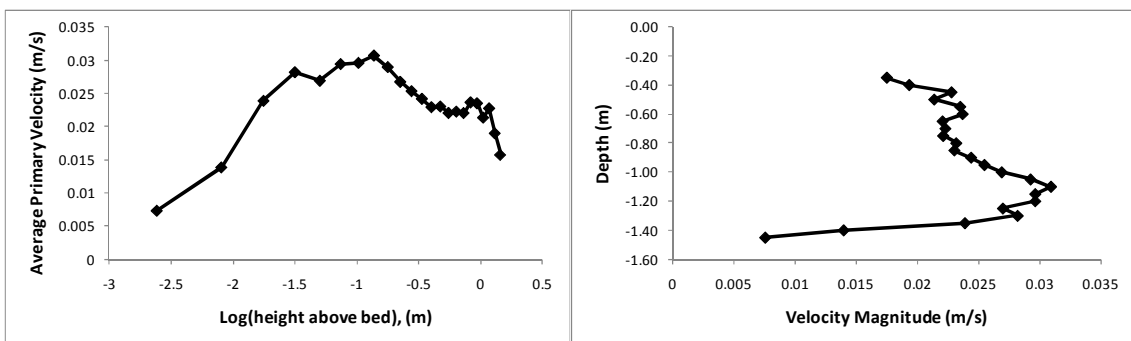
Profile Location# 18

Water cover depth = 1.24 m, and average current direction = 4.63 radians



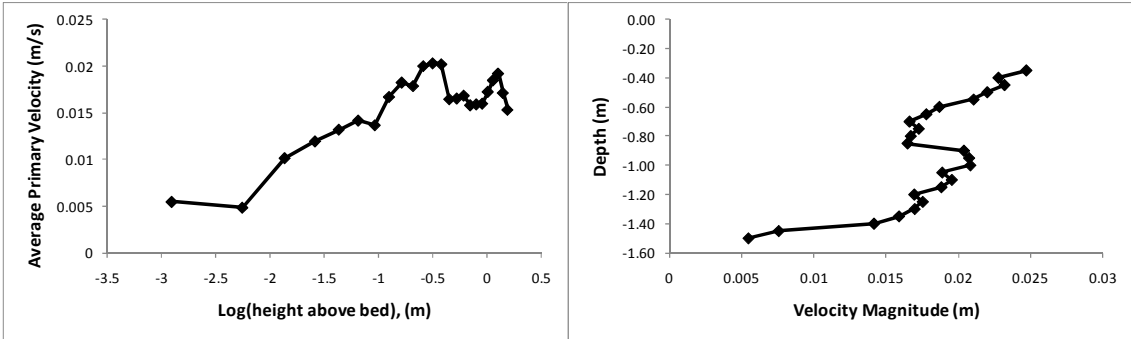
Profile Location# 19

Water cover depth = 1.52 m, and average current direction = 4.75 radians



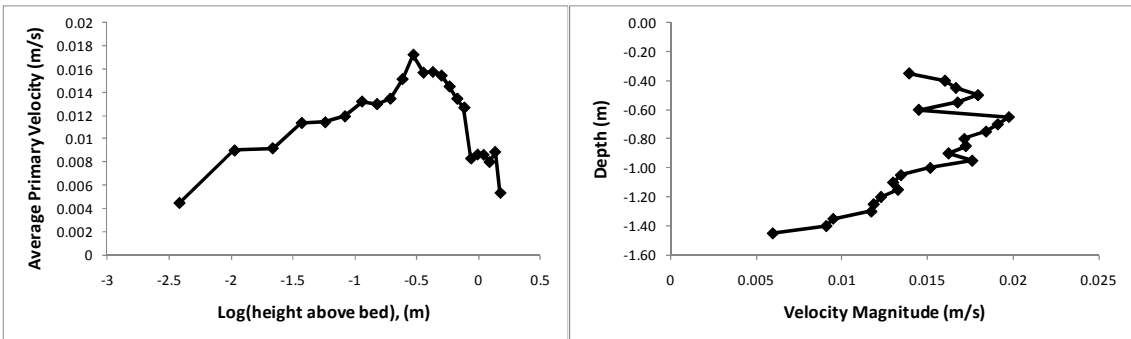
Profile Location# 20

Water cover depth = 1.55 m, and average current direction = 4.20 radians



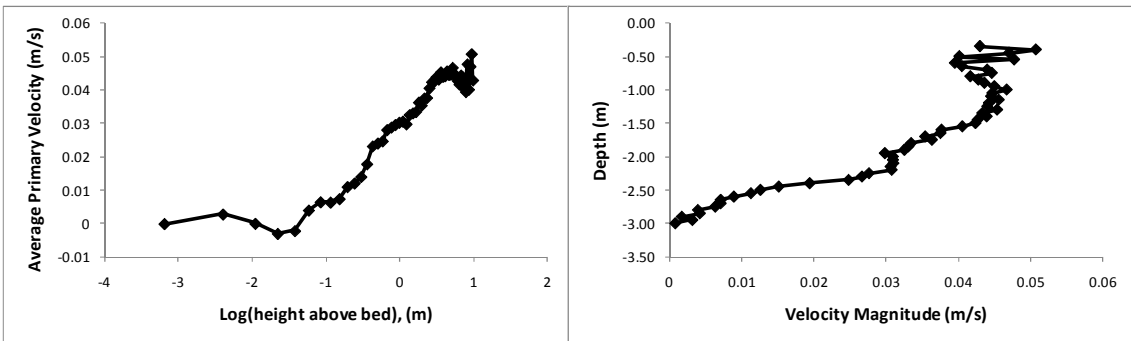
Profile Location# 21

Water cover depth = 1.54 m, and average current direction = 2.07 radians



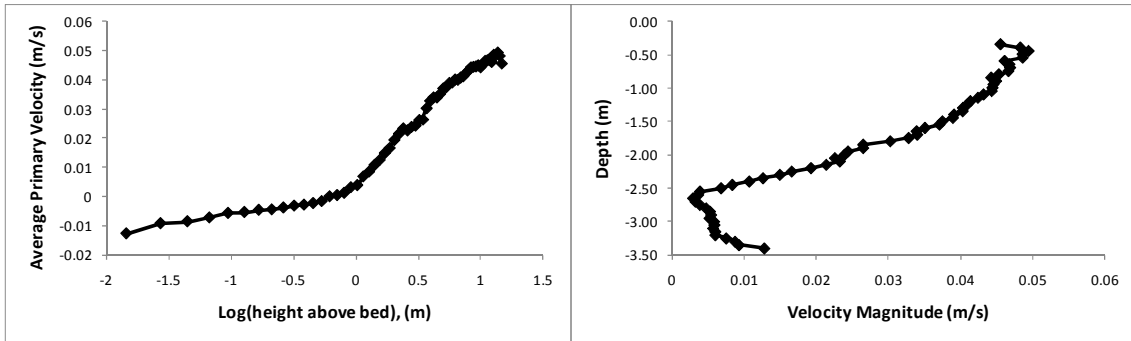
Profile Location# 22

Water cover depth = 3.04 m, and average current direction = 1.49 radians



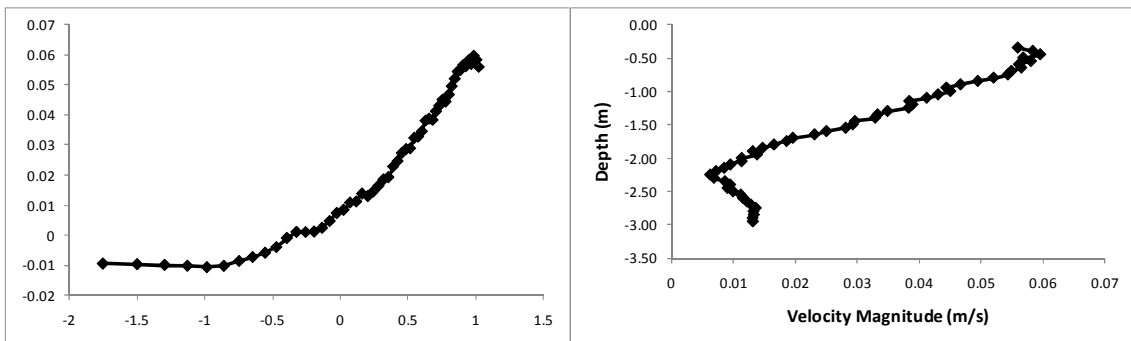
Profile Location# 25

Water cover depth = 3.56 m, and average current direction = 1.43 radians



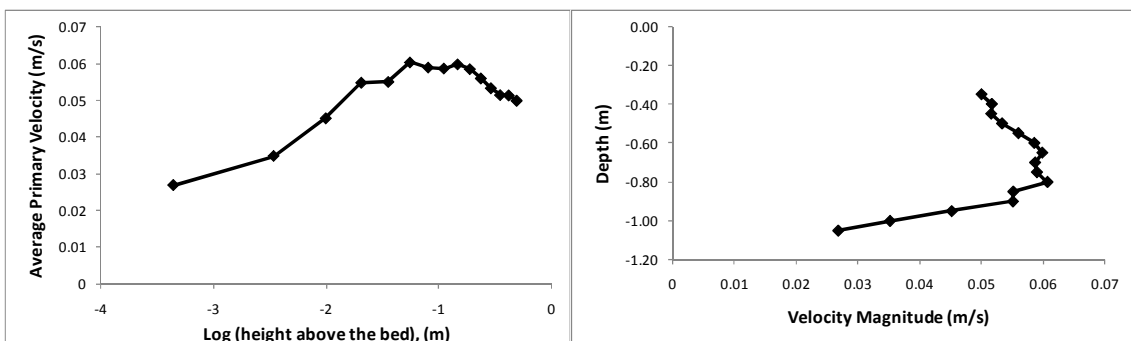
Profile Location# 26

Water cover depth = 3.12 m, and average current direction = 1.62 radians



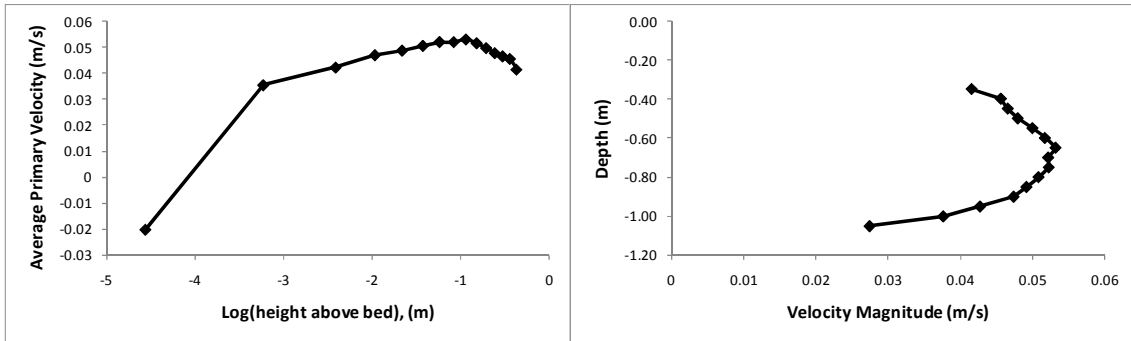
Profile Location# 28

Water cover depth = 1.08 m, and average current direction = 1.50 radians



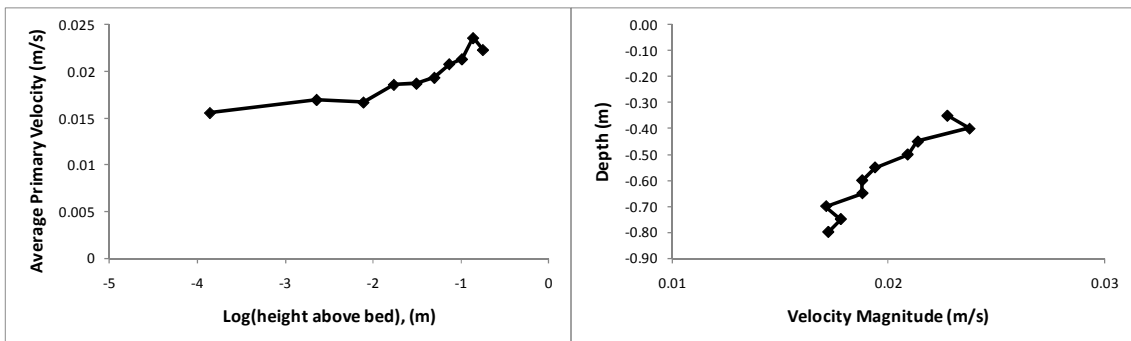
Profile Location# 29

Water cover depth = 1.04 m, and average current direction = 1.33 radians



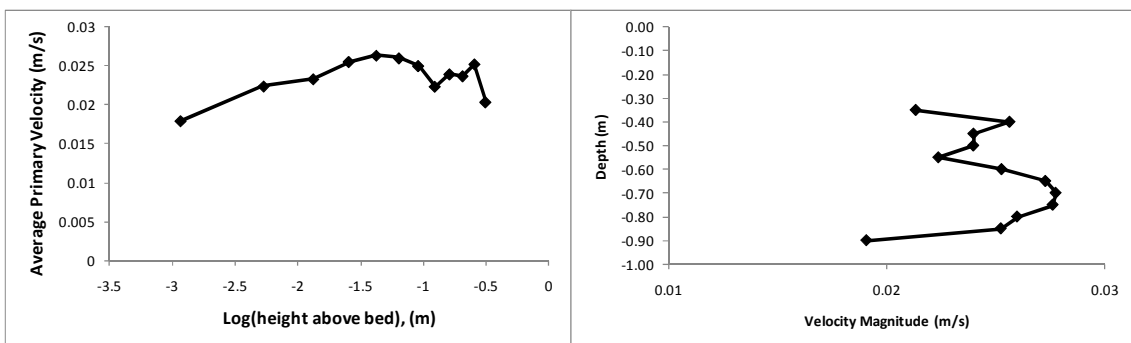
Profile Location# 30

Water cover depth = 0.82 m, and average current direction = 3.11 radians



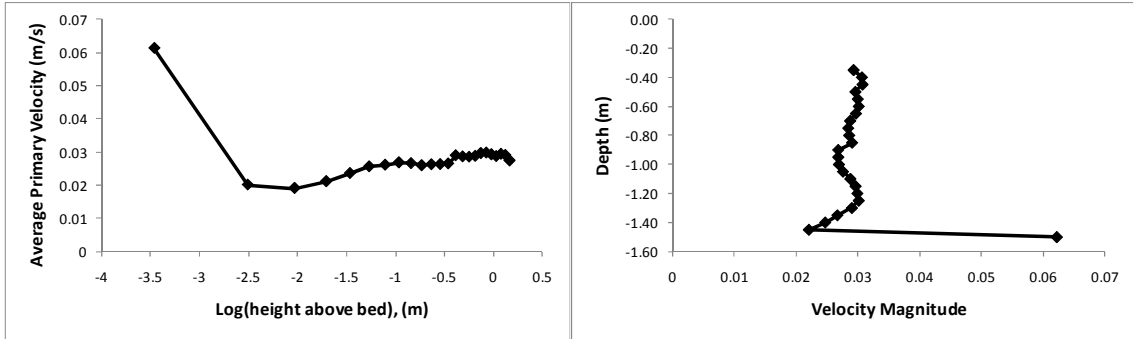
Profile Location# 31

Water cover depth = 0.95 m, and average current direction = 2.88 radians



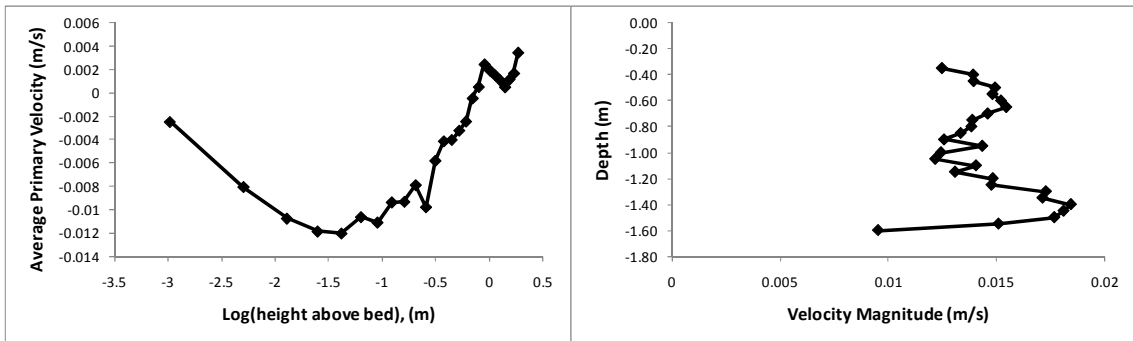
Profile Location# 32

Water cover depth = 1.53 m, and average current direction = 2.60 radians



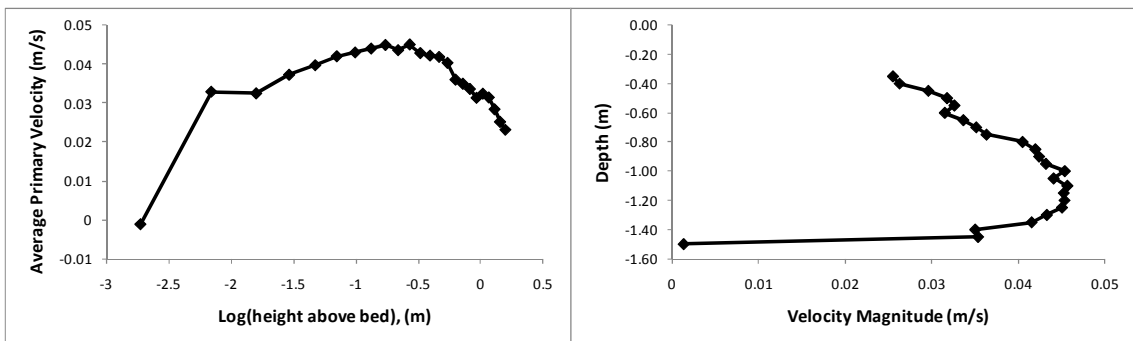
Profile Location# 33

Water cover depth = 1.65 m, and average current direction = 4.26 radians



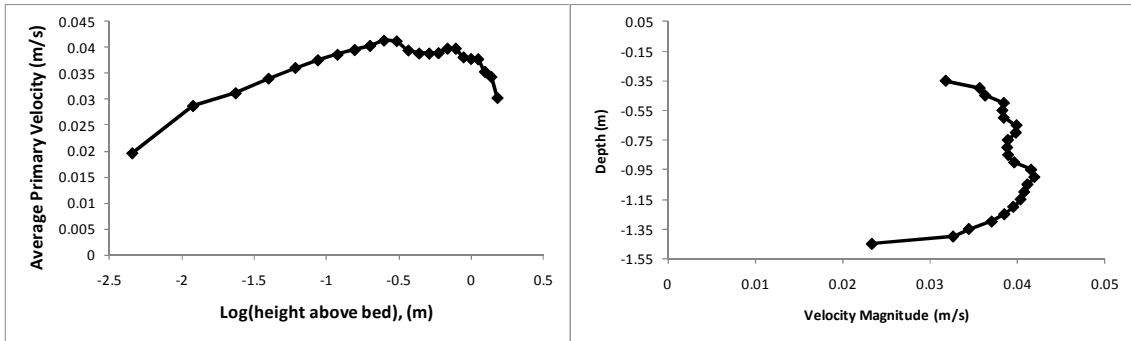
Profile Location# 34

Water cover depth = 1.57 m, and average current direction = 5.55 radians



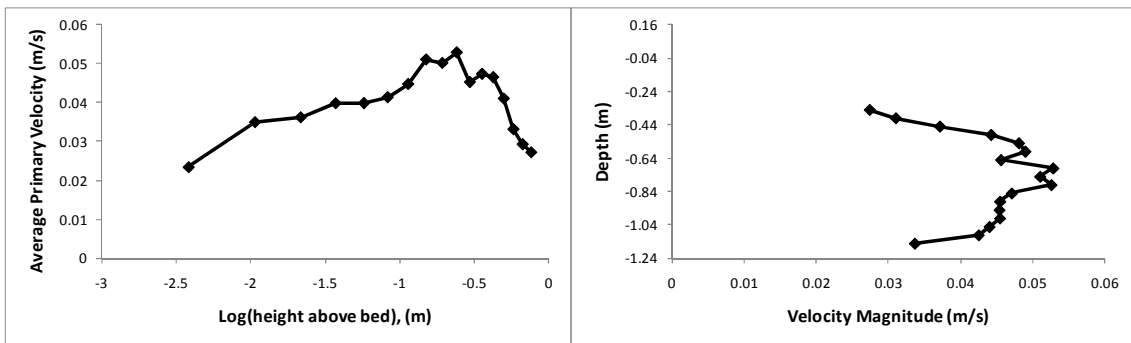
Profile Location# 36

Water cover depth = 1.55 m, and average current direction = 4.99 radians



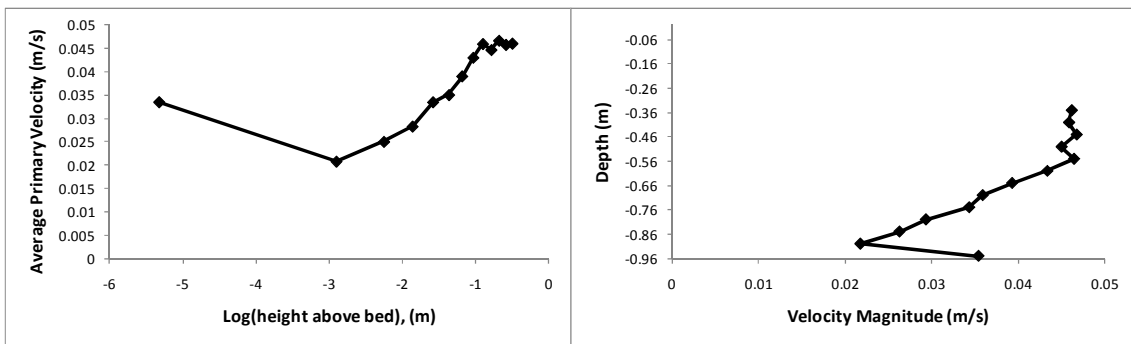
Profile Location# 37

Water cover depth = 1.24 m, and average current direction = 4.69 radians



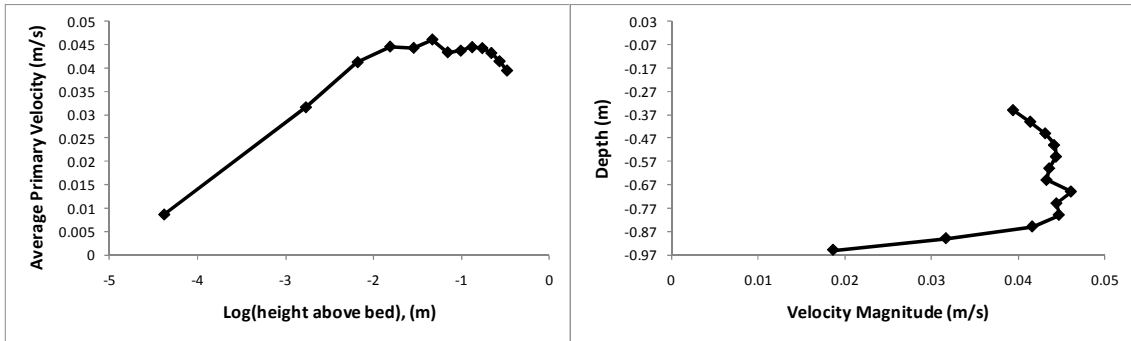
Profile Location# 39

Water cover depth = 0.96 m, and average current direction = 4.93 radians



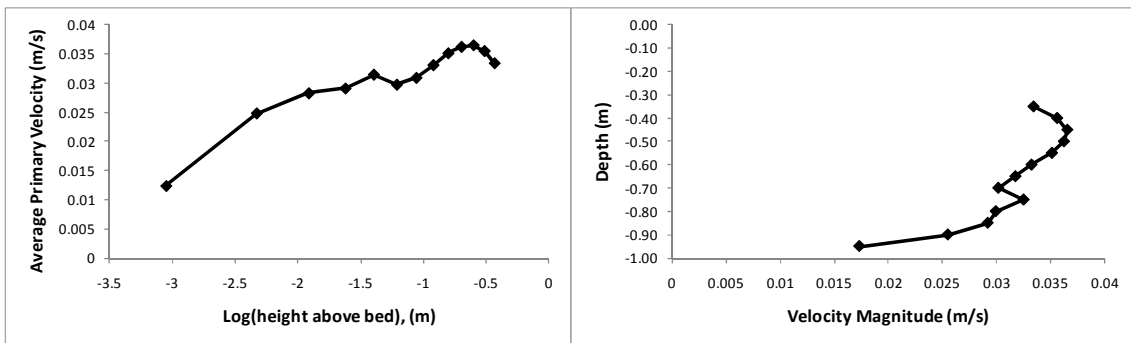
Profile Location# 40

Water cover depth = 0.97 m, and average current direction = 5.07 radians



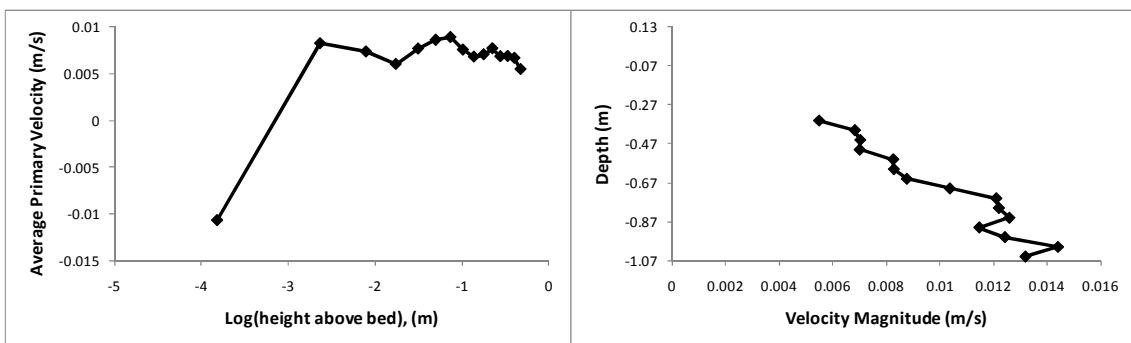
Profile Location# 41

Water cover depth = 1.00 m, and average current direction = 5.00 radians



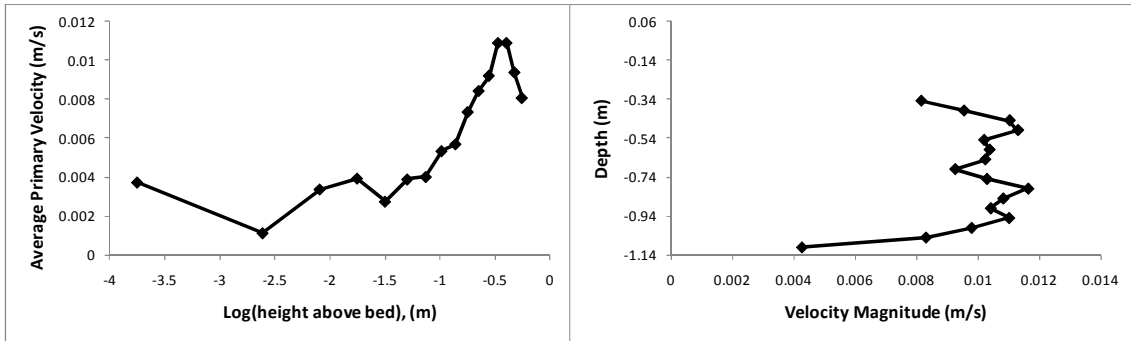
Profile Location# 44

Water cover depth = 1.07 m, and average current direction = 4.07 radians



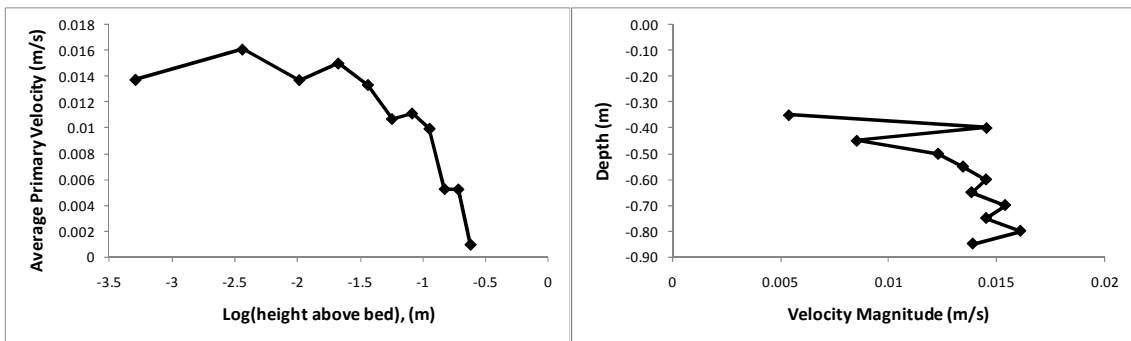
Profile Location# 45

Water cover depth = 1.14 m, and average current direction = 4.35 radians



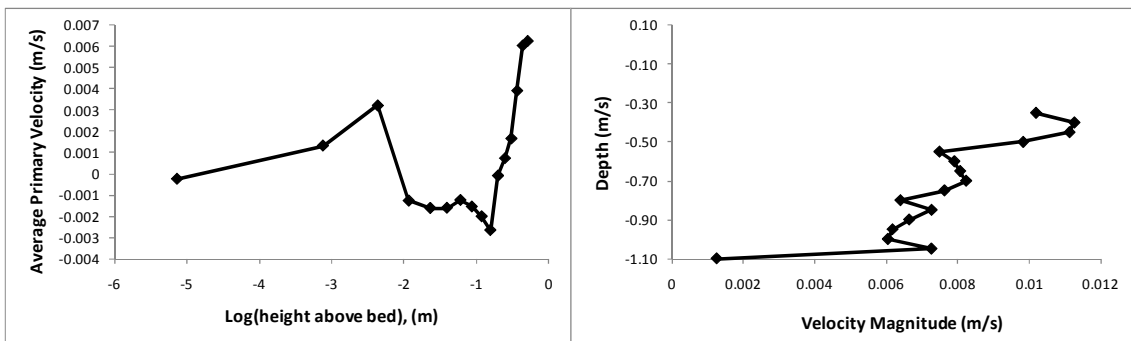
Profile Location# 48

Water cover depth = 0.89 m, and average current direction = 3.80 radians



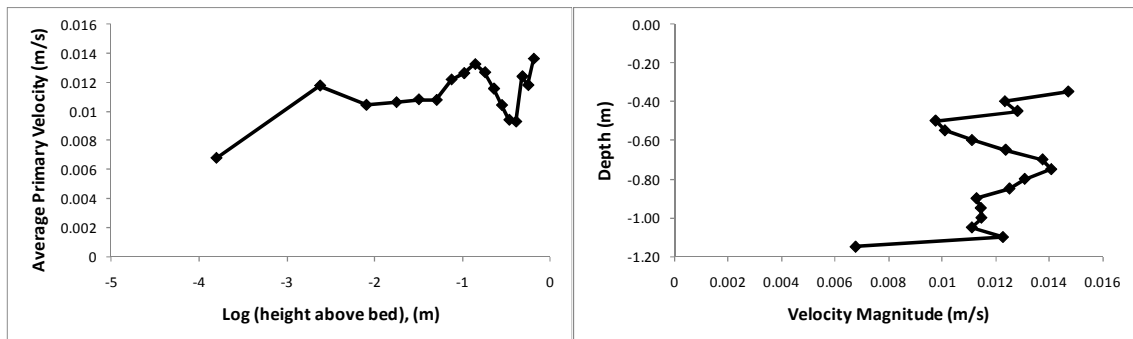
Profile Location# 50

Water cover depth = 1.10 m, and average current direction = 3.64 radians



Profile Location# 51

Water cover depth = 1.17 m, and average current direction = 4.77 radians



APPENDIX-IV: DERIVATION OF SIMPLIFIED EQUATION FOR TOTAL BED SHEAR STRESS

In section 5.3 of chapter 5 in this thesis, a simplified equation (Equation 5.5) of the total bed shear stress estimation under shallow water conditions was used. This equation facilitates the direct estimation of the total bed shear stress under shallow water conditions for known values of water depth (h), wind speed (U), and fetch length (F) instead of a lengthy step by step approach used in chapter 3 of this thesis. Derivation of the simplified equation has been provided below.

The total bed shear stress from non-linear wave-current interaction can be given by the following equation:

$$\tau_b = \tau_c + \tau_w + 2\sqrt{\tau_c \tau_w} \cos \theta_c \quad (1)$$

where, τ_w and τ_c are the bed shear stress due to waves and currents, respectively; θ is the angle between waves and currents which varies between 0 to 90° , assuming simple harmonic motion of waves. The third term in Equation 1 is due to non-linear wave current interaction.

(1) Bed shear stress due to waves

The total bed shear stress due to wind induced waves can be determined using the SMB (Sverdrup-Munk-Bretschneider) method with linear wave theory as detailed in section

3.3.4 of chapter 3 in this thesis. In shallow water conditions ($h/L < 0.5$), wave parameters, significant wave height (H), significant wave period (T), and wave length (L) may be calculated using following equations:

$$H_s = 0.283 \frac{U_a^2}{g} \tanh \left[0.530 \left(\frac{gh}{U_a^2} \right)^{3/4} \right] \tanh \left\{ \frac{0.00565 \left(\frac{gF}{U_a^2} \right)^{1/2}}{\tanh \left[0.530 \left(\frac{gh}{U_a^2} \right)^{3/4} \right]} \right\} \quad (2)$$

$$T_s = 7.54 \frac{U_a}{g} \tanh \left[0.833 \left(\frac{gh}{U_a^2} \right)^{3/8} \right] \tanh \left\{ \frac{0.0379 \left(\frac{gF}{U_a^2} \right)^{1/3}}{\tanh \left[0.833 \left(\frac{gh}{U_a^2} \right)^{3/8} \right]} \right\} \quad (3)$$

$$L = \frac{gT^2}{2\pi} \sqrt{\tanh \left[\frac{4\pi^2 h}{T^2 g} \right]} \quad (4)$$

Taylor expansion series were for hyperbolic tangent function is shown below:

$$\tanh(x) = x - \frac{x^3}{3} + \frac{2x^5}{15} - \dots \text{ for all finite } x < \frac{\pi}{2} \text{ values} \quad (5)$$

For small values of x, the second and higher order terms will be very small comparatively to x and can be ignored. Using only first order terms Equations 2, 3, and 4 can be simplified without compromising much in accuracy as written in following equations:

$$H = 1.6 \times 10^{-3} * \left(\frac{U_a^2}{g} \right) * \left(\frac{gF}{U_a^2} \right)^{0.5} \quad (6)$$

$$T = 0.286 * \left(\frac{U_a}{g} \right) * \left(\frac{gF}{U_a^2} \right)^{0.33} \quad (7)$$

$$L = \frac{gT^2}{2\pi} \quad (8)$$

The wind stress factor can be written in term of wind speed U as follows:

$$U_a = 0.71 * U^{1.23} \quad (9)$$

The maximum horizontal bottom velocity in shallow water is calculated using equation:

$$u_{bm} = \frac{\pi H}{T} \left[\frac{1}{\sinh\left(\frac{2\pi h}{L}\right)} \right] \quad (10)$$

The maximum displacement of fluid particles corresponding to maximum bottom velocity can be obtained as:

$$a_m = \frac{H}{2 \sinh\left(\frac{2\pi h}{L}\right)} \quad (11)$$

Substituting the values of H, T, L, and U_a from Equations 6, 7, 8, and 9 respectively into

Equations 10, and 11, the following equations were obtained.

$$\sinh\left(\frac{2\pi h}{L}\right) = \sinh\left(\frac{1287 * h}{U^{0.820} * F^{0.667}}\right) \quad (12)$$

$$u_{bm} = \frac{0.0205 * U^{0.820} * F^{0.167}}{\sinh\left(\frac{1287 * h}{U^{0.820} * F^{0.667}}\right)} \quad (13)$$

$$a_m = 1.81 \times 10^{-4} * U^{1.23} * F^{0.5} \quad (14)$$

The wave friction factor is given by

$$f_w = \frac{2}{\sqrt{R_w}} \quad (15)$$

and Reynolds number by

$$R_w = \frac{u_{bm} a_m}{\nu} \quad (16)$$

where, the kinematic viscosity of water $\nu = 10^{-6} \text{ m}^2/\text{s}$ at 20° C . On substituting the values of u_{bm} and a_m into the Equation 15, the wave friction factor can be written as:

$$f_w = 1.0384 * (U^{-1.025} * F^{-0.334}) * \sinh\left(\frac{1287 * h}{U^{0.820} * F^{0.667}}\right) \quad (17)$$

Using the above simplified parameters, the bed shear stress due to wind induced waves can be calculated as:

$$\tau_w = \frac{1}{2} f_w \rho u_{bm}^2 \quad (18)$$

After substituting appropriate simplified parameters, the bed shear stress due to wind waves in terms of water depth (h), wind speed (U), and fetch length (F) can be written as:

$$\tau_w = \frac{0.2182 * U^{0.613}}{\sinh\left(\frac{1287 * h}{U^{0.820} * F^{0.667}}\right)} \quad (19)$$

In above equation, numerical value in the hyperbolic sine function was adjusted to increase the accuracy of the equation and following corrected equation was obtained.

$$\tau_w = \frac{0.2182 * U^{0.613}}{\sinh\left(\frac{1541.5 * h}{U^{0.820} * F^{0.667}}\right)} \quad (20)$$

(2) Bed shear stress due to currents

Shear stress at the bed due to wind induced return currents can be calculated using the following equations as already described in section 3.3.4 of chapter 3.

$$\tau_c = \rho_w u_{*s}^2 \lambda_{z_{bh}} (z_{sh} + 1) \times \left(\frac{A}{z_{bh}} - \frac{B}{z_{sh} + 1} \right) \quad (21)$$

The variables A and B in the above equation are given as:

$$A = \frac{q_2}{p_1 q_2 - p_2 q_1} \quad \text{and} \quad B = \frac{-q_1}{p_1 q_2 - p_2 q_1}$$

where,

$$p_1 = \lambda z_{sh};$$

$$p_2 = \lambda z_{sh} / z_{bh};$$

$$q_1 = (1 + z_{sh}) \ln\left(1 + \frac{1}{z_{sh}}\right) - 1; \text{ and}$$

$$q_2 = z_{sh} \ln\left(1 + \frac{1}{z_{bh}}\right) - 1;$$

where, the surface characteristics length $z_{sh} = 2.2 \times 10^{-4}$;

the bottom characteristics length $z_{bh} = 1.4 \times 10^{-4}$; and

the constant $\lambda = 0.35$

The surface shear velocity of water

$$u_{*s} = 0.035U \sqrt{\frac{\rho_a}{\rho_w}} \tag{22}$$

On substituting the values of z_{sh} , z_{bh} , and λ and solving above parameters, the bed shear stress due to return currents can be written as:

$$\tau_c = 3.734 \times 10^{-4} * U^2 \tag{23}$$

It is evident that the bed shear stress due to return currents is a function of wind speed only and it does not depend on the water depth (h) and fetch length (F).

(3) *Total bed shear stress*

The total bed shear stress in simplified form can be obtained by substituting values of τ_w and τ_c from Equations 7 and 8 respectively into equation 1. Here, the waves and currents are assumed collinear (Angle $\theta = 0$ or 180 degrees) to obtain maximum total bed shear stress. The simplified equation of the total bed shear stress can be written as:

$$\tau_b = \frac{0.2182 * U^{0.613}}{\sinh \left[\frac{1541.5 * h}{U^{0.820} * F^{0.667}} \right]} + 3.734 \times 10^{-4} * U^2 + \frac{0.0180 * U^{1.307}}{\sqrt{\sinh \left[\frac{1541.5 * h}{U^{0.820} * F^{0.667}} \right]}} \quad (24)$$

In the Equation 24, the first term on the right-hand-side is the bed shear stress due solely to wind waves, the second term defines the bed shear stress due to currents, and the third term shows the enhancement in bed shear stress due to non-linear wave-current interactions.

**APPENDIX-V: MISCELLANEOUS PICTURES OF SITE SHOWING
DEPLOYMENT OF VARIOUS INSTRUMENTS**



Figure IV-1 Shebandowan Mine tailings storage facility, located near Thunder Bay, ON, Canada



Figure IV-2 Main entrance to the Shebandowan tailings storage facility



Figure IV-3 Pictures of open spillway (outlet) and a wave break, which separates the cells in tailings pond



Figure IV-4 Weather station installed at the Shebandowan tailings storage facility



Figure IV-5 Deployment of sediment traps by professional divers in the tailings pond



Figure IV-6 Deployment of sediment traps by professional divers under supervision of Prof. Ernest K. Yanful (on right) and a properly installed sediment trap



Figure IV-7 Sampling process of the sediment traps and samples collected from each sediment trap stored in 4 liter containers

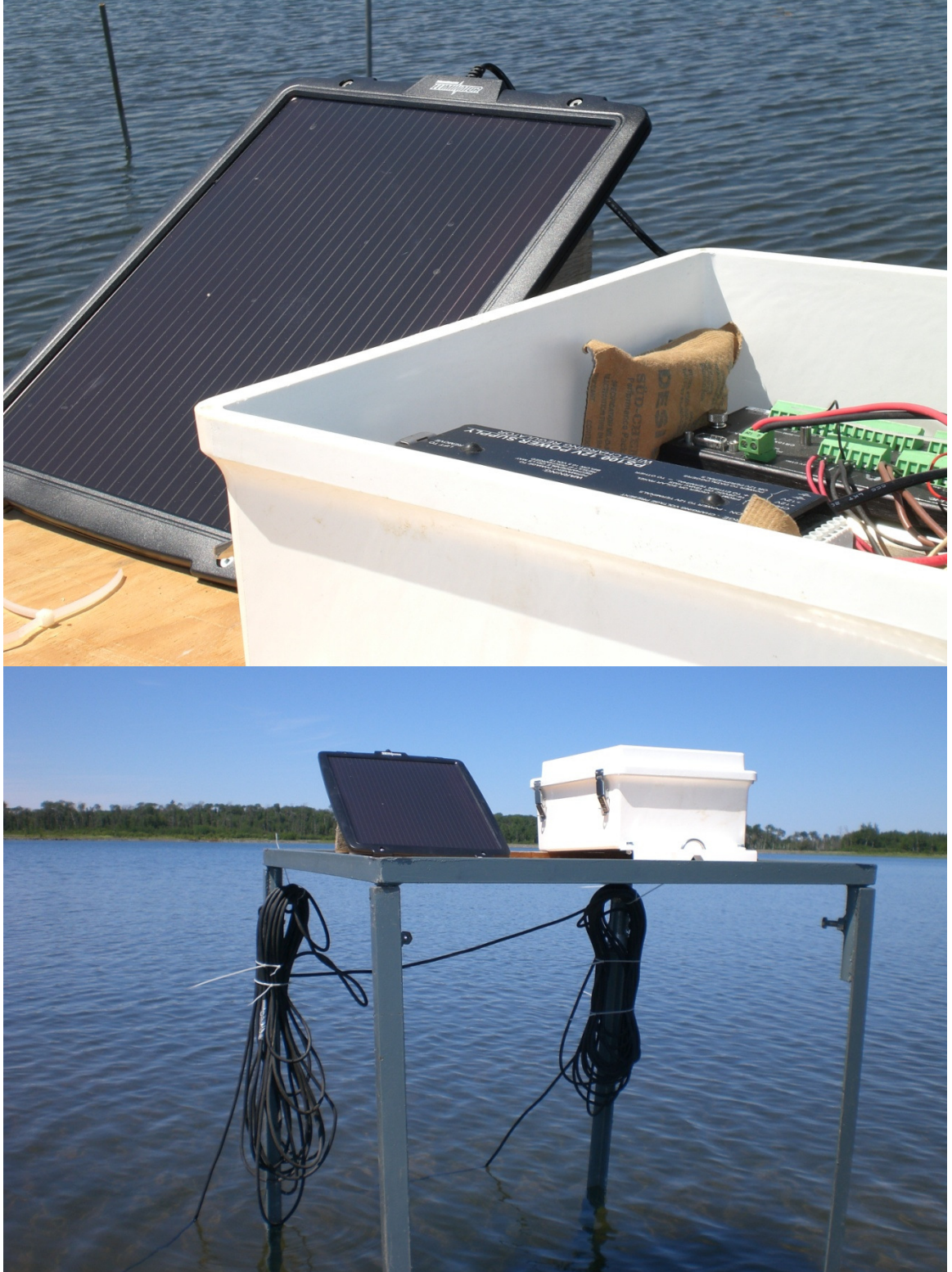


Figure IV-8 Deployment of OBS sensors in the middle cell with datalogger and solar panel sitting on a steel fabricated platform



Figure IV-9 Testing of ADCP and peripherals prior to deployment in the tailings pond



Figure IV-10 ADCP and GPS mounted on the boat with especially fabricated mounting assembly



Figure IV-11 Stationary boat data circulation current data collection with ADCP in the middle cell of the tailings pond

**APPENDIX-VI: COPYRIGHT LICENSE FOR PUBLICATION OF
CHAPTER 3**

**SPRINGER LICENSE
TERMS AND CONDITIONS**

Jan 26, 2011

This is a License Agreement between Laxmi Kant Kachhwal ("You") and Springer ("Springer") provided by Copyright Clearance Center ("CCC"). The license consists of your order details, the terms and conditions provided by Springer, and the payment terms and conditions.

All payments must be made in full to CCC. For payment instructions, please see information listed at the bottom of this form.

License Number	2593780385694
License date	Jan 21, 2011
Licensed content publisher	Springer
Licensed content publication	Water, Air, and Soil Pollution
Licensed content title	Water Cover Technology for Reactive Tailings Management: A Case Study of Field Measurement and Model Predictions
Licensed content author	Laxmi Kant Kachhwal
Licensed content date	Jan 1, 2010
Volume number	214
Issue number	1
Type of Use	Thesis/Dissertation
Portion	Full text

Number of copies	1
Author of this Springer article	Yes and you are the sole author of the new work
Order reference number	
Title of your thesis / dissertation	Evaluation of Wind-Induced Resuspension on the Performance of a Mine Tailings Storage Facility
Expected completion date	Apr 2011
Estimated size(pages)	260
Total	0.00 USD

Terms and Conditions:

Introduction

The publisher for this copyrighted material is Springer Science + Business Media. By clicking "accept" in connection with completing this licensing transaction, you agree that the following terms and conditions apply to this transaction (along with the Billing and Payment terms and conditions established by Copyright Clearance Center, Inc. ("CCC"), at the time that you opened your Rightslink account and that are available at any time at <http://myaccount.copyright.com>).

Limited License

With reference to your request to reprint in your thesis material on which Springer Science and Business Media control the copyright, permission is granted, free of charge, for the use indicated in your enquiry. Licenses are for one-time use only with a maximum distribution equal to the number that you identified in the licensing process.

This License includes use in an electronic form, provided it is password protected or on the

university's intranet, destined to microfilming by UMI and University repository. For any other electronic use, please contact Springer at (permissions.dordrecht@springer.com or permissions.heidelberg@springer.com)

The material can only be used for the purpose of defending your thesis, and with a maximum of 100 extra copies in paper.

Although Springer holds copyright to the material and is entitled to negotiate on rights, this license is only valid, provided permission is also obtained from the (co) author (address is given with the article/chapter) and provided it concerns original material which does not carry references to other sources (if material in question appears with credit to another source, authorization from that source is required as well). Permission free of charge on this occasion does not prejudice any rights we might have to charge for reproduction of our copyrighted material in the future.

Altering/Modifying Material: Not Permitted

However figures and illustrations may be altered minimally to serve your work. Any other abbreviations, additions, deletions and/or any other alterations shall be made only with prior written authorization of the author(s) and/or Springer Science + Business Media. (Please contact Springer at permissions.dordrecht@springer.com or permissions.heidelberg@springer.com)

Reservation of Rights

Springer Science + Business Media reserves all rights not specifically granted in the combination of (i) the license details provided by you and accepted in the course of this

licensing transaction, (ii) these terms and conditions and (iii) CCC's Billing and Payment terms and conditions.

Copyright Notice:

Please include the following copyright citation referencing the publication in which the material was originally published. Where wording is within brackets, please include verbatim.

"With kind permission from Springer Science+Business Media: <book/journal title, chapter/article title, volume, year of publication, page, name(s) of author(s), figure number(s), and any original (first) copyright notice displayed with material>."

Warranties: Springer Science + Business Media makes no representations or warranties with respect to the licensed material.

Indemnity

You hereby indemnify and agree to hold harmless Springer Science + Business Media and CCC, and their respective officers, directors, employees and agents, from and against any and all claims arising out of your use of the licensed material other than as specifically authorized pursuant to this license.

No Transfer of License

This license is personal to you and may not be sublicensed, assigned, or transferred by you to any other person without Springer Science + Business Media's written permission.

No Amendment Except in Writing

This license may not be amended except in a writing signed by both parties (or, in the case of Springer Science + Business Media, by CCC on Springer Science + Business Media's behalf).

Objection to Contrary Terms

Springer Science + Business Media hereby objects to any terms contained in any purchase order, acknowledgment, check endorsement or other writing prepared by you, which terms are inconsistent with these terms and conditions or CCC's Billing and Payment terms and conditions. These terms and conditions, together with CCC's Billing and Payment terms and conditions (which are incorporated herein), comprise the entire agreement between you and Springer Science + Business Media (and CCC) concerning this licensing transaction. In the event of any conflict between your obligations established by these terms and conditions and those established by CCC's Billing and Payment terms and conditions, these terms and conditions shall control.

Jurisdiction

All disputes that may arise in connection with this present License, or the breach thereof, shall be settled exclusively by the country's law in which the work was originally published.

Other terms and conditions:

v1.2

Gratis licenses (referencing \$0 in the Total field) are free. Please retain this printable license for your reference. No payment is required.

If you would like to pay for this license now, please remit this license along with your payment made payable to "COPYRIGHT CLEARANCE CENTER" otherwise you will be invoiced within 48 hours of the license date. Payment should be in the form of a check or money order referencing your account number and this invoice number RLNK10918195.

Once you receive your invoice for this order, you may pay your invoice by credit card. Please follow instructions provided at that time.

Make Payment To:

Copyright Clearance Center

Dept 001

P.O. Box 843006

Boston, MA 02284-3006

If you find copyrighted material related to this license will not be used and wish to cancel, please contact us referencing this license number 2593780385694 and noting the reason for cancellation.

Questions? customercare@copyright.com or +1-877-622-5543 (toll free in the US) or +1-978-646-2777.

CURRICULAR VITAE

Name: Laxmi Kant Kachhwal

Date and Place of Birth: March 01, 1981
Ratangarh, Rajasthan, India

Post-secondary Education and Degrees:

The University of Rajasthan
Jaipur, Rajasthan, India
1997-2000 B.Sc. Physics

The University of Rajasthan
Jaipur, Rajasthan, India
2000-2003 M.Sc. Physics

Indian Institute of Technology Roorkee
Roorkee, Uttarakhand, India
2003-2005 M.Tech. Hydrology

The University of Western Ontario
London, Ontario, Canada
2006-2010 Ph.D.

Honours and Awards:

Ministry of Human Resources Development
Scholarship,
Government of India
2003-2005

University Grant Commission-National
Eligibility Test Junior Research Fellowship,
Government of India
2003-2005

Publications:

Kachhwal, L.K., Singhal, D.C., Kumar, B., Sharma, V.K., Verma, S.K., Israil, M. (2009). Hydrogeological investigations in Pathri-Rao watershed Uttarakhand, India using an integrated isotopes technique. Chapter 19, In: Ramanathan, A.L., Bhattacharya, P., Keshari, A.K., Bundschuh, J., Chandrasekharam, D., Singh, S.K. (Editors), Assessment of Groundwater Resources and Management, I.K. International Pvt. Ltd., New Delhi, India, pp. 192-200.

- Singhal, D.C., **Kachhwal, L.K.**, Israil, M., Kumar, B. (2010). Estimation of ground water recharge in the Upper Piedmont Zone of a hilly watershed, district Haridwar, Uttarakhand. National Conference on Groundwater Resources Development and Management in Hard Rocks, Department of Geology, University of Pune, India, February 2010.
- Kachhwal, L.K.**, Yanful, E.K., Lanteigne, L. (2009). Evaluation of wind-induced resuspension of flooded mine tailings at Shebandowan mine site, Ontario, Canada. Proceeding. 8th International Conference on Acid Rock Drainage (ICARD) and Securing the Future: Mining, Metals, & the Environment in a Sustainable Society 2009, Skelleftea, Sweden, June 22-26, 2009, vol. 2, pp. 1009-1018.
- Kachhwal, L.K.**, Yanful, E.K., Lanteigne, L. (2010). Water cover technology for reactive tailings management: a case study of field measurement and model predictions. Water, Air and Soil Pollution, DOI 10. 1007/s11270-010-0429-6.
- Kachhwal, L.K.**, Yanful, E.K., Rennie, C.D. (2010). Field measurements of resuspension in a tailings pond by acoustic and optical backscatter instruments. Proceedings 63rd Canadian Geotechnical Conference, Calgary, Canada, September 12-16, 2010.
- Kachhwal, L.K.**, Yanful, E.K., Rennie, C.D. (2011). A semi-empirical approach for estimation of bed shear stress in a tailings pond. Environmental Earth Sciences, Reviews submitted.
- Kachhwal, L.K.**, Yanful, E.K. (2011). Estimating the erosion characteristics of tailings using field resuspension data. Marine Geology, submitted.